



UNIVERSIDAD DE LA REPÚBLICA
FACULTAD DE INGENIERÍA



Stochastic models for Cognitive Radio Networks

TESIS PRESENTADA A LA FACULTAD DE INGENIERÍA DE LA
UNIVERSIDAD DE LA REPÚBLICA POR

Claudina Rattaro Eugui

EN CUMPLIMIENTO PARCIAL DE LOS REQUERIMIENTOS
PARA LA OBTENCIÓN DEL TÍTULO DE
DOCTORA EN INGENIERÍA ELÉCTRICA.

DIRECTORES DE TESIS

Dr. Pablo Belzarena Universidad de la República
Dra. Paola Bermolen Universidad de la República

TRIBUNAL

Dr. Héctor Cancela Universidad de la República, Uruguay
Prof. María Simon Universidad de la República, Uruguay
Dra. Sandrine Vaton Telecom Bretagne, Francia
Dr. Andrés Ferragut (Revisor) Universidad ORT, Uruguay
Dr. Matthieu Jonckheere (Revisor) Universidad de Buenos Aires,
Argentina

DIRECTOR ACADÉMICO

Dr. Pablo Belzarena Universidad de la República

Montevideo
Friday 23rd February, 2018

Stochastic models for Cognitive Radio Networks, Claudina Rattaro Eugui.

ISSN 1688-2784

Esta tesis fue preparada en \LaTeX usando la clase iietesis (v1.1).

Contiene un total de 180 páginas.

Compilada el Friday 23rd February, 2018.

<http://iie.fing.edu.uy/>



ACTA DE DEFENSA

TESIS DE DOCTORADO

Fecha: Viernes 8, de diciembre, de 2017 .-

Lugar: Montevideo, Facultad de Ingeniería – Universidad de la República.-

Plan de Estudio: Doctorado en Ingeniería Eléctrica.-

Aspirante: Claudina Isabel Rattaro Eugui.-

Documento de Identidad: 3.599.265-4

Director/es de Tesis: Dr. Pablo Belzarena (DT); Dra. Paola Bermolen (coDT).-

Tribunal: Dr. Matthieu Jonckheere (Univ. Buenos Aires);
Dr. Andrés Ferragut (Univ. ORT);
Dra. Sandrine Vaton (Telecom Bretagne, Institut Mines Télécom Atlantique, Francia);
Dr. Héctor Cancela (INCO, FING, UdelaR);
Prof. María Simon (IIE, FING, UdelaR).-

Los miembros del Tribunal hacen constar que en el día de la fecha la **Sra. Ing. Claudina Rattaro** ha sido **APROBADA** en la defensa de su **Tesis de Doctorado** titulada: “**Stochastic models for Cognitive Radio Networks**”

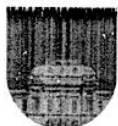
La resolución del Tribunal se fundamenta en los puntos detallados a continuación:

En esta tesis se analiza por diferentes técnicas matemáticas el problema de asignación de recursos de ancho de banda en el contexto de redes cognitivas (Cognitive Radio Networks), en el que los recursos de espectro electromagnético son compartidos por sus licenciatarios originales, que los ponen a disposición de un mercado de agentes secundarios, manteniendo la prerrogativa de uso correspondiente a la licencia. Esto permite el reuso en tiempo real de recursos de radio previamente bloqueados por la licencia, conformando un uso oportunista por parte de los agentes secundarios.

Dentro de este contexto general la candidata propone, mediante la utilización de modelos matemáticos, caracterizar en primer lugar políticas de control de admisión para los usuarios secundarios que permitan un uso adecuado de los recursos. Partiendo de la revisión profunda del estado del arte, relevando la bibliografía más actualizada pertinente para la tesis, se formula el problema mediante modelos Markovianos de decisión (Markov Decision Processes, MDP). Estos problemas se resuelven aplicando técnicas de programación dinámica (Dynamic Programming). A continuación, se analiza el comportamiento de estas políticas mediante la utilización de técnicas recientes de límites fluidos en presencia de discontinuidades. En una segunda parte de la tesis, el foco se concentra en la perspectiva geométrica de la red y su impacto en el uso del medio inalámbrico. Mediante modelos de geometría estocástica y de grafos aleatorios, se propone calcular la probabilidad de acceso al medio (MAP) y la probabilidad de cobertura (COP) resultante de aplicar tanto técnicas clásicas de acceso al medio (tipo ALOHA), como otros mecanismos de detección de portadora (CSMA).

Los problemas de ingeniería abordados en esta tesis son de gran importancia y actualidad. La asignación del espectro es un problema central y desafiante, cuya importancia no ha dejado de crecer y se prevee que aumente a medida que las redes crecen en ubicuidad y diversidad. Las contribuciones realizadas por la candidata son originales y aportan de manera muy relevante al conocimiento en la temática. Se basan en un abanico muy amplio de técnicas matemáticas avanzadas, sobre las cuales demuestra un profundo dominio, y que incluyen varias de las más recientes y potentes que están disponibles para la evaluación de desempeño de sistemas complejos. Complementan este abanico de técnicas un conjunto de simulaciones de validación para cada uno de los puntos abordados, que muestran un análisis crítico y metódico por parte de la candidata, así como una preocupación de acercar las políticas, algoritmos y reglas de decisión a implementaciones prácticas.

El documento de tesis es de muy alta calidad, con una excelente organización general y de cada parte y capítulo. La candidata se preocupa por la claridad de las demostraciones buscando que el lector pueda realizar un seguimiento de los temas abordados, sin exceso de detalles, pero sin por ello perder rigurosidad. La notación elegida es especialmente elegante y adecuada para expresar los problemas y los resultados obtenidos. También las publicaciones asociadas a la tesis demuestran la calidad del trabajo, y su valoración por la comunidad académica internacional.



UNIVERSIDAD
DE LA REPUBLICA
URUGUAY

UNIVERSIDAD DE LA REPÚBLICA



La presentación oral fue asimismo de excelente calidad, transmitiendo de manera sintética y clara los aspectos más relevantes de su trabajo y poniendo en valor las contribuciones realizadas, y contestando las respuestas formuladas por el jurado de manera clara y precisa.

Para que conste,

Firmas originales

Dr. Matthieu Jonckheere

Dr. Andrés Ferragut

Dra. Sandrine Vaton

Dr. Héctor Cancela

Prof. María Simon

This page was intentionally left blank.

Dans la vie, rien n'est à craindre, tout est à comprendre.

MARIE CURIE

This page was intentionally left blank.

Acknowledgements

This work was partially supported by Comisión Académica de Posgrado de la UdelaR (CAP) with a PhD grant, Plan Ceibal (Centro Ceibal para el Apoyo a la Educación de la Niñez y la Adolescencia) with another PhD grant, Agencia Nacional de Investigación e Innovación del Uruguay (ANII) with the R&D project “Grafos aleatorios y límites fluidos en el modelado de redes inalámbricas”, and Comisión Sectorial de Investigación Científica de la UdelaR (CSIC) under two projects: R&D Group ARTES “Análisis de redes, tráfico y estadísticas de servicio” and R&D project “Límites fluidos, aproximación por difusión y grandes desvíos en sistemas de comunicación de gran dimension”.

Luego de los agradecimientos formales, paso a los agradecimientos personales. En primer lugar debo agradecer a mi familia, por el apoyo fundamental para realizar el doctorado. En particular, tengo que agradecerle a Marco por todo su apoyo, compañía, confianza y por todo su amor.

Luego, agradezco a mis tutores Paola y Pablo, quienes me brindaron su apoyo incondicional durante todos estos años, así como la guía necesaria para llevar este trabajo a buen puerto. Paola fue una de las mejores profesoras que tuve durante mi carrera y la verdad que ha sido un lujo que me dirigiera el trabajo de doctorado. Hablando de Pablo, es a él a quien tengo que agradecerle el crecimiento que he tenido en todos estos años, comenzando allá por el 2007 cuando realicé mi proyecto de fin de carrera, luego en mis primeros pasos en el IIE, luego motivándome para realizar la maestría y finalmente dándome el empujoncito final para realizar el doctorado y dedicarme de lleno a la vida académica. En todas las etapas siempre guiándome, confiando en mi y aconsejándome.

Quiero agradecer a toda la familia del IIE y a los integrantes del grupo ARTES. Agradezco a todos con los que he trabajado durante estos años en diversos proyectos, muy especialmente a Laurita y a Federico quienes han colaborado directamente con este trabajo y de quienes he aprendido muchísimo. En particular Federico oficiando muchas veces de un tercer tutor.

Quiero agradecer a mis compañeros de “la ex 110”, comenzando por Fernanda con quien compartí larguísimas charlas formando una muy linda amistad, luego a Martín quién me ha contagiado su gran pasión por la política universitaria, y por último a Sebastián quien soportó el tramo final de esta aventura.

Por último agradezco a los integrantes del tribunal, quienes amablemente aceptaron evaluar esta tesis.

This page was intentionally left blank.

A Marco.

This page was intentionally left blank.

Abstract

During the last decade we have seen an explosive development of wireless technologies. Consequently the demand for electromagnetic spectrum has been growing dramatically resulting in the spectrum scarcity problem. In spite of this, spectrum utilization measurements have shown that licensed bands are vastly underutilized while unlicensed bands are too crowded. In this context, Cognitive Radio emerges as an auspicious paradigm in order to solve those problems. Even more, this concept is envisaged as one of the main components of future wireless technologies, such as the fifth-generation of mobile networks.

In this regard, this thesis is founded on cognitive radio networks. We start considering a paid spectrum sharing approach where secondary users (SUs) pay to primary ones for the spectrum utilization. In particular, the first part of the thesis bears on the design and analysis of an optimal SU admission control policy; i.e. that maximizes the long-run profit of the primary service provider. We model the optimal revenue problem as a Markov Decision Process and we use dynamic programming (and other techniques such as sample-path analysis) to characterize properties of the optimal admission control policy. We introduce different changes to one of the best known dynamic programming algorithms incorporating the knowledge of the characterization. In particular, those proposals accelerate the rate of convergence of the algorithm when is applied in the considered context.

We complement the analysis of the paid spectrum sharing approach using fluid approximations. That is to say, we obtain a description of the asymptotic behavior of the Markov process as the solution of an ordinary differential equation system. By means of the fluid approximation of the problem, we propose a methodology to estimate the optimal admission control boundary of the maximization profit problem mentioned before. In addition, we use the deterministic model in order to propose some tools and criteria that can be used to improve the mean spectrum utilization with the commitment of providing to secondary users certain quality of service levels.

In wireless networks, a cognitive user can take advantage of either the time, the frequency, or the space. In the first part of the thesis we have been concentrated on time-frequency holes, in the second part we address the complete problem incorporating the space variable. In particular, we first introduce a probabilistic model based on a stochastic geometry approach. We focus our study in two of the main performance metrics: medium access probability and coverage probability.

Finally, in the last part of the thesis we propose a novel methodology based on configuration models for random graphs. With our proposal, we show that it is possible to calculate an analytic approximation of the medium access probability (both for PUs and, most importantly, SUs) in an arbitrary large heterogeneous random network. This performance metric gives an idea of the possibilities offered by cognitive radio to improve the

spectrum utilization. The introduced robust method, as well as all the results of the thesis, are evaluated by several simulations for different network topologies, including real scenarios of primary network deployments.

Keywords:

Markov decision process, fluid limit, stochastic geometry, random graphs, dynamic spectrum assignment, cognitive radio.

Resumen

Hace ya un buen tiempo que las redes inalámbricas constituyen uno de los temas de investigación más estudiados en el área de las telecomunicaciones. Actualmente un gran porcentaje de los esfuerzos de la comunidad científica y del sector industrial están concentrados en la definición de los requerimientos y estándares de la quinta generación de redes móviles. 5G implicará la integración y adaptación de varias tecnologías, no solo del campo de las telecomunicaciones sino también de la informática y del análisis de datos, con el objetivo de lograr una red lo suficientemente flexible y escalable como para satisfacer los requerimientos para la enorme variedad de casos de uso implicados en el desarrollo de la “sociedad conectada”.

Un problema que se presenta en las redes inalámbricas actuales, que por lo tanto genera un desafío más que interesante para lo que se viene, es la escasez de espectro radioeléctrico para poder asignar bandas a nuevas tecnologías y nuevos servicios. El espectro está sobreasignado a los diferentes servicios de telecomunicaciones existentes y las bandas de uso libre o no licenciadas están cada vez más saturadas de equipos que trabajan en ellas (basta pensar lo que sucede en la banda no licenciada de 2.4 GHz). Sin embargo, existen análisis y mediciones que muestran que en diversas zonas y en diversas escalas de tiempo, el espectro radioeléctrico, si bien está formalmente asignado a algún servicio, no se utiliza plenamente existiendo tiempos durante los cuales ciertas bandas están libres y potencialmente podrían ser usadas. Esto ha llevado a que las Redes Radios Cognitivas, concepto que existe desde hace un tiempo, sean consideradas uno de los pilares para el desarrollo de las redes inalámbricas del futuro.

Este paradigma busca romper con el esquema tradicional de asignación de espectro de bandas licenciadas para uso exclusivo, permitiendo que los usuarios secundarios puedan usar aquellas bandas licenciadas, de manera oportunista, cuando los usuarios primarios no están presentes. Otro modelo posible dentro de las redes cognitivas, complementario al anterior, es pensar que el usuario primario es quien asigna a operadores secundarios el espectro que en ese momento no está utilizando a cambio de un cierto beneficio para él o para sus usuarios. Esto introduce diversos problemas económicos y de teoría de juegos aplicados a las redes cognitivas.

Un aspecto fundamentalmente buscado es que los usuarios primarios no se vean afectados (o sean afectados lo menos posible) al participar en estos mecanismos. Para ello, un modelo posible consiste en establecer prioridad absoluta a los primarios en el uso del espectro. Esto es, en caso de que un primario necesite un cierto ancho de banda y no exista capacidad suficiente en el sistema, al menos un secundario debe ser desalojado para ceder los recursos al primario. En este contexto, las comunicaciones de los secundarios pueden

ser abruptamente interrumpidas generándoles cierto perjuicio. Es entonces que resulta necesario desarrollar los mecanismos adecuados para mantener el cumplimiento de calidad de servicio necesario, en particular para aplicaciones con requerimientos exigentes, tanto para los usuarios primarios como para los secundarios.

Sumado a lo anterior, el Internet de las Cosas (IoT) dibuja un futuro de miles de millones de dispositivos interconectados. Concretamente, en 2022 se prevé que existan en todo el mundo 29.000 millones de dispositivos conectados según el último Mobility Report de Ericsson (Junio 2017). En escenarios de este tipo, los modelos y algoritmos más usados para el análisis de redes muchas veces resultan inaplicables. Esto trae otro desafío: lograr comprender el comportamiento de estas redes cuando la cantidad de usuarios y la cantidad de conexiones es inmensamente grande. Esta tesis es una contribución en esta dirección.

Con lo anterior en mente, en esta tesis se destacan cuatro grandes áreas de trabajo que se resumen a continuación. Considerando un número finito pero grande de recursos para compartir entre usuarios primarios y secundarios, y considerando el esquema de prioridad absoluta para las comunicaciones de los primarios, a lo largo de la tesis se aplican modelos de límites fluidos para analizar y caracterizar el comportamiento de la asignación de espectro en un sistema de redes radio cognitivas. A partir del análisis y la caracterización se aborda el problema de garantizar ciertos niveles de calidad de servicio a los usuarios secundarios tratando de utilizar de forma inteligente el espectro radioeléctrico disponible. En particular, se proponen criterios prácticos para reducir la probabilidad de interrupción de conexión de los secundarios.

En la tesis se analiza la siguiente pregunta: ¿cómo incentivar a los usuarios primarios a participar en este modelo? En otras palabras, ¿cómo motivarlos para que cedan sus bandas (por las que generalmente han pagado grandes sumas de dinero) a los usuarios secundarios? Un modelo razonable es que los secundarios paguen al operador primario por la utilización del espectro. Por otro lado, bajo la consigna de prioridad absoluta de las comunicaciones primarias, surge otra pregunta: ¿qué hacer cuándo se tiene que abortar abruptamente la comunicación de un secundario siendo que este ya pagó por el recurso? Contestando a esto último, en la literatura se observó que una opción razonable es reembolsar al secundario afectado (provocando un costo para el operador primario). Dicho lo anterior, resulta natural la aplicación de un control de admisión de secundarios de forma de que el operador primario no se vea afectado económicamente, al contrario, logre obtener algún beneficio por la participación en el mecanismo de espectro compartido. Bajo esta temática, se trabaja bajo dos enfoques. Por un lado se continúa el análisis realizado con modelos fluidos incorporando el aspecto económico. Y por el otro, se modela el problema utilizando procesos de decisión Markovianos. En ambos casos, el problema abordado consiste en encontrar y caracterizar la política de admisión de usuarios secundarios que maximice la ganancia del operador primario. En el estudio de procesos Markovianos, una vez caracterizado el sistema, se utiliza dicho análisis para optimizar algoritmos de programación dinámica utilizados para la resolución de este tipo de problemas (ej: Policy Iterator) y por otro lado, como contribución del enfoque de límite fluido se presenta una metodología que permite obtener una estimación de la política óptima basada en la resolución de ecuaciones diferenciales sencillas.

Complementando el trabajo realizado y de forma de darle completitud al estudio de

las posibilidades que las redes radio cognitivas ofrecen se integran a los modelos anteriores aspectos geométricos como por ejemplo: la distribución de usuarios primarios y secundarios en el espacio, modelos de propagación, etc. Por este motivo, se incorpora al modelado herramientas de geometría aleatoria. En este sentido se trabaja en responder las siguientes preguntas: ¿qué posibilidades brindan las redes cognitivas desde el punto de vista de los usuarios secundarios considerando re-utilización espacial de frecuencias?, ¿cómo se ven afectadas las comunicaciones de los primarios debido a la interferencia causada por los secundarios? En este aspecto se dan los primeros pasos en un modelado y análisis de un sistema de redes cognitivas considerando varios canales y re-asignación espacial. Se determinan distintas métricas de desempeño que contribuyen a responder las preguntas mencionadas.

Debido a la alta experiencia del grupo ARTES¹ en el modelado y análisis de grafos aleatorios y de herramientas del tipo límite fluido, se trabaja en un modelo de asignación de espectro donde las características de la red son abstraídas a un grafo. En particular, los nodos del grafo representan a los usuarios primarios y secundarios; y las aristas definen que aquellos nodos que tienen una en común no pueden transmitir simultáneamente. Con este modelado, trabajando con un caso particular de grafos aleatorios (aquellos definidos por la distribución de grados), se logran resultados más generales que con el enfoque de geometría aleatoria debido a que estos últimos tienen hipótesis muy fuertes requeridas para la obtención de expresiones analíticas tratables de las métricas deseadas.

Es importante resaltar que todos los resultados y las contribuciones de la tesis son verificados mediante simulaciones en diversos escenarios.

Palabras Claves:

Procesos de decisión Markovianos, límites fluidos, geometría aleatoria, grafos aleatorios, asignación dinámica del espectro, redes radio cognitivas.

¹<https://iie.fing.edu.uy/investigacion/grupos/artes/en/home/>

This page was intentionally left blank.

Contents

Acta de Defensa	i
Acknowledgements	vii
Abstract	xi
Resumen	xiii
1 Introduction	1
1.1 Context and motivation	1
1.2 Summary and contributions	3
1.2.1 Part I: Spectrum resource assignment: a paid sharing approach based on secondary users admission control	3
1.2.2 Part II: Spectrum resource assignment: user interactions and geo- metric aspects in cognitive radio networks	5
1.3 Structure of the document	6
I Spectrum resource assignment: a paid sharing approach based on secondary users admission control	9
2 Introduction to Part I	11
3 Markov decision process based models	13
3.1 Markov decision processes	14
3.1.1 Definitions and notation	14
3.1.2 Discounted infinite horizon models	15
3.2 Related work	19
3.3 Model description	19
3.4 Analysis and characterization of optimal admission control policies	22
3.4.1 Uniformization and dynamic programming formulation	22
3.4.2 Optimal control policies analysis and characterization	25
3.5 Alternative version of MPI Algorithm	28
3.5.1 Modified Policy Iteration algorithm	28
3.5.2 Modification of “policy improvement step”	30
3.5.3 Modification of “policy evaluation step”	31

Contents

3.5.4	Linear approximation of MPI when $b_1 = b_2 = 1$	34
3.5.5	Linear approximation of MPI	35
3.6	Simulated experiments and results	38
3.6.1	Performance tests of <i>newMPI</i>	38
3.6.2	Performance tests of <i>linMPI</i>	39
3.7	Conclusions	41
4	Fluid Limits Approximation	43
4.1	Preliminaries and motivation	43
4.1.1	Discontinuous drift	45
4.2	Related work	46
4.3	Fluid analysis of the dynamic of the spectrum sharing mechanism	46
4.3.1	Spectrum sharing without SU's admission control	48
4.3.2	Spectrum sharing with SU's admission control	53
4.4	Fluid analysis of the paid sharing approach	57
4.4.1	Multidemand system in the limit	57
4.4.2	Optimization problem formulation	60
4.4.3	Simulated experiments and results	61
4.5	Fluid analysis and QoS for secondary users	65
4.5.1	Possible criteria and actions	66
4.6	Conclusions	71
5	Conclusions of Part I	73
 II Spectrum resource assignment: user interactions and geometric aspects in cognitive radio networks		75
6	Introduction to Part II	77
7	A stochastic geometry analysis of multichannel CR network	79
7.1	Introduction	79
7.2	Related work	80
7.3	Problem formulation	81
7.4	Performance metrics estimation of particular case: two frequency bands and a random sensing mechanism	84
7.4.1	MAP of secondary users - MAP_s	84
7.4.2	COP of primary users - COP_p	85
7.4.3	COP of secondary users - COP_s	86
7.4.4	Simulation results	86
7.5	Performance metrics estimation of the general case	90
7.5.1	MAP of secondary users - MAP_s	90
7.5.2	COP of primary users - COP_p	91
7.5.3	COP of secondary users - COP_s	92
7.6	Conclusions	92

8	Capacity analysis using random graphs	93
8.1	Introduction	93
8.2	Context and assumptions	94
8.3	Random graphs and configuration algorithm	95
8.3.1	Preliminaries and motivation	95
8.3.2	Configuration model	96
8.3.3	Markov process and fluid limit	98
8.4	Simulated experiments and results	104
8.5	Comparison with spatial models	106
8.5.1	An approximation of the medium access probability using a stochastic geometry analysis	106
8.5.2	Numerical examples	108
8.6	Conclusions	115
9	Conclusions of Part II	117
III	General conclusions and future work	119
10	General conclusions and perspectives	121
	Appendices	123
A	Stochastic geometry essentials	123
A.1	Definitions	123
A.1.1	Point process	123
A.1.2	Laplace functional	124
A.1.3	Palm distribution	125
A.1.4	Campbell's formula	125
A.1.5	Marked point process	125
A.2	Poisson point process	125
A.3	Shot-noise	126
A.3.1	Additive Shot-noise	126
A.3.2	Extremal Shot-noise	127
B	Proposition proofs of Chapter 2	129
B.1	Proof of Proposition 1	129
B.2	Proof of Proposition 2	131
B.3	Proof of Proposition 3	132
B.4	Proof of Proposition 4	134
C	Stochastic Geometry proofs	137
C.1	Proof of Proposition 10	137
C.2	Proof of Proposition 11	140

Contents

D Proposition proofs of Chapter 8	143
D.1 A Proof of Theorem 2	143
D.2 A Proof of Theorem 4	145
References	147

Chapter 1

Introduction

1.1 Context and motivation

During the last two decades we have seen an explosive development of wireless networks which is reflected on the widely extended use of wireless technologies in our everyday lives (e.g. mobile phones, sensors, laptops). Consequently the demand for electromagnetic spectrum has increased to unprecedented levels resulting in the spectrum scarcity problem. This is evident by a glance at the National Telecommunications and Information Administration's frequency allocation chart¹, which reveals that almost all frequency bands have been assigned. In spite of this, spectrum utilization measurements have shown that licensed bands (except for radio frequencies for both 3G and 4G) are vastly underutilized while unlicensed bands are too crowded [1–5]. The significant underutilization occurs even in densely populated urban areas. Therefore, it is vital to move forward with a means for better utilization of the spectrum.

The new era of communications will be dominated by 5G (fifth-generation of mobile networks). Industrial and academic communities are defining the key requirements, technical specifications and also developing the correspondent 5G standards. These efforts are reflected by the number of publications and conferences in this area, see for example the recent articles [6–8] and the references therein. 5G is not just limited to mobile broadband, it is envisaged to support a diverse variety of use cases which can be divided into three categories: enhanced mobile broadband, ultra-reliable and low latency communications, and massive machine type communications. It is expected that 5G connections will appear on the scene in 2020 and will grow more than a thousand percent from 2.3 million in 2020 to over 25 million in 2021 [9]. With this in mind, how to optimize the spectrum capacity becomes a key ingredient in 5G system design.

In this regard, Cognitive Radio represents an attractive candidate, especially for 5G networks [7, 10–14]. The concept of Cognitive Radio (CR) is not new, it was first introduced by Mitola in his PhD thesis [15]. CR represents a promising technology which, based on dynamic spectrum access, strives at solving the important problems that we mentioned before: spectrum underutilization and spectrum scarcity. The importance of wireless networks today has shifted the attention and efforts of many researchers all over

¹https://www.ntia.doc.gov/files/ntia/publications/january_2016_spectrum_wall_chart.pdf

Chapter 1. Introduction

the world towards the study of CR networks (see for example [16–20]). Also, it has attracted the interest of industrial communities resulting in several approved standards (IEEE 802.22 [21], 802.11af [22], 802.16h [23], 802.19.4 [24] and 802.15.4m [25]) and the development of software defined radio (SDR) platforms which seems to be the most suitable technology to support CRs [26, 27].

In this paradigm we can identify two classes of users: primary and secondary. Primary users (PUs) or licensed users are those for which a certain portion of the spectrum has been assigned to (often in the form of a paid contract). The main advantage of the licensing approach is that the licensee completely controls its assigned spectrum, and can thus unilaterally manage interference between its users and hence their quality of service. Secondary users (SUs) or unlicensed users are devices which are capable of detecting unused licensed bands and adapt their transmission parameters for using them. The key requirement in this context is that the PUs ought to be as little affected as possible by the presence of SUs. In the ideal case, PUs would use the network without being affected at all by SUs, which will in turn make use of whatever resources are left available. This dynamic spectrum assignment (DSA), although a rather large number of solutions already exist in the literature, is still one of the main challenges in the design of CR due to the requirement of “peaceful” coexistence of both types of users.

There are roughly two different approaches for dynamic spectrum sharing: paid-sharing or free-sharing [20, 28–30]. Free-sharing spectrum is also known as opportunistic spectrum access. In this context, a SU has to monitor licensed bands and opportunistically transmit (without payments) whenever no primary signal is detected. There is no motivation for PUs to participate in this process because they do not obtain any benefit from it. However, it could be an impulse for regulators in order to improve the spectrum usage. On the other hand, another approach is considering paid-sharing models, where unoccupied channels are assigned to SUs which have to pay to the correspondent PU’s Service Provider (SP) for the spectrum utilization. The paid-sharing models have drawn more attention recently because they can provide an economic incentive to the SP and/or to its PUs. PU’s charge and SU’s payments are vital to the PUs-SUs interactions: PUs are motivated to share their own underutilized licensed resource and SUs are persuaded to wisely use the PU’s spectrum avoiding an aggressive usage. One of the main question that motivates our work is: how to encourage the spectrum sharing behavior of primary users? In this context, paid-sharing methods seem to be the most suitable. We thus focus on this kind of mechanisms in the first part of the thesis.

As we mentioned, while CR is one of the most discussed topics in contemporary spectrum management, there are still many issues and challenges to be solved, even more when we think in large random networks (e.g. V2V (vehicle to vehicle), M2M (machine to machine) and the whole range of IoT topologies). It is known that wireless networks are fundamentally limited by the intensity of the received signals and by users interference. These quantities depend on many aspects like: the spatial location of the users, users mobility, channel models, fading, etc. In order to explore in depth the possibilities offered by cognitive radio to improve the effectiveness of spectrum utilization, in the second part of the thesis we analyze a cognitive system using stochastic geometry and random graphs to model interactions between nodes considering large random networks. In particular we propose a framework for network capacity analysis.

1.2. Summary and contributions

The thesis is divided in two main parts, each one dedicated on different but complementary topics. En each part we analyze the following research questions:

Part I: Which models are most appropriate to represent a spectrum assignment mechanism in CRs? Which models can reflect economic interactions between PUs and SUs? Which control policies a primary service provider must apply in order to obtain the maximum possible profit from SUs? Is it possible to estimate those policies using deterministic models? How admission control mechanisms can be used to protect SUs communications?

Part II: How to estimate the portion of spectrum “wasted” by PUs and which may be leveraged by SUs? When or how can cognitive techniques be applied? Once applied, how much value can be captured? Are PUs communications severely affected by the presence of SUs? Is it possible to estimate the degradation of PU’s communications when they participate in a CR scenario?

With that inspiration in mind, in the following section we detail the different problems addressed in each part of the thesis and we summarize the main contributions.

1.2 Summary and contributions

1.2.1 Part I: Spectrum resource assignment: a paid sharing approach based on secondary users admission control

Spectrum regulatory bodies such as the Federal Communications Commission (FCC²) in the United States, the European Telecommunications Standards Institute (ETSI³) in Europe, or the Unidad Reguladora de Servicios de Telecomunicaciones (URSEC⁴) in Uruguay, have always allocated spectral frequency blocks for specific uses and assigned licenses for these blocks to specific groups or companies. Generally, they use an auction system to sell the rights (licenses) to transmit signals over specific bands. In this traditional static assignments, the licensee for each band has generally an exclusive use of the band. The scarcity in some frequency bands, while others are unused, opens the door for a more dynamic system where that exclusive use disappears. Since its introduction, the idea of cognitive radio has evoked much enthusiasm about its possibilities to improve spectral efficiency with a dynamic spectrum assignment.

As we explain in the previous section, an effective collaboration is achieved when the spectrum sharing behavior of primary service providers is encouraged. In this context, paid-sharing methods (i.e. where SUs pay for spectrum utilization) seem to be most suitable. There are different proposals to implement paid spectrum sharing techniques. These can be grouped into two big classes: dynamic spectrum auctions [31–33] and admission control mechanisms [34–36]. Generally, the aim of all the approaches is to maximize the revenue of the primary service provider (SP). While much research has been recently

²<https://www.fcc.gov/>

³<http://www.etsi.org/>

⁴<https://www.ursec.gub.uy/>

Chapter 1. Introduction

dedicated to paid spectrum sharing methods, most of the works have mainly focused on auction processes based on conventional spectrum auctions, which is not always consistent with the original intention of dynamic spectrum sharing. In this context admission control policies might play a key role. There is no doubt that admission control strategies and pricing rules [37, 38] are strongly related. Prices, SU's demand and admission control boundaries are correlated variables because SU's behavior is sensitive to spectrum utility (costs and benefits) and QoS guarantees. Another challenge in these mechanisms is what to do when a PU needs a channel and there are not enough free channels to satisfy its demand. Some works permit SU's interference over PU's communications and in this context SUs pay the corresponding interference cost to the PUs [39, 40]. Other studies assume a channel reservation scheme only for PUs [33]. On the other hand, fewer works contemplate preemptive situations [34] implying a preemption cost for the primary SP. This last alternative of termination model is already defined by FCC in a different scenario (Block D at 700 MHz), therefore, it would represent a natural way to implement that situation.

Keeping this in mind, the focus of our analysis is a paid spectrum sharing method based on admission control decisions over SUs. In particular, in the first part of the thesis we consider a scenario without spatial reuse of channels where if a PU arrives and does not find enough free channels in the system, at least one of the SUs will be deallocated immediately. In other words, a preemptive system is considered where some SUs communications will be aborted whenever a PU needs certain amount of bandwidth and the system has an insufficient number of free bands. In addition, we assume that the affected SUs (the ones that are deallocated before their services are finished) will be reimbursed, implying some cost for the PUs service provider (SP). We address the problem of maximizing the total expected discounted revenue of the SP over an infinite horizon. That is to say, the goal is to find the optimal admission control policy a SP must apply in order to obtain the maximum possible profit from SUs. We look for a solution capable of optimally balancing a fast calculation, low computational cost and a robust performance.

For the formulation of the problem we start using a continuous time Markov Decision Process (MDP) where the objective function we seek to maximize is defined as the expected discounted reward obtained by a primary SP. This Markovian structure allows us to analyze its asymptotic behavior by means of a simpler deterministic approximation: the fluid limit (see for example [41, 42] where there are examples of control queueing problems analyzed through a fluid approximation). Then, we complement the analysis introducing a fluid approximation of the stochastic control problem. The problem formulation addressed in this part of the thesis is much more general than a cognitive radio network analysis, since it can also model many other economic scenarios of dynamic control of queueing systems which consider two different classes of users (or services), one with strict priority, and contemplate preemptive situations with reimbursement, admission control decisions and multi-resource assignment. To the best of our knowledge, this general admission control problem has not been deeply explored yet in the literature (see Chapters 3 and 4 where we discuss in detail the most relevant works related to control queueing system).

On the one hand, an important contribution of this part of the thesis is the analysis and characterization of this general asymmetric queueing system and its application to the par-

1.2. Summary and contributions

ticular context of cognitive radio networks where PUs and SUs represent the two classes. We use dynamic programming and other techniques such as sample-path analysis to make a complete study of the properties of the optimal admission control policies. Not only is the analysis the main contribution, but also we propose many alternatives to improve the dynamic programming algorithms performance based on the system characterization. On the other hand, another contributions of this part consists in the definition and analysis of a fluid model of the MDP. Based on the deterministic approximation we develop a methodology in order to obtain an estimation of the optimal admission control boundary. The methodology combines fast calculation with a robust performance. We also perform a comparison between the approximation presented here with the optimal one. As a further contribution, we use the fluid approximation so as to define some practical criteria that can be used to improve the mean spectrum utilization with the commitment of providing to SUs a satisfactory grade of service and a small interruption probability.

1.2.2 Part II: Spectrum resource assignment: user interactions and geometric aspects in cognitive radio networks

The second part of this thesis is dedicated to another approach of resource assignment problem in cognitive radio networks. In wireless networks, a cognitive user can take advantage of either the time (when a primary user is not transmitting), the frequency (when a primary user is transmitting at a different frequency band), or the space (when a primary user is far away). In the first part of the thesis we have been concentrated on time-frequency holes, in this part we address the complete problem incorporating the space variable.

In this context, a wireless network can be viewed as a collection of users located in an area where there are a large amount of concurrent transmissions. The idea here is to integrate into the model: user interactions, interference, channel characteristics, user mobility, spatial reuse of frequency bands and geometric aspects. Then, we address a depth network capacity analysis based on two of the most powerful mathematical and analytical tools for the modeling, analysis and design of wireless networks with random topologies: random graphs and stochastic geometry. These tools had been applied to different network paradigms, see for example some relevant previous works in [43–48].

In this part of the thesis, we consider two large wireless networks, one composed by PUs and the other by SUs. We first introduce a probabilistic model based on a stochastic geometry approach. We focus on those scenarios where more than one band is available, a natural situation in CR networks. Quite surprisingly, and to the best of our knowledge, such scenario has not been deeply explored yet in the literature. In particular, we focus our study in the two main performance metrics: medium access probability (MAP) and coverage probability (COP). The former is the probability that a user gets access to a channel band. Due to the interference, not every transmission attempt is successful. In this sense, COP measures this success probability. We complement the analysis with the proposal of a methodology, based on configuration models for random graphs, to estimate the medium access probability of secondary users. In particular we present an analytic approximation of the MAP based on ordinary differential equations. We perform simulations to illustrate the accuracy of our results and we also make a performance comparison between our

estimation and one obtained by a stochastic geometry approach. We demonstrate the versatility of our technique, including also simulations in real scenarios of primary network deployments.

1.3 Structure of the document

The next four chapters constitute the first part of the thesis, concerning the study of a spectrum paid-sharing mechanism. Chapter 2 is devoted to set the problem and an introduction of our economic model. In Chapter 3, based on paper [J2], we define the Markov Decision Process (MDP) and we explain our analysis and characterization of the optimal admission policies. We finish the chapter with a discussion about how to integrate this characterization into the best known dynamic programming algorithms in order to improve their performance (e.g. reducing its running time). Chapter 4, which is based on papers [CP1,CP2,J3,J4], derives a fluid model of the MDP defined in Chapter 3. Through a deterministic approximation, we also develop a methodology to obtain an estimation of the optimal admission control boundary. The methodology combines fast calculation with a robust performance. We also describe the asymptotic distribution related with the fluid limit. We demonstrate that this distribution strongly depends on the fixed points of the deterministic approximation, and we find, depending on the parameters of the model, gaussian and non-gaussian asymptotic distributions. We present some criteria that can be used in order to improve the mean spectrum utilization while ensuring a small interruption probability to secondary communications. We perform simulations to illustrate the accuracy of all the results. Finally, we make some first conclusions in Chapter 5.

The second part of the thesis starts in Chapter 6. This chapter covers the presentation of the problem and a brief literature review introducing the nomenclature used along the chapters. It also includes the definition of the performance metrics handled in this part of the thesis. Then, Chapter 7 describes a probabilistic model based on a stochastic geometry approach to analyze CR networks on scenarios where more than one band is available (i.e. multichannel environment). This is a generalization of the framework proposed in [49]. We evaluate our proposal through simulations. In Chapter 8 we propose a methodology, based on configuration models for random graphs, to estimate the medium access probability of secondary users. We perform simulations to illustrate the accuracy of our results and by the end of this chapter, we present the comparative analysis between our estimation and an analogous one obtained by a stochastic geometry approach. The principal conclusions of this part of the thesis are summarized in Chapter 9. The contents of these chapters are based on the paper [CP3] and the article [J1].

In order to close the thesis, in Chapter 10 the general conclusions of this work are presented and future prospects are discussed as well.

List of publications

International Conference Papers

- CP1** C. Rattaro, L. Aspirot and P. Belzarena, “Analysis and characterization of dynamic spectrum sharing in Cognitive Radio Networks,” International Wireless Communications and Mobile Computing Conference (IWCMC), Dubrovnik, 2015, pp. 166-171. doi: 10.1109/IWCMC.2015.7289076
- CP2** C. Rattaro and P. Belzarena. “Cognitive Radio Networks: Analysis of a Paid-Sharing Approach based on a Fluid Model.” In Proceedings of the 2016 workshop on Fostering Latin-American Research in Data Communication Networks (LAN-COMM ’16). ACM, New York, NY, USA, 40-42. DOI: <https://doi.org/10.1145/2940116.2940120>
- CP3** C. Rattaro, P. Bermolen, F. Larroca, and P. Belzarena. “A Stochastic Geometry Analysis of Multichannel Cognitive Radio Networks.” In Proceedings of the 9th Latin America Networking Conference (LANC ’16). ACM, New York, NY, USA, 32-38. DOI: <https://doi.org/10.1145/2998373.2998450>

Journal Articles

- J1** C. Rattaro, F. Larroca, P. Bermolen, P. Belzarena, “Estimating the medium access probability in large cognitive radio networks”, Ad Hoc Networks, Volume 63, 2017, Pages 1-13, ISSN 1570-8705, <http://dx.doi.org/10.1016/j.adhoc.2017.05.003>.
- J2** C. Rattaro and P. Belzarena, “Cognitive Radio Networks: Analysis of a Paid-Sharing Approach based on Admission Control Decisions”, Preprint submitted in Jan 2017 to Wireless Personal Communications (Springer). Under review.
- J3** C. Rattaro, P. Bermolen and P. Belzarena, “Multi-resource allocation: Analysis of a paid spectrum sharing approach based on fluid models”, Preprint submitted in Sep 2017 to IEEE Transactions on Cognitive Communications and Networking. Under review.
- J4** C. Rattaro, L. Aspirot, E. Mordecki and P. Belzarena, “QoS provision in a dynamic channel allocation based on admission control decisions”, Preprint submitted in Dec 2017 to Queueing Systems (Springer). Under review.

This page was intentionally left blank.

Part I

Spectrum resource assignment: a paid sharing approach based on secondary users admission control

Chapter 2

Introduction to Part I

The widely extended use of wireless technologies in our everyday lives, together with the prediction that the mobile data traffic will increase 7-fold between 2016 and 2021 [9], have shifted the attention and efforts of many researchers all over the world towards the study of Cognitive Radio networks (see for example [16–19]). Cognitive Radio have emerged in last decades as a solution for two problems: spectrum underutilization and spectrum scarcity. The main idea is to manage the radio spectrum more efficiently, where secondary users (SUs) are allowed to exploit the spectrum holes in primary user's (PUs) frequency bands. The design of an efficient and fair spectrum sharing mechanism is then crucial.

There are two ways to acquire the spectrum holes: free or paid. Free acquisition can be done through spectrum sensing or free access to geo-location data base. On the other hand, a paid acquisition is a bit tricky because it involves, in addition to the previous ones, economic aspects. The main question that motivates the first part of the thesis is: how to encourage the spectrum sharing behavior of primary users? A possible answer is to consider a scenario where SUs pay to the primary service provider for its spectrum utilization. With this in mind, the focus of our analysis is a special paid spectrum sharing method.

Remembering that PUs have legacy rights on the usage of a specific part of the spectrum, in order to emphasize the importance of PUs, we model the PUs as the higher priority users whereas the SUs are the lower priority ones. We consider a mechanism that allows SUs in the system when there is unused capacity and aborts some SUs communications whenever a PU needs service and there is insufficient free capacity. In this sense, other questions that motivates this work are: which models are most appropriate to represent the paid spectrum assignment mechanism together with the preemptive dynamic? and what happens when a SU is abruptly deallocated? A possible approach to deal with these issues is to consider reimbursements and admission control decisions over SUs. That is to say, the affected SUs (the ones which communications are aborted before finish) are reimbursed implying a punishment for the SP. We have a control problem where the goal is to find the best admission control policy in order to maximize the SP profit.

We address the optimization problem with two different approaches: using Markov Decision Processes and using fluid limits. In Chapter 3 we start modeling the optimal revenue problem as a continuous time Markov Decision Process (MDP) where the ar-

Chapter 2. Introduction to Part I

rivals of each class are independent Poisson processes and the service durations are also independent and exponentially distributed. We further assume that each class of user demands b_i resources, with b_i integer (i.e. a PU requests b_1 channel bands and a SU requests b_2). The set of available actions of the MDP are reflected in the admission control policy: accept or reject a new SU. In this part we concentrate on analyzing and characterizing the optimal admission control policies and also on exploiting their properties to design computational procedures for efficiently finding the parameters of such policies. Then, in order to simplify the problem, both for payment and for reimbursement we assume static prices.

This part continues in Chapter 4 where we derive a fluid model of the MDP. We developed a computationally efficient way to find an estimation of the admission control boundary based on the solution of an ordinary differential equation system. In addition, we exploit the fluid model to perform a quality of service (QoS) analysis. In particular we concentrate in the QoS of SUs. Through extensive simulations we have validated all the proposals and the obtained results.

General conclusions are discussed in a separate chapter at the end of this part (see Chapter 5).

Chapter 3

Markov decision process based models

This chapter bears on the design and analysis of a paid spectrum sharing mechanism based on admission control decisions over SUs. We consider a scenario without spatial reuse of channels where if a PU arrives and does not find enough free channels in the system, at least one of the SUs will be deallocated immediately. We model the optimal revenue problem as an infinite-horizon Markov Decision Process (MDP).

The main contribution of this part of the thesis is the analysis and characterization of a general dynamic control of an asymmetric queueing system. We use dynamic programming and other techniques such as sample-path analysis to make a complete study of the properties of the optimal admission control policy. Moreover, we go further and we propose many alternatives to improve the dynamic programming algorithms performance based on the system characterization. The proposed alternatives decrease the computational complexity as well as the large running time introduced by methods like Value Iteration and Policy Iteration (commonly used to solve MDP problems). In particular, as one of the results of this work, we have obtained a customized version of Modified Policy Iteration Algorithm (MPI [50]) which combines faster calculation with a robust performance.

This chapter provides a quick review on the basic components of Markov decision processes (MDPs) in Section 3.1. This thesis deals with discounted infinite horizon problems, then the revision is focused in that particular subclass of MDPs. The rest of the chapter is structured as follows. Some related works are introduced in Section 3.2. In Section 3.3 we describe our economic model of dynamic spectrum sharing in cognitive radio networks. We introduce most of the notation, in particular, we define the components of our Markov decision process. The chapter continues in Section 3.4 where we explain the analysis and characterization of the optimal admission policy. In Section 3.5 we propose changes to the Modified Policy Iteration algorithm in order to significantly decrease its running time. In Section 3.6 we include some numerical examples to validate our results. Finally, the general conclusions are presented in Chapter 5.

3.1 Markov decision processes

We start this section introducing the principal definitions which are essential to understanding the rest of the chapter. Finally, we present the main results for discounted infinite horizon problems.

As described in depth in Puterman [50] and Bertsekas [51], a MDP consists in five elements: decision epochs, states, actions, transitions probabilities and rewards. The goal is to choose a sequence of actions which cause the system to perform optimally with respect to some criterion. For instance, an optimal criterion could be “maximizing the expected total discounted reward”.

3.1.1 Definitions and notation

Decision epoch: points in time at which decisions are made. Let T be the set of decision epochs and its components will be denoted by t . T may be classified in two ways, discrete or continuous. For example, in discrete time problems $T = \{0, 1, \dots, N\}$. When N is finite, the decision problem will be called a *finite horizon* problem, otherwise it will be called an *infinite horizon* problem. An analogous situation we have in continuous time models.

State set: the set of all possible values of dynamic information relevant to the decision process. Let S be the state space and each state will be denoted by s .

Action set: for any state $s \in S$, A_s represents the action space, the set of possible actions that the decision maker (or controller) can take at state s .

Rewards and Transitions probabilities: as a result of choosing $a \in A_s$ in state s at decision epoch t

- the decision maker receives a reward $r_t(s, a)$, and
- the system state at the next decision epoch is determined by the probability distribution $p_t(\cdot|s, a)$.

The reward may be positive or negative (an income or a cost). In a stationary problem the rewards and transitions probabilities do not vary from decision epoch to decision epoch, i.e. $r_t(s, a) = r(s, a)$ and $p_t(\cdot|s, a) = p(\cdot|s, a)$.

Decision rule: A decision rule d_t prescribes a procedure for action selection in each state at a specified decision epoch. We can classify decision rules as history dependent and randomized (HR), history dependent and deterministic (HD), Markovian and randomized (MR), and Markovian and deterministic (MD).

Policy: A policy or strategy (π) specifies the decision rule to be used at all decision epoch. It is a sequence of decision rules $\pi = \{d_0, d_1, \dots\}$. Let Π be the policy space. In particular we denote:

- Π^{HR} : the set of history dependent and randomized policies,
- Π^{HD} : the set of history dependent and deterministic policies,

3.1. Markov decision processes

- Π^{MR} : the set of Markovian and randomized policies, and
- Π^{MD} the set of Markovian and deterministic policies.

We refer to the collection of objects $\{T, S, A_s, p_t(\cdot|s, a), r_t(s, a)\}$ as a MDP.

Given these ingredients, the basic question is how to choose the actions on a dynamic basis such that the objective function reaches a maximum value.

Please note that under a fixed policy, the process behaves according to a Markov chain.

3.1.2 Discounted infinite horizon models

In this thesis we study infinite-horizon MDPs with the expected total discounted reward optimality criterion. The infinite number of decision epochs is a mathematical formalization and constitutes a reasonable approximation for problems involving finite but very large number of stages. In many contexts, a specific finite time horizon is not easily specified, and the infinite horizon formulation is more natural. On the other hand, the role of the discount rate is to emphasize short-term rewards vs. rewards that might be obtained in a more distant future. If the reward is financial (like in our formulation), immediate rewards may earn more interest than delayed rewards. Discounted models, besides a mathematical convenience or an economic argument, play a central role because numerous computational algorithms are available for their solution. More importantly, in these cases (discounted infinite-horizon) optimal policies are typically stationary, which offer great simplicity for practical implementations.

Firstly, we will describe discrete time models. A further analysis on this models will enable to understand the continuous case. Finally, we will explain how to convert continuous MDPs to an equivalent model (more easily analyzed process) through *uniformization*.

Some remarks are listed below:

1. In the next subsections we assume stationary and bounded rewards $r(s, a) < M < \infty$, stationary transitions probabilities $p(\cdot|s, a)$, a discount factor β ($0 \leq \beta < 1$) and a finite (or countable) discrete state space S . As we will see in the next sections, these hypothesis are satisfied in our problem formulation.
2. In [50], the authors show that in infinite horizon models, given any history-dependent policy and starting state, there exists a randomized Markov policy with the same expected total discounted reward. Then, we need not consider history dependent policies, it suffices to consider Π^{MR} policies (see details in Theorem 5.5.3.b in [50]).
3. Let $\mathbb{R}^{|S|}$ denote the space of functions $V : S \rightarrow \mathbb{R}$, the set of bounded real-valued functions on S . Note that V can be viewed as an $|S|$ -dimensional vector (being $|S|$ the size of the state space).

Chapter 3. Markov decision process based models

Discrete time MDPs

The expected total discounted reward $V^\pi(s) \in \mathbb{R}^{|S|}$ of a policy $\pi = \{d_0, d_1, \dots\} \in \Pi^{MR}$, when rewards are bounded, is defined by

$$V^\pi(s) = E^\pi \left[\sum_{t=0}^{\infty} \beta^t r(s_t, d_t(s_t)) \mid s_0 = s \right]. \quad (3.1)$$

We say that a policy π^* is discount optimal for fixed β whenever

$$V^{\pi^*}(s) \geq V^\pi(s) \forall s \in S, \forall \pi \in \Pi^{MR}. \quad (3.2)$$

The value $V^*(s) \in \mathbb{R}^{|S|}$ of a β -discounted MDP is defined by

$$V^*(s) = \sup_{\pi \in \Pi^{MR}} V^\pi(s), \forall s \in S. \quad (3.3)$$

Then, we say that a discount optimal policy exists whenever

$$V^*(s) = V^{\pi^*}(s), \forall s \in S. \quad (3.4)$$

Dynamic Programming (DP) [51] is a mathematical technique based on the *principle of optimality* that provides the basis for the iterative algorithms. It can be used in a variety of contexts and it is usually based on a recursive formula and initial states. When π is stationary¹ ($d_t = d \forall t$), the finite-horizon optimality equations may be expressed as:

$$V_t(s) = \sup_{a \in A_s} \left\{ r(s, a) + \sum_{j \in S} \beta p(j|s, a) V_{t-1}(j) \right\}. \quad (3.5)$$

Please note that $V_t(s)$ is the maximum total expected reward starting in state s with t decision epochs remaining.

Passing to the limit ($t \rightarrow \infty$) on both sides, we have the Bellman equation:

$$V^*(s) = \sup_{a \in A_s} \left\{ r(s, a) + \sum_{j \in S} \beta p(j|s, a) V^*(j) \right\}. \quad (3.6)$$

Please note that the value of the MDP (Eq. (3.3)) satisfies the optimality equation.

If A_s is finite, which is the case of our work, we can replace “sup” by “max”, then, the optimality equation becomes:

$$V^*(s) = \max_{a \in A_s} \left\{ r(s, a) + \sum_{j \in S} \beta p(j|s, a) V^*(j) \right\}, \quad (3.7)$$

where the action a defines policy π^* such that

$$\pi^* = \arg \max_{a \in A_s} \left\{ r(s, a) + \sum_{j \in S} \beta p(j|s, a) V^*(j) \right\}. \quad (3.8)$$

¹We restrict attention to stationary policies from the perspective of implementation.

3.1. Markov decision processes

In [50] the authors show that the optimality equation has a unique solution $V^*(s)$ in $\mathbb{R}^{|S|}$ in discounted infinite horizon problems when the rewards are bounded and S is countable (or finite). They also prove that when S is discrete and A_s is finite for each $s \in S$, then there is always an optimal deterministic stationary policy $\pi^* \in \Pi^{MD}$ such that $V^*(s) = V^{\pi^*}(s), \forall s \in S$ (Proposition 6.2.1 in [50]). Therefore, in this thesis we focus on deterministic Markovian decision rules, where such rules are functions $d_t : S \rightarrow A_s$ which specify the action choice when the system occupies state s at the decision epoch t . The term deterministic is because it chooses an action with certainty. As we mentioned before, in this thesis we analyze stationary policies, that means $d_t = d \forall t$, which are essential to the theory of infinite horizon MDPs (in this context we indistinctly use d or π).

Bellman equation is typically very hard to solve (direct solution only possible for small MDPs), in this sense Value and Policy iteration are the most widely used and best understood algorithms for solving discounted Markov decision problems.

Continuous time MDPs

Some applications, like queueing control, are more naturally modeled by allowing action choice at random times in $[0, \infty)$. Such problems can be modeled using continuous-time models. Semi-Markov decision processes (SMDPs) a class of continuous-time models, generalize discrete-time Markov decision processes (DTMDPs) by allowing state changes to occur randomly over continuous time and letting or requiring decisions to be taken whenever the system state changes.

Continuous-time Markov decision processes (CTMDPs) constitute a special type of SMDPs in which the transition times between decisions are exponentially distributed and actions are taken at every transition.

In CTMDPs we have an analogous equation to (3.1) but in continuous time:

$$V^\pi(s) = E^\pi \left[\int_0^\infty r(s(t), a(t)) e^{-\alpha t} dt \right], \quad (3.9)$$

where α is defined as the discount rate. Later on we will discuss the relation between α and β for equivalent systems.

The most common way to analyze CTMDPs consists in converting the model to a more easily analyzed process through *uniformization*. Next, we briefly describe the most important aspect of this procedure, for more details we suggest [52] and Chap. 11 of [50].

Uniformization

Let X be a CTMDP with transition probabilities $p(\cdot|s, a)$. Let $\gamma(s, a)$ denote the transition rate out of state s when action a is taken, that is: $p(j|s, a) = \frac{\gamma(j|s, a)}{\gamma(s, a)}$. Let Γ be the uniformization constant; Γ is chosen such that $\Gamma > \gamma(s, a), \forall s \in S, \forall a \in A_s$. Then, we can define the transition probabilities of the “uniformed process” \hat{X} as:

$$\hat{p}(j|s, a) = \frac{\gamma(j|s, a)}{\Gamma} = \frac{\gamma(s, a)}{\Gamma} p(j|s, a), \forall j \in S, j \neq s,$$

$$\hat{p}(s|s, a) = 1 - \frac{\gamma(s, a)}{\Gamma}.$$

Chapter 3. Markov decision process based models

By creating fictitious transitions (from a state to itself), we are creating a stochastically equivalent process in which the transitions occur more often. We refer to \hat{X} as the uniformization of X because it has an identical (or uniform) sojourn time distribution in every state. Please note that the two processes are equal in distribution so they have the same probabilistic behavior.

Now, consider the infinite-horizon discounted CTMDP with the following reward function:

$$\lim_{n \rightarrow \infty} E \left[\int_0^{t_n} e^{-\alpha t} r(s(t), a(t)) dt \right], \quad (3.10)$$

where t_n represents the time of n -th transition.

Generally, $r(s(t), a(t))$ consists in two parts: a lump reward $L(s(t), a(t))$ and a continuous accumulated reward $C(s(t), a(t))$. We define s_n and a_n , the state and the action selected in time t_n (i.e. $a_n = a(t_n)$ and $s_n = s(t_n)$). By definition, the state of CTMDP does not change between decision epochs, therefore, the value function of a given policy π is

$$V^\pi(s) = E^\pi \left[\sum_{n=0}^{\infty} e^{-\alpha t_n} L(s_n, a_n) \right] + E^\pi \left[\sum_{n=0}^{\infty} e^{-\alpha t_n} C(s_n, a_n) \int_0^{\tau_{n+1}} e^{-\alpha t} dt \right],$$

where $\tau_{n+1} = t_{n+1} - t_n$.

Working with the previous equation and considering the uniform version of the CTMDP (i.e. the sojourn times at each state $\tau_n, n = 1, \dots$ are assumed to be independent and identically distributed with exponential distribution of parameter Γ and independent of the state s_n), we can obtain:

$$V^\pi(s) = \sum_{n=0}^{\infty} E^\pi [L(s_n, a_n)] \beta^n + \sum_{n=0}^{\infty} E^\pi [C(s_n, a_n)] \frac{1}{\alpha + \Gamma} \beta^n, \quad (3.11)$$

where $\beta = \frac{\Gamma}{\Gamma + \alpha}$. Therefore:

$$V^\pi(s) = E^\pi \left[\sum_{n=0}^{\infty} \beta^n \left(L(s_n, a_n) + \frac{C(s_n, a_n)}{\alpha + \Gamma} \right) \right], \quad (3.12)$$

which has the same form we saw for DTMDP (see Eq. (3.1)). Therefore, it can be solved using conventional DTMDP solution techniques such as value iteration, policy iteration, or linear programming. The corresponding DP equations are then:

$$V_n(s) = \max_{a \in A_s} \left\{ \frac{C(s, a)}{\alpha + \Gamma} + L(s, a) + \sum_{j \in S} \beta \hat{p}(j|s, a) (l(s, a, j) + V_{n-1}(j)) \right\}. \quad (3.13)$$

Please note that we have included in the above expression $l(s, a, j)$ which represents the lump reward (or cost) incurred in each state transition.

Before presenting in detail our model and results, some related works are discussed in the next section.

3.2 Related work

In this chapter the focus of our analysis is a paid spectrum sharing method based on admission control decisions over SUs. We assume a multi-resource allocation problem with preemption where PUs have strict priority over SUs; when a PU arrives to the system and there are not enough free channels to accommodate the new user, one or more SUs will be deallocated. The affected SUs will then be reimbursed, implying some cost for the PUs service provider (SP).

There are some previous works which contribute in the direction of dynamic control of queueing systems and preemption [42, 53–55], being the most representative examples [34, 56]. In particular, in [34] the authors assume that call durations are exponentially distributed with identical means for both classes. This hypothesis strongly simplifies the problem (it can be analyzed as a one-dimensional Markov Chain) and does not represent the most common real scenarios in cognitive radio networks. The vast majority of the CR related articles consider different primary and secondary services (e.g. Internet access provided using White Space frequency bands [57]), then the natural situation is to model them with different arrival and service rates as we do in this work. Although in [56] the authors consider preemptive situations and different service rates, they study a symmetric problem where all users (of both classes) have to pay for the spectrum utilization and the service abrupt termination can occur in both classes. Due to these characteristics, their analysis is not totally applicable to our context.

On the other hand, an important hypothesis assumed in the cited articles is to consider that all users (PUs and SUs) request the same amount of bandwidth. Even more, they assume “one user with one channel” representing a particular scenario of the problem. This hypothesis implies that the preemption only occurs when the system is full of users. More general, in our scenario the preemption occurs when there are not enough free resources to satisfy primary demand.

Finally, but not less important, our work differs from [34, 56] in the payment mechanism. In the preceding works, the reward per user accepted in the system is collected after the SU leaves the system with successful completion of service implying that a SU could earn money without paying anything. In our case, the reward is collected at the moment when the user is accepted in the system (independent if it successfully completes its service or it is deallocated). Even though our formulation is more complex, we consider it more realistic.

In the next section we present our dynamic spectrum allocation problem modeled as a CTMDP. Motivated by the results of the previous section, our first aim will be to convert our continuous time MDP to an uniform sojourn time version.

3.3 Model description

Let us begin by describing our working scenario and introducing the notation, definitions and hypothesis. We assume that the spectrum is divided into C non-overlapping orthogonal channels to be distributed between PUs and SUs. In a LTE system (for example), we can consider a channel as one resource block.

Let $X(t)$ and $Y(t)$ be the number of PUs and SUs in the system at time t respectively

Chapter 3. Markov decision process based models

(in order to simplify the notation, we indistinctly use X and $X(t)$, as well as Y and $Y(t)$). Let λ_1 and μ_1 be the arrival and departure rates for PUs respectively (independent Poisson arrivals and exponentially distributed service times). In the same way, λ_2 and μ_2 represent the arrival and departure rates for SUs. We assume that each PU demands b_1 resources, and analogously each SU requires b_2 channel bands to its transmission. Even more general, our analysis can be generalized to different primary (and/or secondary) demands working with more than two classes of users.

We consider a paid-sharing mechanism where SUs pay to the primary SP for its spectrum utilization. We assume static prices similar to the ones considered in previous articles [34, 36, 58]. Let $R > 0$ be the reward collected for each band when a SU is allowed to exploit the PU's resource (i.e. b_2R is the collected reward when a SU is accepted in the system). We also consider a preemptive system where PUs have strict priority over SUs. This means that SUs can be removed from the system if there is insufficient free capacity when a PU arrives. In this model, these affected SUs will be reimbursed with b_2K ($K > 0$), implying a punishment for the SP. We take into account a discount rate $\alpha > 0$, that is, the rewards and costs at time t are scaled by a factor $e^{-\alpha t}$.

According to the definitions of Section 3.1, the process $(X(t), Y(t))$ results then in a Continuous Time MDP (CTMDP) with state space $S = \{(X, Y) : 0 \leq b_1X + b_2Y \leq C\}$ with the following optimal criterion

$$\max_{\pi \in \Pi^{MD}} E^\pi \left[\int_0^\infty r(s(t), a(t)) e^{-\alpha t} dt \right], \quad (3.14)$$

where $r(s(t), a(t))$ is a lump reward (or cost) related with R , K , b_1 and b_2 ; and $s(t)$ and $a(t)$ are the state and the admission control action in the decision epoch t . Please note that according to the explanation of Section 3.1, due to the fact that the rewards are bounded, S is discrete and the set of actions is finite (accept or reject a new user), in the maximization problem we have considered $\pi \in \Pi^{MD}$. Therefore, the objective is to find the optimal stationary policy $\pi^* \in \Pi^{MD}$ that defines the admission control action $a(s) \in A_s$ in each state $s \in S$ maximizing the primary SP's revenue.

In this thesis we consider a deterministic admission control mechanism, then the action space is $A_s = \{0, 1\}$ or $A_s = \{0\}$, depending on $s \in S$, where action 0 corresponds to refusing a SU's arrival and 1 to admitting it (please note that for all $s = (X, Y)$ such that $b_1X + b_2Y > C - b_2$ the action space is $A_s = \{0\}$ since the system has an insufficient number of free bands).

According to the previous definitions, the transition rates $q((X, Y), (X', Y'))$ between states (X, Y) and (X', Y') of the CTMDP are:

- $q((X, Y), (X + 1, Y)) = \lambda_1$ if $b_1X + b_2Y \leq C - b_1$,
- $q((X, Y), (X - 1, Y)) = \mu_1X$,
- $q((X, Y), (X, Y + 1)) = a(X, Y)\lambda_2$ if $b_1X + b_2Y \leq C$,
- $q((X, Y), (X, Y - 1)) = \mu_2Y$,
- $q((X, Y), (X + 1, Y - Z)) = \lambda_1$ if $C - b_1 < b_1X + b_2Y \leq C$ and $Y \geq Z$ (preemption),

3.3. Model description

where $a(X, Y) \in A_s$ represents the admission control decision in each state and Z represents the number of preempted SUs:

$$Z = \left\lfloor \frac{b_1 X + b_2 Y - C + b_1}{b_2} + \mathbb{1}_{\{\text{mod}\{b_1 X + b_2 Y - C + b_1, b_2\} \neq 0\}} \right\rfloor. \quad (3.15)$$

In Eq. (3.15) $\lfloor \cdot \rfloor$ represents the integer part and we use $\text{mod}\{m, n\}$ operator to get the remainder after division of m by n . Please note that if the system is in state $s = (X, Y)$ and a SU arrives, only if $a(X, Y) = 1$ will it enter to the system.

In Figure 3.1 we represent the state space S and the different economic zones in the particular case where there is no admission control (i.e. $a(X, Y) = 1 \forall (X, Y)$ such that $b_1 X + b_2 Y \leq C - b_2$). For the illustration we assume that $b_1 > b_2$. In this case, we can divide the state space S in three economic zones:

- Zone I: SUs are accepted into the system and for each SU that enters, the SP earns $b_2 R$.
- Zone II: the SP has to pay $Z b_2 K$ when a PU arrives (if $Y \geq Z$). In addition, it also earns $b_2 R$ for each SU accepted.
- Zone III: the SP only pays $Z b_2 K$ (if $Y \geq Z$) for each PU arrived.

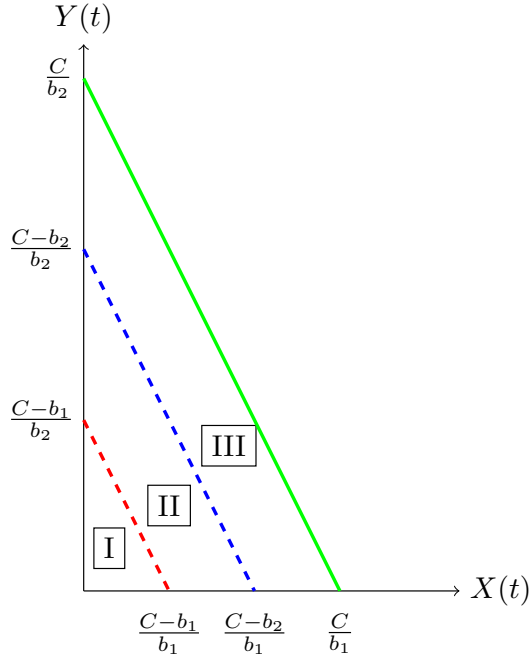


Figure 3.1: The state space is $S = \{(X, Y) : 0 \leq b_1 X + b_2 Y \leq C\}$, then $0 \leq X \leq \frac{C}{b_1}$ and $0 \leq Y \leq \frac{C}{b_2}$. If $a(X, Y) = 1 \forall (X, Y) : b_1 X + b_2 Y \leq C - b_2$ and $b_1 < b_2$, we can divide the state space in three economic zones: I, II and III. The condition $Y \geq Z$ is not represented.

Please note the scalability of our model. For instance, if we considered different primary demands (e.g. b_1, b'_1), the MDP would have a greater dimensional state space

(e.g. $S = \{(X, X', Y) : 0 \leq b_1 X + b'_1 X' + b_2 Y \leq C\}$, where X and X' would represent the number of PUs that use b_1 and b'_1 bands respectively). The same consideration is valid if we considered different secondary bandwidth requirements. We will not deal with that generalization here, but our results can be extended for this more general case.

Summing up, the objective is to find π^* , that is to say, the rule that maps each system state s to its optimal action a , in each decision epoch, maximizing SP's benefits. Using *uniformization* technique, as was explained in Section 3.1, we can develop an equivalent model with uniform transition rates and thus the algorithms for discrete time MDP can be used directly. In the next section, we will discuss how to solve our optimization problem starting with the uniformization. In particular, we will characterize some properties of the optimal admission control policy. Using this characterization we will propose some alternatives to improve the performance of the most commonly used dynamic programming algorithms.

3.4 Analysis and characterization of optimal admission control policies

In this section we focus on the characterization of the optimal admission control policy in the described context. To this end, we formulate the problem using Dynamic Programming and after that, we prove some properties of the control policies.

3.4.1 Uniformization and dynamic programming formulation

Let Γ be the uniformization constant. It is chosen, as was explained in Section 3.1, such that $\Gamma > \gamma(s, a) = \sum_{j \in S} \gamma(j|s, a)$, $\forall s \in S$, then in this work we choose $\Gamma = \lambda_1 + \lambda_2 + C(\frac{\mu_1}{b_1} + \frac{\mu_2}{b_2})$. Figure 3.2 shows a generic state $s = (X, Y)$ when the uniformization has been performed. In particular it is a state where the system has enough free capacity for primary demand ($b_1 X + b_2 Y \leq C - b_1$).

As we explain in Section 3.1 the equivalent discrete time MDP (DTMDP) has a discount factor $\beta = \frac{\Gamma}{\Gamma + \alpha}$ ($0 < \beta < 1$) and the optimization problem can be written as:

$$V^*(s) = \max_{\pi \in \Pi^{MD}} E^\pi \left[\sum_{n=0}^{\infty} \beta^n r(s_n, a_n) | s_0 = s \right], \forall s \in S; \quad (3.16)$$

where:

- $V^*(s)$ is the maximal expected β -discounted reward for the system with initial state s ,
- Π^{MD} represents all the possible Markov deterministic policies,
- t_n is the time of n-th transition (n-decision epoch),
- $a_n = a(t_n)$ and $s_n = s(t_n)$, and

3.4. Analysis and characterization of optimal admission control policies

- $r(s_n, a_n) = l(s_n, a_n, s_{n+1})$ (a lump reward at the moment of the transition) such that

$$l(s_n, a_n, s_{n+1}) = \begin{cases} b_2 R & \text{if } a_n = 1, s_n = (X_n, Y_n) \text{ and } s_{n+1} = (X_n, Y_n + 1), \\ -Z_n b_2 K & \text{if } s_n = (X_n, Y_n) \text{ and } s_{n+1} = (X_n + 1, Y_n - Z_n), \\ 0 & \text{otherwise.} \end{cases} \quad (3.17)$$

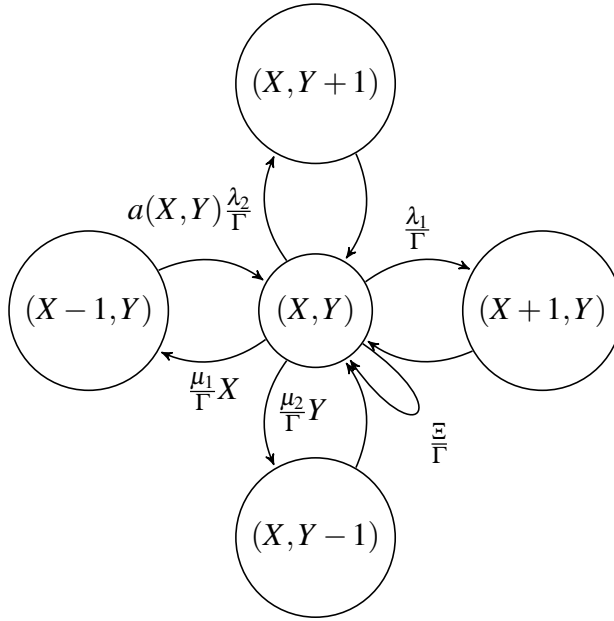


Figure 3.2: Discrete time model for a generic state (X, Y) obtained after the uniformization process. Observe that this transformation implies “fictitious” transitions from a state to itself, $\Xi = C(\frac{\mu_1}{b_1} + \frac{\mu_2}{b_2}) - \mu_1 X - \mu_2 Y + \lambda_2(1 - a(X, Y))$.

Let $V_n(s)$ be the maximal expected discounted profit for the system starting in the state $s = (X, Y)$ when n observation points remain in the horizon. $V_n(s)$ is referred as the value function of state (X, Y) in n -steps. After the uniformization process is done, we are now able to formulate the problem using DP according to Eq. (3.13), in particular considering a stationary π :

$$V_n(s) = \max_{a \in A_s} \left\{ \sum_{j \in S} \beta \hat{p}(j|s, a) (l(s, a, j) + V_{n-1}(j)) \right\}, \quad (3.18)$$

where

$$\hat{p}(j|s, a) = \frac{\gamma(j|s, a)}{\Gamma}, \forall j \in S, j \neq s,$$

$$\hat{p}(s|s, a) = 1 - \frac{\gamma(s, a)}{\Gamma}.$$

Chapter 3. Markov decision process based models

Defining $\lambda'_i = \lambda_i/(\Gamma + \alpha)$ and analogously $\mu'_i = \mu_i/(\Gamma + \alpha)$, the corresponding DP equations are:

For $n = 0$:

$$V_0(X, Y) = 0,$$

For $n \geq 1$:

- if $b_1X + b_2Y \leq C - b_1$:

$$V_n(X, Y) = \lambda'_1 V_{n-1}(X+1, Y) + \lambda'_2 \max\{V_{n-1}(X, Y), V_{n-1}(X, Y+1) + b_2 R\} + \mu'_1 X V_{n-1}(X-1, Y) + \mu'_2 Y V_{n-1}(X, Y-1) + \left(C\left(\frac{\mu'_1}{b_1} + \frac{\mu'_2}{b_2}\right) - \mu'_1 X - \mu'_2 Y\right) V_{n-1}(X, Y),$$

- if $C - b_1 < b_1X + b_2Y \leq C - b_2$ and $Y \geq Z$:

$$V_n(X, Y) = \lambda'_1 (V_{n-1}(X+1, Y-Z) - Z b_2 K) + \lambda'_2 \max\{V_{n-1}(X, Y), V_{n-1}(X, Y+1) + b_2 R\} + \mu'_1 X V_{n-1}(X-1, Y) + \mu'_2 Y V_{n-1}(X, Y-1) + \left(C\left(\frac{\mu'_1}{b_1} + \frac{\mu'_2}{b_2}\right) - \mu'_1 X - \mu'_2 Y\right) V_{n-1}(X, Y),$$

- if $C - b_2 < b_1X + b_2Y \leq C$ and $Y \geq Z$:

$$V_n(X, Y) = \lambda'_1 (V_{n-1}(X+1, Y-Z) - Z b_2 K) + \lambda'_2 V_{n-1}(X, Y) + \mu'_1 X V_{n-1}(X-1, Y) + \mu'_2 Y V_{n-1}(X, Y-1) + \left(C\left(\frac{\mu'_1}{b_1} + \frac{\mu'_2}{b_2}\right) - \mu'_1 X - \mu'_2 Y\right) V_{n-1}(X, Y),$$

- if $b_1X + b_2Y = C$ and $b_1X = C$:

$$V_n(X, Y) = \lambda'_1 V_{n-1}(X, Y) + \lambda'_2 V_{n-1}(X, Y) - \frac{\mu'_1}{b_1} C V_{n-1}(X-1, Y) + \frac{\mu'_2}{b_2} C V_{n-1}(X, Y).$$

Please note that we have considered $b_1 \geq b_2$ in order to simplify the notation. As we can see, there are four different DP equations for $n \geq 1$. The first one represents the situation when there are enough idle channels in the system to satisfy primary demand. The second and the third equations are for the preemptive situations, and the last one is for the case when all the channels are used by PUs. Another observation is that the ‘‘fictitious’’ transitions do not affect the total reward of the system. Finally, it is important to remark that we can assume that the process terminates with probability $\alpha' = \alpha/(\Gamma + \alpha)$ and after that no more profits will be earned [50].

Passing to the limit ($n \rightarrow \infty$) in the DP formulation, we have the Bellman equations which characterize the values and optimal policies in infinite horizon models:

$$V^*(s) = \max_{a \in A_s} \left\{ \sum_{j \in S} \beta \hat{p}(j|s, a) (l(s, a, j) + V^*(j)) \right\}, \quad (3.19)$$

where π^* satisfies $V^{\pi^*}(s) = V^*(s)$, in other words:

$$\pi^* = \arg \max_{a \in A_s} \left\{ \sum_{j \in S} \beta \hat{p}(j|s, a) (l(s, a, j) + V^*(j)) \right\}. \quad (3.20)$$

3.4. Analysis and characterization of optimal admission control policies

As we explain at the beginning of the chapter, the best known practical algorithms for solving bellman equation are: Value Iteration (VI) and Policy Iteration (PI and its several modifications, i.e. Modified Policy Iteration (MPI)) [50]. In [59], there is a complete analysis of these techniques. The rate of convergence of both is strongly related with β (discount factor) and also with the total number of channels considered (C). It is important to highlight that if $\beta < 1$, all the iterative DP algorithms are guaranteed to converge [50].

In the following subsection we prove several results to characterize the optimal admission control policies for SUs that maximize the SP profit. This analysis will be used, as an example of application, to improve the performance of the mentioned DP algorithms.

3.4.2 Optimal control policies analysis and characterization

In this subsection the structure of the optimal policies is determined. We address the cases $K \geq R$ and $K < R$ separately. For $K \geq R$, we first prove monotonicity properties of $V^*(s)$, then we prove that the admission control boundary is a “switching curve” policy, and finally we demonstrate the concavity of the value function under certain conditions. These properties are analogous to the ones presented in [34, 42, 53, 56, 60] but based on our specific context. For the other case, when the SP’s punishment is less than the SU’s payments ($K < R$), we prove an evident result: the optimal policy is the one that always accepts SUs independently of the system parameters $\lambda_i, \mu_i, b_i, \beta$ and C . In the proofs we use induction and sample-path arguments [61] [62]. These techniques are used in most of the cited references in Section 3.2 in order to characterize the value function and the optimal policies in a variety of scenarios.

Proposition 1. $V_n(X, Y + 1) \leq V_n(X, Y), \forall (X, Y) : b_1 X + b_2(Y + 1) \leq C, \forall n.$

See Appendix B.1 for the proof of the general case ($b_1 \geq 1$ and $b_2 \geq 1$) using induction arguments on n . For better understanding this result, we explain here the proof using sample-path methods [63] for the particular case: $b_1 = b_2 = 1$. Please note that in this situation the preemption only occurs when the system is full of users.

Proof. Consider two processes on the same probabilistic space. Process 1 starting in the state (X, Y) and process 2 in $(X, Y + 1)$. We couple this two systems, by considering that all service and arrival times in one and the other are the same. Suppose the optimal policy of system 2 (π_2^*) is followed in both systems. Let $V_n^{\pi_2^*}(X, Y)$ and $V_n^{\pi_2^*}(X, Y + 1)$ be the value functions of system 1 and 2 using policy π_2^* respectively, so $V_n^{\pi_2^*}(X, Y + 1) = V_n(X, Y + 1)$.

Now since both processes use the same policy, as long as system 1 has one less user than system 2, then $V_n^{\pi_2^*}(X, Y) = V_n(X, Y + 1)$ (they see the same arrivals and departures, and, therefore the same rewards and costs). This situation could change only in the following critical case:

- Consider the first time the process 2 enters a state with the number of users equal to C and system 1 has exactly $C - 1$ users (this situation will never occur if the extra SU in system 2 leaves the system before the first time that system reaches C users). In this case, if a PU arrives, both systems must accept the new user. System 2 has to remove one of the SUs allocated, thus system 1 will have K more profit than

Chapter 3. Markov decision process based models

system 2. This implies that $V_n^{\pi_2^*}(X, Y) > V_n(X, Y + 1)$. After this point, the systems will be in the same state and therefore that difference will continue unchanged.

Finally, considering that the reward obtained in this way for system 1 will not be greater than its optimal reward ($V_n^{\pi_1^*}(X, Y) \leq V_n(X, Y)$), and examining that the initial state was arbitrary considered, the result follows. \square

As we have explained, we study the behavior of the system for all values of K and R . Then, Propositions 2, 3 and 4 are for the case where $K \geq R$, that is, when the reimbursement obtained by an affected SU is greater than its payment. This scenario plays a key role in motivating the SU's participation in the spectrum sharing (in particular, it is very important when the SU's service interruption causes a big damage affecting the QoS of their communications). On the other hand, Proposition 5 is for the complementary case ($R > K$). In this particular situation, if the objective is to maximize the SP's profit, we prove that the optimal policy is the one which defines $a(X, Y) = 1, \forall (X, Y)$ such that $b_1X + b_2Y \leq C - b_2$.

Proposition 2. *If $K \geq R$ and $\forall (X, Y) : b_1X + b_2(Y + 1) \leq C$, then*

$$V_n(X, Y + 1) - V_n(X, Y) \geq -b_2K \forall n.$$

The proof of this proposition can be found in Appendix B.2. As in the previous proposition, we present here the proof for the same particular case ($b_1 = b_2 = 1$) using sample-path arguments.

Proof. Considering system 1 starting in (X, Y) and system 2 in $(X, Y + 1)$. In this case, we assume that system 1 follows its optimal admission policy (π_1^*) and system 2 imitates all decisions of system 1 whenever it is feasible. When $X + Y + 1 = C$, we can identify two critical cases which may alter the difference between the profit of the systems.

In other words, when system 2 reaches C users:

- If a SU arrives, system 2 will reject it. System 1 can accept or reject, it will depend on its optimal policy π_1^* . If the SU is accepted in system 1, the inequality holds only if $K \geq R$. After that, the difference of the profit of both systems will not change because the systems will be in the same state. This implies that if $K \geq R$, then $V_n^{\pi_1^*}(X, Y + 1) - V_n(X, Y) \geq -K$.
- If a PU arrives, both systems have to accept it. System 2 will remove one of the secondary users paying K , so the equality holds. After that, the two will be coupled (they will be in the same state).

Due to the fact that $V_n^{\pi_1^*}(X, Y + 1) \leq V_n(X, Y + 1)$, the result is proved. \square

Proposition 3. *If $K \geq R$ and $\forall (X, Y) : b_1(X + 1) + b_2(Y + 1) \leq C$, then*

$$V_n(X + 1, Y + 1) - V_n(X + 1, Y) \leq V_n(X, Y + 1) - V_n(X, Y) \forall n.$$

Proof. The detailed proof can be found in appendix B.3 and it is based on induction arguments on n . \square

3.4. Analysis and characterization of optimal admission control policies

Intuitively, we can interpret this last result as: we expect that it should be more difficult to accept SUs when there are more PUs in the system. This gives us the idea that the admission control (AC) boundary that maximize the SP profit is a “switching curve” (see Definition 1).

Definition 1. *Switching curve: For every y , we define a level $l(y)$ such that when the system is in state (x, y) decision 1 is taken if and only if $x \leq l(y)$ and 0 otherwise. The mapping y with $l(y)$ is called a “switching curve”.*

In the particular case that $\mu_1 = \mu_2$ and $b_1 = b_2 = 1$ (see the analysis in [34]) we have $V_n(X+1, Y+1) - V_n(X+1, Y) = V_n(X, Y+2) - V_n(X, Y+1)$, $\forall (X, Y) : X+Y+2 \leq C$, $\forall n$. This means that the admission control boundary only depends on the number of busy channels at the system.

In what follows, we prove the concavity property of the value function. This would lead to monotony of the thresholds. In addition, the concavity will play a key role in the proposals of the next section.

Proposition 4. *If $K \geq R$ and $\forall (X, Y) : b_1X + b_2(Y+2) \leq C$, then*

$$V_n(X, Y) - V_n(X, Y+1) \leq V_n(X, Y+1) - V_n(X, Y+2) \quad \forall n.$$

Proof. The proof can be found in appendix B.4. In the same way as in the previous case, the proof is based on induction arguments. \square

Proposition 5. *If $R > K$ and π is an admission control policy which satisfies that*

$$a(X, Y) = \begin{cases} 1 & \text{if } b_1X + b_2Y \leq C - b_2, \\ 0 & \text{otherwise,} \end{cases} \quad (3.21)$$

then π is the optimal one ($\pi = \pi^$).*

Proof. Using sample-path arguments in the particular case $b_1 = b_2 = 1$, we will prove that $V_n^\pi(X, Y) \geq V_n^{\pi'}(X, Y) \quad \forall \pi' \neq \pi$ (where π' represents a policy that has at least one state $(X, Y) / X+Y < C$ where $a(X, Y) = 0$).

Considering two systems starting in the same state (X, Y) , system 1 following policy π and system 2 policy π' . It is easy to note that the number of PUs will always be the same in both systems, they could only differ in the number of SUs. If system 2 is in state (X', Y') then system 1 will be in state $(X', Y' + W)$, $W \geq 0$.

As long as a preemptive situation does not occur, $V_n^\pi(X, Y) - V_n^{\pi'}(X, Y) \geq WR$. On the other hand, considering the times when the process 1 enters a state with the number of users equal to C ($X' + Y' + W = C$), in this situation the worst-case is when at least W successive PU arrivals occur (that implies WK of punishment for the SP). Then, $V_n^\pi(X, Y) - V_n^{\pi'}(X, Y) \geq W(R - K)$. Due to the fact that $R \geq K$ and the initial state was arbitrary considered, the desired result is proved.

It is possible to prove the general case ($b_1 \neq b_2$) using induction arguments in the same way as in previous propositions. \square

So far, previous propositions were proven by working on the finite horizon discounted profit to be able to use induction on n . When the state space is countable, the action space is finite, and the absolute values of rewards and costs are bounded, all conclusions apply to the infinite horizon β -discounted case by taking the limit $n \rightarrow \infty$. Even more, given that rewards and transition probabilities are stationary, we consider bounded rewards and finite state space; and we restrict the attention to stationary policies; then the results of the analysis and characterization of the optimal policy and of the value function are also valid for the average reward problem (i.e. when $\beta \rightarrow 1$).

3.5 Alternative version of MPI Algorithm

In this section we propose a possible application of the system characterization of previous section. In particular, we use those properties in order to improve the performance of a specific DP algorithm: the Modified Policy Iteration (MPI). The goal is to present a new version of that algorithm such that the running time drastically decreases respect to the original one when is applied to our problem. We consider the case of $K \geq R$ because in the other case the optimal control is already known.

First of all, we introduce the DP algorithm that we have used and optimized. In the rest of the section, we present some alternatives in order to modify the algorithm including the knowledge of the characterization of Section 3.4. As a result we obtain two customized versions of MPI: *newMPI* and *linMPI*. Also we present an extended version of [34] that can be used when $b_1 = b_2 = 1$ and $\mu_1 \neq \mu_2$.

3.5.1 Modified Policy Iteration algorithm

As aforementioned, Value Iteration (VI) and Policy Iteration (PI) are the most usual DP mechanisms for solving MDPs. This subsection begins by presenting these algorithms in their most basic form.

The following value iteration algorithm finds a stationary ε -optimal policy within a finite number of iterations.

Value iteration

1. Select $V_0(s) \forall s$, specify $\varepsilon > 0$, and set $n = 0$.
2. For each $s \in S$, compute $V_{n+1}(s)$ by

$$V_{n+1}(s) = \max_{a \in A_s} \left\{ \sum_{j \in S} \beta \hat{p}(j|s, a) (l(s, a, j) + V_n(j)) \right\}.$$

3. If $\|V_{n+1} - V_n\| < \varepsilon \frac{(1-\beta)}{2\beta}$ go to step 4, otherwise $n = n + 1$ and go to step 2.
4. For each $s \in S$, we have:

$$\pi_\varepsilon \in \arg \max_{a \in A_s} \left\{ \sum_{j \in S} \beta \hat{p}(j|s, a) (l(s, a, j) + V_n(j)) \right\}$$

3.5. Alternative version of MPI Algorithm

and stop.

It is possible to demonstrate that V_n converges in norm to V^* , $\|V_{n+1} - V^*\| < \varepsilon/2$, and the stationary policy π_ε is ε -optimal.

Definition 2. *ε -optimal policy:* Let $V^*(i)$ be the maximum expected total discounted reward over an infinite horizon starting in state i . It is well known that V^* satisfies the Bellman equation. Then, a policy π is ε -optimal for $\varepsilon > 0$ if $\|V^\pi - V^*\| < \varepsilon$.

In practice, choosing ε small enough ensures that the algorithm stops with a policy that is very close to optimal.

On the other hand, the policy iteration algorithm manipulates the policy directly, rather than finding it indirectly via the optimal value function. It operates as follows:

Policy iteration

1. Set $n = 0$ and select an arbitrary decision rule π_0 .
2. Policy evaluation: solve the linear equations

$$V_n(s) = \sum_{j \in S} \beta \hat{p}(j|s, \pi_n(s))(l(s, \pi_n(s), j) + V_n(j)).$$

3. Policy improvement: Choose π_{n+1} to satisfy

$$\pi_{n+1} = \arg \max_{a \in A_s} \left\{ \sum_{j \in S} \beta \hat{p}(j|s, a)(l(s, a, j) + V_n(j)) \right\}.$$

4. If $\pi_{n+1} = \pi_n$ stop and $\pi^* = \pi_n$, otherwise $n = n + 1$, $\pi_n = \pi_{n+1}$ and go to step 2.

Policy iteration mainly applies to stationary infinite-horizon problems. When S is finite and for each $s \in S$, A_s is finite, then it is possible to demonstrate that policy iteration algorithm terminates in a finite number of iterations with a solution of the optimality equation and a discount optimal policy. Please note that when no improvements are possible, then the policy is guaranteed to be optimal.

Comparing PI with VI, the first one is desirable to be used in practice because of its finite-time convergence to the optimal policy. That is the main reason why in this work we have chosen PI.

Policy iteration mainly consists of two iteration steps: policy evaluation and policy improvement. The most tricky part is the ‘‘Policy Evaluation’’. It consists in solving a system of linear equations to calculate $V_n(s) \forall s \in S$ (considering a fixed policy). The most common method to work it out is the Gaussian elimination, but when you have a model with q states, this requires on the order of q^3 multiplications and divisions. So, for a large q (in our case q is related with C , b_1 and b_2), obtaining an exact value function for a specific policy might be computationally prohibitive.

There are many proposals for the implementation of this algorithm. In particular, in [50,64] the authors proposed the Modified Policy Iteration (MPI) algorithm to improve the

efficiency of PI when there is a large state space involved. In MPI the idea is to implement the “Policy Evaluation” step similar to the VI algorithm with the only difference that the value functions are computing for a fixed policy instead of computing the maximum of the value function for all possible actions in each state. As we mentioned before, VI finds a stationary policy that is ϵ -optimal within a finite number of iterations (ϵ is related with the stop criterion). Therefore, due to the fact that this implementation of MPI combines features of policy iteration and value iteration, the policy obtained is also ϵ -optimal.

Numerical results reported in [59, 64] suggest that MPI is more efficient than either value iteration or policy iteration in practice. Then, in this thesis we have worked with that MPI algorithm definition. However, depending of the number of system states, the running time of MPIs could also blow up to impractical levels. Table 3.2 shows the average running time of the MPI algorithm when applied to our problem for different system parameters. In the second column of the table it is shown the size of the state space $|S|$. Those large running times motivate us to work in improving the algorithm performance.

Table 3.1: Performance of MPI algorithm. All the measurements were taken on a i7 3770/16GB with execution times averaged over ten repetitions.

Parameters	$ S $	Running time
$C = 500, \lambda_1 = 200, \lambda_2 = 500, \mu_1 = 0.1, \mu_2 = 1, \alpha = 2, R = 1, K = 3, b_1 = 5, b_2 = 1$	25351	32267 seg
$C = 100, \lambda_1 = 200, \lambda_2 = 500, \mu_1 = 3, \mu_2 = 1, \alpha = 2, R = 1, K = 3, b_1 = 1, b_2 = 1$	5151	9045 seg
$C = 100, \lambda_1 = 200, \lambda_2 = 500, \mu_1 = 3, \mu_2 = 1, \alpha = 2, R = 1, K = 3, b_1 = 5, b_2 = 1$	1071	46 seg

Following we present some alternatives in order to modify the MPI algorithm using the knowledge of the previous section. One proposal is based on the fact that it is not necessary to consider all actions in each state while improving the policy. Another consists in picking a subset of states in order to apply the “policy evaluation step”. In addition, at the end of this section, we also present a way to modify the MPI to obtain a linear approximation of the optimal admission control boundary.

3.5.2 Modification of “policy improvement step”

We incorporate the information given in Props. 3 and 4 in order to reformulate “Policy Improvement” step of the MPI algorithm. In this Step the idea is to improve the policy at each state of the system, therefore the original MPI algorithm has to evaluate it in the whole state space. Our proposal consists in evaluating the policy improvement only in few states. In other words, the idea is to consider a subset of policies (i.e. the feasible policies). In the original MPI algorithm when is applied to our deterministic admission control context, the total number of policies to be considered is $\approx 2^q$ (letting q the total number of states and 2 is the maximum number of possible actions in a typical state).

3.5. Alternative version of MPI Algorithm

In our proposal we only consider the policies whose boundaries represent a “switching curve” verifying Props. 3 and 4.

According to Prop. 3, we can infer that:

$$\boxed{\text{if } a(X^+, Y^+) = 1 \text{ for a particular state } (X^+, Y^+), \text{ then } a(X, Y^+) = 1 \forall X < X^+ .}$$

In addition, please note that using Prop. 4, we can conclude that:

$$\boxed{\text{if } a(X^+, Y^+) = 0 \text{ for a particular state } (X^+, Y^+), \text{ then } a(X^+, Y) = 0 \forall Y > Y^+ .}$$

We present in Alg. 1 an alternative way to implement “Policy Improvement” step of MPI using the above explanation. In particular in Figure 3.3 we illustrate the system states where this particular step of the algorithm is evaluated. In the other states the policy is deduced.

Algorithm 1 Alternative Policy Improvement step

```

1: for  $Y := 0 : \lfloor C/b_2 \rfloor - 1$  do
2:   if  $(Y = 0)$  then
3:      $X := \lfloor C/b_1 \rfloor - 1;$ 
4:   else
5:      $X := X_b;$ 
6:   end if
7:    $\text{out} := \text{false};$ 
8:   while not out do
9:      $a(X, Y) := \arg \max_{a \in A_{(X, Y)}} \{ \sum_{j \in S} \beta \hat{p}(j|s, a) (l(s, a, j) + V_n(j)) \}$ 
10:    if  $(a(X, Y) = 1)$  then
11:       $\text{out} := \text{true}$ 
12:       $\forall X' < X$  SET  $a(X', Y) := 1$  (all the states  $(X', Y) : X' < X$  have the
        same admission control decision as state  $(X, Y)$ );
13:    else
14:       $X := X - 1;$ 
15:    end if
16:  end while
17:   $X_b := X;$ 
18: end for
19:  $\pi := \{a(X, Y), \forall (X, Y)\};$ 
20: return  $\pi_{n+1} = \pi$ 

```

3.5.3 Modification of “policy evaluation step”

In [50] there is a detailed demonstration of the non-necessity of determining the exact value function ($V_n(s)$) to identify an improved policy. The fundamental concept behind is to make a finite number of iterations in order to obtain an approximation of $V_n(s) \forall s \in S$. It represents the essential part of the MPI algorithm which differentiates it from PI. The

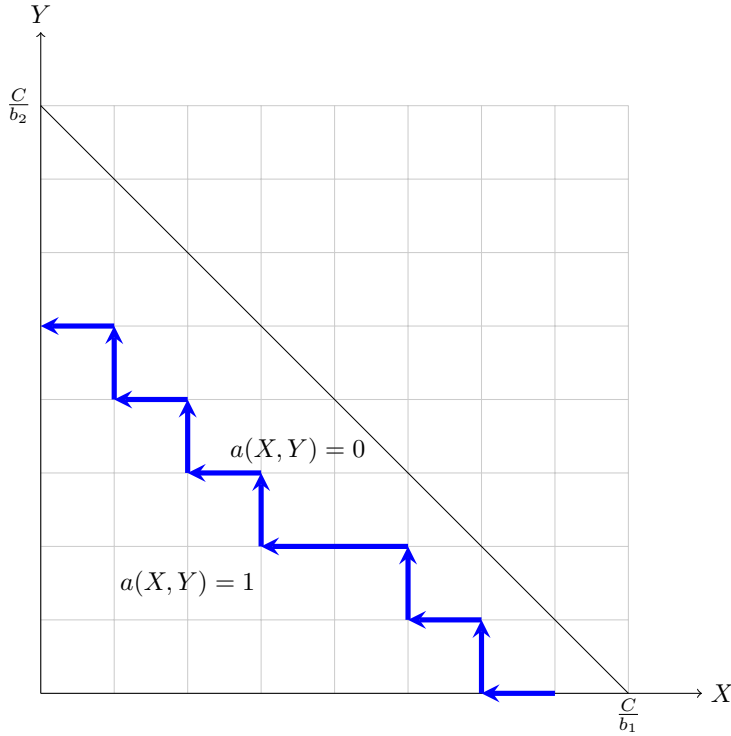


Figure 3.3: Illustration of alternative of Alg. 1: Policy Improvement step is evaluated only in the states located on the path of arrows.

convergence in this scenario is also proven in [50]. For a better understanding, a pseudo code of the “policy evaluation step” (from original MPI) is presented in Alg. 2. We have used it as a pattern to compare with our proposals.

Please note that the existence of the parameter m_n in Alg. 2 represents the main characteristic of the original “policy evaluation step” from MPI. It is proved that the algorithm converges for any order sequence $\{m_n\}$ and the rate of its convergence is related with $\{m_n\}$. In the numerical examples of Section 3.6 we have chosen a fixed value of $m_n = m, \forall n$ and it has remained unchanged in all the simulations (both in the original MPI and in the new proposals), then we can affirm that the comparative results of Section 3.6 are independent of m_n .

In this subsection (and also in Subsection. 3.5.5) we propose heuristic modifications to this step of the algorithm which are focused on reducing the number of system states that participate directly in “policy evaluation step”. With that in mind, we introduce into the algorithm the information that the value function is concave for a fixed value of PU (see Prop. 4). This property allows us to apply linear interpolation (when the difference $V_n(X, Y) - V_n(X, Y + 1)$ is small) reducing the computational complexity of the algorithm. The idea is to sacrifice the precision of the value determination without affecting the final result. In other words, the new value determination will be applied only on certain states ($S' \subseteq S$, including in S' the states where the difference $V_n(X, Y) - V_n(X, Y + 1)$ is higher) and for the others, it will be estimated using piecewise linear interpolation. In Alg. 3 a pseudo code of the explained alternative is presented. Please note that the policy

Algorithm 2 Original Policy evaluation Step (from MPI Algorithm)**Require:** $\varepsilon > 0, m_n, V_n, \pi_n$;

```

1:  $k := 0$ ;
2:  $u_n^k(s) := \max_{a \in A_s} \{ \sum_{j \in S} \beta \hat{p}(j|s, a)(l(s, a, j) + V_n(j)) \}$ ;
3: if ( $\|u_n^k - V_n\| < \varepsilon \frac{(1-\beta)}{2\beta}$ ) then
4:   MPI finishes and the result is  $\pi_n$ ;
5: else
6:   if ( $k = m_n$ ) then
7:     go to step 13;
8:   else
9:      $u_n^{k+1}(s) := \sum_{j \in S} \beta \hat{p}(j|s, a)(l(s, a, j) + u_n^k(j)), \forall s \in S$ ;
10:     $k := k + 1$ ;
11:    go to step 6;
12:   end if
13:    $V_{n+1} := u_n^{m_n}$ ;
14:   return  $V_{n+1}$ 
15: end if

```

evaluation is executed only in $s \in S'$.

It is important to highlight that the computational complexity of linear interpolation is one multiplication and two additions per sample of output. On the other hand, the evaluation of $u_n^{k+1} = \sum_{j \in S} \beta \hat{p}(j|s, a)(l(s, a, j) + u_n^k(j))$, in most of the states, implies: ten multiplications and seven additions (see the DP formulation of Subsection 3.4.1).

The question is how to chose the subset S' and how many elements include in it. Observing the DP formulation, it is easy to note that the value function of each state only depends on the value function (in the previous iteration) of its “neighbor states”. However, it is a recursive dependency because the value function of the neighbors of an specific state also depends on their neighbors’ functions and so on. In this context, we propose that the subset S' must include the states that are located near the admission control (AC) boundary and also their nearest neighbors. We do not know a priori where is going to be located the AC boundary, but, we can infer it by using the results of the next two subsections.

Therefore, in order to define the set S' we define two parameters (K^* and L) and we proceed in the following way:

- choose the parameters $K^* \in \mathbb{N}$ ($K^* < C$) and $L \in \mathbb{N}$ ($L \leq \frac{K^*/b_2(K^*/b_1+1)}{2}$),
- randomly choose a set of states $I = \{(X, Y) \text{ such that } b_1X + b_2Y < K^*\}$ and $|I| = L$,
- define $S' = \{I \cup \{(X, Y) : K^* \leq b_1X + b_2Y \leq C\}\}$.

The result of this proposal is sub-optimal and its performance will be associated with the parameters K^* and L . In particular, because of the concavity of $V_{nX}(Y)^2$, its piecewise linear estimation (the segments) will be always under the corresponding MPI’s value

² $V_{nX}(Y)$ is $V_n(X, Y)$ for fixed X .

Algorithm 3 Alternative Policy Evaluation Step**Require:** $\varepsilon > 0, m_n, V_n, \pi_n$

- 1: $k := 0$;
- 2: $u_n^k(s) := \max_{a \in A_s} \{r(s, a) + \sum_{j \in S} \beta p(j|s, a) V_n(j)\}$;
- 3: **if** ($\|u_n^k - V_n\| < \varepsilon \frac{(1-\beta)}{2\beta}$) **then**
- 4: MPI finishes and the result is π_n ;
- 5: **else**
- 6: **if** ($k = m_n$) **then**
- 7: go to step 14;
- 8: **else**
- 9: $u_n^{k+1}(s) := \sum_{j \in S} \beta \hat{p}(j|s, a)(l(s, a, j) + u_n^k(j)), \forall s \in S'$;
- 10: With the results of the previous step, use linear interpolation to estimate $u_n^{k+1}(s) \forall s \in S \setminus S'$;
- 11: $k := k + 1$;
- 12: go to step 6;
- 13: **end if**
- 14: $V_{n+1} := u_n^{m_n}$;
- 15: **return** V_{n+1}
- 16: **end if**

function. As a consequence, the admission boundary obtained by this modification will be more conservative than the original MPI's solution. It is important to remark that choosing appropriate values of K^* and L , the interpolation error could be as small as you want, therefore the results could be optimal (or nearly optimal).

Which are good options of these parameters? In the following we list some important considerations. The smaller is K^* , more accurate will be the value determination, but the running time will have a smaller impact in its reduction. On the other hand, for larger values of K^* , although the algorithm running time will decrease, the admission control boundary might be not optimal. The opposite effect occurs with L : if larger values of L are considered, more precision will be reached, but less impact in the running time. As a conclusion, the values of these new parameters are related with the system parameters ($\lambda_1, \lambda_2, \mu_1, \mu_2, b_1, b_2, R, K$ and β). The proposals of next subsections gives heuristic methods for K^* ; once K^* is chosen, an upper bound to L is implicitly determined.

As a result of using the proposals of Subsection 3.5.2 and 3.5.3 we have developed a new version of MPI called *newMPI*. In Section 3.6 we present some simulation experiments and a performance comparison between MPI and *newMPI*.

3.5.4 Linear approximation of MPI when $b_1 = b_2 = 1$

Based on [34], in this subsection we extend the work [34] to be applied to our problem in the particular case when $b_1 = b_2 = 1$ and $\mu_1 \neq \mu_2$. Another motivation is to propose a fast heuristic method for choosing the parameter K^* defined before. In other words, we want to know which area (i.e. which set of states) is most likely to contain the optimal AC

3.5. Alternative version of MPI Algorithm

border.

The authors in [34] studied a similar problem (preemption with reimbursement in a cognitive scenario) with different hypotheses: call durations are exponentially distributed with identical means ($\mu_1 = \mu_2 = \mu$), the reward per SU accepted is collected after the SU leaves the system with successful completion of its service, and each user demand is one channel, independently of the class ($b_1 = b_2 = 1$). According to the first hypothesis, they demonstrated that the optimal admission control decision only depends on the total number of occupied channels, in other words the admission control boundary is a line with equation $X + Y - T^* = 0$.

As a consequence, it is possible to use an unidimensional birth-death MDP with state space $S_{1d} = \{i \in \mathbb{N} | 0 \leq i \leq C\}$ to determine the optimal threshold (T^*). Adapting their model in order to satisfy our assumptions (in particular the difference with their second hypothesis) the problem is reduced to solve the next optimization problem:

$$\max_T \lambda_2 R \left(1 - \sum_{T \leq i \leq C} \pi_T(i) \right) - K \lambda_1 \pi_T(C) + K \lambda_1 E_b \left(\frac{\lambda_1}{\mu_1}, C \right) \quad (3.22)$$

where $\pi_T(i), 0 \leq i \leq C$ is the steady state probability with threshold T and $E_b(\frac{\lambda_1}{\mu_1}, C)$ corresponds to Erlang-B formula.

Due to the fact that the above formulation can be used only when the mean service time of both classes are identical, using the idea of [42] we propose to transform our general system to be in that particular context. Our proposal consists of obtaining a μ -scaled system with parameters $\lambda_1^s, \lambda_2^s, \mu, b_1, b_2, K$, and R , and after solving Eq. (3.22) an estimation of the admission control boundary is possible to obtain.

In particular, the μ -scaled system has the following parameters:

$$\mu_1^s = \mu_2^s = \mu, \lambda_1^s = \frac{\lambda_1 \mu}{\mu_1} \text{ and } \lambda_2^s = \frac{\lambda_2 \mu}{\mu_2}.$$

Observe that $\frac{\lambda_1^s}{\mu} = \frac{\lambda_1}{\mu_1}$ and $\frac{\lambda_2^s}{\mu} = \frac{\lambda_2}{\mu_2}$. Choosing $\mu = \mu_1$ in Figures 3.4 and 3.5 there are two simulated examples that show the optimal admission control boundary obtained using MPI and the line obtained applying the results of our adaptation of the model of [34] (Eq. (3.22)) to the μ -scaled version of our problem.

In both examples the threshold T^* gives an estimation of the location of the optimal boundary. In the case of Figure 3.5 the estimation is excellent. In the other case, the estimated AC boundary is nearly optimal. If more accurate is required, we can use this deterministic result as an input of the proposal of the previous subsection.

That is to say, this result can be used in order to choose an appropriate value of K^* to our proposal of *newMPI*. For instance, in Figure 3.4 being conservative a possible value of K^* is 10, while in the other one $K^* = 15$ can be a reasonable option. As we will see in Section 3.6, by adequate selection of the parameters K^* and L , *newMPI* obtains the optimal AC boundary.

3.5.5 Linear approximation of MPI

In order to continue improving the computational efficiency of the DP algorithm, we use the results of Prop. 3 and 4 to obtain another alternative version of Modified Policy

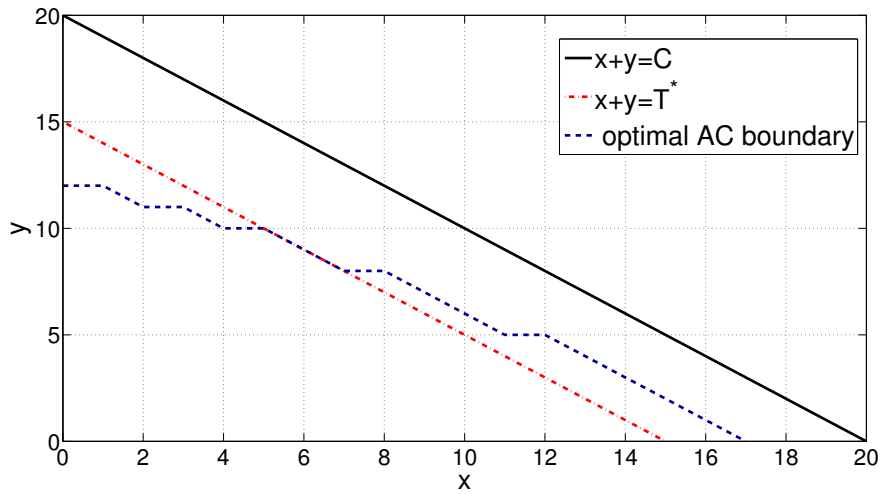


Figure 3.4: Performance comparison between Eq. (3.22) and the optimal AC boundary obtained by MPI. Parameters: $\lambda_1 = 20$, $\lambda_2 = 5$, $\mu_1 = 1$, $\mu_2 = 4$, $\mu = 1$, $b_1 = b_2 = 1$, $C = 20$, $R = 1$, $K = 10$.

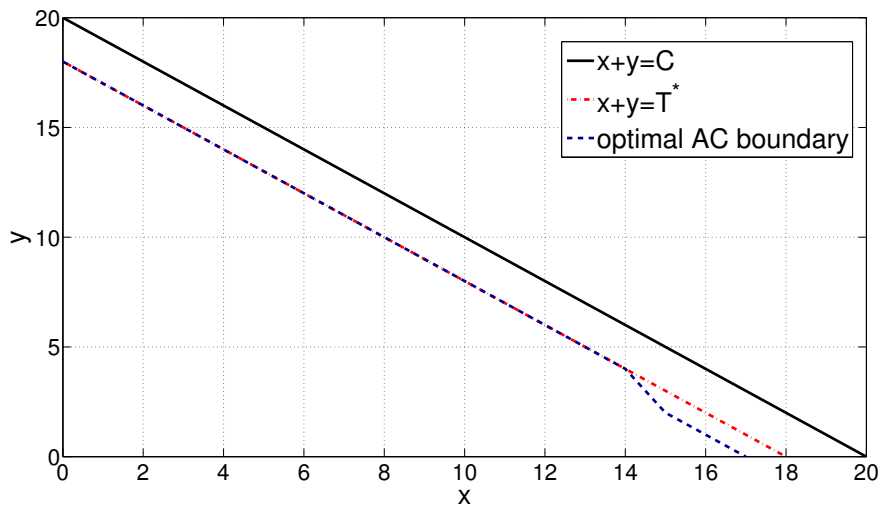


Figure 3.5: Performance comparison between Eq. (3.22) and the optimal AC boundary obtained by MPI. Parameters: $\lambda_1 = 20$, $\lambda_2 = 5$, $\mu_1 = 3$, $\mu_2 = 4$, $\mu = 3$, $b_1 = b_2 = 1$, $C = 20$, $R = 1$, $K = 10$.

Iteration algorithm (*linMPI*). It returns a linear approximation of the optimal admission boundary. Because of its characteristics, the optimal AC boundary achieved by MPI could be approximated by a line with equation $Y = AX + B$ (for instance see the optimal AC boundaries in Figures 3.4 and 3.5). In this new proposal, the idea is to reach a policy that its reward is nearly optimal implying less computational effort than *newMPI* and MPI. The difference between *linMPI* and the proposal of Subsection 3.5.4 is that *linMPI* can

3.5. Alternative version of MPI Algorithm

be applied for the general case $b_1 \geq 1$ and $b_2 \geq 1$.

Prop. 3 is used in order to optimize “Policy Improvement Step” of MPI in a similar way as we described before and Prop. 4 to reduce the running time of “Policy Evaluation Step” of MPI. In this new proposal we define two parameters k^* and L , then the policy evaluation defined in the original MPI is executed only in a set of the system states: $S^* = \{(X, Y) : X \leq k^* \text{ or } Y \leq k^*\} \cup \{I\}$ where I represents a group of randomly chosen states of $S \setminus \{(X, Y) : X \leq k^* \text{ or } Y \leq k^*\}$ such that $|I| = L$. Using the concavity property, the value functions of the not considered states are obtained by linear interpolation based on the value of $s \in S^*$. Note that L , as in Subsection 3.5.3, represents the number of states chosen randomly. On the other hand, the parameter k^* defines a band in $X = 0$ and $Y = 0$ axes. This proposal has the advantage that we do not need to know, a priori, the possible location of the optimal policy.

Due to the fact that we are looking for a line as an approximation of the AC boundary, in this case the “Policy Improvement Step” is only evaluated over the states that satisfy $X = 0$ or $Y = 0$ (we only need two points to determine the line $Y = AX + B$). That is the reason of the parameter k^* . After having done many simulations with different system parameters, we conclude that using the pair $(k^* = \frac{C}{10}, L = \frac{C/b_1 C/b_2}{4})$ the results obtained are nearly optimal (see simulated examples in Section 3.6).

In this alternative, the policy π is translated as a pair of parameters $\pi = (A, B)$. Therefore, the stop criterion of the *linMPI* is when $A = A'$ and $B = B'$, letting $\pi = (A, B)$ and $\pi' = (A', B')$ be two policies in two different and consecutive iterations of the algorithm (see Alg. 4 where it is explained the “Policy improvement step” proposed). Please note that Alg. 4 has to be executed for $Y = 0$ and for $X = 0$, when it is running for $X = 0$ the parameter B is obtained, otherwise is obtained $\frac{-B}{A}$.

Algorithm 4 Alternative Policy improvement step - linMPI

```

1:  $Y := 0; X := \lceil C/b_1 \rceil - 1$  (or  $X := 0; Y := \lceil C/b_2 \rceil - 1$ );
2: out:=false;
3: while not out do
4:   compute  $a(X, Y) := \arg \max_{a \in A_{(X, Y)}} \{ \sum_{j \in S} \beta \hat{p}(j|s, a)(l(s, a, j) + V_n(j)) \}$  at
      state  $(X, Y)$ ;
5:   if  $(a(X, Y) = 1)$  then
6:     out:=true;
7:      $-B/A := X$  (or  $B := Y$ )
8:   else
9:      $X := X - 1$  (or  $Y := Y - 1$ );
10:  end if
11: end while
12:  $\pi' := (A, B)$ ;
13: return  $\pi'$ 

```

Complementing *linMPI*, in this case “Policy evaluation step” is implemented in a similar way to *newMPI* but considering the defined set S^* . In Section 3.6 we show some examples of the performance of *linMPI*.

3.6 Simulated experiments and results

In order to test the proposed algorithms we consider different simulation experiments. In the first case we evaluate the *newMPI* algorithm and finally, the last experiments corresponds to *linMPI* proposal.

3.6.1 Performance tests of *newMPI*

As we explained before, we developed a new version of MPI called *newMPI* using the proposals of Subsections 3.5.2 and 3.5.3. We expect to get the optimal admission control boundary reducing the total CPU-time consumed in comparison to the MPI pattern (original version).

After having tested the algorithm with both proposed modification versus the original MPI, we have identified that in most cases the number of states evaluated in “Policy Improvement Step” in the *newMPI* represents less than 5% of the whole space and the obtained results are excellent approximations of the optimal AC policy.

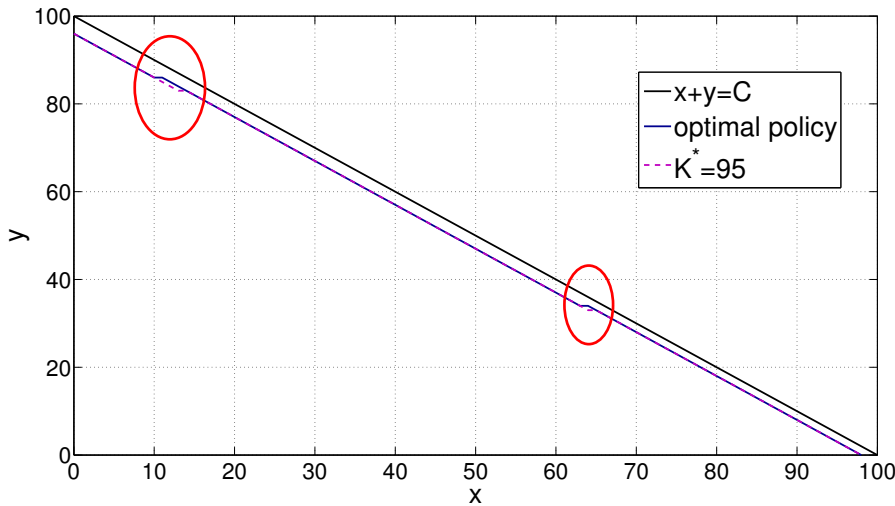


Figure 3.6: Parameters: $\lambda_1 = 200$, $\lambda_2 = 300$, $\mu_1 = 3$, $\mu_2 = 1$, $b_1 = b_2 = 1$, $C = 100$, $R = 1$, $K = 3$, $\beta = 0.9474$. The circles show the differences between the AC boundary obtained with *newMPI* using $K^* = 95$ and $L = 2280$ and the optimal boundary. In terms of SP's profit that difference is insignificant. As we explained before, the AC boundary obtained by *newMPI* is the optimal or is more conservative.

In the experiments we have chosen L proportional to K^{*2} such that $L = \frac{K^*(K^*+1)}{4}$. For instance, in Figure 3.6 it is shown an example where *newMPI* is applied. In this example, we have tested the new version of the algorithm for different values of parameters K^* and L , and only when $K^* = 95$ (and $L = \frac{K^*(K^*+1)}{4}$) there is a minimal difference between the optimal AC boundary and the AC obtained in the *newMPI* (for $K^* < 95$ the resulted boundaries are the same as the optimal one). In particular in Figure 3.7 there is a performance comparison showing $\frac{T_{newMPI}}{T_{MPI}}$ for different values of K^* and L . T_{MPI} and T_{newMPI}

3.6. Simulated experiments and results

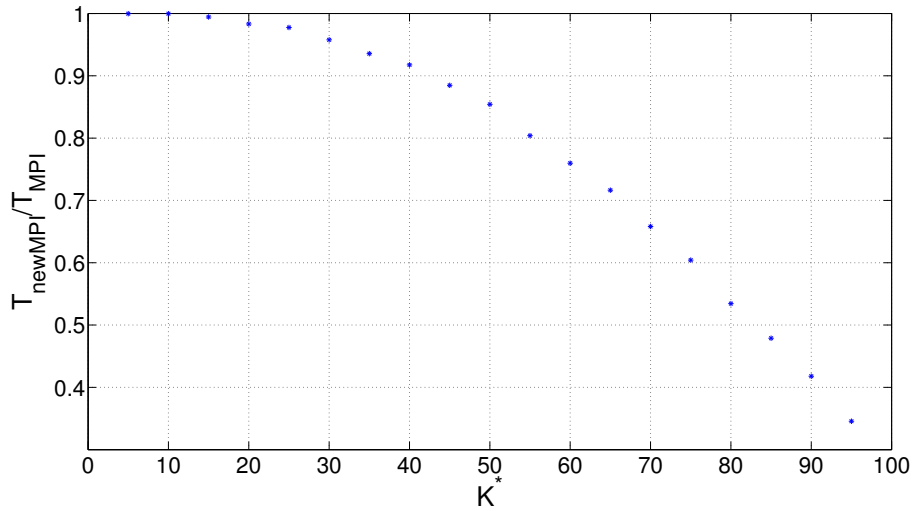


Figure 3.7: Comparison between MPI and *newMPI* (improving Steps 4 and 5). L is chosen proportional to K^{*2} : $L = \frac{K^*(K^*+1)}{4}$.

represent the running times of the original MPI algorithm and of our new version respectively. It is clear that the running time has a big impact as bigger is K^* . For example for $K^* = 85$ (and $L = 1827$) the running time of the new version is less than $0.5T_{\text{MPI}}$ and the AC boundary obtained is the optimal.

It is important to remark that a practical determination of K^* value can be done using the results of Subsec. 3.5.4 or Subsec. 3.5.5. The proposed methods in these subsections give us “instantaneously” the knowledge of where is going to be located the optimal admission control boundary. Knowing that, a reasonable value of K^* will be if the boundary is totally located in the area $b_1X + b_2Y - K^* \geq 0$. The parameter L is related with K^* because it represents the number of states to be evaluated that are not considered when K^* is chosen.

3.6.2 Performance tests of *linMPI*

In Figures 3.8 and 3.9 we present some numerical examples of two different systems. T_{linMPI} and T_{MPI} represent the algorithm’s running time of *linMPI* and MPI respectively. It is shown that the linear AC boundaries are good approximations to the optimal ones in both cases. Using $k^* = C/10$ and $L = C^2/4$, we can see that the running time of the new version decreases by 75%. In Case 1 $T_{\text{linMPI}} = 0.25T_{\text{MPI}}$ and in Case 2 $T_{\text{linMPI}} = 0.2T_{\text{MPI}}$.

In order to test how closely to the optimal are the approximations of the admission control boundary, we have made several experiments (n) with both boundaries (the optimal and its approximation using *linMPI*) and compute the profit of the SP. Each experiment consists in one realization of the continuous time markov chain using the appropriate AC boundary. In each transition the discount profit of the SP is computed. In Table 3.2 the results are summarized for both cases. Based on these results we can conclude that

Chapter 3. Markov decision process based models

Table 3.2: Examples considering cases of Figures 3.8 and 3.9. Confidence Interval: $n = 30$, confidence level= 0.95.

Case	Method	Reward Confidence Interval
1	MPI	6.32 ± 0.57
	<i>linMPI</i>	6.34 ± 0.57
2	MPI	41.75 ± 1.85
	<i>linMPI</i>	41.54 ± 1.59

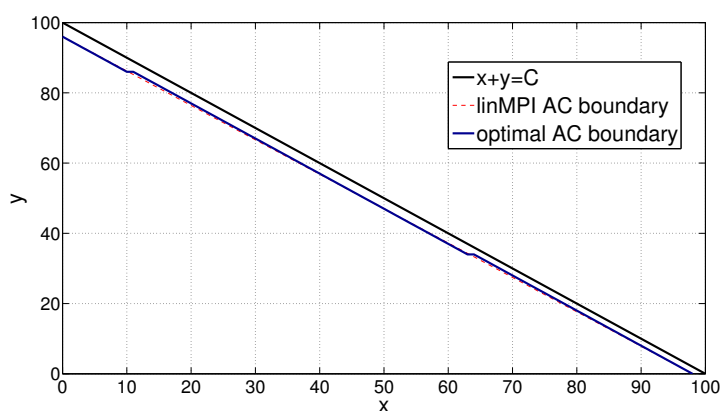


Figure 3.8: Optimal Boundaries MPI vs linMPI. Case 1 parameters: $\lambda_1 = 200$, $\lambda_2 = 300$, $\mu_1 = 3$, $\mu_2 = 1$, $b_1 = b_2 = 1$, $C = 100$, $R = 1$, $K = 3$, $\beta = 0.9474$. Performance result: $\frac{T_{linMPI}}{T_{MPI}} = 0.25$.

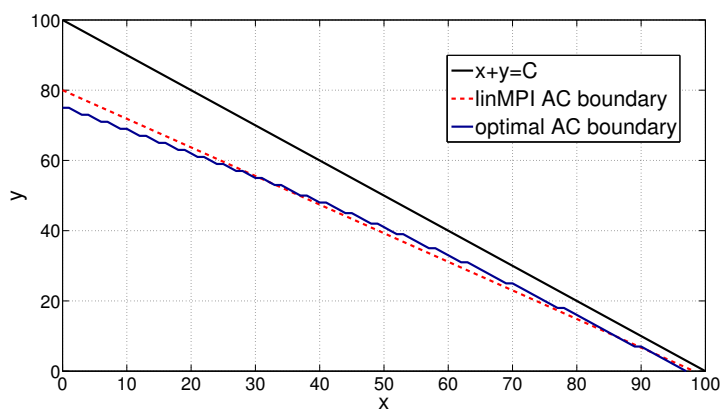


Figure 3.9: Optimal Boundaries MPI vs linMPI. Case 2 parameters: $\lambda_1 = 200$, $\lambda_2 = 500$, $\mu_1 = 3$, $\mu_2 = 0.5$, $b_1 = b_2 = 1$, $C = 100$, $R = 1$, $K = 3$, $\beta = 0.9953$. Performance result: $\frac{T_{linMPI}}{T_{MPI}} = 0.2$.

the reward of the approximated boundary has a good accuracy.

3.7 Conclusions

In this chapter we have analyzed the profit maximization problem of preemptive systems. Summarizing, we have presented our stochastic model, we defined the objective as a dynamic programming (DP) problem, and we have characterized some properties of the optimal admission control boundary using the DP formulation. Using this information we have proposed some alternatives to implement modifications to DP algorithms whose running times are much smaller than the original used algorithms. In particular we have formulated two new versions of the Modified Policy Iteration algorithm: *newMPI* and *linMPI*. We have presented some simulations and numerical examples that validate our results. The results obtained show an excellent performance of *newMPI* and *linMPI*. The presented stochastic model will be the starting point for the next chapter.

This page was intentionally left blank.

Chapter 4

Fluid Limits Approximation

There are several examples of complex stochastic systems for which analytical expressions cannot be derived, or that are even difficult to simulate. However, in many cases they can be studied much more easily by analyzing deterministic systems, obtained as asymptotic approximations of the original ones which are denominated “fluid limits”. The complexity of the system may be due to its size, its dependence structure, etc. In particular, in this thesis we deal with deterministic approximations of: Continuous Time Markov Chains (CTMC) and Markov Decision Processes (MDPs).

This chapter provides a quick review on the main results of fluid limits presenting classical and non-classical results (see Section 4.1). After the introductory section, in Section 4.2 we describe some previous work and highlight some recent papers. The chapter continues in Section 4.3 where the fluid limit technique is used to analyze and characterize the dynamic of a spectrum sharing mechanism where primary users have strict priority over secondary ones. In Section 4.4 we return to the problem presented in Chapter 3, of maximizing the total expected discounted revenue of the primary service provider applying admission control decisions over secondary users, by means of the fluid approximation of the control problem. Finally, in Section 4.5, we use the deterministic model in order to present some tools and criteria that can be used to improve the mean spectrum utilization with the commitment of providing to secondary users a satisfactory grade of service and a small interruption probability.

4.1 Preliminaries and motivation

In a nutshell, we can say that by choosing a convenient scaling of a Markov process it is possible to obtain in the limit, a description of the asymptotic behavior of the process as the solution of an ordinary differential equation system (hopefully deterministic) which is denominated “fluid limit”. Whereas the stochastic process is a microscopic description of the system, the corresponding differential equation gives a macroscopic description that captures the main characteristics of the system. For a survey about this topic see [65, 66], and for a more general reference about limits of stochastic processes we suggest [67].

The proof of this approximation result is generally based on a semi-martingale decomposition of the Markov process, which shows that the main characteristic of the stochastic

Chapter 4. Fluid Limits Approximation

process are captured by the drift part while the stochastic fluctuation of second order (corresponding to the martingale) vanishes with the scaling and limit procedure. More specifically, consider a Markov process $\tilde{X}^N(t)$ parametric in N and its martingale decomposition:

$$\tilde{X}^N(t) = \tilde{X}^N(0) + \int_0^t Q_N(\tilde{X}^N(s))ds + M^N(t), \quad (4.1)$$

where $Q_N(l)$ is the so-called drift of the process at state l which may be calculated as

$$Q_N(l) = \sum_m (l-m)q(l,m), \quad (4.2)$$

being $q(l,m)$ the transition rate from state l to m and $M^N(t)$ is a Martingale. Consider now the scaled process $X^N(t) = \frac{\tilde{X}^N(t)}{N}$, then:

$$X^N(t) = X^N(0) + \frac{1}{N} \int_0^t Q_N(\tilde{X}^N(s))ds + \frac{M^N(t)}{N}. \quad (4.3)$$

If there exist a Lipschitz function Q such that

$$\lim_{N \rightarrow \infty} \left\| \frac{Q_N(\tilde{X}^N(t))}{N} - Q(X^N(t)) \right\| = 0$$

and $\frac{M^N(t)}{N}$ converges to zero in probability, then $X^N(t)$ converges in probability, when $N \rightarrow \infty$, over compact time intervals to a deterministic process $x(t)$, described by the ordinary differential equation (ODE):

$$x'(t) = Q(x(t)). \quad (4.4)$$

The drift Q may be interpreted as the expected rate of change of the process. See an illustrative example in Figure 4.1.

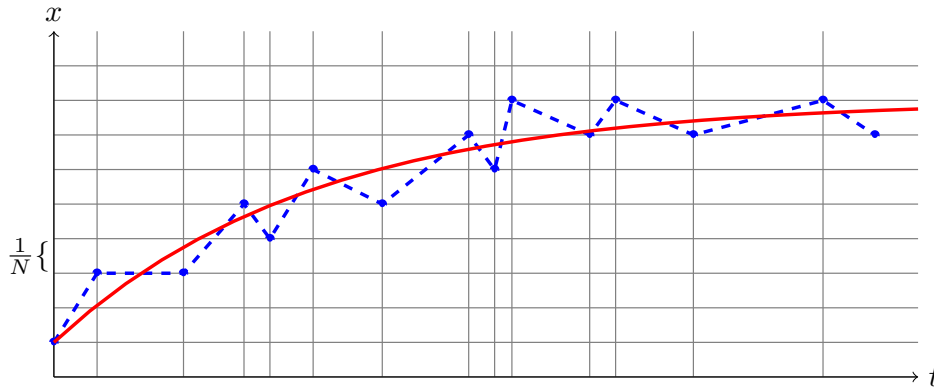


Figure 4.1: Illustration of the Markov process convergence. The continuous red line represents the solution of the ODE and the dashed blue one is a trajectory of $X^N(t)$.

As previously mentioned, classical results on convergence of Markov processes assume some regularity properties of the fluid ODE, i.e. the vector field defining the ODE must be a Lipschitz continuous function in the domain of interest. This condition is enforced to guarantee the existence and uniqueness of the solution of the ODE for fixed initial conditions. As we will see later, due to the existence of an admission control and preemption policies, in our system this regularity condition does not hold.

4.1.1 Discontinuous drift

In the case of non-continuous right hand side, the differential equation Eq (4.4) is not well-defined since there exists no function x that is differentiable and that satisfies Eq (4.4). The proper way to define its solutions is to use Differential Inclusions (DI) [68]. The trajectories of a fluid equivalent system near a point of discontinuity may enter “sliding modes” and the differential equation Eq (4.4) has to be replaced by a new dynamical system defined piece-wise by differential equations:

$$x'(t) \in \tilde{Q}(x(t)).$$

where \tilde{Q} is a set-value mapping defined as the convex null of the accumulation points of the drift [69–71].

In this new context, our explanations and demonstrations are inspired by the methodology proposed by Bortolussi in [72, 73], where the author demonstrates that generally it is possible to determine a piecewise-smooth (PWS) system (i.e. a dynamical system in which the vector field is discontinuous in the domain of interest, but with a controlled form of discontinuity). That is to say, considering $\mathbf{x}'(t) = f(\mathbf{x}), f : E \rightarrow \mathbb{R}^n, E \subseteq \mathbb{R}^n, \bigcup R_i \supseteq E$ (R_i $i = 1 \dots s$ is a finite set of disjoint regions), a PWS system is when f is smooth on R_i and can be discontinuous only on the boundaries of R_i . In [72], they also prove that the sequence of CTMC converges to the trajectories of this hybrid dynamical system when the size of the system N goes to infinity.

Let us give an informal explanation of Bortolussi results restricting our attention to a system with two regions (R_1 and R_2). In this context we have f_1 and f_2 the velocity vectors, both continuous in R_1 and R_2 respectively and we define γ as the boundary between R_1 and R_2 . In R_1 and R_2 we can apply the classical results on convergence of Markov processes (Eq. (4.4)). The question is what happen on γ . If we are in a point \mathbf{x} of γ and $n(\mathbf{x})$ is the normal vector to γ at \mathbf{x} (consider that $n(\mathbf{x})$ points to R_1), we find the following behaviors of a solution starting in \mathbf{x} depending on the value of $n^T(\mathbf{x})f_1(\mathbf{x})$ and $n^T(\mathbf{x})f_2(\mathbf{x})$:

- **transversal crossing:** if $n^T(\mathbf{x})f_1(\mathbf{x})$ and $n^T(\mathbf{x})f_2(\mathbf{x})$ are non zero and have the same sign, e.g. if $n^T(\mathbf{x})f_1(\mathbf{x}) > 0$ and $n^T(\mathbf{x})f_2(\mathbf{x}) > 0$ a solution starting in R_2 will cross γ and continues in R_1 (see Figure 4.2(a));
- **sliding motion:** if $n^T(\mathbf{x})f_1(\mathbf{x}) < 0$ and $n^T(\mathbf{x})f_2(\mathbf{x}) > 0$ the system cannot escape from γ , then the solution follows a vector field obtained as convex combination of f_1 and f_2 (see Figure 4.2(b));
- **tangential crossing:** if $n^T(\mathbf{x})f_1(\mathbf{x}) = 0$ or $n^T(\mathbf{x})f_2(\mathbf{x}) = 0$, e.g. if $n^T(\mathbf{x})f_1(\mathbf{x}) > 0$ and $n^T(\mathbf{x})f_2(\mathbf{x}) = 0$ then the trajectory continues in the region pointed by f_1 .

It is important to highlight that these results will be used in the proofs of the following sections.

In this thesis we indistinctly use PWS system or ODE, but the reader must note that when there are involved discontinuous transition rates, fluid limit is represented as a piece-wise smooth dynamical system (PWS).

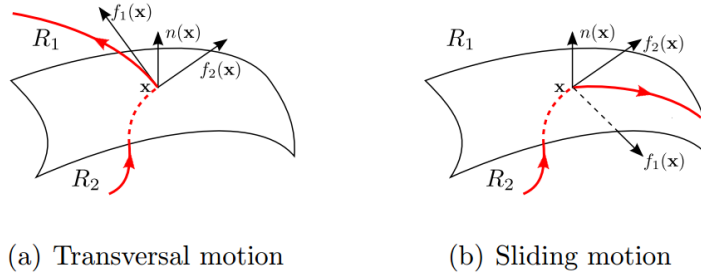


Figure 4.2: Schematic representations of transversal crossing and sliding motion (source: [72]). Please note that tangential crossing can be seen as a particular case of transversal crossing.

4.2 Related work

Applications of fluid models to telecommunications appeared in the literature and were widely developed in the last decade. Some recent examples include for instance: peer-to-peer systems, load balancing and mobile networks (see for example [74–79] and references therein). In particular, in [74] the authors dealt with vector fields with discontinuities and they applied the results described in [72] in the same way as ours. On the other hand, there are examples of control queueing problems analyzed through a fluid approximation. Some of the most representative examples are [41, 42, 80]. Our work differs from the preceding works by focusing on preemptive queueing systems with multi-resource demand.

In particular, applications to Cognitive Radio networks there are some recent related works that we would like to highlight. In [81] the authors use a fluid model to study SUs queueing delay performance. In [82] they study the coexistence of two wireless networks with different priorities and compare throughput and delay obtained in both networks. On the other hand, in [83], they focus on the collaborative sensing within the SUs and its impact in its QoS. In these papers the authors analyze the delay and throughput in different CR scenarios, so their results can be complementary to our QoS analysis of Section 4.5.

4.3 Fluid analysis of the dynamic of the spectrum sharing mechanism

The main contribution of this section is the fluid approximation of the stochastic system defined in the previous chapter. In particular we will concentrate on the CTMC which models the number of primary and secondary users allocated in the system. Based on this analysis, in the next section we will deal with the complete economic control problem.

Generally speaking, starting from a stochastic model the objective is to find a deterministic approximation for the original process. This introduces the problem of finding the suitable scale for the approximation. A typical scaling procedure consists in dividing

4.3. Fluid analysis of the dynamic of the spectrum sharing mechanism

by N , and in considering transition rates multiples of N (jumps are of order $1/N$ and transition rates are of order N , which means that the product remains or tends to a constant as N increases). In this regard, we consider a properly scaled sequence in order to study and characterize the evolution of the system when the number of channels as well as the arrival rates are arbitrary large, a representative scenario in IoT applications.

In the direction of introducing the deterministic approximation, we make some important definitions. Let $\tilde{X}^N(t)$ and $\tilde{Y}^N(t)$ be the number of PUs and SUs in the system considering a N -parametric version of the original stochastic model presented in Chapter 3. That means that the parameters of this new process are: $\tilde{C} = CN$, $\tilde{\lambda}_i = \lambda_i N$ and $\tilde{\mu}_i = \mu_i$, $i = 1, 2$.

For the sequence of stochastic processes $(\tilde{X}^N(t), \tilde{Y}^N(t))$, the transition rates between states $(\tilde{X}^N, \tilde{Y}^N)$ and $(\tilde{X}^N, \tilde{Y}^N)$ are defined by:

- $\tilde{q}((\tilde{X}^N, \tilde{Y}^N), (\tilde{X}^N + 1, \tilde{Y}^N)) = \lambda_1 N$ if $b_1 \tilde{X}^N + b_2 \tilde{Y}^N \leq CN - b_1$,
- $\tilde{q}((\tilde{X}^N, \tilde{Y}^N), (\tilde{X}^N - 1, \tilde{Y}^N)) = \mu_1 \tilde{X}^N$,
- $\tilde{q}((\tilde{X}^N, \tilde{Y}^N), (\tilde{X}^N, \tilde{Y}^N + 1)) = a(\tilde{X}^N, \tilde{Y}^N) \lambda_2 N$ if $b_1 \tilde{X}^N + b_2 \tilde{Y}^N \leq CN$,
- $\tilde{q}((\tilde{X}^N, \tilde{Y}^N), (\tilde{X}^N, \tilde{Y}^N - 1)) = \mu_2 \tilde{Y}^N$,
- $\tilde{q}((\tilde{X}^N, \tilde{Y}^N), (\tilde{X}^N + 1, \tilde{Y}^N - \tilde{Z}^N)) = \lambda_1 N$ if $CN - b_1 < b_1 \tilde{X}^N + b_2 \tilde{Y}^N \leq CN$ and $\tilde{Y}^N \geq \tilde{Z}^N$ (preemption).

Remember that \tilde{Z}^N is defined in Eq. (3.15) and represents the number of preempted SUs. On the other hand, $a(\tilde{X}^N, \tilde{Y}^N)$ represents the admission control decision in state $(\tilde{X}^N, \tilde{Y}^N)$. In this thesis we have defined a deterministic admission control¹ $a(\tilde{X}^N, \tilde{Y}^N) = \{0, 1\}$, then when the system is in state $(\tilde{X}^N, \tilde{Y}^N)$ and a secondary user arrives, it will be accepted if $a(\tilde{X}^N, \tilde{Y}^N) = 1$, otherwise it will be rejected.

Consider now the scaled process $(X^N(t), Y^N(t)) = \frac{1}{N}(\tilde{X}^N(t), \tilde{Y}^N(t))$, using the arguments of the previous section it is possible to demonstrate that $(X^N(t), Y^N(t))$ converges in probability over compact time intervals to a deterministic process $(x(t), y(t))$, described by the equation:

$$(x'(t), y'(t)) = \tilde{Q}(x(t), y(t)). \quad (4.5)$$

In the next subsections, we will calculate the drift Q and we will use the methodology proposed by Bortolussi for two different scenarios (with and without an admission control mechanism) obtaining \tilde{Q} as a convex combination of the drifts of points in the neighborhood of the discontinuity. As a result we will obtain, for each case, a dynamical system defined piece-wise by differential equations.

It is important to highlight that in our considered scenario we can obtain an explicit expression of $(x(t), y(t))$. We will also support our results with representative simulated examples. We will assume $b_1 = b_2 = 1$ to simplify the analysis, but in Section 4.4 we will extend the results to the general case.

¹In paper [J4], that is under review, we include the analysis of a probabilistic admission control.

4.3.1 Spectrum sharing without SU's admission control

For the deterministic approximation of our system we denote points in the state space by (x, y) such that $\{(x, y) : x + y \leq C\}$. First of all, we assume that $a(x, y) = 1$ for all $(x, y) : x + y < C$. Please note that with the assumption $b_1 = b_2 = 1$, the preemption only occurs when the system is full of users (i.e. $\{(x, y) : x + y = C\}$). The idea in this section is to study the behavior of the system without any intervention: if a SU arrives and there is at least one unoccupied channel, the SU will enter (see Figure 4.3).

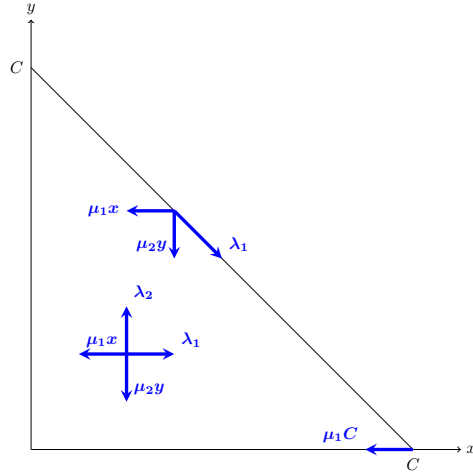


Figure 4.3: Schematic representation of the drift vector fields.

We have in this case that the drift is

$$Q(x, y) = \begin{cases} \lambda_1(1, 0) + \lambda_2(0, 1) + \mu_1 x(-1, 0) + \mu_2 y(0, -1) & \text{if } x + y < C, \\ \lambda_1(1, -1) + \mu_1 x(-1, 0) + \mu_2 y(0, -1) & \text{if } x + y = C \text{ and } y > 0, \\ \mu_1 x(-1, 0) & \text{if } x + y = C \text{ and } y = 0. \end{cases} \quad (4.6)$$

Please note that both coordinates of the process are independent, except when $x + y = C$. In addition, the behavior of PUs is as in a $M/M/C/C$ queue, independent of the SUs. In this simplified version of the problem ($b_1 = b_2 = 1$), when $\mu_1 \neq \mu_2$ it is not possible to obtain a close expression of its stationary distribution, then the fluid approximation will allow us to study the behavior of the system and analyze the influence of admission control decisions in a more feasible way than computing it numerically.

We determine,

- if $Q(x, y)$ is continuous in a point (x, y) , $\tilde{Q}(x, y) = \{Q(x, y)\}$, and
- if $Q(x, y)$ is discontinuous in (x, y) being η the border of discontinuity, $\tilde{Q}(x, y)$ as $co\{\lim_{k \rightarrow \infty} Q(x_k, y_k) \text{ such that } (x_k, y_k) \rightarrow (x, y), (x_k, y_k) \notin \eta\}$

In order to be in the context of [72] (see Section 4.1), as a way to see the above explanation, it is useful to artificially extend our processes outside the region $R_1 = \{x + y \leq C\}$, assuming that in the region $R_2 = \{x + y > C\}$ the vector field is $(\lambda_1 - \mu_1 x, -\lambda_1 - \mu_2 y)$. This leads to a different behavior of the fluid limit in the region $\{x + y = C\}$, where the deterministic system is driven by the following equations:

4.3. Fluid analysis of the dynamic of the spectrum sharing mechanism

If $x + y - C < 0$ (R_1) or $\lambda_1 + \lambda_2 \leq \mu_1 x + \mu_2 y$:

$$\begin{cases} x' = \lambda_1 - \mu_1 x, \\ y' = \lambda_2 - \mu_2 y; \end{cases}$$

else, if $x + y - C = 0$ (γ) or $\lambda_1 + \lambda_2 > \mu_1 x + \mu_2 y$:

$$\begin{cases} x' = \lambda_1 - \mu_1 x, \\ y' = -\lambda_1 + \mu_1 x. \end{cases}$$

This equation has a unique solution with initial condition $(x(0), y(0))$. When $\lambda_1 + \lambda_2 \leq \mu_1 x + \mu_2 y$ it is easy to demonstrate that the solutions are asymptotically stable.

Please note that the equations defined for γ (sliding motion) is obtained considering the convex combination:

$$\begin{cases} x' = \theta(x, y)(\lambda_1 - \mu_1 x) + (1 - \theta(x, y))(\lambda_1 - \mu_1 x), \\ y' = \theta(x, y)(\lambda_2 - \mu_2 y) + (1 - \theta(x, y))(-\lambda_1 - \mu_2 y); \end{cases}$$

where $\theta(x, y)$ is calculated by requiring that the resulting vector field should be tangential to γ . Then,

$$\theta(x, y) = \frac{\mu_1 x + \mu_2 y}{\lambda_1 + \lambda_2}. \quad (4.7)$$

Recapitulating, we can say that if

$$\lim_{N \rightarrow \infty} (X^N(0), Y^N(0)) = (x(0), y(0))$$

then, for all $T > 0$,

$$\lim_{N \rightarrow \infty} \sup_{t \in [0, T]} \|(X^N(t), Y^N(t)) - (x(t), y(t))\| = 0$$

in probability where $(x(t), y(t))$ are the solutions of the previous system of differential equations.

The proof of the previous result follows straightforward the proof of Theorem IV.2 in [72]. Concerning fluid limits, including systems with discontinuous rates and presence of sliding motion, a more general framework is presented by Bortolussi in [73].

In the presence of fluid limits it is usual to infer from the fixed point analysis of the deterministic system the behavior of the stochastic one in the stationary regime. A general result says that for large N the stationary distribution is supported by the Birkhoff center² of the fluid limit. In particular, if there is a unique fixed point that is a global attractor, the stochastic invariant distributions converge in probability to this fixed point [84, 85]. According to that, one of our main results is that the position of the ODE (or PWS) fixed points is decisive in defining an effective operating point of the system (we will see the application of this result in Sections 4.4 and 4.5). Then, in the following proposition we study the behavior of $(x(t), y(t))$, in particular we analyze its fixed points and asymptotic behavior when time goes to infinity. We will show that we have different cases depending on the system parameters.

²Birkhoff center definition in Section 7 of [84]

Chapter 4. Fluid Limits Approximation

Proposition 6. *Considering $a(x,y) = 1$ for all $(x,y) : x + y < C$, letting R_1, R_2 be the above defined zones and defining (x^*, y^*) as the PWS system fixed point, then:*

- a. *If $\frac{\lambda_1}{\mu_1} + \frac{\lambda_2}{\mu_2} < C$, then $(x^*, y^*) = \left(\frac{\lambda_1}{\mu_1}, \frac{\lambda_2}{\mu_2}\right) \in R_1$ and the mean system utilization will be $\frac{\lambda_1}{\mu_1} + \frac{\lambda_2}{\mu_2}$.*
- b. *If $\frac{\lambda_1}{\mu_1} + \frac{\lambda_2}{\mu_2} \geq C$ and $\frac{\lambda_1}{\mu_1} < C$, then $(x^*, y^*) = \left(\frac{\lambda_1}{\mu_1}, C - \frac{\lambda_1}{\mu_1}\right) \in \gamma$ and the mean system utilization will be C .*
- c. *If $\frac{\lambda_1}{\mu_1} \geq C$, then $(x^*, y^*) = (C, 0) \in \gamma$ and the mean system utilization will be C .*

Sketch of the proof. Let f_1 and f_2 be the velocity vectors, both continuous in R_1 and R_2 respectively:

$$f_1(x,y) = \begin{pmatrix} \lambda_1 - \mu_1 x \\ \lambda_2 - \mu_2 y \end{pmatrix}, f_2(x,y) = \begin{pmatrix} \lambda_1 - \mu_1 x \\ -\lambda_1 - \mu_2 y \end{pmatrix},$$

and let $n(x,y)$ be the normal vector to the surface $\gamma: x + y - C = 0$, therefore $n^T = (1, 1) \forall (x,y) \in \gamma$ and it points to R_2 .

We have $n^T f_1(x,y) = 0 \Leftrightarrow \lambda_1 + \lambda_2 - \mu_1 x - \mu_2 y = 0$ and $n^T f_2(x,y) = 0 \Leftrightarrow -\mu_1 x - \mu_2 y = 0$. Therefore, for studying $n^T f_i(x,y)$ we have several cases depending on the position of the line $\lambda_1 + \lambda_2 - \mu_1 x - \mu_2 y = 0$. It is clear that it depends on the values of $\lambda_1, \lambda_2, \mu_1$ and μ_2 . In particular, we have that $n^T f_1(x) > 0$ if $\lambda_1 + \lambda_2 - \mu_1 x - \mu_2 y > 0$, f_1 and n are tangent in the points over the line $\lambda_1 + \lambda_2 - \mu_1 x - \mu_2 y = 0$ and $n^T f_1(x) < 0$ if $\lambda_1 + \lambda_2 - \mu_1 x - \mu_2 y < 0$. On the other hand, $n^T f_2(x) < 0$ in R_2 independently of the parameters λ_i and μ_i .

All possible cases, for different values of the parameters, can be categorized in two groups (Group 1 and Group 2) shown in Figures 4.4 and 4.5. In those figures, the continuous line represents γ , the dotted line is $\lambda_1 + \lambda_2 - \mu_1 x - \mu_2 y = 0$ and the vectors are f_1 and f_2 in R_1 and R_2 respectively. In Group 1, see Cases 1a, 1b and 1c, the PWS system fixed point is in R_1 (Proposition 6.a). It is easy to note that $(x^*, y^*) = (\lambda_1/\mu_1, \lambda_2/\mu_2)$. On the other hand, in Group 2, represented by Case 2a, 2b and 2c, the fixed point is on γ and its value is $(x^*, y^*) = (\lambda_1/\mu_1, C - \lambda_1/\mu_1)$, (Proposition 6.b). Based on the explanation of Section 4.1, in Group 2 we can identify a sliding motion behavior near the fixed point, more precisely we can affirm that the PWS system trajectory will live on γ most of the time. Please note that all the examples of Figures 4.4 and 4.5 consider $\lambda_1/\mu_1 < C$. Finally, when the system is saturated by PUs ($\lambda_1/\mu_1 \geq C$), as a corollary from Proposition 6.b the fixed point is $(x^*, y^*) = (C, 0)$ (Proposition 6.c). □

In Figures 4.6 and 4.7 we show two examples, one of each group. In each one, in the left graphic we show the simulation of one trajectory of the scaled Markov process and the solution of the PWS system. On the other hand, in the right we show for the same simulation the evolution on the plane of the Markov Chain and the PWS system. In Figure 4.6 the fixed point is in R_1 and in Figure 4.7 it is on γ (the boundary between R_1 and R_2). It is important to note that in both cases, for large time values, the scaled number of users in the stochastic process is around the PWS system fixed point (x^*, y^*) , in other

4.3. Fluid analysis of the dynamic of the spectrum sharing mechanism

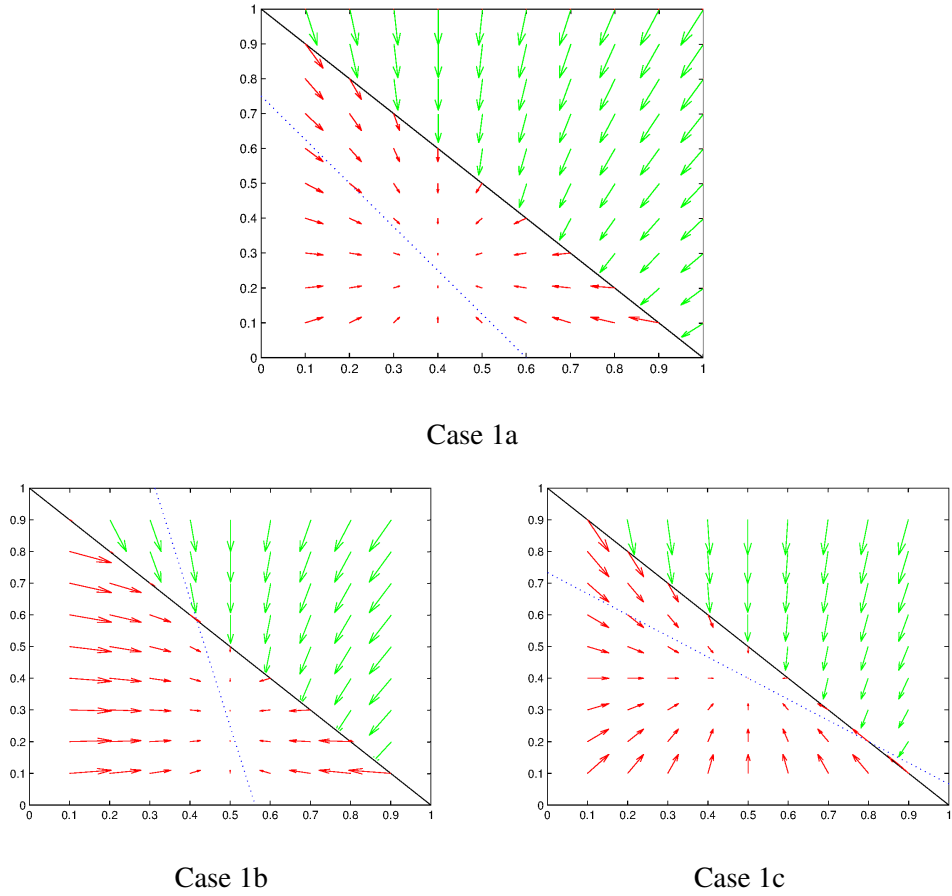
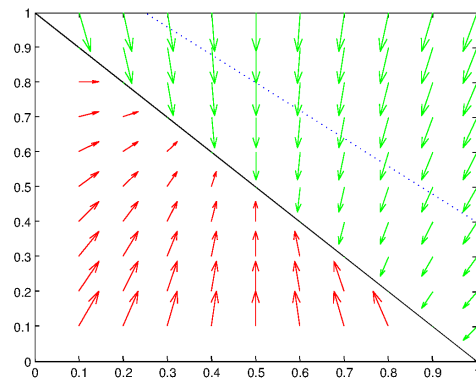


Figure 4.4: Group 1. Vector field for Case 1a: $N = 100$, $\lambda_1 = 2$, $\lambda_2 = 1$, $\mu_1 = 5$, $\mu_2 = 4$ and Case 1b: $N = 100$, $\lambda_1 = 4$, $\lambda_2 = 0.5$, $\mu_1 = 8$, $\mu_2 = 2$ and Case 1c: $N = 100$, $\lambda_1 = 5$, $\lambda_2 = 6$, $\mu_1 = 10$, $\mu_2 = 15$. The continuous line represents γ and the dotted line is $\lambda_1 + \lambda_2 - \mu_1 x - \mu_2 y = 0$.

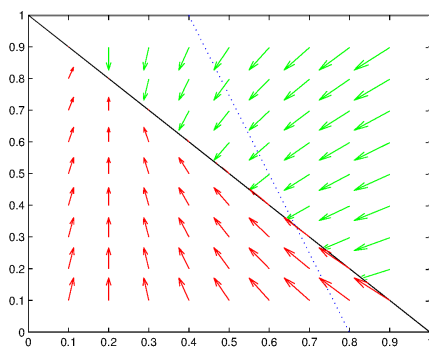
words $\lim_{N \rightarrow \infty} (X^N(\infty), Y^N(\infty)) = (x^*, y^*)$, being $(X^N(\infty), Y^N(\infty))$ the system in stationary regime. As a result, the mean system utilization is $x^* + y^*$ ($x^* + y^* = \lambda_1/\mu_1 + \lambda_2/\mu_2 < C$ or $x^* + y^* = C$ in Group 1 and 2 respectively). Comparison with simulation results show that the fluid limit accurately predicts the corresponding behavior of finite systems of interest (see Figures 4.6 and 4.7). Then, the deterministic approximation allows us to study and characterize the evolution of the system when the number of channels as well as the arrival rates are arbitrary large.

In the next subsection we will analyze the system when an admission control policy is applied.

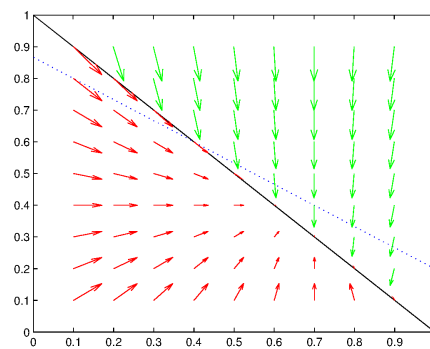
Chapter 4. Fluid Limits Approximation



Case 2a



Case 2b



Case 2c

Figure 4.5: Group 2. Vector field for Case 2a: $N = 100$, $\lambda_1 = 2$, $\lambda_2 = 4$, $\mu_1 = 4$, $\mu_2 = 5$, Case 2b: $N = 100$, $\lambda_1 = 1$, $\lambda_2 = 3$, $\mu_1 = 5$, $\mu_2 = 2$, and Case 2c: $N = 100$, $\lambda_1 = 7$, $\lambda_2 = 6$, $\mu_1 = 10$, $\mu_2 = 15$. The continuous line represents γ and the dotted line is $\lambda_1 + \lambda_2 - \mu_1 x - \mu_2 y = 0$.

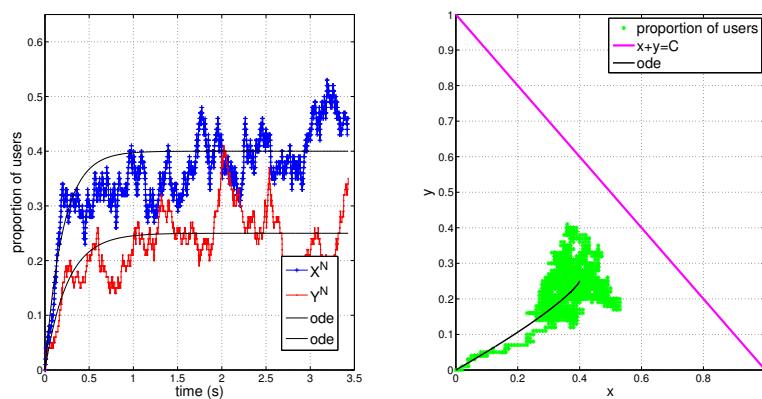


Figure 4.6: Group 1, parameters: $N = 100$, $C = 1$, $\lambda_1 = 2$, $\lambda_2 = 1$, $\mu_1 = 5$ and $\mu_2 = 4$

4.3. Fluid analysis of the dynamic of the spectrum sharing mechanism

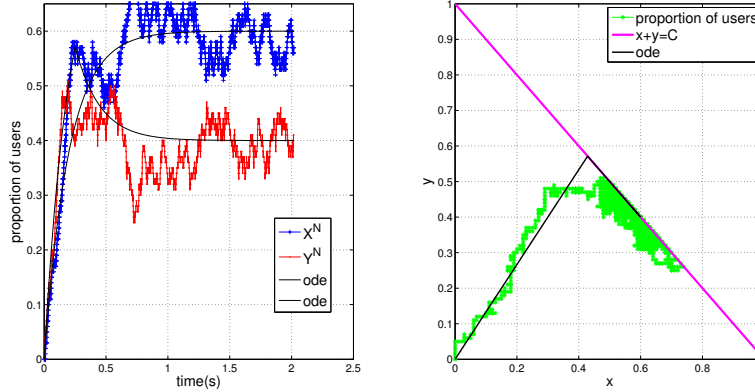


Figure 4.7: Group 2, parameters: $N = 100$, $C = 1$, $\lambda_1 = 3$, $\lambda_2 = 4$, $\mu_1 = 5$ and $\mu_2 = 5$

4.3.2 Spectrum sharing with SU's admission control

We have in this case that the drift is

$$Q(x, y) = \begin{cases} \lambda_1(1, 0) + a(x, y)\lambda_2(0, 1) + \mu_1x(-1, 0) + \mu_2y(0, -1) & \text{if } x + y < C, \\ \lambda_1(1, -1) + \mu_1x(-1, 0) + \mu_2y(0, -1) & \text{if } x + y = C \text{ and } y > 0, \\ \mu_1x(-1, 0) & \text{if } x + y = C \text{ and } y = 0. \end{cases} \quad (4.8)$$

Please note that Eq. (4.8) differs from Eq. (4.6) by the inclusion of the admission control $a(x, y)$ when $x + y < C$.

If $\mu_1 = \mu_2$, for some type of admission policies $a(x, y)$, the process can be represented as a one-dimensional CTMC and the stationary distribution can be computed explicitly. However, as happened in the case studied in the previous section, when $\mu_1 \neq \mu_2$ it is not possible to obtain a closed form expression of its stationary distribution (see for example [86, 87] and the references therein). This represents the great advantage in analyzing the behavior of the system by means of its fluid approximation.

As a first step, for simplicity and without loss of generality, we consider the case where the admission control boundary is the line with equation $-x - y + \delta = 0$ for $0 < \delta < C$. That is to say, $a(x, y) = 1$ if $y \leq -x + \delta$ and $a(x, y) = 0$ if $y > -x + \delta$. The advantage of this basic case is its simple practical implementation: primary SP only need to know the number of occupied bands to decide whether a SU is accepted to the system or not. As we will see in the next section, the optimal admission control boundary of the maximization profit problem of Chapter 3, in the limit, can be assumed as a line. Therefore, this study will be the basis for the analysis of next section.

Please note that the fixed-point's abscissa (λ_1/μ_1) is not affected by the control action $a(x, y)$. Another observation is that the domain where the ordinate could live is the segment $[0, \psi]$ where ψ represents the "original ordinate", that is the ordinate when $a(x, y) = 1$ for all (x, y) . The fixed point ordinate domain for Group 1 is $[0, \lambda_2/\mu_2]$ and for Group 2 is $[0, C - \lambda_1/\mu_1]$. In the particular case when $x^* = C$, the admission control does not change the position of the fixed point.

In the next proposition we study the behavior of $(x(t), y(t))$ when an admission control

Chapter 4. Fluid Limits Approximation

is applied and in particular we analyze its fixed points in the same way as we did in Prop. 6.

Proposition 7. *Let $\gamma' : -x - y + \delta = 0$ be the admission control boundary, if the system parameters satisfy $\frac{\lambda_1}{\mu_1} < C$, then the PWS system fixed point is*

$$(x^*, y^*) = \begin{cases} \left(\frac{\lambda_1}{\mu_1}, \frac{\lambda_2}{\mu_2} \right) & \text{if } \frac{\lambda_1}{\mu_1} + \frac{\lambda_2}{\mu_2} \leq \delta, \\ \left(\frac{\lambda_1}{\mu_1}, \delta - \frac{\lambda_1}{\mu_1} \right) & \text{if } \frac{\lambda_1}{\mu_1} < \delta, \\ \left(\frac{\lambda_1}{\mu_1}, 0 \right) & \text{if } \frac{\lambda_1}{\mu_1} \geq \delta. \end{cases} \quad (4.9)$$

In addition, the mean system utilization will be δ or $\frac{\lambda_1}{\mu_1}$ respectively.

Sketch of the proof. When there is an admission control like we explained above, in the PWS system we identify three zones (R_1 , R_2 and R_3^3) and two surfaces (γ and γ'), so:

If $x + y - \delta < 0$ (R_1):

$$\begin{cases} x' = \lambda_1 - \mu_1 x, \\ y' = \lambda_2 - \mu_2 y; \end{cases}$$

else, if $x + y - \delta = 0$ (γ'):

$$\begin{cases} x' = \lambda_1 - \mu_1 x, \\ y' = -\lambda_1 + \mu_1 x; \end{cases}$$

else, if $x + y - \delta > 0$ and $x + y - C < 0$ (R_2):

$$\begin{cases} x' = \lambda_1 - \mu_1 x, \\ y' = -\mu_2 y; \end{cases}$$

else, if $x + y - C = 0$ (γ):

$$\begin{cases} x' = \lambda_1 - \mu_1 x, \\ y' = -\lambda_1 + \mu_1 x. \end{cases}$$

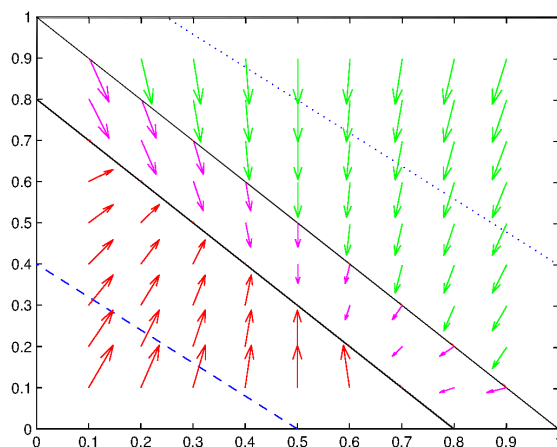
Defining f_i (velocity vectors) in the same way as in the previous subsection, the first case of the proposition ($\lambda_1/\mu_1 + \lambda_2/\mu_2 \leq \delta$) is analogous to cases of Group 1 of Prop. 6. We can infer that a solution starting in R_1 will die in R_1 (its fixed point is in R_1).

Now, concentrating in a case from the Group 2 defined before, the most representative scenarios we have are shown in Figure 4.8. They differ in the relative position of the admission control border:

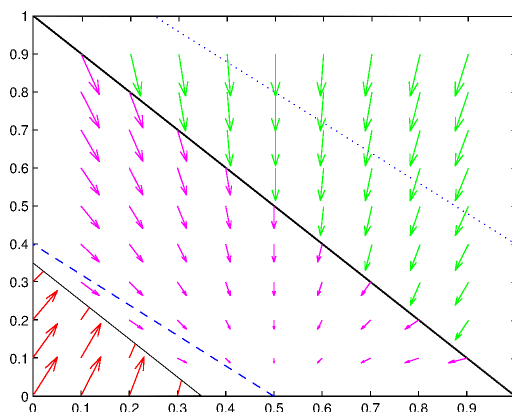
- Case A: $\frac{\lambda_1}{\mu_1} < \delta$,
- Case B: $\frac{\lambda_1}{\mu_1} > \delta$.

³ $R_3 = \{x + y - C > 0\}$ is an artificially zone defined for a better understanding of the fluid determination.

4.3. Fluid analysis of the dynamic of the spectrum sharing mechanism



Case A, the fixed point is $(x^*, y^*) = (0.5, 0.3)$, $\gamma' : x + y - 0.8 = 0$.



Case B, the fixed point is $(x^*, y^*) = (0.5, 0)$, $\gamma' : x + y - 0.35 = 0$.

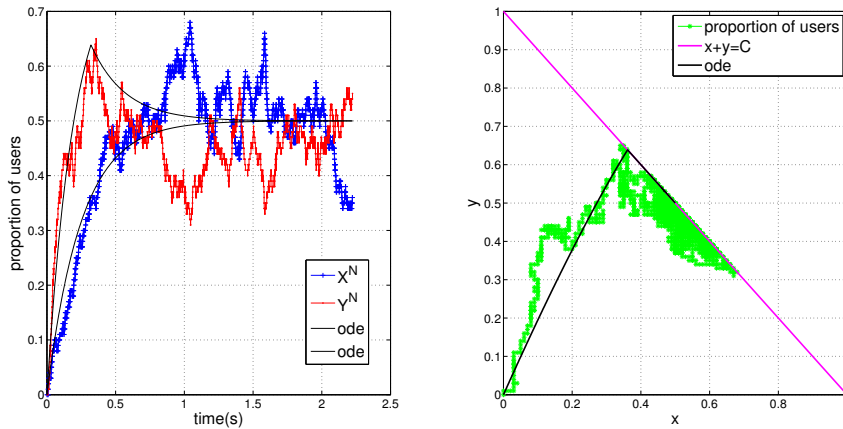
Figure 4.8: $N = 100$, $\lambda_1 = 2$, $\lambda_2 = 4$, $\mu_1 = 4$, $\mu_2 = 5$. Dashed line is $\lambda_1 - \mu_1 x - \mu_2 y = 0$ (where $(1, 1)^T f_2(x, y) = 0$), and dotted line is $\lambda_1 + \lambda_2 - \mu_1 x - \mu_2 y = 0$.

Working with the explanation of Section 4.1, in Case A the solution of the PWS system can not scape from γ' (sliding motion). However, in Case B the vector fields show that on γ' a transversal motion occurs. As we explained before, the abscissa of the fixed point is λ_1/μ_1 (it is not affected by the admission control), therefore the fixed point will be in the intersection of $x = \lambda_1/\mu_1$ and γ' . When that intersection is empty in the domain of interest, the fixed point will be $(\lambda_1/\mu_1, 0)$. Looking Case A, it is easy to notice that the fixed point is $(x^*, y^*) = (\lambda_1/\mu_1, \delta - \lambda_1/\mu_1)$, on the other hand in Case B it is $(x^*, y^*) = (\lambda_1/\mu_1, 0)$.

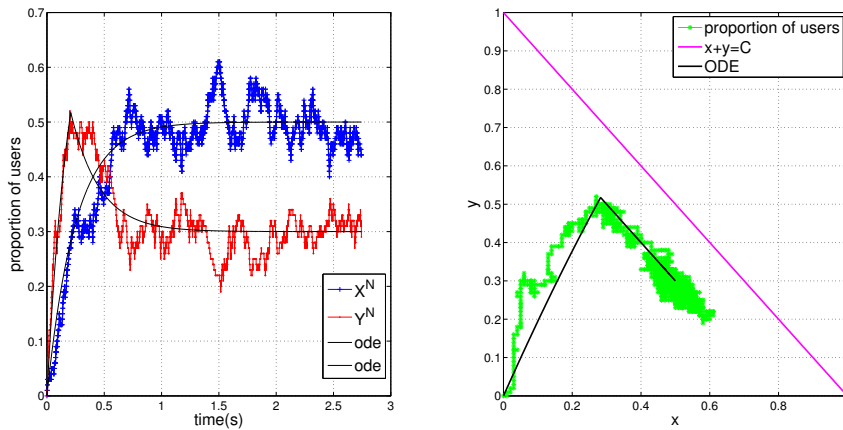
□

From Prop. 7 we can conclude that if you want to improve the spectrum usage, the location of admission control boundary is restricted by $\frac{\lambda_1}{\mu_1} < \delta$.

Chapter 4. Fluid Limits Approximation



Without Admission Control.



With Admission Control, AC boundary $\gamma'_1 : x + y - 0.8 = 0$.

Figure 4.9: Comparing the same system ($N = 100$, $\lambda_1 = 2$, $\lambda_2 = 4$, $\mu_1 = 4$, $\mu_2 = 5$) without and with admission control decisions. For each case we show the fluid limit and one trajectory of the corresponding Markov Chain.

In the graphics of Figure 4.9 we have the same system without and with an admission control. It is possible to observe that the fixed point changes its position, in particular, its ordinate. When there is no admission decisions, the fixed point is on γ then the mean spectrum utilization is C , we can say that most of the time the system is full. From the point of view of the SUs, they are strongly affected by the priority of PUs. In the other case, when the admission mechanism is considered, the fixed point is on γ' , then the mean spectrum utilization is $\delta = 0.8$. Please note that in this case the interruption probability (caused by preemptive behavior) is reduced.

The previous proposition can be extended to other types of admission control boundaries. As a general result, the fixed point, with an arbitrary access boundary defined by an equation $\Delta(x, y) = 0$, will be located at (x^*, y^*) with $x^* = \frac{\lambda_1}{\mu_1}$ and $\Delta(x^*, y^*) = 0$.

We have presented the analysis and characterization of a simple model of spectrum

4.4. Fluid analysis of the paid sharing approach

sharing in cognitive radio networks. We have considered a Markov Chain that represents the population of the different types of users in the system. We formulated the associated fluid model and we studied its solutions. In the next section we will use this analysis, incorporating the multichannel and economic aspects, to solve the optimization problem defined in Chapter 3.

4.4 Fluid analysis of the paid sharing approach

In this section, we will use the previous analysis in order to obtain a deterministic approximation of the optimal admission control boundary when payments and reimbursement are considered. Therefore, in this part of the thesis we will concentrate on the economic problem which objective consists in maximizing the total expected discounted profit of the primary service provider when there is an admission control policy over secondary users.

Recalling the multiresource economical problem formulated in Chapter 3, in this section we start from an infinite horizon Markov Decision Process (MDP) where the user arrivals are independent Poisson processes and the service durations are also independent and exponentially distributed. It is also assumed that each class of user demands b_i resources (each PU demands b_1 resources, and analogously each SU requires b_2 channel bands to its transmission). The state space of the MDP is thus defined by $S = \{(X, Y) : 0 \leq b_1X + b_2Y \leq C\}$. The economic parameters to be considered are: $R > 0$ (the reward collected for each band when a SU is allowed to exploit the PU's resource), $K > 0$ (the reimbursement when a preemption occurs) and α (the discount rate). Finally, it is important to remark that the set of available actions of the MDP are reflected in the admission control policy: accept or reject a new SU.

4.4.1 Multidemand system in the limit

Before we start with the analysis, a question that arises is: do optimal admission control boundaries have a particular shape? In Figure 4.10 we show two generic AC (admission control) boundaries⁴ obtained by Modified Policy Iteration algorithm for two sets of system parameters. We can see the linear correlation between X and Y in the AC boundaries, in both cases linear correlation coefficients are $|r| = 0.999$. Other examples to see this characteristic are located in Chapter 3.

Figure 4.10 suggests that the admission control boundary in the limit can be assumed as a line with equation $y = Ax + \delta$ with unknown A and δ ($A < 0$ and $0 \leq \delta \leq C$). This hypothesis will be used in the following analysis but it is important to highlight that our results and methodology can be extended to other characteristics of the admission control boundary.

In this context we have the three economic zones illustrated in Figure 4.11 (I, II and III). Please note that in the limit ($N \rightarrow \infty$) zone III converges to the line $b_1x + y - C =$

⁴AC boundary represents the optimal policy, in particular it divides the state space in two zones: one where SUs are accepted and the other one where they are refused.

Chapter 4. Fluid Limits Approximation

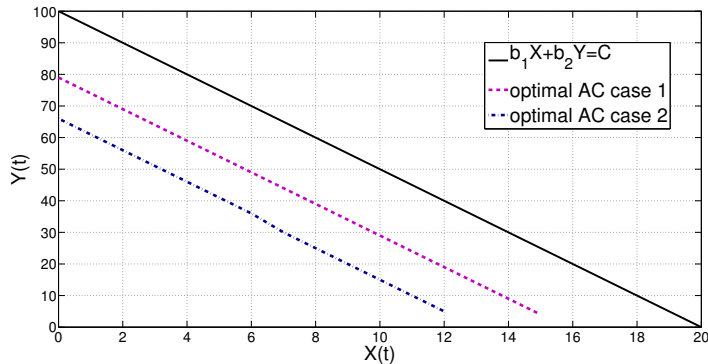


Figure 4.10: Optimal AC boundaries. Parameters of case 1: $\lambda_1 = 200$, $\lambda_2 = 500$, $\mu_1 = 0.1$, $\mu_2 = 1$, $R = 1$, $K = 3$, $C = 100$, $b_1 = 5$, $b_2 = 1$ and $\alpha = 50$. Parameters of case 2: $\lambda_1 = 300$, $\lambda_2 = 500$, $\mu_1 = 0.1$, $\mu_2 = 0.5$, $R = 1$, $K = 3$, $C = 100$, $b_1 = 5$, $b_2 = 1$ and $\alpha = 50$. The state space is the same in both cases ($\{(X, Y) : 0 \leq b_1X + b_2Y \leq C\}$) and linear correlation coefficient $|r| = 0.999$.

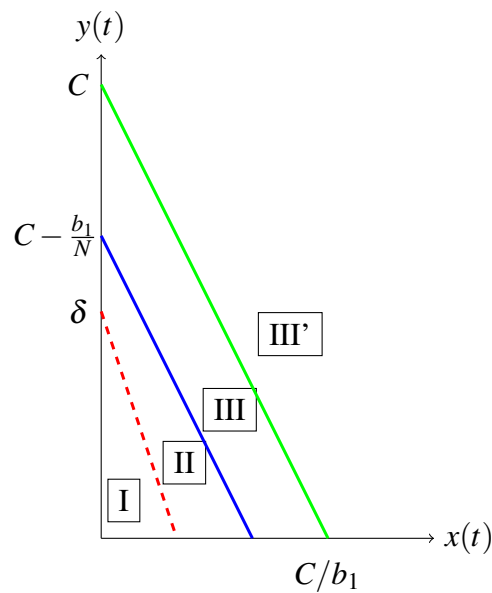


Figure 4.11: Considering $b_2 = 1$, we can divide the state space in three different economic zones. SUs are accepted in zone I and rejected in zones II and III. Zone III includes the states where SUs are deallocated and Zone II represents the “neutral” one (neutral in the sense that the SP does not earn nor lose). Zone III' is an “artificial zone” used to the definition of the fluid approximation.

0^5 (i.e. in the limit zone III disappears), then $z(t) = b_1x(t) + y(t) - C + b_1 = b_1$. As a consequence, in the limit we can think the system with only two economic zones (I and II).

If we turn our attention to these two regions (I and II), we have $f_1(x, y) = (\lambda_1 -$

⁵ $b_2 = 1$ for the explanation

4.4. Fluid analysis of the paid sharing approach

$\mu_1x, \lambda_2 - \mu_2y$) and $f_2(x, y) = (\lambda_1 - \mu_1x, -\mu_2y)$ the velocity vectors, both continuous in I and II respectively. In order to be in the context of [72] it is useful to artificially extend our processes beyond the region $\{b_1x + y \leq C\}$, assuming that in the region $\{b_1x + y > C\}$ (zone III') the vector field is $f_3 = (\lambda_1 - \mu_1x, -\lambda_1b_1 - \mu_2y)$ (representing the preempted scenario). Then, in our PWS system we identify three zones (I, II and III') and two lines ($\gamma' : -Ax + y - \delta = 0$ and $\gamma : b_1x + y - C = 0$). According to that and excluding the behavior on the lines, the deterministic system is driven by the following differential equations:

If $-Ax + y - \delta < 0$ (I):

$$\begin{cases} x' = \lambda_1 - \mu_1x, \\ y' = \lambda_2 - \mu_2y; \end{cases}$$

else, if $-Ax + y - \delta > 0$ and $b_1x + y - C < 0$ (II):

$$\begin{cases} x' = \lambda_1 - \mu_1x, \\ y' = -\mu_2y. \end{cases}$$

Some remarks are in order concerning the results. Firstly, the ODE in zones I and II are obtained directly using classical results on convergence of Markov processes. The difficult task consists in analyzing the system on γ and γ' .

Secondly, in the same way as in the previous sections, we have to study:

- $n'^T(x, y)f_1(x, y)$ and $n'^T(x, y)f_2(x, y) \forall (x, y) \in \gamma'$, and
- $n^T(x, y)f_2(x, y)$ and $n^T(x, y)f_3(x, y) \forall (x, y) \in \gamma$,

being $n'(x, y)$ and $n(x, y)$ the normal vectors to γ' and γ respectively. In this sense, we can identify different behaviors of the deterministic system solution in those borders like: transversal (or tangential) crossing and sliding motion (see details in Section 4.1). Please note that the behavior strongly depends on the values of $\lambda_1, \lambda_2, \mu_1, \mu_2, b_1, A$ and δ .

Finally, we can identify two scenarios depending on the value of $\frac{\lambda_1}{\mu_1}$:

- System saturated by PUs: $\frac{\lambda_1}{\mu_1} \geq \frac{C}{b_1}$, or
- System unsaturated by PUs: $\frac{\lambda_1}{\mu_1} < \frac{C}{b_1}$.

System saturated by PUs

If we consider the system in its rush hour traffic, i.e. $\lambda_1/\mu_1 \geq C/b_1$, we have that $n^T(\mathbf{x})f_3(\mathbf{x}) = -\mu_1b_1x - \mu_2y < 0, \forall \mathbf{x} \in \gamma$ and we can deduce that there is an interval of γ (including C/b_1) where $n^T(\mathbf{x})f_2(\mathbf{x}) = \lambda_1b_1 - \mu_1b_1x - \mu_2y > 0$. Then, the sliding motion condition is verified, at least, on an interval of γ . In this case it is possible to demonstrate that the fixed point is $(x^*, y^*) = (\frac{C}{b_1}, 0)$.

The PWS is completely defined including the dynamic on γ , which is:

$$\begin{cases} x' = \lambda_1 - \mu_1x, \\ y' = -\lambda_1b_1 + \mu_1b_1x. \end{cases}$$

Chapter 4. Fluid Limits Approximation

System unsaturated by PUs

On the other hand, if $\frac{\lambda_1}{\mu_1} < \frac{C}{b_1}$ we have three possible cases depending on the unknown values of A and δ . Let us give an intuitive explanation:

1. if $(\frac{\lambda_1}{\mu_1}, \frac{\lambda_2}{\mu_2})$ is in zone I ($-A\frac{\lambda_1}{\mu_1} + \frac{\lambda_2}{\mu_2} < \delta$), the fixed point is $(x^*, y^*) = (\frac{\lambda_1}{\mu_1}, \frac{\lambda_2}{\mu_2})$. Then, a solution starting in zone I will continue in zone I. In this case the admission control does not make sense (i.e. $A = -b_1$ and $\delta = C$). See more details in Proposition 6 of Section 4.3.
2. if $-A\frac{\lambda_1}{\mu_1} + \frac{\lambda_2}{\mu_2} > \delta$ and $\frac{\lambda_1}{\mu_1} > \frac{-\delta}{A}$, the fixed point is $(x^*, y^*) = (\frac{\lambda_1}{\mu_1}, 0)$ located in zone II. Then, a solution starting in zone I will continue in zone II and will die in II (transversal motion occurs on γ'). In the same way as in the previous case, the admission control does not make sense. See more details in Proposition 7 of Section 4.3.
3. if $-A\frac{\lambda_1}{\mu_1} + \frac{\lambda_2}{\mu_2} > \delta$ and $\frac{\lambda_1}{\mu_1} < \frac{-\delta}{A}$, the fixed point is $(x^*, y^*) = (\frac{\lambda_1}{\mu_1}, A\frac{\lambda_1}{\mu_1} + \delta)$ located on γ' (sliding motion). This condition is verified when $(\frac{\lambda_1}{\mu_1}, \frac{\lambda_2}{\mu_2})$ is in zone III' and $\frac{\lambda_1}{\mu_1} < \frac{C}{b_1}$. In this case, the corresponding PWS is completely defined including the dynamic on γ' as:

$$\begin{cases} x' = \lambda_1 - \mu_1 x, \\ y' = A(\lambda_1 - \mu_1 x). \end{cases}$$

In the next subsection we use this fluid approximation in order to solve the non-linear programming problem described in Chapter 3.

4.4.2 Optimization problem formulation

We have characterized the behavior of the dynamical system. Now we will formulate the economic problem using the deterministic approximation.

Let $R_{t_1}(x_0, y_0)$ be the SP profit function,

$$R_{t_1}(x_0, y_0) = \int_0^{t_1} \lambda_2 R e^{-\alpha t} dt - \int_{t_2}^{t_C} \lambda_1 K b_1 e^{-\alpha t} dt, \quad (4.10)$$

where t_1 verifies $-Ax(t_1) + y(t_1) = \delta$, t_2 verifies $b_1x(t_2) + y(t_2) = C$ and t_C is such that $b_1x(t_C) = C$.

Working with the fluid approximations of $x(t)$ and $y(t)$, we can re-write the optimization problem of Eq. (3.16) as:

$$\begin{aligned} & \underset{t_1}{\text{maximize}} && R_{t_1}(x_0, y_0) \\ & \text{subject to} && 0 \leq t_1 \leq t_C \\ & && b_1x(t_2) + y(t_2) = C \\ & && b_1x(t_C) = C. \end{aligned} \quad (4.11)$$

We are interested in obtaining the admission control boundary independently of the initial condition of the system, so we propose the following methodology:

4.4. Fluid analysis of the paid sharing approach

- Step 1: Choose a set of possible initial conditions $\{(x_0^i, y_0^i)\}, i \in \{1, \dots, n'\}$,
- Step 2: Run the optimization problem Eq. (4.11) to obtain $t_1^i, x(t_1^i)$ and $y(t_1^i)$,
- Step 3: Apply least-squares to define A and δ as those that minimize the mean square error.

Please note that when the system is unsaturated by PUs (this implies that $\nexists t_C$), in particular in the third case ($-A \frac{\lambda_1}{\mu_1} + \frac{\lambda_2}{\mu_2} > \delta$ and $\frac{\lambda_1}{\mu_1} < \frac{-\delta}{A}$) when the admission control decision makes sense, the solution of the optimal problem is $t_1 = t_2$ such that $b_1 x(t_2) + y(t_2) = C$. In the next section we shall present some simulations that will help us to gain insight about this methodology and analyze the accuracy of our results.

4.4.3 Simulated experiments and results

In order to validate the proposed approximation we will present some examples considering systems with a large but finite number of channel bands. In each scenario, we calculate the admission control boundary using the proposed methodology and we compare it with the results obtained by Modified Policy Iteration algorithm (one of the best known practical algorithms for solving infinite-horizon MDPs, the algorithm improved in Chapter 3).

We divide the validation tests into three groups. First, we study scenarios where system parameters verify $\frac{\lambda_1}{\mu_1} < \frac{C}{b_1}$. Then, for $\frac{\lambda_1}{\mu_1} \geq \frac{C}{b_1}$ we analyze the impact of the parameter b_1 considering the particular case when $\mu_1 = \mu_2$. In this situation, as we have demonstrated in the previous Chapter, the optimal admission control boundary is a line with equation $b_1 x + b_2 y = \delta$ (being δ the only parameter to be determined). Finally, also for the system in its rush hour, we show the performance of the approximation in general cases (e.g. different arrival and departure rates, and different prices).

System unsaturated by PUs

With the analysis of the fluid limit we concluded that $A = -b_1$ and $\delta < C$ but very closely to C . We can approximate the AC as the line $b_1 x + y = C$. This result is independent of prices and discount rate.

In table 4.1 we present a set of cases which verify $\frac{\lambda_1}{\mu_1} < \frac{C}{b_1}$ and in Figure 4.12 the correspondent AC boundaries obtained by Modified Policy Iteration. We can conclude that the fluid approximation is accurate.

For one of the examples, the one that has $y = h(x)$ as the optimal AC boundary, we run the MPI algorithm considering different N values. In Figure 4.13 we can see that the fluid estimation is more accurate when N is large.

Different primary bandwidth requirements considering $\frac{\lambda_1}{\mu_1} \geq \frac{C}{b_1}$.

As a first illustration of the accuracy of our proposal when the system is operating in saturated traffic conditions of PUs, we consider scenarios where $\mu_1 = \mu_2$ (the same departure rate in both classes of users). In this particular case, where some characteristics of the

Chapter 4. Fluid Limits Approximation

Table 4.1: AC boundaries obtained by Policy Iteration. Parameters common to all cases: $N = 100$, $\mu_1 = 0.1$, $\mu_2 = 1$, $R = 1$, $C = 1$, $b_1 = 5$, $b_2 = 1$ and $\alpha = 5$. The line $b_1 X^N + Y^N(t) = C$ represents an estimation of the AC boundary obtained by our approximation.

K	λ_1	λ_2	AC boundary
3	0.01	2	$y = f(x)$
10	0.01	2	$y = g(x)$
10	0.01	5	$y = h(x)$

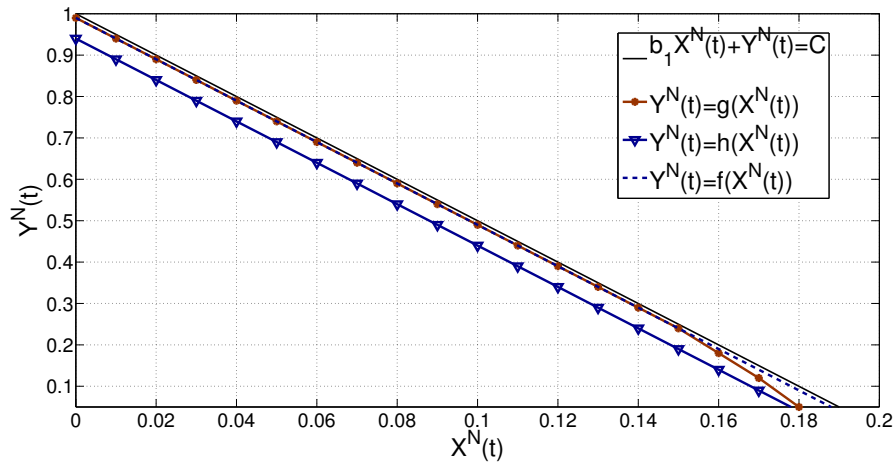


Figure 4.12: Optimal AC boundaries $f(x)$, $g(x)$ and $h(x)$ obtained by Modified Policy Iteration (see Table 4.1).

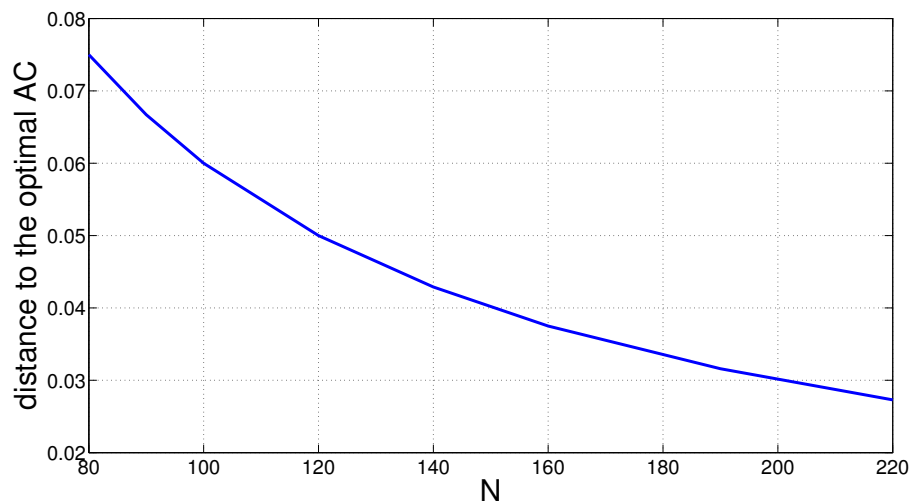


Figure 4.13: Distance between Optimal AC boundary $y = h(x)$ (see Table 4.1) and the fluid AC estimation $b_1 x + b_2 y = C$.

4.4. Fluid analysis of the paid sharing approach

admission control boundary are already known, the methodology requires only one initial condition on Step 1 ($n' = 1$). This represents an immediately calculation of policy parameters. We test the approximation with different b_1 values ($b_1 = 1, 2, 5, 10$). The rest of the network parameters (e.g. rates, prices, number of total channel bands) are the same in all the examples.

In table 4.2 we present the ACs boundaries for all the cases. In order to test how close to the optimal is the approximation, we make several experiments ($n = 30$) with both boundaries (the optimal and its approximation) and compute the profit of the SP. Each experiment consists in one realization of the continuous time Markov chain using the appropriate AC boundary. In each transition the discount profit of the SP is computed. We build the reward confidence intervals and they are included in table 4.2.

Some remarks regarding the obtained results are in order. Firstly, these results lead us to conclude that our fluid limit provides an excellent approximation of the optimal one. Secondly, we observe that the deterministic approximation is more conservative than the stochastic one. This is a direct consequence of the limit of the penalty zone. Lastly, we can observe the quality of our model in the curves of Figure 4.14 where we show the evolution on the plane of two realizations of the MDP together with the PWS system solution.

Table 4.2: AC boundaries and reward confidence intervals (0.95 level of confidence) obtained by both methods. System parameters: $N = 100$, $\lambda_1 = 3$, $\lambda_2 = 5$, $\mu_1 = \mu_2 = 0.1$, $R = 1$, $K = 3$, $C = 1$, $b_2 = 1$ and $\alpha = 50$.

b_1	AC boundary	Modified Policy Iteration		Fluid Model	
		δ	Reward	δ	Reward
1	$x + y = \delta$	0.93	10.6 ± 0.6	0.92	10.7 ± 1.0
2	$2x + y = \delta$	0.86	9.76 ± 0.55	0.85	9.76 ± 0.45
5	$5x + y = \delta$	0.65	5.86 ± 0.74	0.62	5.95 ± 0.65
10	$10x + y = \delta$	0.29	0.66 ± 0.40	0.24	0.81 ± 0.47

Different arrivals and departure rates considering $\frac{\lambda_1}{\mu_1} \geq \frac{C}{b_1}$.

When we think about cognitive radio networks and even more when we think about IoT applications using licensed spectrum as secondaries, we commonly imagine different primary and secondary services (e.g. Internet access provided using White Space frequency bands [57]), then the natural situation is to model them with different arrival and service rates. With that in mind, we test the methodology in generic cases.

In Figure 4.15 and in Table 4.3 we present the results of two examples. The differences between them are the arrival and departure rates of PUs and SUs. The estimation of the AC boundary is obtained using the methodology introduced before for different values of initial conditions. In particular, for each case we have solved the optimization problem using $n' = 5$ different initial conditions and then we have applied least-squares. Please note that the optimal AC boundaries are not necessarily lines when $\mu_1 \neq \mu_2$, in particular see case 2 where the boundary is a piecewise linear function with three line segments (one when $x(t) \in [0, 0.06]$, the second when $x(t) \in [0.06, 0.065]$ and the third when $x(t) \in$

Chapter 4. Fluid Limits Approximation

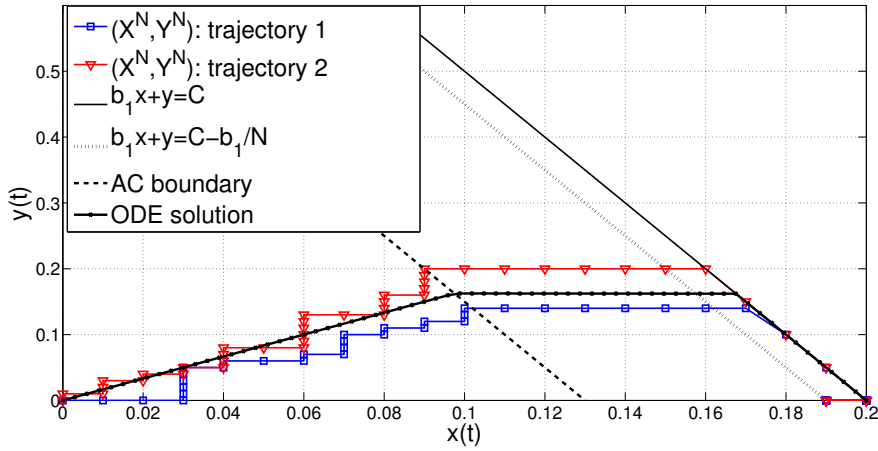


Figure 4.14: Evolution on the plane of the Markov Chain (two realizations) and the PWS. Parameters: $N = 100$, $\lambda_1 = 3$, $\lambda_2 = 5$, $\mu_1 = \mu_2 = 0.1$, $R = 1$, $K = 3$, $C = 1$, $b_1 = 5$, $b_2 = 1$ and $\alpha = 50$. AC boundary: $b_1x + y = 0.63$.

$[0.065, 0.12]$. Continuing with case 2, we can say that for $x(t) > 0.12$ all SU arrivals will be rejected.

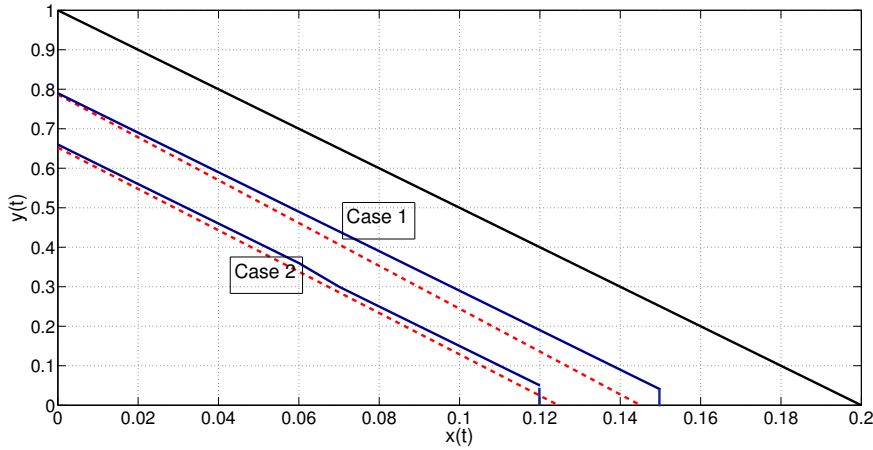


Figure 4.15: Solid and dashed lines represent optimal and estimated AC boundaries respectively. Parameters of case 1: $N = 100$, $\lambda_1 = 2$, $\lambda_2 = 5$, $\mu_1 = 0.1$, $\mu_2 = 1$, $R = 1$, $K = 3$, $C = 1$, $b_1 = 5$, $b_2 = 1$ and $\alpha = 50$. Parameters of case 2: $N = 100$, $\lambda_1 = 3$, $\lambda_2 = 5$, $\mu_1 = 0.1$, $\mu_2 = 0.5$, $R = 1$, $K = 3$, $C = 1$, $b_1 = 5$, $b_2 = 1$ and $\alpha = 50$.

Again, our estimation shows a very good performance in both cases. This demonstrates the versatility of our technique.

4.5. Fluid analysis and QoS for secondary users

Table 4.3: Reward confidence intervals (0.95 level of confidence) obtained by both methods. Parameters of case 1: $N = 100$, $\lambda_1 = 2$, $\lambda_2 = 5$, $\mu_1 = 0.1$, $\mu_2 = 1$, $R = 1$, $K = 3$, $C = 1$, $b_1 = 5$, $b_2 = 1$ and $\alpha = 50$. Parameters of case 2: $N = 100$, $\lambda_1 = 3$, $\lambda_2 = 5$, $\mu_1 = 0.1$, $\mu_2 = 0.5$, $R = 1$, $K = 3$, $C = 1$, $b_1 = 5$, $b_2 = 1$ and $\alpha = 50$.

Case	Policy Iteration	Fluid Model
1	8.16 ± 0.82	7.60 ± 0.70
2	4.87 ± 0.51	4.30 ± 0.70

4.5 Fluid analysis and QoS for secondary users

One challenge today is to distribute the spectrum holes efficiently and fairly. Another goal is to guarantee quality of service (QoS) to the SUs. In this part of the thesis, as another contribution, we will exploit the fluid model in order to analyze two features of the cognitive system: the mean spectrum utilization and the probability that the SUs services can be interrupted. Associated with this last issue we will analyze a possible admission control policy in order to reduce this probability. Our main findings consist in a Gaussian limit theorem in the sub-critical case, and a non-Gaussian limit theorem (under a different scaling scheme) in the critical case. Both these results are based on fluid limits techniques, and the second one is non-classical in this type of problems. The asymptotic distribution allows to analyze the interruption probability for SUs giving some kind of confidence bounds valid when the number of users is large. In the case of non-Gaussian distribution, the stationary regime and its limit is described explicitly in a simplified case. Using our results we also present some practical network design criteria.

In this section we consider $b_1 = b_2 = 1$ to simplify the analysis using directly Propositions 6 and 7. Remembering the description of the system, based on this assumption, if $x + y = C$ and a PU arrives, a SU will be immediately deallocated giving the channel to the new PU. In this case, the QoS perceived by the SU will be affected because of the interruption of its communication. In this part of the thesis, we are interested in SUs whose service cannot be interrupted with high probability (like a phone call or other interactive services). For these services it is preferable to let the connection be rejected to avoid the situation where the connection is established and then interrupted.

As we have analyzed in previous sections, given the fact that the abscissa of the PWS system fixed point is not affected with the control action $a(x, y)$, the objective is to move the fixed point ordinate looking for a better operation point. Working with the zones defined in 4.3:

$$\begin{aligned} \gamma &: x + y = C, \\ R_1 &: x + y < C, \\ R_2 &: x + y > C; \end{aligned}$$

we can make a first conclusion: the fixed point of the fluid limit must be out of γ (it must be in R_1). Even more it has to be far enough from γ to avoid a strong impact on secondary communications, however, it has to be as close as possible to γ to permit more spectrum utilization and a good SU's access probability.

Chapter 4. Fluid Limits Approximation

In the cases of Group 1 of 4.3 (the sub-critical cases where the fixed point is in R_1), if the fixed point is far enough from γ , the admission control does not make sense. So, the first question to be answered is: how can we determine if it is far enough? Obviously, it fully depends on the QoS requirement for the SU's traffic (for example, a criterion could be to guarantee a low value of probability of service interruption). On the other hand, if it is not far enough, how can we move the fixed-point? The cases of Group 2 of 4.3 (critical ones) are totally related with this last question. In these cases, the system in stationary state works near γ , so the probability of service interruption is too large. According to that, the analysis in the following subsections is going to be concentrated on answering the above questions.

4.5.1 Possible criteria and actions

Question 1: Is the fixed point of the PWS system far enough from γ ?

Considering Group 1 cases defined in 4.3 ($\lambda_1/\mu_1 + \lambda_2/\mu_2 < C$) and the PWS system trajectory remains all time in R_1 , it is possible to apply known results (see Theorem 2.3 of Chapter 11 in [67]). That is to say, let (x, y) be the trajectory of the PWS system with initial condition $(x(0), y(0))$, if

$$\lim_{N \rightarrow +\infty} \sqrt{N}[(X^N(0), Y^N(0)) - (x(0), y(0))] = \chi(0) \quad (4.12)$$

with $\chi(0)$ deterministic, then, $\sqrt{N}[(X^N(t), Y^N(t)) - (x(t), y(t))] \Rightarrow \chi(t)$ where $\chi(t)$ is a two-dimensional Gaussian process and its covariance matrix can be determined explicitly by:

$$\text{Cov}(\chi(t), \chi(r)) = \int_0^{t \wedge r} e^{A(t-s)} G(x(s), y(s)) [e^{A(r-s)}]^T ds \quad (4.13)$$

where $A = \begin{pmatrix} -\mu_1 & 0 \\ 0 & -\mu_2 \end{pmatrix}$, $G(x(s), y(s)) = \begin{pmatrix} \lambda_1 + \mu_1 x(s) & 0 \\ 0 & \lambda_2 + \mu_2 y(s) \end{pmatrix}$ and M^T denotes the transpose of matrix M .

In sub-critical cases, we can conclude that $\lim_{N \rightarrow +\infty} P(X_1^N(t) + X_2^N(t) = C) = 0$ for all t . As we have shown in all the simulated examples of the chapter, the fluid limit is an excellent approximation when N is large (and finite). Then, considering the defined Gaussian process and a finite large N we can present a practical criterion to analyze if the PWS system fixed point is far enough from γ . In particular, we can obtain confidence bounds and also infer an adequate number of channels to be consider in the system in order to avoid a high interruption probability for SUs.

Practical criterion for sub-critical cases: If the resulted confidence ellipse is entirely inside R_1 , certain probability of non-interruption is guarantee. Otherwise, we should try to move the fixed point.

In more details, when $\lim_{t \rightarrow +\infty} G(x(s), y(s)) = G(x^*, y^*) = G(\infty)$, we can obtain the covariance matrix $\Sigma(\infty)$ solving (as in [77])

$$A\Sigma(\infty) + \Sigma(\infty)A^T = -G(\infty). \quad (4.14)$$

An example is presented in Figure 4.16 where we show the theoretical 95% confidence ellipse determined by Kurtz's theorem and also a simulated confidence one. We simulated

4.5. Fluid analysis and QoS for secondary users

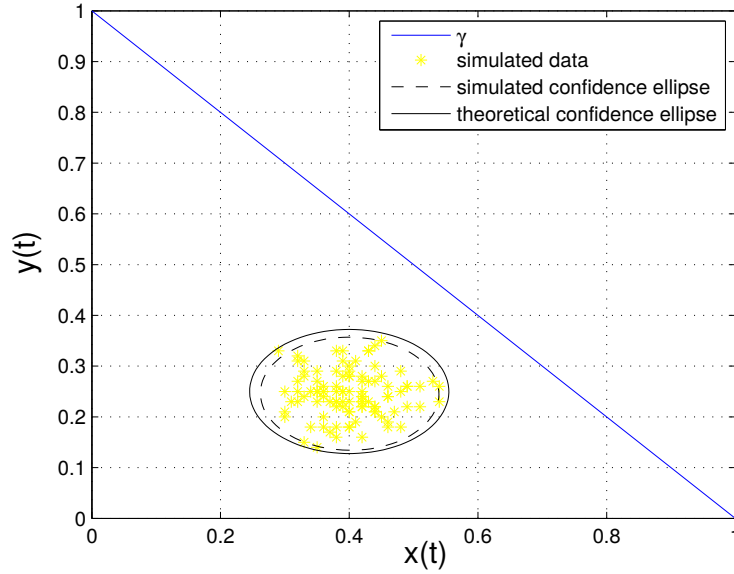


Figure 4.16: Simulated and theoretical 95% confidence ellipses of $(X^N(t), Y^N(t))$, considering a large t value, parameters: $N = 100$, $\lambda_1 = 2$, $\lambda_2 = 1$, $\mu_1 = 5$ and $\mu_2 = 4$. Theoretical is determined using Eq. (4.14).

$n = 100$ independent samples of $(X^N(t), Y^N(t))$ considering the same large t value. The simulated ellipse is obtained from the empirical covariance matrix. In this particular case, an admission control is not necessary because the ellipse is totally in R_1 . In other words, this means that the stochastic system $(X^N(t), Y^N(t))$ has low probability to reach γ .

On the other hand, considering a fixed relation between both classes $\frac{\lambda_1/\mu_1}{\lambda_2/\mu_2} = \text{constant}$, using the deterministic ellipse we can infer which is the ideal scaled parameter. In other words, we can obtain an idea of the optimal number of resources (channels) necessary to guarantee a small interruption probability to SUs. In Figure 4.17 we show the theoretical confidence ellipses considering different values of N for two cases (Case A and Case B). In particular, we have considered $C = 1$, then N represents the number of channels of the system $(\tilde{X}^N(t), \tilde{Y}^N(t))$. For Case A, we have the ellipse tangent to γ when $N = 180$. Therefore, we can conclude that an admission control does not make sense in the system $(\tilde{X}^N(t), \tilde{Y}^N(t))$ when $N \geq 180$. For Case B, an analogous conclusion we have when $N \geq 120$.

Question 2: How can we move the fixed point of the PWS system?

As we saw before in Section 4.3, the fixed point can be moved by applying admission control decisions. Working with cases of Group 2 of Section 4.3 and continuing the example of $\gamma' : x + y - \delta = 0$ as the admission control border, the question is: what is a reasonable value of δ ? In this case, the hypotheses of Theorem 2.3 of Chapter 11 in [67] are not verified. We have convergence of the stationary regime to the PWS system fixed point but there is not a general framework that allows to state a Gaussian asymptotic

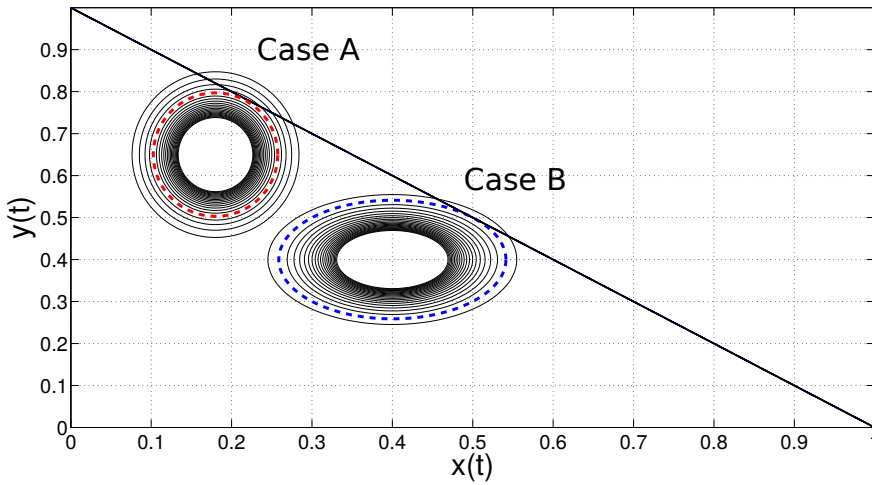


Figure 4.17: Theoretical 95% confidence ellipses of $(X^N(t), Y^N(t))$, considering different N values ($N = 100, 120, 140, 160, \dots, 500$). Parameters of Case A: $C = 1$, $\lambda_1 = 9$, $\lambda_2 = 13$, $\mu_1 = 50$ and $\mu_2 = 20$. Parameters of Case B: $C = 1$, $\lambda_1 = 10$, $\lambda_2 = 12$, $\mu_1 = 25$ and $\mu_2 = 30$.

distribution. In this case, we proceed computing the asymptotic stationary distribution of the total number of users in the particular case when service rates are the same for primary and secondary users. Using the limit of the invariant distribution for the particular case, we can build some design criteria in order to find an estimation of the optimal δ value for certain maximum level of interruption probability. We will see that the criteria can also be used when $\mu_1 \neq \mu_2$.

Consider the Markov chain when $\mu_1 = \mu_2$. If we consider $W = Y + X$ we have a one dimensional Markov chain with state space $E = \{0, 1, \dots, C\}$, and non-zero transition rates from i to j , $q(i, j)$, given by:

$$q(i, i+1) = \begin{cases} \lambda_1 + \lambda_2 & \text{for } 0 \leq i < \delta \\ \lambda_1 & \text{for } \delta \leq i < C \end{cases}, \quad q(i, i-1) = i\mu \text{ for } 0 < i \leq C,$$

where $\delta \in E$ denotes the border of the admission control, that is when we have δ or more users we prohibit the access of new secondary users.

In order to simplify notation in what follows let us call $v_2 = \lambda_1 + \lambda_2$, and $v_1 = \lambda_1$, then we have the following transition rates:

$$q(i, i+1) = \begin{cases} v_2 & \text{for } 0 \leq i < \delta \\ v_1 & \text{for } \delta \leq i < C \end{cases}, \quad q(i, i-1) = i\mu \text{ for } 0 < i \leq C,$$

with $v_1 < v_2$. W is a modification of a $M/M/C/C$ queue, where the arrivals change their rate depending on number of clients in the queue. Please note that we can compute analytically the stationary distribution $\pi(i) \forall i = 0 \dots C$ for this Markov chain [88]:

$$\begin{aligned} \pi(i)v_2 &= \pi(i+1)(i+1)\mu \text{ for } 0 \leq i < \delta, \\ \pi(i)v_1 &= \pi(i+1)(i+1)\mu \text{ for } \delta \leq i < C. \end{aligned}$$

4.5. Fluid analysis and QoS for secondary users

Defining $\rho_1 = \frac{v_1}{\mu}$ and $\rho_2 = \frac{v_2}{\mu}$, we have:

$$\begin{aligned} \pi(i) &= \frac{\rho_2^i}{i!} \pi(0) \quad \text{for } 0 \leq i \leq \delta, \\ \pi(i) &= \left(\frac{\rho_2}{\rho_1}\right)^\delta \frac{\rho_1^i}{i!} \pi(0) \quad \text{for } \delta < i \leq C, \end{aligned}$$

where

$$\pi(0)^{-1} = \sum_{i=0}^{\delta} \frac{\rho_2^i}{i!} + \left(\frac{\rho_2}{\rho_1}\right)^\delta \sum_{i=\delta+1}^C \frac{\rho_1^i}{i!}.$$

Using the results of Prop. 7 and working with the scaled process $\tilde{W}^N = \tilde{X}^N + \tilde{Y}^N$ with the scaling parameters: v_1N , v_2N , CN and δN , we also have that $W^N = \frac{1}{N}\tilde{W}^N$ converges in probability, uniformly over compact time intervals to w , given by the following equations, for $0 \leq \delta \leq C$.

If the initial condition is $w(0) < \delta$

$$w' = \begin{cases} v_2 - \mu w & \text{if } w < \delta \\ 0 & \text{if } w = \delta. \end{cases}$$

If the initial condition is $w(0) > \delta$

$$w' = \begin{cases} v_1 - \mu w & \text{if } w < \delta \\ 0 & \text{if } w = \delta. \end{cases}$$

As follows from Section 4.3, from the study of the scaled system, its fluid approximation and the stationary points of the deterministic approximation, we have that when $\rho_1 = \frac{v_1}{\mu} < \delta < \frac{v_2}{\mu} = \rho_2$ the fixed point for the deterministic approximation in dimension 2 is in the admission control border $\{(x, y) : x + y = \delta\}$.

In the next proposition we present a geometric distribution that characterizes $\tilde{W}^N - N\delta$. It will be useful in order to estimate the δ value.

Proposition 8. *The stationary distribution of $\tilde{W}^N - N\delta$ converges to the distribution of an integer variable Z given by*

$$P(Z = j) = \begin{cases} \rho \left(\frac{\rho_2}{\delta}\right)^j & \text{if } j < 0, \\ \rho \left(\frac{\rho_1}{\delta}\right)^j & \text{if } j \geq 0, \end{cases}$$

where $\rho_1 = \frac{v_1}{\mu}$, $\rho_2 = \frac{v_2}{\mu}$, $\rho = \left(\frac{\rho_1}{\delta - \rho_1} + \frac{\rho_2}{\rho_2 - \delta}\right)^{-1}$.

Proof. The proof is in L. Aspirot PhD thesis [89]. □

Chapter 4. Fluid Limits Approximation

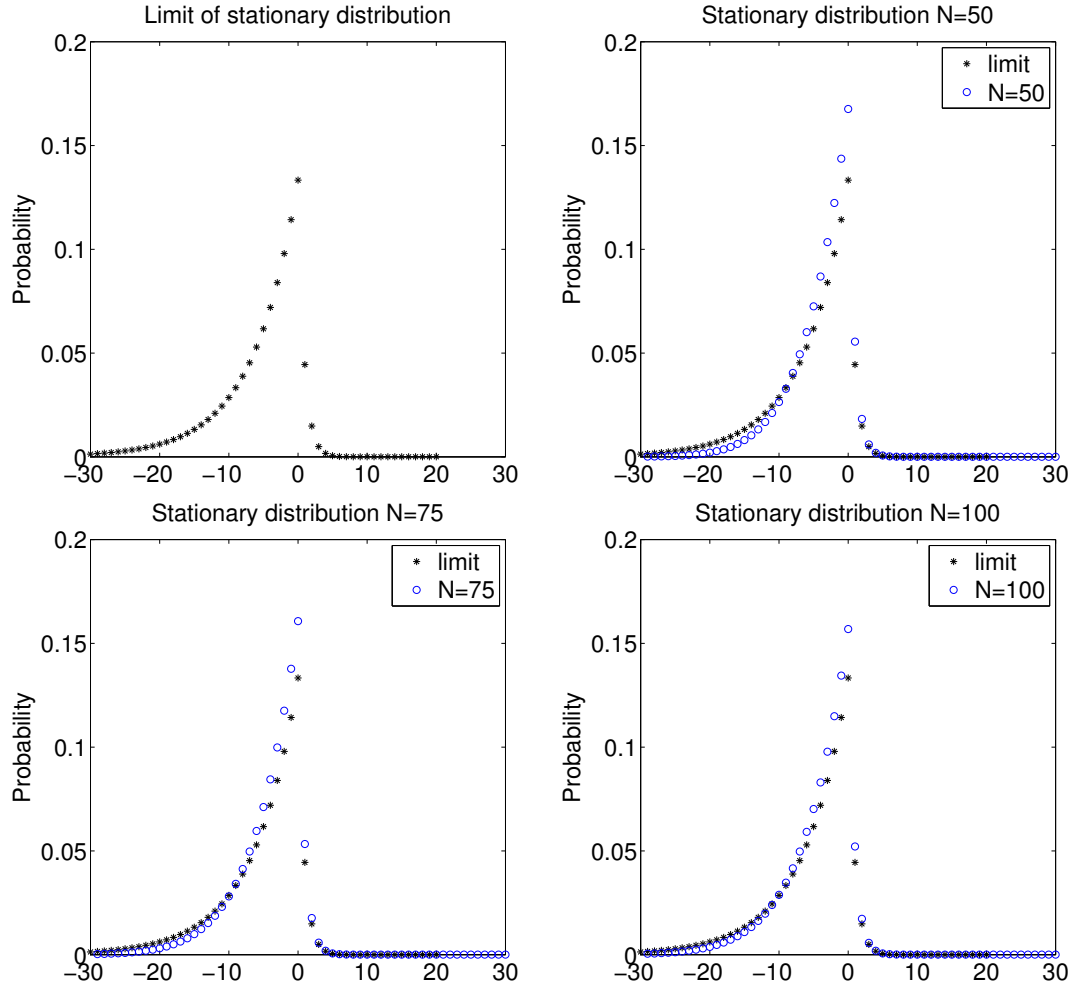


Figure 4.18: Limit ($N \rightarrow \infty$) of stationary distribution and stationary distributions for different N values. Parameters: $C = 5$, $\delta = 3$, $\rho_1 = 1$, $\rho_2 = 3.5$.

In Figure 4.18 we show the limit distribution and the stationary distribution for different values of N . We can conclude that the limit distribution represents a good estimation of the stationary one for all N values.

Using this result we can improve the average utilization of the spectrum while ensuring a small probability of interruption to the secondary users. Please note that the result is valid for $\mu_1 = \mu_2$. For the general case, we can not obtain an analytical expression of the distribution but we can estimate δ considering $\mu = \min\{\mu_1, \mu_2\}$ (the worst case).

Our proposal consists in relate the value of δ with the probability that the process lives on γ , then

$$P(\tilde{X}^N + \tilde{Y}^N = CN) = P(\tilde{W}^N = CN) = P(\tilde{W}^N - N\delta = CN - N\delta).$$

According to Prop. 8 we can assume that

$$P(\tilde{X}^N + \tilde{Y}^N = CN) \approx \rho \left(\frac{\rho_1}{\delta} \right)^{N(C-\delta)} \quad (4.15)$$

for large values of N .

Assuming a threshold on the probability of interruption which can be represented by $P(\tilde{X}^N + \tilde{Y}^N = CN) \leq \varepsilon$ for certain ε and considering CN as the total number of channels in the system, using Eq. (4.15) it is possible to obtain an upper bound of $\hat{\delta} = \delta(N, C, \varepsilon)$.

As an example we made different sets of simulations changing the value of N considering the parameters $\lambda_1 = 2$, $\lambda_2 = 4$, $\mu_1 = 4$ and $\mu_2 = 5$. In Figure 4.19 it is shown the probability that the system is full for different N values. In this case we have used $\mu = 4$ (the most critical case). Considering $\varepsilon = 0.1$ we can conclude that if we need $P(\tilde{X}^N + \tilde{Y}^N = CN) \leq 0.1$, we obtain an upper bound of δ ($\hat{\delta}$) depending on N (see Table 4.4).

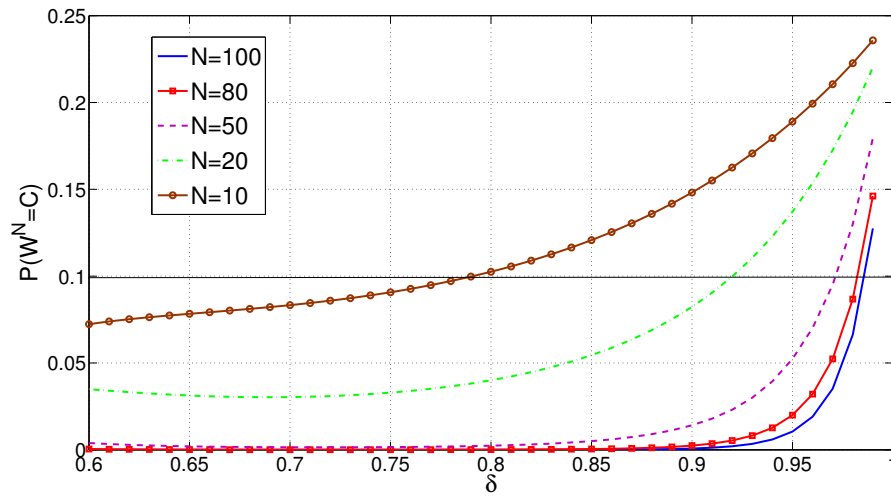


Figure 4.19: Parameters: $\lambda_1 = 2$, $\lambda_2 = 4$, $\mu_1 = 4$, $\mu_2 = 5$.

N	$\hat{\delta}$
100	0.986
80	0.982
50	0.951
20	0.920
10	0.791

Table 4.4: Upper bounds to δ in order to ensure $P(\tilde{X}^N + \tilde{Y}^N = CN) \leq 0.1$.

4.6 Conclusions

Throughout this chapter we have worked with the fluid approximation of the number of users in the network. We have successfully addressed two main problems: maximizing the primary SP reward and improving QoS of secondary users. We have presented some

Chapter 4. Fluid Limits Approximation

tools and approaches that can be used to deal with those problems when the number of channels is large as well as the user arrival rates. In the next chapter we will summarize the main contributions of Part I of the thesis.

Chapter 5

Conclusions of Part I

We have studied a general asymmetric queueing system and we have applied the obtained results to the cognitive radio network context. In particular we have characterized a paid-sharing approach as a spectrum allocation mechanism where SUs pay for the spectrum utilization and preemptive situations are also contemplated. In this model when a PU arrives to the system and the free capacity is insufficient, at least one SU is deallocated and reimbursed for its service interruption implying some cost for the primary SP. This interruption also has an impact in the QoS perceived by SUs.

We have considered a general model with different demands, different arrivals and different departure rates between PUs and SUs. We have proposed distinct alternatives to obtain the admission control policy for SUs that maximize the long-run discount profit of the SP. Different techniques have been used to achieve completeness in the analysis of the problem.

On the one hand, we have modeled the optimal revenue problem as a Markov decision process. As one of the main contribution, we have characterized many properties of the structure of the optimal admission control policies. As an example of application of these results, we have proposed different alternatives to improve the performance of Modified Policy Iteration (MPI) algorithm which is one of the most used mechanisms for solving MDP problems. Our new versions of the algorithm show drastically shorter running-times than the original MPI. The simulation experiments indicate the time efficient can be improved in more than 70%. On the other hand, we have studied the behavior of the control system using a fluid approximation of the MDP. We have developed a computationally efficient way to find an estimation of the optimal admission control boundary using the deterministic approximation. Through extensive simulations we have verified that the obtained approximation is accurate.

Finally, we have considered a Markov Chain that represents the population of the different types of users in the system. Using the fluid approximation we have proposed different network design criteria, for a system with a large number of users, which guarantee with high probability that secondary users in the system will not have service interruptions. This criteria is suggested by a theoretical analysis and supported by simulations. It is important to remark that all the contributions have been evaluated through extensive sets of simulations.

This page was intentionally left blank.

Part II

Spectrum resource assignment: user interactions and geometric aspects in cognitive radio networks

Chapter 6

Introduction to Part II

The second part of this thesis is dedicated to another approach of resource allocation problem in cognitive radio networks. A wireless network can be viewed as a collection of user located in an area where there are a large amount of concurrent transmissions. The idea here is to incorporate into the model: user interactions, interference, channel characteristics, spatial reuse of frequency bands and geometric aspects. Then, we address a network capacity analysis based on random graphs and stochastic geometry tools.

Let us define the most important performance metrics in these kind of networks: the Medium Access Probability (MAP) and the Coverage Probability (COP). The former represents the mean number of concurrent transmissions that take place in a network divided by the total number of nodes. Given the network and the PUs utilization, one of the main performance metrics of interest here is naturally the MAP of SUs. This value measures the portion of spectrum “wasted” by PUs and which may be leveraged by SUs. Due to the interference, not every transmission attempt is successful. In this sense, COP measures this probability of success. In this context, primary COP value gives an idea of the degradation of PU’s communications caused by the presence of SUs. COP is also a key value to estimate the throughput obtained by primary and secondary users.

Many works like [43–48] have demonstrated that mathematical techniques such as stochastic geometry [90] and random graphs [91, 92] are excellent tools in order to estimate diverse wireless network performance metrics. They are specially useful to model interactions between nodes in large random networks. This randomness may include node positions, node mobility, fading, or traffic (stochastic arrivals and departure).

Stochastic geometry allows to study the average behavior over many spatial realizations of a network whose nodes are placed according to some spatial probability distribution. Generally, the location of the nodes is assumed to be a realization of an homogeneous Poisson point process (PPP). Moreover, and for particular cases, these probabilistic models may include other factors such as propagation models, transmitting power, receiving sensitive, antenna radiation patterns, signal polarization, and power/interference thresholds. The articles [49, 93, 94] are the most representative examples of the use of stochastic geometry in cognitive radio networks. The authors obtained closed formulas for bounds of some performance metrics (such as MAP) in different CR network contexts. However, in some scenarios the obtained bounds are very conservative. Moreover, in more general cases (e.g. when the processes involved are not Poisson or when the fading variables are

not independent), determining these bounds is a difficult task, if not impossible.

On the other hand, since we are interested in the MAP, many network characteristics (e.g. propagation models, transmitting power, etc.) can be abstracted into a (random) graph. Vertices in the graph represent nodes (or links) of the wireless network, and two nodes (or links) are connected by an edge when they cannot transmit simultaneously (as a consequence of the medium access mechanism, or the spectrum sensing capabilities of SUs). Then, the study of these structures provides an alternative route in order to predict performance metrics such as the MAP. In particular, recently the authors of [95] proposed a methodology for very general random graphs (characterized by the node's degree distribution), and they proved that some key properties of the system can be captured by ordinary differential equations. Authors of [45] applied this method in a wireless environment (RTS/CTS CSMA network) and obtained accurate results in the estimation of the MAP, whereas the methodology was further refined and simplified in [96].

The main questions that motivate this part of the thesis are: what are the possibilities offered by cognitive radio to improve the effectiveness of spectrum utilization? and what is the impact in PUs communications caused by the presence of SUs? With this in mind, firstly in Chapter 7 we choose an approach based on stochastic geometry and we extend the probabilistic framework developed in [49] to a multichannel scenario in CR. Secondly, in Chapter 8 we propose a methodology, based on configuration models for random graphs, to estimate the medium access probability of secondary users. We perform simulations to illustrate the accuracy of our results and we also make a performance comparison between our estimation based on random graph and one obtained by a stochastic geometry approach. Finally, this part of the thesis closes with Chapter 9.

Chapter 7

A stochastic geometry analysis of multichannel CR network

7.1 Introduction

Stochastic geometry is a powerful tool that allows to define and compute macroscopic properties of a wireless network by averaging over all potential geometrical patterns of the nodes (see [97] for a survey). In this context, point processes are used to represent the spatial distribution of the network entities being the Poisson point process (PPP) the most popular and well-understood point process in the literature due to its simplicity and tractability. Some of the pioneering works in this field are [43, 44] and the references therein.

Stochastic geometry is specially useful to model interactions between nodes in large random networks. This randomness may include node positions, node mobility, fading, and/or traffic (stochastic arrivals and departure). Mathematical preliminaries for stochastic geometry modeling and point processes are presented in Appendix A. This will allow to better understand the discussion and results presented later in this chapter and in Chapter 8.

The articles [49, 93] are the most representative examples of the use of this technique in CR networks. In those works, the authors developed a probabilistic model to analyze the performance of different MAC protocols within this context. They concentrated their analysis in a unique cell; that is to say, all users can transmit in the same channel band. We aim at generalize these results in the multichannel case. In particular, we are interested in estimating MAP and COP in scenarios where more than one band is available, which is a natural situation in cognitive radio networks. We want to concentrate our analysis in large random ad hoc or wireless sensor networks, not precisely in infrastructure-based networks.

A large volume of research has been conducted in the cognitive radio area over the last decade (some of the last examples are [16, 98]). However, it is important to highlight that to our knowledge, a multichannel scenario in CR, which considers geometric characteristics such as nodes positions, has not been deeply explored yet. Motivated by this fact and to help in filling this gap, we choose an approach based on stochastic geometry and we

extend the probabilistic framework developed in [49] to that context in CR. In particular, in the analysis exposed in this chapter we consider ALOHA to schedule primary transmissions in each frequency band and we also consider that all SU transmitters are saturated, i.e. have a packet ready to be sent in every time slot. In this situation, MAP and COP give an idea of the possibilities offered by cognitive radio to improve the spectrum utilization. Those metrics are also useful to explore how PUs are affected under the spectrum sharing context.

The rest of the chapter is structured as follows. In the next section we present the previous related work and highlight some recent papers. In Section 7.3 we introduce our scenario and the notation. In Section 7.4 we present our main results in a specific scenario that consists in two channel bands and a particular sensing mechanism. We validate our results presenting numerical examples based on simulations. In Section 7.5 we show the MAP and COP estimation for a general case. We present analytical expressions for those metrics. Finally, we conclude and discuss future work in Section 7.6.

7.2 Related work

In the context of multichannel CR Networks the most representative previous examples are based on the theory of queues and priority queues (see for example [99, 100] and the references therein). In those articles, authors use queueing results to find several network statistics. However, there are few works that capture random features such as user locations, fading/shadowing and path loss; which play a crucial role in network performance. According to that, Stochastic Geometry is the natural tool to be used in these scenarios; even more, when the interest is to analyze the impact of those features.

Some of the most representative previous works in CR area using this technique are [49, 93, 94, 101–105]. However, only in [94] and [104, 106] the authors analyze a multichannel environment. In particular, in [94] the authors analyze ad hoc networks where each SU previously selects a channel and then, if that channel is primary-free it will transmit; therefore the MAP is strictly dependent of the selected channel band. In our case, each SU determines which channels are primary-free and then it selects one of them to transmit. When the interest is to know the opportunities in CR networks, our assumption is more reasonable. Also, in [94] the impact of the SU presence in PUs communications has not been studied.

On the other hand in [104] and its extension [106], the authors investigate a channel assignment and opportunistic spectrum access in two-tier cellular networks with cognitive small cells. In particular, we can say that they have modeled femtocells as secondary networks and macrocells as primary ones. We would like to emphasize that our model is completely different from that because their calculus and results are based on cellular cells and our approach is thinking about ad hoc networks, more focused on massive machine type communications. Another main difference to our work is that in their scenario there is no notion of priority between primaries and secondaries in the sense of network optimization criteria (i.e. performances of both femtocell and macrocell users are considered to maximize the overall network performance). In our case, we analyze different design network parameters in order to maximizing the spectrum usage based on the requirement that PUs ought to be as little affected as possible by the presence of SUs.

7.3 Problem formulation

Let us begin by describing our working scenario and introducing the notation, definitions and hypotheses. The location of the nodes of the network is seen as the realization of two point processes [107], one for PUs and the other for SUs. This means that the network can be considered as a snapshot of a stationary random model in the (Euclidean) space and that it is possible to analyze it in a probabilistic way. The time is divided into slots (see the time slot structure in Fig. 7.1) and one slot is needed to transmit a packet for all users. Then, one snapshot represents the nodes spatial distribution in one time slot.

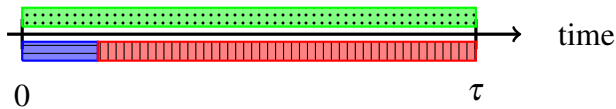


Figure 7.1: Time slot structure (τ in the duration of one slot time). PUs transmissions occur in the whole time slot (green dotted area). SUs first sense the spectrum during the sensing time (representing with the blue horizontal line pattern) and then (those which can) transmit in the remaining slot time (red vertical line pattern).

In the particular case of this work, the users of the network are assumed to be a realization of two independent homogeneous PPP, $\Phi_p = \{X_i^p\}$ and $\Phi_s = \{X_i^s\}$ with intensities λ_p and λ_s on \mathbb{R}^2 respectively. Specifically, $\{X_i^p\}$ and $\{X_i^s\}$ denote the positions of the potential primary and secondary transmitters respectively. The advantages of using spatial Poisson processes for modeling the locations of the wireless devices have been stated in many articles. As we mention before, they are easy to handle analytically, and they provide bounds for the performance of more general network models. We also assume that each transmitter has its intended receiver uniformly distributed in a circle of radius r centered in each transmitter location. We define $r(x)$ as the relative location of the receiver of a transmitter located in x .

In order to introduce the multichannel aspect, we define $f = \{f_1, f_2, \dots, f_n\}$ as the set of channel bands to be used by PUs or SUs. We consider ALOHA in the primary transmissions. We can define a new PPP $\Phi_p^* = \{X_i^p : e(X_i^p) = 1\}$ where $e(X_i^p)$ is a $\{0, 1\}$ -value r.v. indicating whether X_i^p chooses to transmit in the current time slot or not ($P(e(X_i^p) = 1) = p_e$). Φ_p^* represents the process of the active primary transmitters and it is an independent thinning of the original Poisson, then it is a PPP with intensity $\lambda_p p_e$. Each PU also has to choose its frequency band for its transmission. We assume that each band f_k has probability p_{f_k} to be selected by any active PU. Therefore we can define Φ_{p, f_k}^* , a PPP with intensity $\lambda_p p_e p_{f_k}$, as the process of the active primary transmitters using band f_k .

A deterministic attenuation $\alpha > 2$ is also assumed; that is, the signal power decays with the distance between two nodes. Given two nodes x and y , the power received from x by y is $P(x, y) = P(x)l(\|y - x\|)$ where $P(x)$ is the transmission power of node x and $l(\|y - x\|)$ is the path loss function from x to y which depends on the distance between

nodes. Different path loss functions can be considered. For our specific calculus we have considered $l(\|y - x\|) = \|x - y\|^{-\alpha}$ with $\alpha > 2$ but they are totally adaptable to other models.

In the literature, there are many proposals of spectrum sensing methodologies for cognitive radio networks (for instance: energy detection, cyclostationary sensing techniques [108], and/or limited channel feedback [12]). We assume that SUs implement a sensing method based on energy detection to detect primary activity. More specifically, a SU y detects the presence of a PU x if $P(x, y) > \rho$ where ρ is a pre-set constant (one of the design network parameters to be analyzed). Each SU has to sense the bands to know the set of primary-free channels. If there is at least one free band of primary users, it can transmit. This behavior is represented in Figures 7.1 and 7.2. Analogously to the PUs case, we define Φ_s^* as the process of active SU and Φ_{s, f_k}^* the one of active SUs using band f_k . Note that these processes are dependent thinning of the original Poisson process Φ_s .

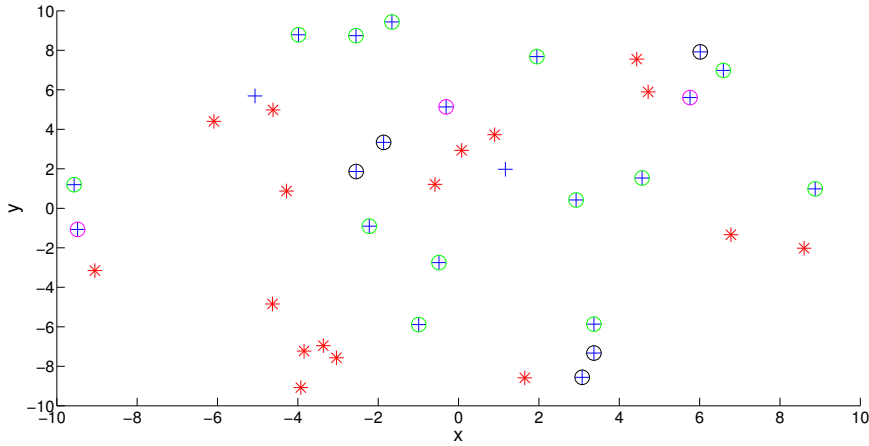


Figure 7.2: A snapshot of the nodes of the network defined by Φ_p (stars) and Φ_s (crosses) processes using the parameters $\lambda_p = 0.05$, $\lambda_s = 0.1$, two frequency bands $\{f_1, f_2\}$, $p_e = 1$, $p_f = 0.5$, $\alpha = 3$ and $\rho = 0.1$. SUs that are surrounded by a circle are the active ones. In particular, SUs that have a green circle have detected both primary-free channels. On the other hand, the ones that are surrounded by black and magenta circles have detected only one primary-free band, f_1 or f_2 respectively.

In order to model the random variations of the channel conditions, we consider two families of i.i.d. random variables: $F_k = \{F_k(i, j)_{i,j}\}$ and $F_k^r = \{F_k^r(i, j)_{i,j}\}$. The first one represents the fading of the channel k from primary transmitter i to secondary transmitter j . It will be used in the sensing mechanism implementation. The second one models the fading of the channel k from transmitter i to receiver of transmitter j (being i and j two arbitrary transmitters, PU or SU) being essential for the COP calculus. In order to simplify the notation we assume $F_k = F = \{F(i, j)_{i,j}\} \forall k$ and $F_k^r = F^r = \{F^r(i, j)_{i,j}\} \forall k$.

In our particular case, we consider a Rayleigh fading (suitable when many obstacles are present and there is no line of sight between transmitter and receiver) therefore, the random variables $\{F(i, j)_{i,j}\}$ and also $\{F^r(i, j)_{i,j}\}$ are assumed to be independent and exponentially distributed with parameter μ . Including this new feature, we can say that

7.3. Problem formulation

the power received from y by x is:

$$P(x, y) = P(x)F(x, y)l(\|y - x\|); \quad (7.1)$$

analogously if $F^r(x, y)$ is considered.

As usual, we model interference as noise. In this work, we do not consider the co-channel interference (i.e. non-overlapping orthogonal channels). Hence, a transmission in frequency f_k will be successful if the *SINR* is higher than a certain threshold considering only the signals operating in the same spectrum band. The interference is assumed to be the sum of signal strengths generated by all the other nodes transmitting in the same time slot (i.e. aggregate interference). Let t_i and r_i be the locations of a pair of primary transmitter and its receiver using band f_k (please note that r_i is the relative location of the transmitter t_i). We will assume that the communication between t_i and r_i will be successful if the following condition is verified:

$$SINR^p(t_i, r_i, f_k) = \frac{P(t_i, r_i)}{N + I_{pp}^{f_k}(r_i) + I_{sp}^{f_k}(r_i)} \geq \gamma \quad (7.2)$$

where $I_{pp}^{f_k}(\cdot)$ and $I_{sp}^{f_k}(\cdot)$ represents the aggregate interference associated to the active primaries and secondaries transmitters using band f_k respectively:

$$I_{pp}^{f_k}(r_i) = \sum_{y \in \Phi_{p, f_k}^* \setminus \{t_i\}} P(y)F^r(y, t_i)l(\|y - t_i - r_i\|) \quad (7.3)$$

$$I_{sp}^{f_k}(r_i) = \sum_{y \in \Phi_{s, f_k}^*} P(y)F^r(y, t_i)l(\|y - t_i - r_i\|) \quad (7.4)$$

I_{pp} denotes the interference from primary transmitters to a primary receiver. On the other hand I_{sp} denotes the influence of the secondary communications in a specific primary receiver.

Analogously, when t_i and r_i are a pair of secondary users, the transmission will be successful if

$$SINR^s(t_i, r_i, f_k) = \frac{P(t_i, r_i)}{N + I_{ss}^{f_k}(r_i) + I_{ps}^{f_k}(r_i)} \geq \gamma \quad (7.5)$$

$$I_{ps}^{f_k}(r_i) = \sum_{y \in \Phi_{p, f_k}^*} P(y)F^r(y, t_i)l(\|y - t_i - r_i\|) \quad (7.6)$$

$$I_{ss}^{f_k}(r_i) = \sum_{y \in \Phi_{s, f_k}^* \setminus \{t_i\}} P(y)F^r(y, t_i)l(\|y - t_i - r_i\|) \quad (7.7)$$

where γ is a selectable threshold and it is strongly related with the receiver sensitivity. Please note that this threshold can be different between classes of users. The aggregate interference, as we explain in the Appendix A when we define the characteristics of the additive shot-noise, is usually characterized by using the Laplace transform.

In the following sections we present the calculus for the estimation of the performance metrics *MAP* and *COP*, in particular we start with a particular scenario where those metrics can be obtained exactly. Then, we continue with a more general case for which upper bounds are derived since exact results can not be obtained.

7.4 Performance metrics estimation of particular case: two frequency bands and a random sensing mechanism

The aim of this section is to investigate the MAP and COP calculus of a particular scenario. For this purpose, first we define the new assumption which represents a simplification in SU's sensing mechanism. Finally, we include a validation section.

In this scenario, we consider only two possible frequency bands $f = \{f_1, f_2\}$ with probabilities p_f and $1 - p_f$ to be chosen by PUs respectively. We also add a new hypothesis: a SU will transmit if and only if in a ball centered at it with random radius q there is at least one primary-free channel (radius q are considered as i.i.d. random variables with $G(q)$ distribution). This is an alternative version of the described sensing mechanism. In other words, we can assume that distance between transmitters, fading and path loss function ($F(i, j), l(\|i - j\|), \rho$) are abstracted into the random radius q . This represents a reasonable hypothesis for radio propagation in a very dense urban area, even more where beamforming and MIMO techniques are used.

The major consequence of this new assumption is that Φ_s^* is now an independent thinning of the original Poisson process Φ_s . Let us first begin with the MAP calculus. In our model, due to the fact that PUs access to the network according to ALOHA protocol, the MAP_p is already known. Thus, we are only interested in the MAP of a secondary users.

7.4.1 MAP of secondary users - MAP_s

Conforming to the previous description, a typical SU potential transmitter ($0 \in \Phi_s$) will access the medium with probability:

$$\int 1 - P(\Phi_{p,f_1}^*(B(0, q)) > 0) P(\Phi_{p,f_2}^*(B(0, q)) > 0) dG(q). \quad (7.8)$$

Φ_{p,f_1}^* and Φ_{p,f_2}^* are PPP in \mathbb{R}^2 , then

- $P(\Phi_{p,f_1}^*(A) = 0) = e^{-\lambda_p p_e p_f |A|}$ and
- $P(\Phi_{p,f_2}^*(A) = 0) = e^{-\lambda_p p_e (1-p_f) |A|}$,

where $|A|$ is the area of A . According to that and considering A as the ball centered at 0 with random radius q , we have

$$MAP_s = \int (1 - (1 - e^{-\lambda_p p_e p_f \pi q^2})(1 - e^{-\lambda_p p_e (1-p_f) \pi q^2})) dG(q). \quad (7.9)$$

It is easy to note that the MAP_s calculus can be easily generalized to the case of n frequency bands ($n > 2$).

7.4. Performance metrics estimation of particular case: two frequency bands and a random sensing mechanism

7.4.2 COP of primary users - COP_p

Under the same hypothesis that were explained before (i.e. $f = \{f_1, f_2\}$ with probabilities p_f and $1 - p_f$) and given the MAP_s (Eq. (7.9)), we will compute the COP of primary users. The COP measures the probability of a success transmission and is computed as the probability that the SINR of the tagged user is larger than a pre-set constant γ .

Now, the first question we have is: if a SU finds both bands available, which one is going to be selected? In this work, as a first step, we consider that each band has a fixed probability (p'_f and $1 - p'_f$) to be chosen. Therefore, we can express the probability that a SU transmits in f_1 as:

$$P(f_1) = \int e^{-\lambda_p p_e p_f \pi q^2} (1 - e^{-\lambda_p p_e (1-p_f) \pi q^2}) dG(q) + p'_f \int e^{-\lambda_p p_e p_f \pi q^2} e^{-\lambda_p p_e (1-p_f) \pi q^2} dG(q)$$

complementary, the probability that a SU transmits in f_2 is:

$$P(f_2) = \int (1 - e^{-\lambda_p p_e p_f \pi q^2}) e^{-\lambda_p p_e (1-p_f) \pi q^2} dG(q) + (1 - p'_f) \int e^{-\lambda_p p_e p_f \pi q^2} e^{-\lambda_p p_e (1-p_f) \pi q^2} dG(q).$$

In this context we have

$$\begin{aligned} P_{\Phi_p}^0(\text{SINR}^p(0, r(0), f_1) > \gamma) &= P\left(\frac{F_r(0, 0)l(|r(0)|)}{N + I_{pp}^{f_1}(0) + I_{sp}^{f_1}(0)} > \gamma\right) \\ &= P\left(F_r(0, 0) > \frac{\gamma(N + I_{pp}^{f_1}(0) + I_{sp}^{f_1}(0))}{l(|r(0)|)}\right) = \\ &\int \int e^{-\frac{\mu\gamma(N+x+y)}{l(|r(0)|)}} F_{I_{pp}^{f_1}}(dx) F_{I_{sp}^{f_1}}(dy) = \\ &e^{-\frac{\mu\gamma N}{l(|r(0)|)}} \mathcal{L}_{I_{pp}^{f_1}}\left(\frac{\mu\gamma}{l(|r(0)|)}\right) \mathcal{L}_{I_{sp}^{f_1}}\left(\frac{\mu\gamma}{l(|r(0)|)}\right) \end{aligned}$$

where \mathcal{L} is the Laplace transform (see more details in Appendix A).

Please note that we have identified the Laplace transforms of the additive shot noises associated with the point processes of active primary and secondary transmitters using f_1 band. Due to the fact that Φ_{p,f_1}^* and Φ_{s,f_1}^* are PPP with intensities $\lambda_p p_e p_f$ and $\lambda_s P(f_1)$, the corresponding Laplace transforms are:

$$\begin{aligned} \mathcal{L}_{I_{pp}^{f_1}}(s) &= \exp\left\{-2\pi\lambda_p p_e p_f \int_0^\infty 1 - \frac{\mu}{\mu + sl(|r(0)|)} r dr\right\} \\ \mathcal{L}_{I_{sp}^{f_1}}(s) &= \exp\left\{-2\pi\lambda_s P(f_1) \int_0^\infty 1 - \frac{\mu}{\mu + sl(|r(0)|)} r dr\right\} \end{aligned}$$

The calculus of $P_{\Phi_p}^0(\text{SINR}^p(0, r(0), f_2) > \gamma)$ is analogous and the COP_p is totally determined.

7.4.3 COP of secondary users - COP_s

Using the same arguments explained before, we can express the probability of a successful secondary transmission by conditioning on the selected band as:

$$P_{\Phi_s^*}^0(SINR^s(0) > \gamma) = \frac{P_{\Phi_s}^0(SINR^s(0, r(0), f_1) > \gamma)P(f_1)}{MAP_s} + \frac{P_{\Phi_s}^0(SINR^s(0, r(0), f_2) > \gamma)P(f_2)}{MAP_s}$$

where the calculus of the different involved terms are analogous to the COP_p .

7.4.4 Simulation results

In this subsection we introduce some numerical examples related to the results presented in the previous subsection. To do that, we implement a set of simulations following the hypotheses of the presented particular case.

The set of transmitters (PUs and SUs) are distributed according of two PPPs in \mathbb{R}^2 with intensities λ_p and λ_s . Therefore we generate two Poisson processes in a circle of radius $R = 30$ and consider only those points that fall into a circle of radius $R = 15$ to minimize border effects (see Figure 7.3). For each transmitter we simulate each receiver uniformly distributed in a circle of radius 1 centered at each transmitter.

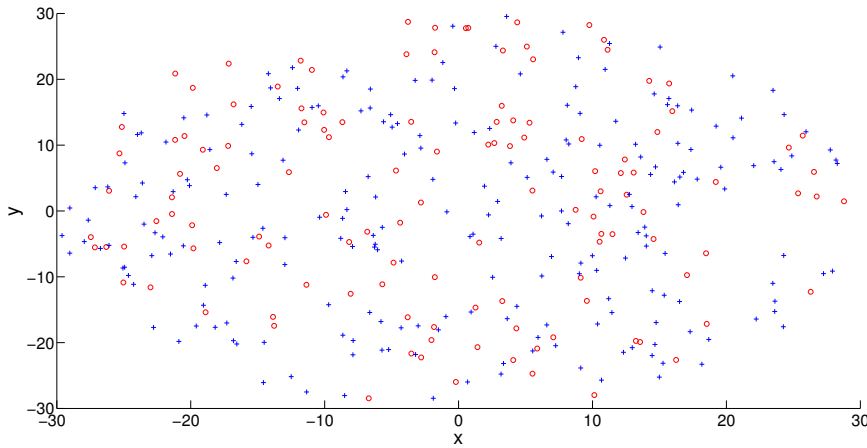


Figure 7.3: An example of the simulated sets of points of Φ_p (circles) and Φ_s (crosses). Parameters: $\lambda_p = 0.05$ and $\lambda_s = 0.08$.

The network parameters that we use in the simulations are:

- $\lambda_p = \lambda_s = 0.8$.
- $p_e = 1$: all PUs are active.

7.4. Performance metrics estimation of particular case: two frequency bands and a random sensing mechanism

- $p_f = 0.3$: probability to be selected f_1 band by an active PU transmitter.
- $p'_f = 0.5$: probability to be selected f_1 band by a SU when both bands are primary-free.
- $\mu = 2$: parameter of the fading random variables.
- $\alpha = 3$: path loss coefficient.
- $\gamma = 0.1$: successful detection threshold.
- $G(q)$ is an uniform distribution with parameter a, b ; $\mathcal{U}[a, b]$, considering $a = 0$ and varying b . This is used to implement the sensing mechanism of SUs.

Figures 7.4, 7.5 and 7.6 show the results corresponding to MAP_s , COP_p and COP_s respectively in the described scenario for different values of the parameter b . For each b value, we run 20 independent simulations and we can observe the analytical results together with the correspondent simulated boxplot representation. Our calculus are validated with the presented numerical examples.

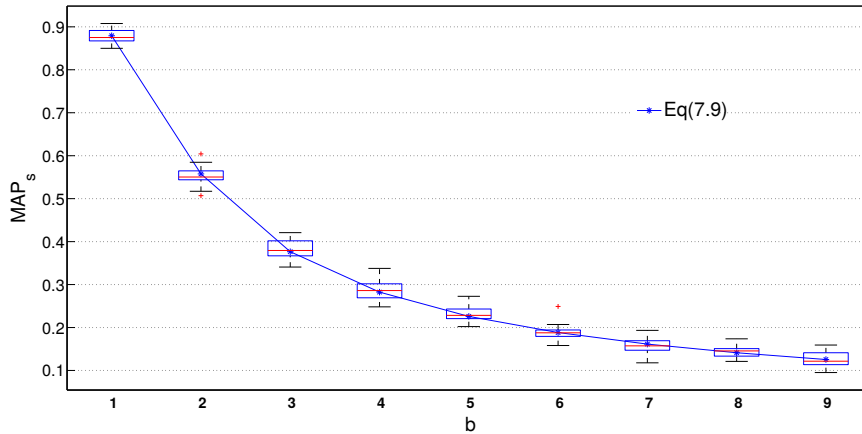


Figure 7.4: MAP_s : The evaluation of Eq. (7.9) along with the boxplot of the numerical results of 20 simulations.

In Figures 7.7 and 7.8 we analyze the impact of the presence of secondary user. The network parameters are the same that we described before. We can observe in Figure 7.7 the COP value of PU with and without SUs for different b values. Please note that parameter b is used by SU in the sensing algorithm, therefore, COP_p in a traditional network composed only by PUs is independent of b . On the other hand, in the CR scenario, when b increases PUs are less affected by SUs interference. The results obtained are coherent: for large b values, SUs have less probability to access to the network (see figure 7.4) and also, SUs that reach a channel to transmit have a high probability of being away from PU's protection zones.

In Figure 7.8 it is shown the impact of the successful probability of PUs when the detection threshold varies. In addition we can see the impact of the presence of SUs that will be directly reflected in PU's throughput.

Chapter 7. A stochastic geometry analysis of multichannel CR network

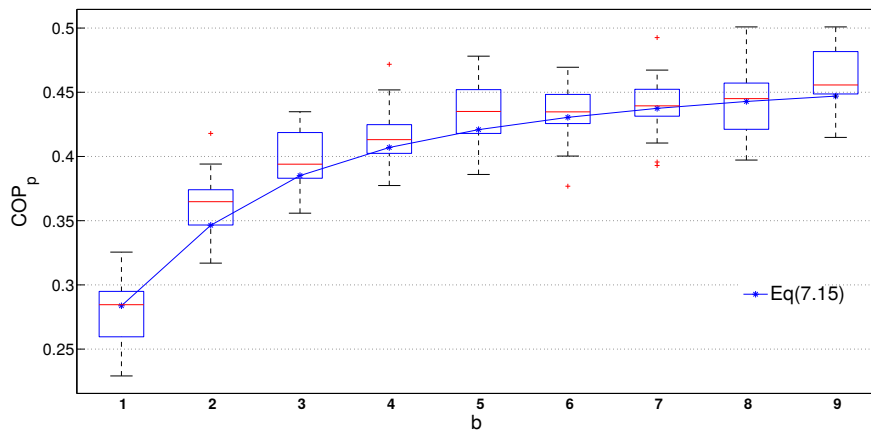


Figure 7.5: COP_p : The evaluation of Eq. (7.15) for the particular case along with the boxplot of the numerical results of 20 simulations.

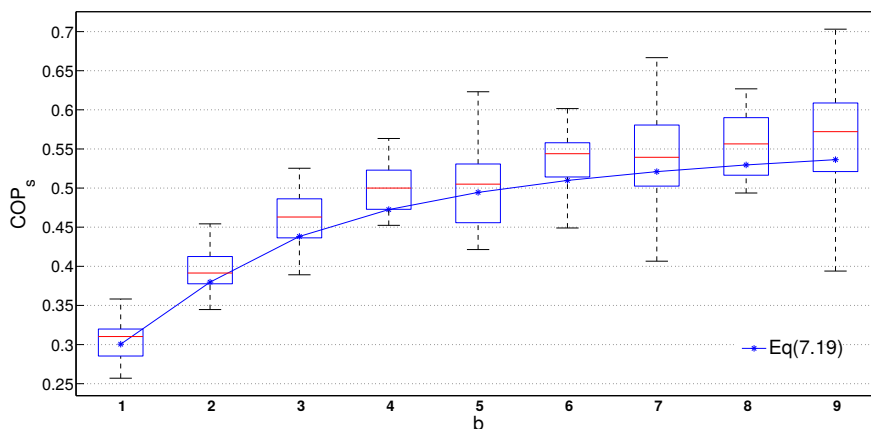


Figure 7.6: COP_s : The evaluation of Eq. (7.19) for the particular case along with the boxplot of the numerical results of 20 simulations.

Extending Eq. (7.9) for the case when there are more than two channels in the system and applying it to our context we obtain the results of Figure 7.9. In this example, we show the MAP_s for different number of channel bands in the system ($f = \{f_1\}$, $f = \{f_1, f_2\}$, ..., and $f = \{f_1, f_2, \dots, f_{10}\}$) and considering different λ_p values. In the simulated examples of this figure each PU selects each channel with the same probability $p_f = 1/|f|$ where $|f|$ is the number of frequency bands. This scenario allows to analyze, from other point of view, the possibilities offer by CR networks.

In the next section we present the metrics in the general case.

7.4. Performance metrics estimation of particular case: two frequency bands and a random sensing mechanism

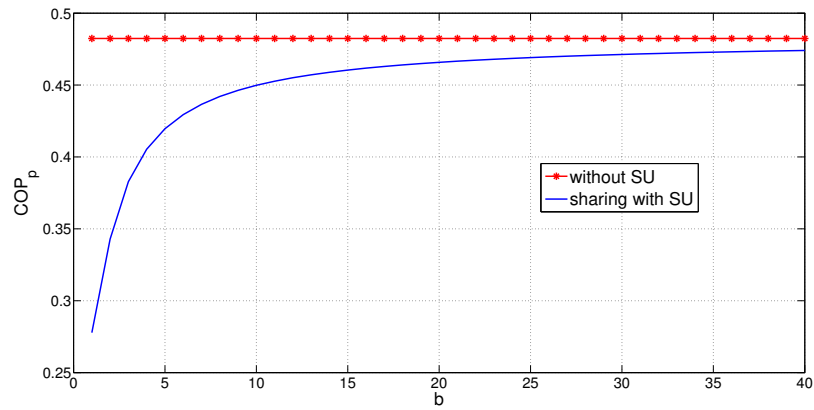


Figure 7.7: COP_p with and without SUs for different b values.

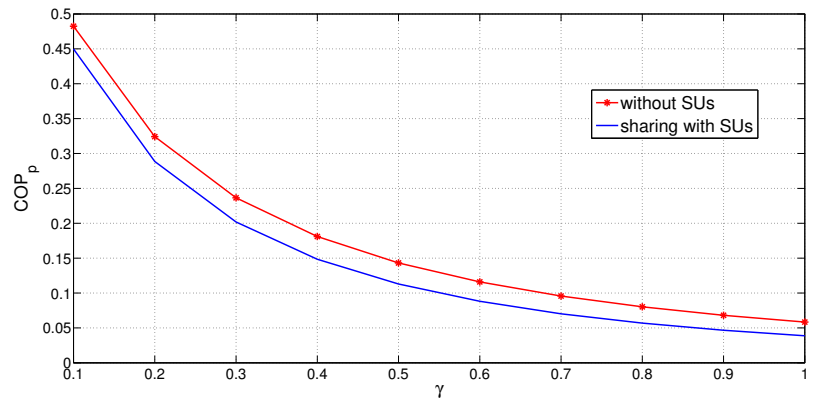


Figure 7.8: COP_p with and without SUs for different γ values. We consider a fixed $b = 10$.

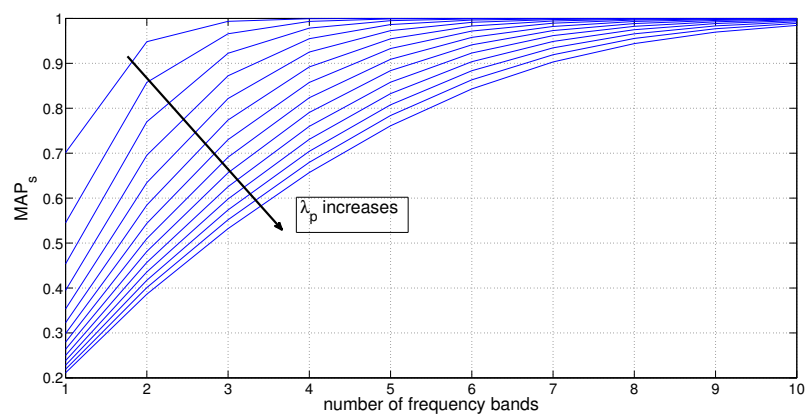


Figure 7.9: MAP_s considering different number of channel bands. Parameters: $\lambda_p = 0.1; 0.2; 0.3; \dots; 1.5$, $\lambda_s = 1$, $p_e = 1$, $p_f = 1/|f|$ and $\alpha = 3$.

7.5 Performance metrics estimation of the general case

In this subsection we present the performance metrics in the general scenario described in Section 7.3. As in the particular case, we begin with the MAP estimation.

7.5.1 MAP of secondary users - MAP_s

Proposition 9. *The medium access probability of a SU in a multichannel scenario is*

$$MAP_s = 1 - \prod_k (1 - e^{-\lambda_p p_e P_{f_k} \bar{N}_0}), \quad (7.10)$$

where $\bar{N}_0 = \int_{\mathbb{R}^2} e^{-\frac{\mu\rho}{l(y)}} dy$ is the mean number of active primary contenders of a typical secondary user in a network of intensity 1.

Proof. For a typical secondary potential transmitter located at 0, in a general way it is possible to define the set of primary contenders in the different frequency bands as:

$$N_0^{p,f_k} = \{y \in \Phi_{p,f_k}^* : F(y,0)l(|y-0|) > \rho\}. \quad (7.11)$$

That is to say, N_0^{p,f_k} is the set of active primary transmitters using f_k that are detected by the typical SU with the considered sensing mechanism. With this in mind, we can say that the typical SU is in the protection zone of the PUs defined by N_0^{p,f_k} . Without loss of generality we have considered $P(y) = 1, \forall y$ (or $P(y)$ might have been assumed constant and included in $F(y,0)$).

Please note that Φ_{p,f_k}^* is a PPP and a secondary user will transmit if and only if there is at least one primary-free channel. Considering f_k , the probability that band the typical SU finds f_k band free of primary transmissions is:

$$P(|N_0^{p,f_k}| = 0) = e^{-\lambda_p p_e P_{f_k} \bar{N}_0}, \quad (7.12)$$

where $|N_0^{p,f_k}|$ is a Poisson random variable that represents the number of active primary user using f_k . Therefore, the medium access probability can be written as:

$$MAP_s = 1 - \prod_k (1 - e^{-\lambda_p p_e P_{f_k} \bar{N}_0}) \quad (7.13)$$

where $\bar{N}_0 = \int_{\mathbb{R}^2} e^{-\frac{\mu\rho}{l(y)}} dy$. □

It should be noted that, in this general case, the process of active secondary users Φ_s^* is a dependent thinning of the original Poisson process Φ_s but it is not itself a PPP. Moreover, it is the sum of k Matérn Hard Core Point processes (one corresponding to each frequency band), i.e. SUs which fall within a PU protection zone are automatically silenced in that specific primary frequency band. For that reason, the COP calculus for this general case is approximate; more precisely it is possible to obtain analytical expression of an upper bound of the COPs.

Now, the question again is: if a SU finds many bands available, which one is going to be selected? In this work, we consider that each band has the same probability to be

7.5. Performance metrics estimation of the general case

chosen. Therefore, we can express the probability that a SU transmits in f_k as $P(f_k) = \frac{1}{C_f}$ being C_f the number of free-primary bands detected and f_k one of these bands. For example, considering $p_{f_k} = p \forall k$ (i.e. each band has the same probability to be chosen by a PU), please note that the probability of a SU finds c free channels is

$$P(C_f = c) = C_c^n \left(e^{-\lambda_p p_e p \bar{N}_0} \right)^c \left(1 - e^{-\lambda_p p_e p \bar{N}_0} \right)^{n-c}. \quad (7.14)$$

In the next subsections we will present the COP calculus. In particular, the COP of primary users is important to analyze the impact of the presence of secondary user in PUs QoS.

7.5.2 COP of primary users - COP_p

Considering 0 as the typical active primary transmitter (with its corresponding receiver in the relative position $r(0)$), the transmission will be successful with probability:

$$\begin{aligned} COP_p &= P_{\Phi_p^*}^0 (SINR^p(0, r(0)) > \gamma) \\ &= \sum_k P_{\Phi_{p, f_k}^*}^0 (SINR^p(0, r(0), f_k) > \gamma) p_{f_k} \end{aligned} \quad (7.15)$$

where p_{f_k} represents the probability that the typical primary node uses f_k to transmit.

Proposition 10. $P_{\Phi_{p, f_1}^*}^0 (SINR^p(0, r(0), f_1) > \gamma)$, considering $\{f_1, f_2\}$ as the set of possible frequency bands and assuming that an active primary transmitter chooses f_1 with p_f probability (i.e. f_2 is chosen with $(1 - p_f)$), is upper bounded by

$$e^{\frac{-\mu \gamma N}{l(r_p)}} \left(e^{-\lambda_p p_e p_f c(r_p)} - \frac{(1 - e^{-\lambda_p c(r_p)})}{c(r_p)} \int_{\mathbb{R}^2} \frac{\gamma l(|x - r(0)|)}{\gamma l(|x - r(0)|) + l(r_p)} (AB + \frac{1}{2}AC) dx \right),$$

where:

$$A = (1 - e^{\frac{-\mu \rho}{l(|x|)}}) \exp \left\{ -\lambda_p p_e p_f \int_{\mathbb{R}^2} \frac{\gamma l(|y - r(0)|) + l(r_p) e^{\frac{-\mu \rho}{l(|y-x|)}}}{l(r_p) + \gamma l(|y-x|)} dy \right\}, \quad (7.16)$$

$$B = 1 - \exp \left\{ -\lambda_p p_e (1 - p_f) \int_{\mathbb{R}^2} e^{\frac{-\mu \rho}{l(|z-x|)}} dz \right\}, \quad (7.17)$$

and

$$C = \exp \left\{ -\lambda_p p_e (1 - p_f) \int_{\mathbb{R}^2} e^{\frac{-\mu \rho}{l(|z-x|)}} dz \right\}. \quad (7.18)$$

The proof is in Appendix C.1.

7.5.3 COP of secondary users - COP_s

In this case, for a typical SU transmitter and its receiver we have:

$$\begin{aligned} COP_s &= P_{\Phi_s^*}^0(SINR^s(0, r(0)) > \gamma) \\ &= \sum_k \frac{P_{\Phi_s}^0(SINR^s(0, r(0), f_k) > \gamma, U_k(0))}{MAP_s} \end{aligned} \quad (7.19)$$

The complete analytical expression and its proof is in Appendix C.2.

7.6 Conclusions

We extended the methodology developed in [49] to the case of a multichannel cognitive radio environment. We made the first steps in order to analyze a scenario which considers more than one channel together with geometric aspects such as random node locations and path loss functions. We showed analytical results for the calculus of the main performance metrics: Medium Access Probability and Coverage Probability. These parameters give information about the possibilities offered by cognitive radio to improve the spectrum utilization and also they give an idea of how much affected are primary users with the presence of secondary ones. We made some simulations in order to show this effect over PU communications.

As a future work, we want to investigate the influence of the different system parameters. In particular, we are interested in answer the following questions: what channel band should SU select if there are more then one available? Is it possible to define an optimal parameters configuration in order to maximize the spectrum utilization minimizing the effects over primary communications?

In the next chapter we will analyze an analogous scenario but considering CSMA as the medium access mechanism for primary users. Considering CSMA in a multichannel analysis increases the complexity of the analytical expressions of the obtained COP upper bounds. In this sense, in the next chapter we will address the problem with random graphs instead of using stochastic geometry.

Chapter 8

Capacity analysis using random graphs

8.1 Introduction

In this chapter, we consider two large wireless networks, one composed by PUs and the other by SUs. As opposed to Chapter 7, we choose an approach based on random graphs. Another difference is that in this part we use CSMA instead of ALOHA as the medium access mechanism. In particular, we extend the methodology developed in [95, 96] to the context of CRs. The main difficulties that arise are related to the interaction between both networks. We show that the methodology yields differential equations for which explicit solutions may be obtained. The differential equations are determined using fluid limits in the same way as in Chapter 4. With our proposal, we show that it is possible to calculate an analytic approximation of the MAP (both for PUs and, most importantly, SUs) in an arbitrary large heterogeneous random network.

As a further contribution of this part of the thesis, we perform a comparison between the approximation presented here, based on random graphs, with that based on a stochastic geometry approach. To perform the comparison we will refer to [49], where the authors studied an analogous problem and they obtained a bound of the MAP of SUs. We also analyze how conservative this bound is in some representative scenarios. On the one hand, these comparisons will be performed on those scenarios where a stochastic geometry approach is valid and possible. On the other hand, we will show that the approach presented here is more general than the one that uses spatial models, analyzing their performance in real network scenarios (e.g. when the involved processes are not necessarily Poisson).

The rest of the Chapter is structured as follows. In section 8.2 we introduce our hypotheses and the main characteristics of the considered MAC protocol. In section 8.3 we present our main results, in particular we show the MAP estimation using a random graph approach based on [95]. In section 8.4 we validate our results presenting numerical examples in several scenarios. In section 8.4, we give an introduction of the stochastic geometric model proposed in [49] and we compare their results with our MAP approximation in representative cases. The conclusions and the discussion of future work is in 8.6.

8.2 Context and assumptions

As we have considered in the whole thesis, this chapter also bears on the analysis of a general scenario where there is a primary wireless network coexisting with a secondary one. In this context, SUs try to exploit the unused licensed spectrum, so the MAC protocol should provide mechanisms to give SUs a way to detect the primary spectrum holes.

In particular, in this part of the thesis we work with the Cognitive-CSMA model introduced in [49] where Carrier Sensing (CS) is used for spectrum sensing and for interference control. In this mechanism, the following principles are verified:

- each PU has a protection zone,
- no SU can transmit inside the protection zone of a PU,
- time is slotted,
- each time slot consists of three phases: primary sensing, secondary sensing and transmission (see Figure 8.1).



Figure 8.1: Each slot is divided in three phases: primary sensing, secondary sensing and transmission. The above bar corresponds to sensing and transmission phases of SUs and the below one corresponds to the behavior of PUs.

During the primary sensing phase, all PUs sample an independent and identically distributed random variable that represents its backoff timer. When the time indicated by its backoff timer is elapsed, the tagged PU checks whether the channel is free (by means of the CS mechanism mentioned before), and if so immediately begins transmitting. In other words, a PU will transmit during a time-slot if and only if its timer is the smallest among all its primary contenders.

Once the primary phase is over, and the corresponding PUs are transmitting, the secondary sensing phase begins. Similarly to the previous phase, all SUs sample a backoff timer, after which time they transmit if the channel is free. The difference in this case is that the CS mechanism has to evaluate the presence of both SUs and, most importantly, PUs. Note that the protection zone of the PUs is thus implicitly defined by the ability of SU's CS mechanism to detect the presence of PUs. All in all, a SU will transmit if and only if it is not in the protection zone of an active primary user and its timer is the smallest among its secondary contenders. In this context, the MAP is defined as the probability that a user be granted the right to transmit in a time slot.

Naturally, the determination of the protection zone and contender transmitters is strongly related with the nodes' positions and propagation conditions (i.e. path-loss and fading

8.3. Random graphs and configuration algorithm

variables). In our present context, and similarly to [49], we will assume that the CS will evaluate the channel as busy if the signal of any other node is received with an energy above a certain threshold. This threshold may be different for secondary and primary nodes.

Finally, and regarding traffic, we will assume that all SUs are saturated, i.e. have a packet ready to be sent in every time slot. This assumption stems from the fact that we are interested in estimating the capacity of SUs to exploit the resources left by the PUs (i.e. the MAP of SUs).

8.3 Random graphs and configuration algorithm

8.3.1 Preliminaries and motivation

As we mentioned above, at any time-slot, and given the nodes' position and propagation conditions, we may determine the protection zone of each PU and all contending nodes. This, together with the backoff timers, will in turn determine which nodes will be allowed to transmit. Note however that what is actually required to determine which nodes will transmit is precisely which pairs of nodes are contenders, and which SUs are in the protection zone of each PU (as opposed to the complete nodes' position and detailed propagation conditions).

The discussion above suggests that the network may be abstracted to a graph $\mathcal{G}(\mathcal{V}, \mathcal{E})$ (the so-called interference graph), where the set of vertices¹ represent the primary and secondary nodes, and the edges model the interference between any two nodes. In other words, if a transmission of node s triggers the CS of node r , then an edge from node s to r will exist. Note that in the particular case where s is a PU and r a SU, then an edge will exist if r is in the protection zone of s .

We will further assume a symmetric channel among PUs and SUs, meaning that the edges between nodes of the same type of user are bidirectional. Note however that the edges between a PU and a SU are directional, since the former are not affected by the latter (in other words, connections from SUs to PUs are meaningless in this context). If an edge exists between two nodes, we say that those nodes are contenders (or neighbors).

Let us now discuss what information we have on $\mathcal{G}(\mathcal{V}, \mathcal{E})$. For instance, if the network is relatively small and static, we may know the graph completely. If on the other hand, the network is very big, has varying propagation conditions, and/or transient or mobile nodes (which is probably the case for SUs), the most natural modeling tool is a random graph.

This in turn induces the question of what probabilistic model use in the construction of the graph. We may for instance expect that on average each PU will have k_{PP} primary neighbors, that k_{PS} SUs are on average on the protection zone of the typical PU, and that each SU has k_{SS} secondary neighbors on average. In this case a reasonable model would be a variation of the well-known Erdős-Rényi model [109], where for instance a link between any two primary nodes will exist with probability $\frac{k_{PP}}{N_P-1}$ (with N_P the total number of primary nodes).

¹We will use *vertices* or *nodes* indistinctly.

Chapter 8. Capacity analysis using random graphs

We may further enrich our model if we have information regarding the distribution of the nodes' degree (and not just its mean as in the previous example). That is to say, we know the counting measure $\mu(i, j)$, representing the number of PUs which have i PU neighbors and j SUs in its protection zone. Furthermore, we also know $\nu(i, j)$, which will count the number of SUs that belong to the protection zone of i PUs, and that have j SUs neighbors (thus $\sum_{i,j} j\mu(i, j) = \sum_{i,j} i\nu(i, j)$). The example considered in the last paragraph may be cast to this context by considering $\mu(i, j)$ and $\nu(i, j)$ as two-dimensional binomial distributions. That is,

$$\begin{aligned}\mu(i, j) &= N_P F_{bin}(N_P - 1, p_{PP}, i) F_{bin}(N_S, p_{PS}, j), \\ \nu(i, j) &= N_S F_{bin}(N_P, p_{PS}, i) F_{bin}(N_S - 1, p_{SS}, j),\end{aligned}$$

where $F_{bin}(n, p, i) = C_i^n p^i (1-p)^{n-i}$ and the probabilities are $p_{PP} = \frac{k_{PP}}{N_P - 1}$, $p_{PS} = \frac{k_{PS}}{N_S}$ and $p_{SS} = \frac{k_{SS}}{N_S - 1}$.

The analysis to calculate the resulting MAP may then be as follows: construct a random graph (randomly chosen from those which comply to the chosen counting measures), analyze the resulting CSMA algorithm on that particular graph, and then weight the result over all possible graphs. However, this naive approach will become impractical as soon as the number of nodes is relatively big. To circumvent this complication, the idea proposed in [95] (and refined in [96]) is to construct the graph at the same time as the nodes transmit. By smartly choosing the variables considered (as we will present in Sec. 8.3.3), a Markov Chain may be constructed such that, when the number of nodes is large, it may be studied by means of a system of differential equations.

The framework discussed above has two implicit approximations. The first one, is that the analysis is valid for an infinite number of nodes, making it valid for moderate to large networks. The second one, which will be clearer when we present with more detail the graph's construction below, is that the counting measures used in the abstraction do not include any spatial information (i.e. the correlation between degree of nodes). However, we will show by means of simulations that, as soon as fading is not negligible, the MAP estimated by means of the set of differential equations constitutes an excellent approximation (and it is still very good when this is not the case).

8.3.2 Configuration model

Let us first focus on the primary sensing phase. As we mentioned before, each PU chooses a random backoff timer, at which time they will check whether the channel is free. This is equivalent to a random ordering of the PU nodes, meaning that any continuous distribution is equivalent for the backoff timer (in terms of the resulting order). We will thus choose, without loss of generality, an exponentially distributed backoff timer with mean equal to one.

The key to our analysis is the procedure by which the graph $\mathcal{G}(\mathcal{V}, \mathcal{E})$ is constructed along with the CSMA algorithm: the so-called configuration model [110]. Please recall that we have N_P and N_S primary and secondary users respectively, and that our a priori information are the counting measures $\mu(i, j)$ and $\nu(i, j)$. In this construction, we start with a "disconnected" graph. By this we mean that we have a set \mathcal{V} of $N_P + N_S$ vertices where, for instance, we have $\mu(i, j)$ nodes with i primary and j secondary neighbors,

8.3. Random graphs and configuration algorithm

but precisely which other nodes are these neighbors is not revealed until the tagged node transmits. In this sense, we will use the term half-edges to refer to these unmatched edges. The methodology considered here constructs $\mathcal{G}(\mathcal{V}, \mathcal{E})$ by pairing the half-edges sequentially as nodes transmit.

Please note that each node has two types of half-edges: some that should be connected to primary nodes, and others that should be connected to secondary nodes. The pairing above should be performed with this in mind. For instance, a half-edge from a PU to a SU should be paired with a half-edge from a SU to a PU.

Let us consider a time t during the primary sensing phase. The set \mathcal{V} may be partitioned into the following subsets:

1. Primary nodes that are already transmitting: \mathcal{A}_t^P (active nodes).
2. Primary and secondary nodes that have been blocked by the ongoing primary transmissions: \mathcal{B}_t^P and \mathcal{B}_t^S (blocked nodes). These nodes will not transmit during this slot.
3. Primary and secondary nodes that are neither transmitting nor blocked: \mathcal{E}_t^P and \mathcal{E}_t^S (unexplored nodes). These are the nodes that may transmit in the future, and will become either active or blocked as the sensing phase advances.

When the slot has just begun, we have $\mathcal{A}_0^P = \emptyset$, $\mathcal{B}_0^S = \mathcal{B}_0^P = \emptyset$, $|\mathcal{E}_0^P| = \sum_{i,j} \mu(i, j) = N_P$ and $|\mathcal{E}_0^S| = \sum_{i,j} \nu(i, j) = N_S$.

Assume that the backoff timer of a node s in \mathcal{E}_t^P expires at time t . The following then occurs (see Figure 8.2 for a toy example):

1. s is moved from \mathcal{E}_t^P to \mathcal{A}_t^P .
2. Each half-edge of s is in turn paired with another uniformly randomly chosen unmatched half-edge. This way, we construct a graph sampled at random and uniformly from all graphs that comply to the measures $\mu(i, j)$ and $\nu(i, j)$.
3. All vertices whose half-edges were chosen in the previous step, and which are still unexplored (some may already be blocked), are moved from \mathcal{E}_t^P to \mathcal{B}_t^P and from \mathcal{E}_t^S to \mathcal{B}_t^S respectively.

The primary sensing phase ends when $|\mathcal{E}_t^P| = 0$. Half-edges to and from primary nodes which are yet to be matched may be safely ignored, since they belong to blocked nodes.

The secondary sensing phase thus begins, which is very similar to what we described before. The most important difference is that we have to consider only vertices of secondary users, several of which are already blocked. Let us somewhat force notation and consider again that time $t = 0$ refers to the beginning of the secondary sensing phase. We thus have that $\mathcal{A}_0^S = \emptyset$, but the other two sets (\mathcal{B}_0^S and \mathcal{E}_0^S) are actually the result of the primary sensing phase described before.

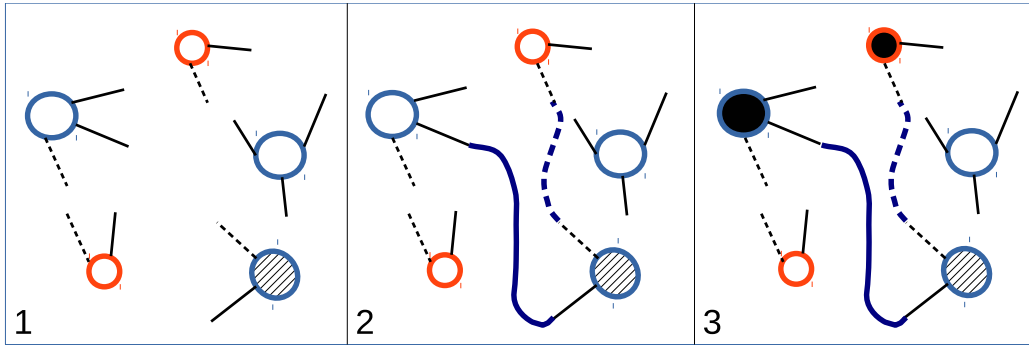


Figure 8.2: Illustration of primary sensing phase. In this toy example, there are represented three PUs (big blue circles) and two SUs (small red circles). Please see their half-edges that are all initially unpaired (solid half-edges will connect PU-PU or SU-SU, and dashed ones will connect PU-SU). In Step 1, a PU is selected and becomes to be an active node (the hatched circle). This node has degree $(1, 1)$ (one solid and one dashed half-edge respectively). This means that the node will have two neighbors: one primary and one secondary. In Step 2, each half-edge of the new active node is in turn paired with another uniformly randomly chosen unmatched half-edge. In other words, in this step the neighbors of the hatched node are defined. Finally, the nodes (PUs and SUs) which are neighbors of the active node (the ones which their half-edges were chosen in step 2) are moved to the blocked set (black nodes).

8.3.3 Markov process and fluid limit

Note that in the configuration model described above, the process given by

$$(|\mathcal{A}_t^P|, |\mathcal{B}_t^P|, |\mathcal{E}_t^P|, |\mathcal{B}_t^S|, |\mathcal{E}_t^S|)$$

constitutes a continuous-time Markov Process during the primary sensing phase, and analogously the process given by $(|\mathcal{A}_t^S|, |\mathcal{B}_t^S|, |\mathcal{E}_t^S|)$ constitutes a Markov Process during the secondary sensing phase. For instance, the time between transitions during the primary sensing phase is exponentially distributed with mean equal to $1/|\mathcal{E}_t^P|$ (since only unexplored nodes may become active at any given time).

However, since we are interested in the number of active nodes resulting from the sensing phases, our goal is to calculate $|\mathcal{A}_\infty^S|$, and not precisely which nodes are active. We thus follow the ideas presented in [95] and particularly [96], which chooses a set of variables that not only conforms a Markov Process, but is also amenable to a relatively simple analysis, in particular when the number of nodes tends to infinity.

Let us then define the following important variables:

- $E_t^P(i, j)$ and $E_t^S(i, j)$: number of unexplored primary and secondary nodes of degree (i, j) at time t .
- U_t^{PP} : number of unpaired half-edges at time t belonging to primary nodes and that should be connected to another primary node.
- U_t^{SS} : same as above but between secondary nodes.

8.3. Random graphs and configuration algorithm

- U_t^{PS} : number of unpaired half-edges at time t that belong to a primary node and should be connected to a secondary node or viceversa.²
- A_t^P and A_t^S : number of active primary and secondary nodes at time t

Initially we have the following conditions:

- all the vertices are unexplored: $E_0^P(i, j) = \mu(i, j)$ and $E_0^S(i, j) = \nu(i, j)$,
- all the half-edges are unpaired:
 - $U_0^{PP} = \sum_{i,j} i\mu(i, j)$,
 - $U_0^{PS} = \sum_{i,j} 2j\mu(i, j) = \sum_{i,j} 2i\nu(i, j) = \sum_{i,j} j\mu(i, j) + \sum_{i,j} i\nu(i, j)$ and
 - $U_0^{SS} = \sum_i \sum_j j\nu(i, j)$,
- no transmitter is active: $A_0^P = A_0^S = 0$.

As we discuss below, during the primary sensing phase the process

$$X_t = (A_t^P, (E_t^P(i, j))_{i,j}, (E_t^S(i, j))_{i,j}, U_t^{PP}, U_t^{PS})$$

also constitutes a continuous-time Markov Process. An analogous process will be defined for the secondary phase. Its Markovian structure, as we explain in details in Section 4.1, allows us to analyze its asymptotic behavior by means of a simpler deterministic approximation which is denominated “fluid limit”. That is, considering $\tilde{X}^N(t)$ as the Markov process parametric in N , then when $N \rightarrow \infty$ $X^N(t) = \frac{\tilde{X}^N(t)}{N}$ converges in probability over compact time intervals to a deterministic process $x(t)$, described by the ODE:

$$x'(t) = Q(x(t)). \quad (8.1)$$

Even if the resulting deterministic differential equation is in many cases an intuitive description of the system, the proof of this kind of convergence or the process X_t is quite technical. The main issue in this case is that the process X_t is a measured-valued Markov process [111], which implies a careful definition of the topologies involved in the convergence result. Examples of formal proofs of convergence for this kind of processes in similar contexts can be found in [45, 95, 96]. In the next section we focus on the calculus of the drift for our process of interest X_t in order to determine the fluid limit (Theorem 1). Moreover, in this case we can obtain an explicit expression of $x(t)$ (solution of Eq. (8.1)).

Primary sensing phase

In this section we discuss the Markov structure of the process

$$X_t = X^{Np}(t) = (A_t^P, (E_t^P(i, j))_{i,j}, (E_t^S(i, j))_{i,j}, U_t^{PP}, U_t^{PS}), \quad (8.2)$$

during the primary sensing phase and we calculate its drift. As we mentioned before, the drift determines the fluid limit. First of all, the times between transitions are exponentially

²Please note that the number of unmatched half-edges that belong to a secondary node and that should be connected to a primary node is at all time equal to $U_t^{PS}/2$.

Chapter 8. Capacity analysis using random graphs

distributed with mean $1/\sum_{i,j} E_t^P(i,j)$, since only primary unexplored nodes are competing for the channel (the rest are either blocked or already active). Let us then consider that at time t a primary node starts transmitting, and thus a transition occurs. Then the transition probabilities may be calculated as follows:

- A random node is uniformly chosen among all unexplored nodes and becomes active. Thus A_t^P increases by one with probability 1.
- The newly active node's degree distribution is simply:

$$\alpha_t(i,j) = \frac{E_t^P(i,j)}{\sum_{k,l} E_t^P(k,l)}.$$

Suppose that the new transmitter has degree (I,J) . This implies that it has I half-edges to be paired with other I unmatched half-edges (belonging to primary nodes), and J half-edges to be paired with other J ones (from secondary nodes). Then the number of unpaired half-edges U_t^{PP} and U_t^{SP} will be reduced by $2I$ and $2J$ respectively³ with probability $\alpha_t(I,J)$.

- Let us focus on the neighbors of the tagged node, which should now be blocked. Assume we have to pair an unmatched half-edge to a primary node (one of the I half-edges from before). The pairing half-edge may be chosen from all those available (U_t^{PP}), of which precisely $iE_t^P(i,j)$ belong to an unexplored node with degree (i,j) . Thus, the probability that any of the I primary neighbors of the tagged node is unexplored and has a degree (i,j) is equal to:

$$\beta_t^P(i,j) = \frac{iE_t^P(i,j)}{U_t^{PP}}.$$

By a similar argument, the probability that any of the J secondary neighbors of the tagged node has a degree (i,j) and is unexplored is equal to:

$$\beta_t^S(i,j) = \frac{iE_t^S(i,j)}{U_t^{PS}/2}.$$

With the discussion above we are in conditions of calculating the drift of the process. For instance, A_t^P has a drift equal to $1 \times \sum_{i,j} E_t^P(i,j)$. Let us then normalize our process by the number of primary and secondary nodes N_P and N_S (where we will assume that N_P/N_S is a constant) and obtain a result such as Eq. (8.1).

Theorem 1. *Consider the configuration model discussed in Sec. 8.3.2 and the processes defined in Sec. 8.3.3 during the primary phase. Let us define the normalized processes, for which N_P/N_S is a constant:*

³Please note that the existence of loops or multi-edges are possible with the configuration model discussed in Sec. 8.3.2. For instance, actually U_t^{PP} should be decreased by $2I - 2L$ (with L the number of self-loops). However, as indicated by intuition, proved in [95, 96], and further discussed in [45], when the number of nodes goes to infinity, as we will consider next, the probability of such occurrences may be neglected in the analysis.

8.3. Random graphs and configuration algorithm

- $\tilde{A}_t^P = A_t^P / N_P$
- $\tilde{E}_t^P(i, j) = E_t^P(i, j) / N_P$ and $\tilde{E}_t^S(i, j) = E_t^S(i, j) / N_S$
- $\tilde{U}_t^{PP} = U_t^{PP} / N_P$ and $\tilde{U}_t^{SP} = U_t^{SP} / N_P$

Let be $\tilde{X}_t^N = (\tilde{A}_t^P, \tilde{E}_t^P(i, j), \tilde{E}_t^S(i, j), \tilde{U}_t^{PP}, \tilde{U}_t^{SP})$. Therefore, as $N_P \rightarrow \infty$, \tilde{X}_t^N converges in probability over compact time intervals to $x^P(t) = (a_t^P, e_t^P(i, j), e_t^S(i, j), u_t^{PP}, u_t^{PS})$ solution of the following differential equation system:

$$\frac{da_t^P}{dt} = \sum_{k,l \in \mathbb{N}} e_t^P(k, l); \quad (8.3)$$

$$\frac{de_t^P(i, j)}{dt} = -e_t^P(i, j) - \frac{ie_t^P(i, j)}{u_t^{PP}} \sum_{k,l \in \mathbb{N}} ke_t^P(k, l); \quad \forall i, j \in \mathbb{N}; \quad (8.4)$$

$$\frac{de_t^S(i, j)}{dt} = -\frac{2ie_t^S(i, j)}{u_t^{PS}} \sum_{k,l \in \mathbb{N}} le_t^P(k, l); \quad \forall i, j \in \mathbb{N}; \quad (8.5)$$

$$\frac{du_t^{PP}}{dt} = -2 \sum_{k,l \in \mathbb{N}} ke_t^P(k, l); \quad (8.6)$$

$$\frac{du_t^{PS}}{dt} = -2 \sum_{k,l \in \mathbb{N}} le_t^P(k, l); \quad (8.7)$$

where

$$\begin{aligned} a_0^P &= 0; \\ e_0^P(i, j) &= \frac{\mu(i, j)}{N_P}; \quad \forall i, j \in \mathbb{N} \text{ and } e_0^S(i, j) = \frac{\nu(i, j)}{N_S}; \quad \forall i, j \in \mathbb{N}; \\ u_0^{PP} &= \frac{1}{N_P} \sum_{i=0}^{\infty} \sum_{j=0}^{\infty} i\mu(i, j) \text{ and } u_0^{PS} = \frac{1}{N_P} \sum_{i=0}^{\infty} \sum_{j=0}^{\infty} 2j\mu(i, j). \end{aligned}$$

Some remarks are in order concerning the result above. Firstly, the original Markov Chain has an absorbing state for which $E_t^P(i, j) = 0 \forall i, j$. This is reflected in the set of equations above, where we have an equilibrium point when $e_t^P(i, j) = 0 \forall i, j$.

Secondly, and as we mentioned before, primary nodes act independently of secondary ones. This is again reflected in the set of equations, where the key is to solve equations (8.4) and (8.6) which are coupled (the rest may be solved once we obtain an analytical expression for $e_t^P(i, j)$, see details in Appendix D.1), and refer to the behavior of these nodes.

Thirdly, we can include into our model unsaturated traffic conditions for primary users. We model this aspect by incorporating the transmission probability p_{PU} . This parameter defines the number of primary transmitters that have packets to be sent in each time slot. In other words, in this phase of the algorithm only the primary unexplored nodes which have packet to be sent are competing for the channel. This only affects $e_0^P(i, j)$ value as $e_0^P(i, j) = p_{PU} \frac{\mu(i, j)}{N_P}; \quad \forall i, j \in \mathbb{N}$.

Chapter 8. Capacity analysis using random graphs

Lastly, we are actually interested in how many secondary nodes are still unexplored after the primary sensing phase is over, so as to study the secondary phase. That is to say, we want to calculate $e_\infty^S(i, j) \forall i, j$, which will in turn become the initial conditions of the secondary sensing phase. This value may be calculated as follows:

Theorem 2. *Consider the processes and variables defined in Theorem 1. Let τ_∞ be the unique value in $(0, \infty]$ such that*

$$\int_0^{\tau_\infty} \frac{u_0^{PP} e^{-2\sigma}}{\sum_{k,l \in \mathbb{N}} k e_0^P(k, l) e^{-k\sigma}} d\sigma = 1. \quad (8.8)$$

Then, the proportion of unexplored secondary nodes at the beginning of the secondary phase converges in probability to:

$$e_\infty^S(i, j) = e_0^S(i, j) \left(\frac{u_{\tau_\infty}^{PS}}{u_0^{PS}} \right)^i \quad \forall (i, j), \quad (8.9)$$

where

$$u_{\tau_\infty}^{PS} = u_0^{PS} - 2 \int_0^{\tau_\infty} \sum_{k,l \in \mathbb{N}} l e_0^P(k, l) e^{-k\sigma} \frac{u_0^{PP} e^{-2\sigma}}{\sum_{k,l \in \mathbb{N}} k e_0^P(k, l) e^{-k\sigma}} d\sigma. \quad (8.10)$$

Proof. See Appendix D.1. □

Some interesting insights may be obtained from the result of equation (8.9). For instance, and as we mentioned before, the result of the primary phase is not influenced by the secondary nodes. This is reflected by the fact that the proportion of secondary nodes that are still unexplored after the primary sensing phase only depends on the degree towards primary nodes (the variable i). More in particular, its form is exponential on i , generating great differences between secondary nodes regarding their access probability. Since $u_{\tau_\infty}^{PS}/u_0^{PS} < 1$, those who belong to the protection zone of several primary nodes will seldomly access the channel.

Please note that $u_{\tau_\infty}^{PS}/u_0^{PS}$ represents the proportion of unpaired half-edges between primary and secondary users at the end of the primary sensing phase. These unpaired half edges correspond to primary users that did not become active. Therefore, the quotient may be interpreted as the probability of a secondary user to be out of the protection zones of active primary nodes.

Secondary sensing phase

Once the primary sensing phase is over, we turn our attention to the secondary sensing phase. The construction of the Markov Process will be very similar to the previous sections, but in this case is a little simpler, since we do not have to take into account primary nodes. In this sense, let us somewhat abuse the notation and define $E_t^S(j)$ as the number of unexplored secondary nodes during the secondary sensing phase that have j half-edges to be paired with other secondary nodes. Then, the initial condition $E_0^S(j)$ is the result

8.3. Random graphs and configuration algorithm

of the primary sensing phase, and will be estimated from $e_\infty^S(k, j)$ as defined in (8.9). It should be noted that the existence of the limit $\lim_{t \rightarrow \infty} e_t^S(k, j)$ (stationary regime) should be guaranteed. The existence of this limit is related to the ergodicity of the process and it can be proved with similar arguments to the ones included in [74] and the references therein.

Finally, with arguments very similar to the ones used in the previous subsection, we reach the following result:

Theorem 3. *Consider the configuration model discussed in Sec. 8.3.2, $E_t^S(j)$ as defined above, and the processes defined in Sec. 8.3.3 during the secondary sensing phase. Furthermore, let $e_\infty^S(i, j)$ be the value defined in (8.9). Let us define the normalized processes $\tilde{A}_t^S = A_t^S/N_S$, $\tilde{E}_t^S(j) = E_t^S(j)/N_S$, and $\tilde{U}_t^{SS} = U_t^{SS}/N_S$.*

Then, as $N_S \rightarrow \infty$, they converge in probability to the solution of the following set of differential equations:

$$\frac{da_t^S}{dt} = \sum_{l \in \mathbb{N}} e_t^S(l); \quad (8.11)$$

$$\frac{de_t^S(j)}{dt} = -e_t^S(j) - \frac{je_t^S(j)}{u_t^{SS}} \sum_{l \in \mathbb{N}} le_t^S(l); \quad \forall j \in \mathbb{N}; \quad (8.12)$$

$$\frac{du_t^{SS}}{dt} = -2 \sum_{l \in \mathbb{N}} le_t^S(l); \quad (8.13)$$

where

$$\begin{aligned} a_0^S &= 0; \\ e_0^S(j) &= \sum_{k \in \mathbb{N}} e_\infty^S(k, j) \quad \forall j \in \mathbb{N}; \\ u_0^{SS} &= \frac{1}{N_S} \sum_{l \in \mathbb{N}} lv(k, l). \end{aligned}$$

Again, we are interested only on the limit of a_t^S as t goes to infinity (when the secondary sensing phase is over). This represents an estimation of the MAP_{SU} . By similar manipulations of the differential equations (Eq. (8.11-8.13) can be resolved explicitly, see details in Appendix D.2) the following result may be obtained:

Theorem 4. *Consider the processes and variables defined in Theorem 3. Let τ_∞ be the unique value in $(0, \infty]$ such that*

$$\int_0^{\tau_\infty} \frac{u_0^{SS} e^{-2\sigma}}{\sum_{l \in \mathbb{N}} le_0^S(l) e^{-l\sigma}} d\sigma = 1. \quad (8.14)$$

Then, the proportion of active secondary transmitters (MAP_{SU}) converges in probability to:

$$a_\infty^S = \int_0^{\tau_\infty} \sum_{j \in \mathbb{N}} e_0^S(j) e^{-j\tau} \frac{u_0^{SS} e^{-2\tau}}{\sum_{j \in \mathbb{N}} je_0^S(j) e^{-j\tau}} d\tau \quad (8.15)$$

Proof. See Appendix D.2. □

Analogously, it is possible to prove that the proportion of active secondary transmitters of degree j , converges in probability to:

$$a_\infty^S(j) = \int_0^{\tau_\infty} e_0^S(j) e^{-j\tau} \frac{u_0^{SS} e^{-2\tau}}{\sum_{k \in \mathbb{N}} k e_0^S(k) e^{-k\tau}} d\tau, \forall j. \quad (8.16)$$

In this phase of the algorithm, the Markov Chain has an absorbing state where $E_t^S(j) = 0 \forall j$ (it finishes when all secondary nodes are active or blocked). This is reflected in the set of equations above, where we have an equilibrium point when $e_t^S(j) = 0 \forall j$. In addition, in Eq. (8.16) we can observe that the medium access probability is influenced by the node's degrees. This is reasonable because the larger j is, the larger the probability of being blocked by another secondary node is.

8.4 Simulated experiments and results

In order to validate the proposed approximation we will present an example considering a large but finite number of nodes. We calculate the MAP_{SU} using our deterministic expression (Eq. (8.15)) and we compare it with the results obtained of several simulations of the stochastic process \tilde{A}_∞^S . We also show the accuracy of our methodology analyzing several realizations of the process $\tilde{E}_t^S(i, j)$ with its associated deterministic estimation $e_t^S(i, j)$ in both phases of the algorithm. In the next section we compare our results with results for spatial models based on stochastic geometry techniques. Finally, we complete our validation by testing the methodology in other representative scenarios.

Before introducing the particular example, let us now explain the validation method. First we simulate a graph that satisfies certain characteristics (the characteristics are defined according to the network we want to simulate). Given the graph, we can extract the counting measures $\mu(i, j)$ and $\nu(i, j)$ and then we apply the results of Theorems 1, 2, 3 and 4 obtaining deterministic approximations of several metrics, in particular the estimation of the MAP_{SU} . On the other hand, having the graph we proceed to simulate several realizations of the stochastic process (its evolution is related with the considered MAC protocol) and as a result we obtain the simulated metrics of interest.

In this section, as a first illustration of the accuracy of our proposal, we choose the variation of the Erdős-Rényi model that was described in Sec. 8.3.1. In particular we consider $k = 1 \dots 10$, where $k = k_{PP} = k_{PS} = k_{SS}$. Consequently, for each k value, we have that on average, each PU has k primary neighbors and k secondary users in its protection zone. In addition, each SU has on average k secondary neighbors.

Several realizations of $\sum_i \sum_j \tilde{E}_t^S(i, j)$, where the graphs have the characteristics explained before, are shown in Figures 8.3 and 8.4 along with the solutions of Eq. (8.5) and Eq. (8.12) respectively. As an example we show the performance of a specific k value ($k = 10$). Figure 8.3 represents the evolution of the proportion of unexplored SUs during the Primary Sensing Phase. We can observe that in Figure 8.4 (which represents the same but during the Secondary Sensing Phase) the initial condition coincides with the limit value in Figure 8.3. As expected, the limit value that is shown in Figure 8.4 is 0

8.4. Simulated experiments and results

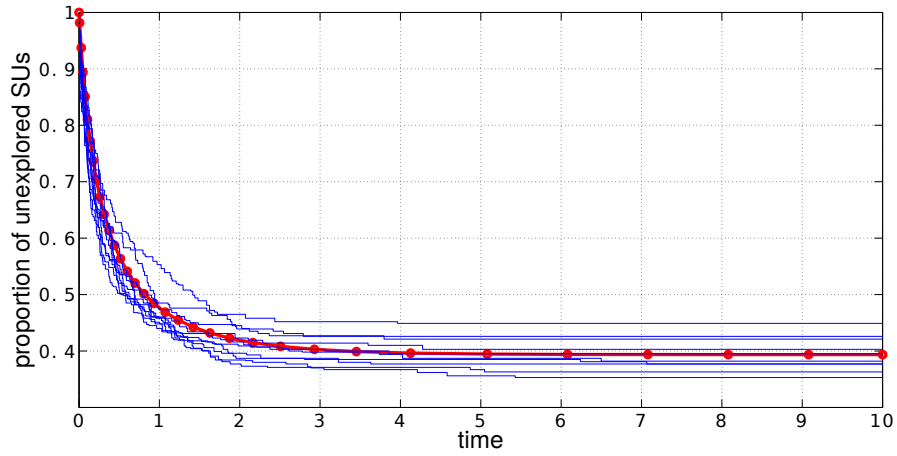


Figure 8.3: $\sum_i \sum_j \tilde{E}_t^S(i, j)$ during the Primary Sensing Phase. The deterministic estimation Eq. (8.5) is marked with circles. Parameters: $N_P = 500$, $N_S = 1000$, $p_{PU} = 0.5$ and $k = 10$.

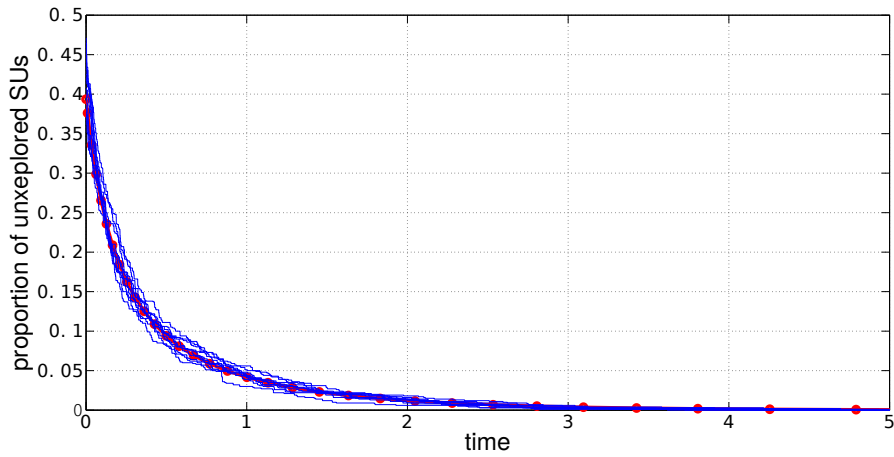


Figure 8.4: $\sum_i \sum_j \tilde{E}_t^S(i, j)$ during the Secondary Sensing Phase. The deterministic estimation Eq. (8.12) is marked with circles. Parameters: $N_P = 500$, $N_S = 1000$, $p_{PU} = 0.5$ and $k = 10$.

(when the process finishes, no SU is unexplored). These figures illustrate how $e_t^S(i, j)$ effectively represents the mean of $\tilde{E}_t^S(i, j)$ in both phases of the algorithm. Similar results were obtained for the other involved stochastic processes.

Finally, in Figure 8.5 we show the performance of the methodology for the different values of the parameter k (k is in the abscissa). The larger k is, the larger the connection probabilities are and then, the smaller the medium access probability of SUs is. We can conclude that Eq. (8.15) provides a very accurate approximation of the access medium probability.

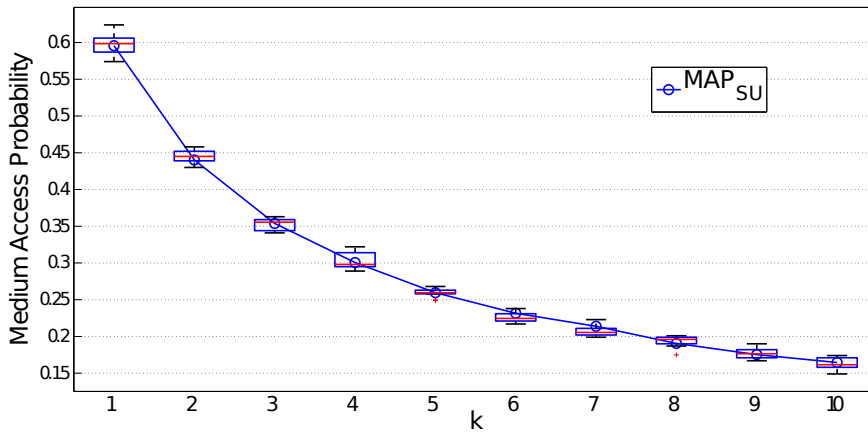


Figure 8.5: The evaluation of Eq. (8.15) along with the boxplot of the numerical results of 10 simulations with parameters: $N_p = 500$, $N_s = 1000$, $p_{PU} = 0.5$ and $k = 1 \dots 10$.

8.5 Comparison with spatial models

In this section we compare our proposal with a result based on stochastic geometry and point processes. This type of analysis focuses on the random spatial location of users and aim at estimating the medium access probability (and other metrics) for a given user configuration. We have chosen to compare the results of the article [49] which have been extended in [93]. In these articles, the authors proposed a probabilistic model to analyze the cognitive radio paradigm in large wireless networks with randomly located users. The authors also used Cognitive-CSMA as the medium access mechanism.

This section is organized as follows. First, we introduce the probabilistic model of [49, 93] and their analytical results. We also propose a modification in their model in order to be in a “comparable” context to ours. Finally we present two representative examples to compare both results.

8.5.1 An approximation of the medium access probability using a stochastic geometry analysis

Using a stochastic geometry approach, the location of the nodes of the network is seen as the realization of one or many point processes. This means that the network can be considered as a snapshot of a stationary random model in the (Euclidean) space which is possible to analyze in a probabilistic way. The time is divided into slots and one slot is needed to transmit a packet for all users. Then, one snapshot represents the nodes spatial distribution in one time slot.

In the articles [49, 93] the users of the network are assumed to be a realization of two independent marked Poisson point processes (PPP) $\Phi_p = \{X_i^p, t_i^p\}$ and $\Phi_s = \{X_i^s, t_i^s\}$ with intensities λ_p and λ_s on \mathbb{R}^2 respectively. $\{X_i^p\}$ and $\{X_i^s\}$ denotes the positions of the potential primary and secondary transmitters, and t_i^p (and t_i^s) models the backoff timers used in the Cognitive-CSMA protocol ($\{t_i^p\}$ and $\{t_i^s\}$ are i.i.d r.v.s. uniformly distributed

8.5. Comparison with spatial models

in $[0, 1]$). The model also features an infinite symmetric matrix $F = \{F(i, j)_{i, j}\}$ which models the fading of the channel from user i to user j (being i and j two arbitrary transmitters, PU or SU). A deterministic attenuation $\alpha > 2$ is also assumed (i.e. $L(d) = d^{-\alpha}$, being d the distance between two nodes). Considering those features we can say that the power received from i by j is:

$$P(i, j) = P(i)F(i, j)L(\|X_j - X_i\|). \quad (8.17)$$

With that in mind, conforming to the medium access mechanism, a primary transmitter will access to the channel if it has the smallest timer among its primary contenders. For secondary transmitters, it will access if it has no active primary contender and it has the smallest timer between its secondary neighbors. Then, for each primary node $i \in \Phi_p$ we can define the set of its primary neighbors (\mathcal{N}_i^p) as

$$\mathcal{N}_i^p = \{j \in \Phi_p : \frac{F(j, i)}{\|X_i^p - X_j^p\|^\alpha} > \rho, j \neq i\}, \quad (8.18)$$

where ρ is a threshold that determines how sensitive the CS is. Please note that in this model, $P(j)$ is assumed constant and included in $F(j, i)$ which is considered as a virtual power.

On the other hand, for each secondary user $i \in \Phi_s$, we need to know the sets of: its active primary contenders (\mathcal{N}_i^p) and its secondary contenders (\mathcal{N}_i^s). Letting Φ_p^* be the process of active primary transmitters, these sets can be defined as

$$\mathcal{N}_i^p = \{j \in \Phi_p^* : \frac{F(j, i)}{\|X_i^s - X_j^p\|^\alpha} > \rho'\} \text{ and} \quad (8.19)$$

$$\mathcal{N}_i^s = \{j \in \Phi_s : \frac{F(j, i)}{\|X_i^s - X_j^s\|^\alpha} > \rho', j \neq i\} \quad (8.20)$$

respectively.

According to that, the primary and secondary retain indicators are:

$$R_i^p = \mathbb{1}_{\{t_i^p < t_j^p \forall X_j^p \in \mathcal{N}_i^p\}} \text{ and} \quad (8.21)$$

$$R_i^s = \mathbb{1}_{\{t_i^s < t_j^s \forall X_j^s \in \mathcal{N}_i^s, \mathbb{1}_{|\mathcal{N}_i^p|=0}\}} \mathbb{1}_{\{|\mathcal{N}_i^p|=0\}}. \quad (8.22)$$

This means that the medium access probabilities are $MAP_{PU} = P(R_i^p = 1)$ and $MAP_{SU} = P(R_i^s = 1)$. The first term of Eq. (8.22) corresponds to the case where the timer of the secondary transmitter i is smaller than all the timers of its secondary neighbors ($t_i^s < t_j^s \forall X_j^s \in \mathcal{N}_i^s$) considering only the ones which are not in a primary protection zone of an active PU ($\mathbb{1}_{|\mathcal{N}_i^p|=0}$). The second term says that the secondary transmitter i is not in a primary protection zone of an active PU ($\mathbb{1}_{|\mathcal{N}_i^p|=0}$).

The authors of [49, 93] obtain a conservative approximation of MAP_{SU} . They simplified the model considering that a SU will be preempted if it has one or more primary contenders no matter whether the contenders are active or not. Therefore, many secondary users, which are in conditions to use the band, might be silenced. In this context, the MAP

Chapter 8. Capacity analysis using random graphs

probability expressions for PUs and SUs are:

$$MAP_{PU} = \frac{1 - e^{-\lambda_p \bar{N}_0}}{\lambda_p \bar{N}_0} \text{ and} \quad (8.23)$$

$$MAP_{SU} \approx \frac{1 - e^{-\lambda_s \bar{N}_0 e^{-\lambda_p \bar{N}_0}}}{\lambda_s \bar{N}_0}, \quad (8.24)$$

where \bar{N}_0 is the mean number of contenders of a typical user in a network of intensity 1 and $G(t) = P(F \leq t)$ is the fading c.d.f.:

$$\bar{N}_0 = \int_{\mathbb{R}^2} (1 - G(\rho|x|^\alpha)) dx. \quad (8.25)$$

Without loss of generality, we have considered $\rho = \rho'$.

The calculus for secondary users MAP is approximated because the authors of [49,93] considered the non preempted secondary users as an independent thinned process from secondary users process with thinning probability $e^{-\lambda_p \bar{N}_0}$. For more details see [49].

Complementing the articles [49, 93] we propose an improvement in the estimation of Eq. (8.24). The idea is to apply an analogous assumption of [49] in order to model the active PU process Φ_p^* as a PPP. Taking this into account, the idea is to approximate the process Φ_p^* by an independent thinning of PU process Φ_p with thinning probability MAP_{PU} . In this context, we can apply the retain indicator defined by Eq. (8.22) obtaining a non conservative estimation of the MAP_{SU} and also more appropriate to compare to our results:

$$MAP_{SU} \approx \frac{1 - e^{-\lambda_s \bar{N}_0 e^{-\lambda_p MAP_{PU} \bar{N}_0}}}{\lambda_s \bar{N}_0}. \quad (8.26)$$

Please note that the fading variables are assumed to be independent of the nodes positions.

8.5.2 Numerical examples

In this section we choose three representative examples in order to illustrate the accuracy and the applicability of both approximations (our estimation using random graphs Eq. (8.15) and the one presented in Eq. (8.26)). In particular, in all cases we have assumed a Rayleigh fading ($G(t) = 1 - e^{-\theta t}$) because in this situation \bar{N}_0 has a closed formula to be used in Eq. (8.26):

$$\bar{N}_0 = \frac{2\pi\Gamma(2/\alpha)}{\alpha(\rho\theta)^{2/\alpha}}, \quad (8.27)$$

where $\Gamma(\cdot)$ is the Euler Gamma function.

We consider different values of fading mean θ . For each θ value, we run several independent simulations of the access process. In order to evaluate the performance of both approaches, we consider as the true MAP the one provided by the average of all the simulations.

Example 1: Poisson Point processes

In this particular case, given a realization of two spatial PPPs (Φ_p and Φ_s with intensities λ_p and λ_s) and the fading variables between any pair of nodes, the conflict graph is built considering also the path-loss phenomenon according to the definitions of \mathcal{N}_i^P , \mathcal{N}_i^S and \mathcal{N}_i^{PS} . Once the graph is obtained, we extract the values of N_S , N_P and the measures $\mu(i, j)$ and $\nu(i, j)$, and we proceed in the same way as in Sec. 8.4.

For each θ value, we run 10 independent simulations and in Figure 8.6 we present the analytical results (of both estimations) together with the corresponding simulated values.

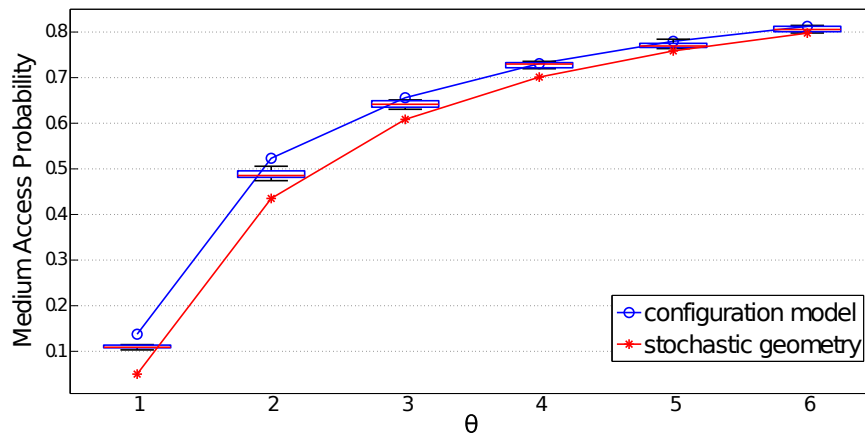


Figure 8.6: Evaluation of Eq. (8.15) and Eq. (8.26) along with the boxplot of the numerical results of 10 simulations with parameters: $\lambda_p = 1.6$ ($p_{PU} = 0.5$ and $\bar{N}_P = 500$), $\lambda_s = 6.4$ ($\bar{N}_S = 2000$), $\alpha = 3$, considering different values of θ .

Some remarks regarding the obtained results. Firstly, our random graph estimation of the MAP_{SU} shows a very good performance complementing the results of Sec. 8.4. Please note that our method considers a graph which is chosen randomly among all graphs that comply with the initial measures $\mu(i, j)$ and $\nu(i, j)$. This means, that in this example our configuration model ignores correlations that appear when spatial features are considered. This explains why the performance results in the Erdős-Rényi case (Figure 8.5) are better than in this case. Even more, this is the reason that justifies the improvement in the accuracy when θ is large. In other words, the effects of the ignored aspects decrease when the amount of noise in the graph increases.

Secondly, we observe that the stochastic geometry estimation has a good accuracy too. Eq. (8.26) was obtained assuming that active primary (and secondary) users are located according to a realization of an homogeneous PPP; consequently the larger θ is, the more reasonable this assumption is, and then, the more accurate the MAP approximation is.

Lastly, we can conclude that in this particular scenario both approaches are suitable despite considering a finite number of nodes.

Example 2: Grid configuration for primary users

A natural scenario for cognitive radio networks, corresponds to a planned primary topology together with a disordered and random secondary one. Therefore, in this second example, we choose a particular fixed configuration for the primary nodes. We consider that PUs are located in a perfect grid configuration and SUs are located according to a realization of a PPP (see for instance Figure 8.7). Please note that this PUs configuration is not in the hypothesis of none of the analyzed methods. In particular, the communication graph is not totally random since the nodes are located in a specific configuration. Despite of this fact, we are going to test how versatile the two approaches are.

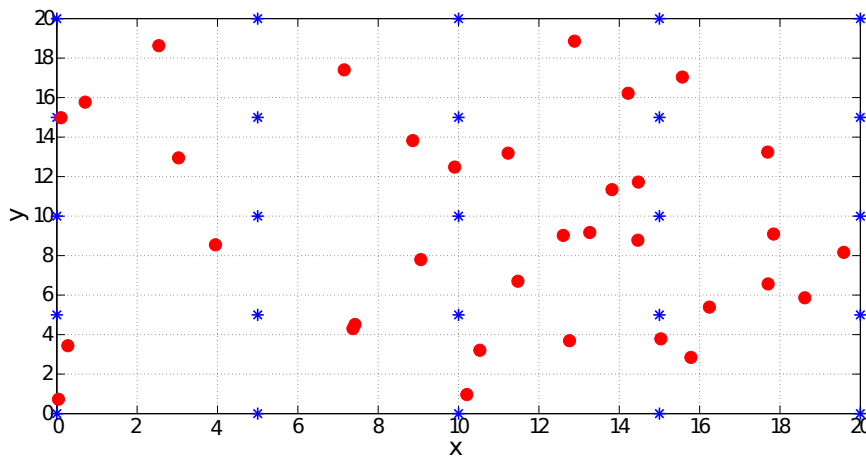


Figure 8.7: Example of a primary grid configuration (stars) with random secondary nodes (circles).

We apply Eq. (8.26) as if the primary process was a PPP. In this case, in order to apply the stochastic geometry expressions, the natural thing to do is to estimate the process intensities. Then, the primary intensity can be calculated as $\lambda_p = \frac{N_p}{L^2}$ where L is the dimension of the grid. For instance, in the example scenario of Figure 8.7 we can say that $\lambda_p = \frac{25}{20^2}$.

In Figure 8.8 we show the performance of both approaches together with the simulated results. The obtained result reflects a poor performance of the spatial model while our random graph approximation shows a better performance. This represents a limitation of the spatial model’s application, more specifically when the involved point processes are not all Poisson. In addition, in this case is more evident the fact that our proposed approximation ignores spatial correlation (see Figures 8.5 and 8.6 and compare them with Figure 8.8). Primary users are located in a specific fixed configuration but thanks to the randomness provided by the fading, the resulting performance indicators still give excellent approximations.

It is important to remark that, if the fading variables were constant, the approximations of Eq. (8.24) and Eq. (8.26) would lack of sense. In addition, in many cases determining closed analytical expression of performance metrics using stochastic geometry techniques represents a difficult task.

8.5. Comparison with spatial models

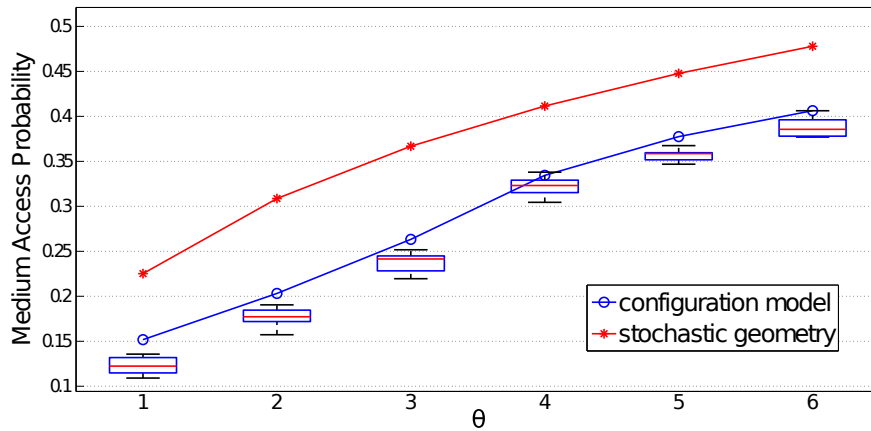


Figure 8.8: Evaluation of Eq. (8.15) and Eq. (8.26) along with the boxplot of the numerical results of 10 simulations with parameters: $\lambda_p = 0.005$ ($p_{PU} = 1$), $\lambda_s = 0.007$, $\alpha = 3$, $L = 360$, considering different values of θ .

Example 3: Real configurations for primary users

We conduct two more realistic experiments to evaluate secondary MAP where locations of PUs are provided by the open source project OpenCellID [112]. This project maintains a complete and open database from which we can easily retrieve latitude and longitude information of the cell-towers of a target geographic area [113].

We consider two different scenarios (see Figure 8.9), one with a high density of users (Case A: center of Paris) and another with a medium density (Case B: Paris suburbs). In both cases PUs are deployed according to data from cell-tower locations of one LTE-operator and SUs are deployed following a PPP. Figures 8.10 and 8.11 show the PU spatial distributions; please note that Case A has approximately twice the user intensity of Case B.

Given the two point process (Φ_p and Φ_s with intensities λ_p and λ_s) and the fading variables between any pair of nodes, the conflict graph (nodes which are neighbors to each other) is built considering also the path-loss phenomenon according to the definitions of \mathcal{N}_i^p , \mathcal{N}_i^p and \mathcal{N}_i^s . We consider different values of fading mean θ , and for each θ the measures $\mu(i, j)$ and $\nu(i, j)$ are obtained. As in Example 2 we apply Eq. (8.26) as if the primary processes were distributed as PPPs.

In Figures 8.12 and 8.13 we show the performance of both approaches together with the simulation results. Some remarks are in order concerning the obtained results. Firstly, our estimation of the MAP_{SU} shows an excellent performance in both cases. This demonstrates the versatility of our technique. We can also see the improvement in the accuracy when θ increases, due to the spatial correlation becoming weaker. Secondly, we observe that the stochastic geometry estimation has a good accuracy in Case A but a poor performance in Case B. The bad performance can be explained by non-homogeneous and non-Poisson characteristics of Φ_p : in Case B there are large areas without the presence of PUs and it also presents some clusters (see for example the airport zone). Maybe the

Chapter 8. Capacity analysis using random graphs

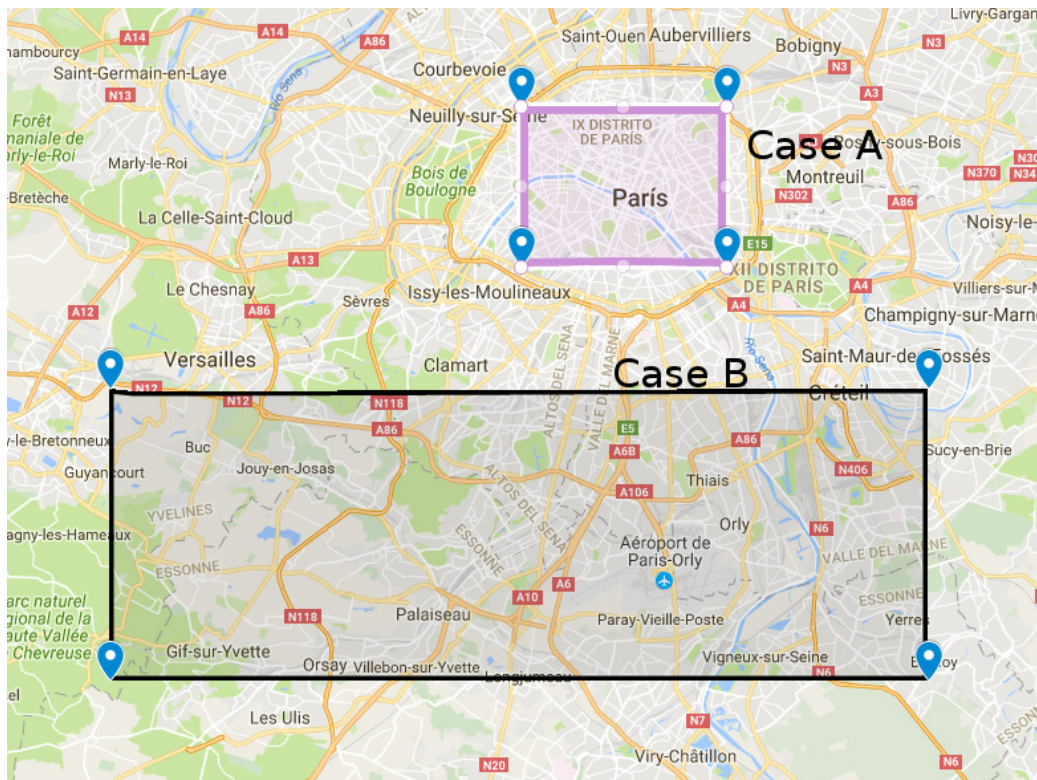


Figure 8.9: Geographical zones chosen for real scenarios: Case A and B. Case A is located in the heart of Paris and Case B in its suburbs.

stochastic geometry performance could be improved in this scenario if Φ_p is represented by a Poisson Cluster Process [114, 115], but this model is out of the scope of the thesis, it is one of our future research lines.

8.5. Comparison with spatial models



Figure 8.10: Case A: Points represent 2412 primary users located in an area of 47km^2 .

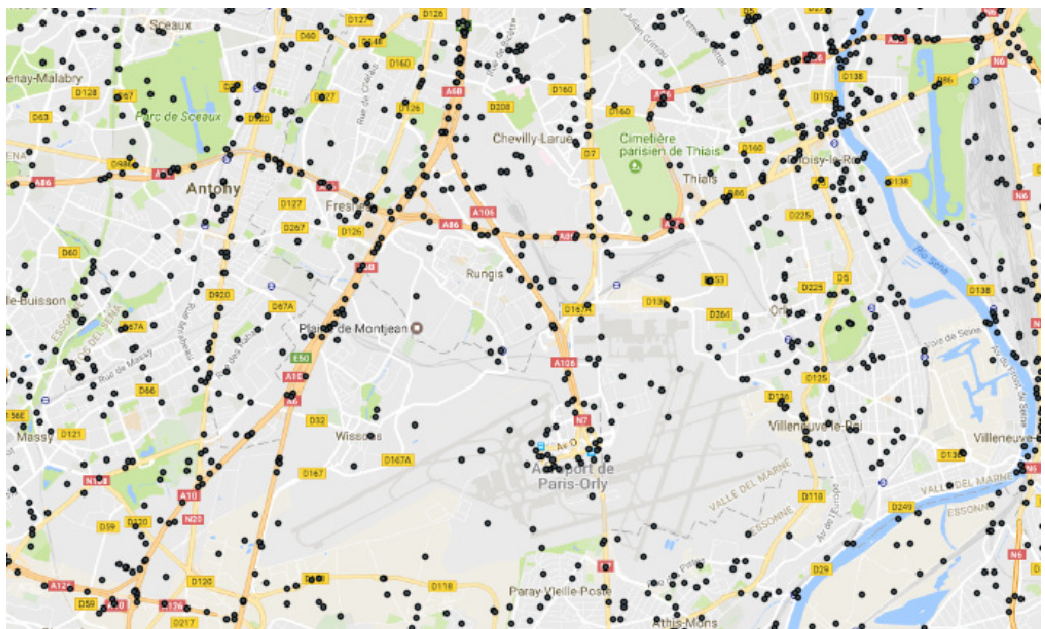


Figure 8.11: Case B: Points represent primary users (for the sake of presentation we show a specific zoom area). Scenario B considers a total of 1996 primary users located in an area of 83km^2 .

Chapter 8. Capacity analysis using random graphs

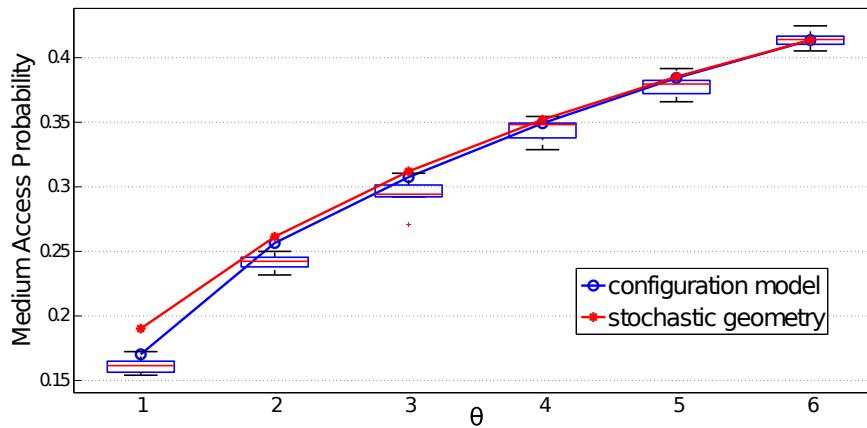


Figure 8.12: Case A performance results. Simulation Parameters: $N_P = 2412$, $N_S = 1800$, $p_{PU} = 0.4$, $\alpha = 3$, considering different values of θ .

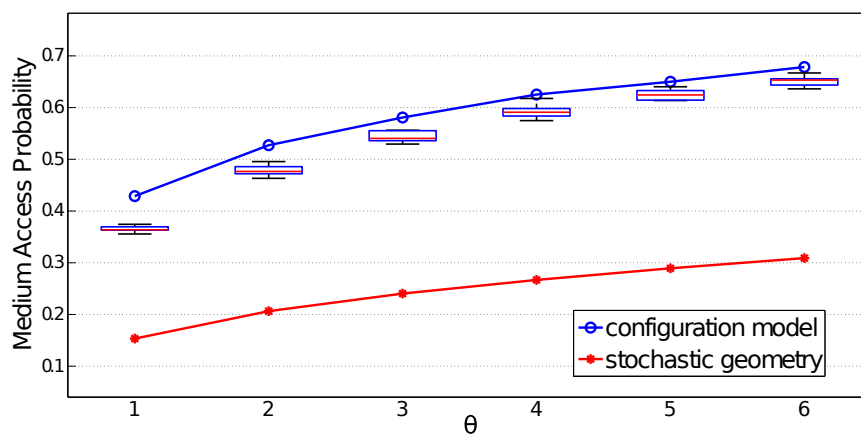


Figure 8.13: Case B performance results. Simulation Parameters: $N_P = 1996$, $N_S = 1237$, $p_{PU} = 0.6$, $\alpha = 3$, considering different values of θ .

8.6 Conclusions

We extended the methodology developed in [95] in the particular case of a cognitive radio network. With our proposal, we showed that it is possible to calculate an analytic approximation of the medium access probability (both for PUs and, most importantly, SUs) in an arbitrary large heterogeneous random network. This performance metric gives an idea of the possibilities offered by cognitive radio to improve the spectrum utilization.

Through extensive simulations, including real scenarios of primary network deployments, we have verified that the approximation obtained is accurate. We have also illustrated a performance comparison between our estimation and the one obtained by a stochastic geometry approach.

This page was intentionally left blank.

Chapter 9

Conclusions of Part II

The spectrum assignment in a cognitive radio network was studied considering stochastic geometry and random graphs. These results can be seen as the continuation of the theory of priorities in queueing theory to spatial processes.

We extended the methodology developed in [49] in the particular case of a multi-channel cognitive radio environment. We showed analytical results for the calculus of the main performance metrics: Medium Access Probability and Coverage Probability. These parameters give information about the possibilities offered by cognitive radio to improve the spectrum utilization and also they give an idea of how affected are primary users with the presence of secondary ones.

We showed how stochastic dynamics on configuration models can provide powerful performance tools for quantifying the effect of interference on the performance of cognitive radio networks. In particular, we developed a methodology to estimate the Medium Access Probability of secondary users based on random graphs. We compared our proposal with a result based on stochastic geometry and point processes.

This page was intentionally left blank.

Part III

General conclusions and future work

Chapter 10

General conclusions and perspectives

In the near future, the telecommunications industry will be faced with two big challenges: a need for more radio spectrum and an ever-increasing demand for data. Spectrum, however, is a finite resource. The concept of cognitive networks has emerged as one of the efficient means for utilizing the scarce spectrum by allowing spectrum sharing between a licensed primary network and a secondary network.

We envision that soon cognitive radio networks will become a reality. However, several challenges still need to be solved, new standards must be approved, new regulation is needed, and the wireless industry will have to develop the necessary equipment. It is also clear that, the necessary mechanisms should be developed in order to maintain the QoS compliance (both for primary and secondary services), particularly for applications with the most demanding requirements. We believe that this thesis is a contribution in this direction.

Thinking in the evolution of wireless technologies, rapidly comes to our minds a world with more and more devices connected to the Internet. In this scenario, Internet of things (IoT) paradigm poses new challenges to the way in which spectrum management is approached and implemented. Experts estimate that the IoT will consist of about 30 billion connected objects by 2022, the vast majority through wireless networks. In this sense, there are several issues that need to be addressed before cognitive radio technology can be used for Internet of things. This thesis contributes in this direction developing methodologies to evaluate the spectrum allocation problem where the number of wireless users is “unlimited”.

Throughout this thesis the resource allocation problem in cognitive radio networks has been studied in depth. We have analyzed the problem according three coordinates: frequency, time and space. In particular, we have made special emphasis in including economic aspects and user interactions, both in large random networks. The organization of this thesis tagged to reflect these two big aspects and so was organized in two parts. The first one was devoted to analyze a paid spectrum sharing mechanism with QoS management based on admission control decisions over secondary users. In the second one we addressed an integral problem of spectrum management including aspects such as: user interactions, interference, channel characteristics and spatial reuse of frequency bands. The research relied on several mathematical tools. The most important were Markov chains, Markov decision process, fluid limits, stochastic geometry and random graphs.

Chapter 10. General conclusions and perspectives

Concerning the paid spectrum sharing mechanism, three alternatives in order to obtain an estimation of the optimal admission control policy were developed. Two of them consisted in improving the time efficiency of one of the most used dynamic programming algorithms. The other was based on the fluid approximation of the control problem. The advantages of the proposed algorithm in comparison with the classical ones, and the accuracy of our results, were illustrated by several simulations.

With respect to the integral problem of spectrum management we addressed a network capacity analysis based on random graphs and stochastic geometry tools. In particular, a methodology based on configuration models for random graphs was adapted to the case of cognitive radio networks. We showed how our proposal can provide powerful performance tools for quantifying the effect of interference on the performance of such networks. We included several simulated examples and we showed the versatility of our proposal in different scenarios.

Finally, for the QoS analysis, we presented some tools and approaches that can be used to improve the average utilization of the spectrum while ensuring a small probability of interruption to the secondary users. In this respect, analytical results based on fluid limits were obtained. In addition, we developed a methodology to estimate two of the main performance metrics: the medium access probability of secondary users and the coverage probability. The last metric gives an idea of the degradation of primary communications caused by the presence of secondary communications.

This research has thrown up many questions in need of further investigation, some of them were listed throughout the document, others we will now highlight:

- Due to the versatility of the proposed methodology based on random graph and according to the complicated analytical expressions obtained by the stochastic geometry analysis of Chapter 7, an interesting analysis for future research is how to include in the random graph analysis the multichannel characteristic.
- Another probable next stage in our research line would be to incorporate, to our paid spectrum model, dynamic pricing features like for example the ones defined in [30] (e.g. a congestion-dependent pricing policies).
- Another open research is how to combine the capacity analysis with the economic aspects in a routing algorithm in cognitive radio networks.
- Once 5G standard is defined, it would be nice to extend the results presented here to the upcoming requirements and use cases where new features appear.
- Additionally, it would be nice to analyze the spectrum situation (utilization and/or underutilization) in Uruguay developing a spectrum observatory.

We believe that the results in this thesis are inspiring and applicable to important emerging classes of wireless networks.

Appendix A

Stochastic geometry essentials

We do not intend here to provide a tutorial about stochastic geometry, we just present a basic introduction of the principal concepts and the involved notation which were extensively used in the thesis. We begin presenting some general definitions and then we concentrate on Poisson point process and its characteristics. For a more rigorous introduction and for the demonstrations of the different results, please refer to [43, 107, 116, 117].

A.1 Definitions

A.1.1 Point process

Consider the d -dimensional Euclidean space \mathbb{R}^d . A spatial point process (PP) Φ is defined as a random, finite or countably-infinite collection of points in the space \mathbb{R}^d , without accumulation points. More formally, $\Phi = \{X_i, i \in \mathbb{N}\}$ where $\{X_i\} \subset \mathbb{R}^d$ (i.e. $\Phi = \sum_i \delta_{X_i}$). In the thesis, we only need the special case where $d = 2$.

Complementary, $\forall A \subset \mathbb{R}^d$ it is possible to define $\Phi(A)$ as the number of point of Φ in A . Note that $\Phi(A)$ is a random variable whose distribution depends on Φ . Consequently, we define $\Lambda(A) = \mathbb{E}(\Phi(A))$ as the intensity of the process Φ .

The most popular PPs in wireless networks are Poisson Point Process (PPP), Binomial Point Process (BPP), Matérn Hard Core Point Process (HCPP) and Poisson Cluster Process (PCP). A formal definition of these PPs can be found in [116]. By way of summary, BPP are usually used to abstract a network when the total number of nodes is known and the network area is finite. PCP are more suitable when the nodes are clustering according to certain social behavior and when its “center” point constitutes a PPP. The Matérn HCPP are used when there is a minimum distance separating the nodes, then they are obtained by applying a dependent thinning to a PPP. In particular, they are suitable to model a cell with CSMA MAC protocol. Among these PPs, PPP is the most popular and well-understood in the literature due to its simplicity and tractability. As an example, Fig. A.1 shows a realization for a PPP. In Fig. A.2 there is a PCP where the center points are the points of Fig. A.1 and each cluster has a Poisson distributed number of points distributed in certain circle neighborhood.

Appendix A. Stochastic geometry essentials

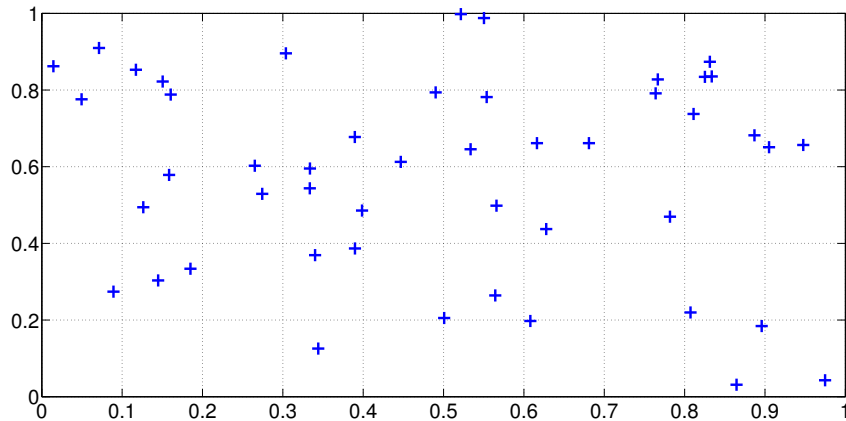


Figure A.1: Poisson Point Process in a $1m \times 1m$ area with intensity $\lambda = 50$ (50 points/ m^2).

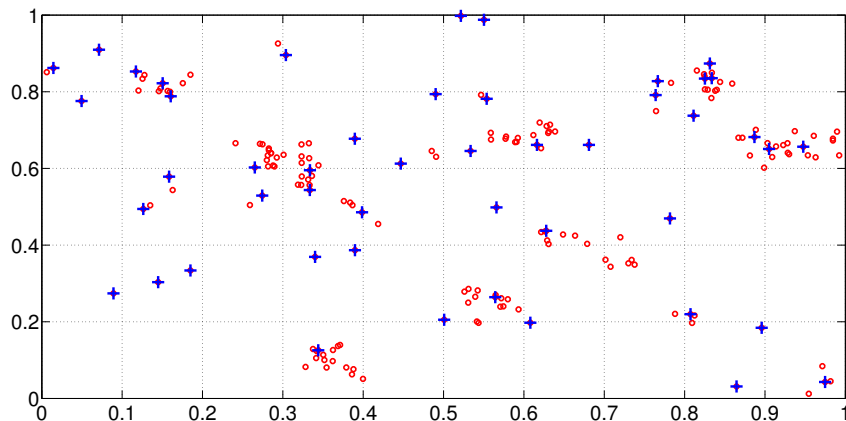


Figure A.2: Poisson Cluster Process in a $1m \times 1m$ area. Center points (crosses) is a PPP with intensity $\lambda = 50$ and each cluster has a Poisson distributed number of points represented by circles ($\lambda_{cluster} = 0.8/m^2$).

A.1.2 Laplace functional

The Laplace functional \mathcal{L} of a PP Φ is defined by the following formula

$$s\mathcal{L}_{\Phi}(f) = \mathbb{E} \left[\exp \left\{ - \int_{\mathbb{R}^d} f(x) \Phi(dx) \right\} \right], \quad (\text{A.1})$$

where f runs over the set of all non-negative functions on \mathbb{R}^d . Note that the Laplace functional (or Laplace transform) completely characterizes the distribution of the PP. In the context of this work, this functional is essential to analyze aggregate interference power.

A.1.3 Palm distribution

Palm theory formalizes the notion of the conditional distribution of a general PP given it has a point at some location. Therefore, the Palm distribution represents how the PP would look when viewed from one of its points.

We call P_x the Palm distribution of Φ :

$$P_x(Y) = P(\Phi \in Y | x \in \Phi), \quad (\text{A.2})$$

where Y is a property that is satisfied by the points of Φ .

In this thesis points represent locations of primary and secondary users.

A.1.4 Campbell's formula

Considering a PP Φ with intensity $\Lambda(\cdot)$, Campbell's theorem offers a way to calculate expectations of a function over the process points ($f: \mathbb{R}^d \rightarrow \mathbb{R}$) as:

$$\mathbb{E} \left[\int f(x) \Phi(dx) \right] = \mathbb{E} \left[\sum_{x \in \Phi} f(x) \right] = \int f(x) \Lambda(dx) \quad (\text{A.3})$$

A.1.5 Marked point process

Consider a d dimensional Euclidean space \mathbb{R}^d as the state space of the point process. Consider a second space \mathbb{R}^l , called the space of marks. A marked PP $\tilde{\Phi}$ is a locally finite random set of points in \mathbb{R}^d with some random vector in \mathbb{R}^l attached to each point. It can be represented as $\tilde{\Phi} = \{(X_i, m_i)\}_i$ where $\Phi = \{X_i\}$ is the set of points and $\{m_i\}$ the set of marks. We say that $\tilde{\Phi}$ is a PP in the space $\mathbb{R}^d \times \mathbb{R}^l$.

An important case of marked PP is the independently marked one, i.e. given the locations of the points $\Phi = \{X_i\}$, we say that it is independently marked if the marks are mutually independent random vectors in \mathbb{R}^l and each mark depends only on the location of the point which is attached.

A.2 Poisson point process

Poisson point processes, a specific category of PPs, have been widely studied to model the wireless network. In particular, PPP are used for modeling the locations of the wireless devices in ad hoc networks and also in planned infrastructure-based networks..

A PP is a Poisson point processes (PPP) iff:

- For an arbitrary $A \subset \mathbb{R}^d$, $\Phi(A)$ is a Poisson random variable;
- For any two disjoint subsets $A_i, A_j \subset \mathbb{R}^d$, $\Phi(A_i)$ and $\Phi(A_j)$ are independent.

If $\Lambda(A) = \lambda|A|, \forall A \subset \mathbb{R}^d$ being $|A|$ the Lebesgue measure (e.g. size) of A^1 , we say that Φ is a homogeneous PPP with intensity parameter λ .

Important properties of a PPP Φ in \mathbb{R}^d of intensity measure Λ :

¹ $|A|$ denotes the area of A or the volume of A for a two or three-dimensional space respectively.

Appendix A. Stochastic geometry essentials

- Superposition, thinning and displacement preserve the Poisson law:
 - Superposition: Let $\{\Phi_k\}_k$ be k PPPs with intensities $\{\Lambda_k\}$, then $\Phi = \sum_k \Phi_k$ is a PPP with intensity $\Lambda = \sum_k \Lambda_k$.
 - Thinning: Consider a function $p : \mathbb{R}^d \rightarrow [0, 1]$, we define Φ^p the thinning of Φ as $\Phi^p = \sum_i \delta_{x_i} \varepsilon_i$ where $p(x_i) = P(\varepsilon_i = 1 | \Phi)$ and $1 - p(x_i) = P(\varepsilon_i = 0 | \Phi)$. If $\{\varepsilon_i\}$ are independent, we say that Φ^p is a PPP with intensity $p\Lambda : p\Lambda(A) = \int_A p(x)\Lambda(dx)$.
 - Displacement: Consider a probability kernel $T(x, B)$ from \mathbb{R}^d to \mathbb{R}^h , then the transformation Φ^T of a PPP Φ by $T(\cdot, \cdot)$ is a PPP in \mathbb{R}^h with intensity $\Lambda_T : \Lambda_T(A) = \int_{\mathbb{R}^d} T(x, A)\Lambda(dx)$.
- Laplace functional is

$$\mathcal{L}_\Phi(f) = \exp \left\{ - \int_{\mathbb{R}^d} (1 - e^{-f(x)})\Lambda(dx) \right\}. \quad (\text{A.4})$$

- Palm distribution verifies $P_0(Y) = P(\Phi \cup \{0\} \in Y)$. This implies that the addition (or removal) of a point does not change the distribution, hence we can always place the point of interest at the origin in coordinates as a typical point (see Slivnyak theorem in [43]).
- An independently marked PPP $\tilde{\Phi}$ with intensity Λ on \mathbb{R}^d and marks with distribution F_X on \mathbb{R}^l is a PPP with intensity

$$\tilde{\Lambda}(A \times K) = \int_A \int_K F_X(dm)\Lambda(dx). \quad (\text{A.5})$$

Therefore, its Laplace functional is

$$\mathcal{L}_{\tilde{\Phi}}(\tilde{f}) = \exp \left\{ - \int_{\mathbb{R}^d} \left(1 - \int_{\mathbb{R}^l} e^{-\tilde{f}(x,m)} F_X(dm) \right) \Lambda(dx) \right\}. \quad (\text{A.6})$$

A.3 Shot-noise

A shot-noise field is a non-negative vector random field $I_\Phi(y)$ defined for all y in some Euclidean space and which is a functional of a marked point process $\tilde{\Phi}$.

Basically, we use shot-noise to model radio interference between wireless users. For example: the total power received from a collection of transmitters at a given location is in essence a shot-noise field at this location.

A shot-noise can be extremal or additive.

A.3.1 Additive Shot-noise

Let $\tilde{\Phi}$ be a marked PP in $\mathbb{R}^d \times \mathbb{R}^l$, an additive shot-noise $I_{\tilde{\Phi}}$ with response function L is defined by

$$I_{\tilde{\Phi}}(y) = \int_{\mathbb{R}^d} \int_{\mathbb{R}^l} L(y, x, m) \tilde{\Phi}(d(x, m)) = \sum_{(X_i, m_i) \in \tilde{\Phi}} L(y, X_i, m_i). \quad (\text{A.7})$$

In the particular case when $\tilde{\Phi}$ is an independently marked PPP, the distribution of the additive shot-noise $I_{\tilde{\Phi}}(y) = (I_1, \dots, I_k)$ is known in terms of its multivariate Laplace transform $\mathcal{L}_{I_{\tilde{\Phi}}(y)}(t_1, \dots, t_k) = E \left[e^{-\sum_i t_i I_i(y)} \right]$ by

$$\mathcal{L}_{I_{\tilde{\Phi}}(y)}(t_1, \dots, t_k) = \exp \left[- \int_{\mathbb{R}^d} \int_{\mathbb{R}^l} \left(1 - e^{-\sum_i t_i L_i(y, x, m)} \right) F_X(dm) \Lambda(dx) \right] \quad (\text{A.8})$$

where the response function is $L = (L_1, L_2, \dots, L_k)$.

Observe that $\mathcal{L}_{I_{\tilde{\Phi}}(y)}(t_1, \dots, t_k) = \mathcal{L}_{\tilde{\Phi}}(\tilde{f})$ being $\tilde{f}(x, m) = \sum_i t_i L_i(y, x, m)$.

A.3.2 Extremal Shot-noise

Let $\tilde{\Phi}$ be a marked PP in $\mathbb{R}^d \times \mathbb{R}^l$, an extremal shot-noise $I_{\tilde{\Phi}}$ with response function L is defined by

$$I_{\tilde{\Phi}}(y) = \sup_{(X_i, m_i) \in \tilde{\Phi}} L(y, X_i, m_i). \quad (\text{A.9})$$

Please note that the extremal shot-noise represents the strongest signal power received at y .

If $\tilde{\Phi}$ is an independently marked PPP we have

$$P(I_{\tilde{\Phi}}(y) \leq t) = \exp \left[- \int_{\mathbb{R}^d} \int_{\mathbb{R}^l} \mathbb{1}(L(y, x, m) > t) F_X(dm) \Lambda(dx) \right]. \quad (\text{A.10})$$

This page was intentionally left blank.

Appendix B

Proposition proofs of Chapter 2

B.1 Proof of Proposition 1

Proof. Inequality holds for $n = 0$ by definition. Assuming the inequality holds for $n - 1$, we show that it holds for n . We divide the problem in two cases: preempted and non-preempted situations.

- case 1: $b_1X + b_2(Y + 1) \leq C - b_1$;

$$V_n(X, Y + 1) = \lambda'_1 V_{n-1}(X + 1, Y + 1) + \tag{B.1}$$

$$\lambda'_2 \max\{V_{n-1}(X, Y + 1), V_{n-1}(X, Y + 2) + b_2R\} + \tag{B.2}$$

$$\mu'_1 X V_{n-1}(X - 1, Y + 1) + \tag{B.3}$$

$$\mu'_2 Y V_{n-1}(X, Y) + \tag{B.4}$$

$$\mu'_2 V_{n-1}(X, Y) + \tag{B.5}$$

$$\left(C \left(\frac{\mu'_1}{b_1} + \frac{\mu'_2}{b_2} \right) - \mu'_1 X - \mu'_2(Y + 1) \right) V_{n-1}(X, Y + 1) \tag{B.6}$$

$$V_n(X, Y) = \lambda'_1 V_{n-1}(X + 1, Y) + \tag{B.7}$$

$$\lambda'_2 \max\{V_{n-1}(X, Y), V_{n-1}(X, Y + 1) + b_2R\} + \tag{B.8}$$

$$\mu'_1 X V_{n-1}(X - 1, Y) + \tag{B.9}$$

$$\mu'_2 Y V_{n-1}(X, Y - 1) + \tag{B.10}$$

$$\mu'_2 V_{n-1}(X, Y) + \tag{B.11}$$

$$\left(C \left(\frac{\mu'_1}{b_1} + \frac{\mu'_2}{b_2} \right) - \mu'_1 X - \mu'_2(Y + 1) \right) V_{n-1}(X, Y) \tag{B.12}$$

Please note that (B.1) \leq (B.7), (B.3) \leq (B.9), (B.4) \leq (B.10), (B.6) \leq (B.12) are proved directly by induction assumption. On the other hand (B.5) = (B.11).

Following we show the justification of (B.2) \leq (B.8):

1. If $(\max\{V_{n-1}(X, Y + 1), V_{n-1}(X, Y + 2) + b_2R\} = V_{n-1}(X, Y + 1)$ and $\max\{V_{n-1}(X, Y), V_{n-1}(X, Y + 1) + b_2R\} = V_{n-1}(X, Y)$) or

Appendix B. Proposition proofs of Chapter 2

$(\max\{V_{n-1}(X, Y + 1), V_{n-1}(X, Y + 2) + b_2R\} = V_{n-1}(X, Y + 2) + b_2R$ and $\max\{V_{n-1}(X, Y), V_{n-1}(X, Y + 1) + b_2R\} = V_{n-1}(X, Y + 1) + b_2R$), the inequality is a direct consequence of induction hypothesis.

2. If $(\max\{V_{n-1}(X, Y + 1), V_{n-1}(X, Y + 2) + b_2R\} = V_{n-1}(X, Y + 1)$ and $\max\{V_{n-1}(X, Y), V_{n-1}(X, Y + 1) + b_2R\} = V_{n-1}(X, Y + 1) + b_2R$), it is simple to note the validity of the demonstration because $R > 0$.
3. If $(\max\{V_{n-1}(X, Y + 1), V_{n-1}(X, Y + 2) + b_2R\} = V_{n-1}(X, Y + 2) + b_2R$ and $\max\{V_{n-1}(X, Y), V_{n-1}(X, Y + 1) + b_2R\} = V_{n-1}(X, Y)$), then we have that $V_{n-1}(X, Y) > V_{n-1}(X, Y + 1) + b_2R \geq V_{n-1}(X, Y + 2) + b_2R$.

- case 2: $C - b_1 < b_1X + b_2(Y + 1) \leq C$;

We define the number of preempted SUs (Z and Z') as:

$$Z = \left\lceil \frac{b_1X + b_2(Y+1) - C + b_1}{b_2} + \mathbb{1}_{\{\text{mod}\{b_1X + b_2(Y+1) - C + b_1, b_2\} \neq 0\}} \right\rceil \text{ and}$$

$$Z' = \max \left\{ \left\lceil \frac{b_1X + b_2Y - C + b_1}{b_2} + \mathbb{1}_{\{\text{mod}\{b_1X + b_2Y - C + b_1, b_2\} \neq 0\}} \right\rceil, 0 \right\}; \text{ we have:}$$

$$V_n(X, Y + 1) = \lambda'_1(V_{n-1}(X + 1, Y + 1 - Z) - Zb_2K) + \tag{B.13}$$

$$\lambda'_2 \max\{V_{n-1}(X, Y + 1), V_{n-1}(X, Y + 2) + b_2R\} + \tag{B.14}$$

$$\mu'_1 X V_{n-1}(X - 1, Y + 1) + \tag{B.15}$$

$$\mu'_2 Y V_{n-1}(X, Y) + \tag{B.16}$$

$$\mu'_2 V_{n-1}(X, Y) + \tag{B.17}$$

$$\left(C \left(\frac{\mu'_1}{b_1} + \frac{\mu'_2}{b_2} \right) - \mu'_1 X - \mu'_2 (Y + 1) \right) V_{n-1}(X, Y + 1) \tag{B.18}$$

$$V_n(X, Y) = \lambda'_1(V_{n-1}(X + 1, Y - Z') - Z'b_2K) + \tag{B.19}$$

$$\lambda'_2 \max\{V_{n-1}(X, Y), V_{n-1}(X, Y + 1) + b_2R\} + \tag{B.20}$$

$$\mu'_1 X V_{n-1}(X - 1, Y) + \tag{B.21}$$

$$\mu'_2 Y V_{n-1}(X, Y - 1) + \tag{B.22}$$

$$\mu'_2 V_{n-1}(X, Y) + \tag{B.23}$$

$$\left(C \left(\frac{\mu'_1}{b_1} + \frac{\mu'_2}{b_2} \right) - \mu'_1 X - \mu'_2 (Y + 1) \right) V_{n-1}(X, Y) \tag{B.24}$$

On the one hand, we have (B.17) = (B.23); and (B.15) \leq (B.21), (B.16) \leq (B.22), (B.18) \leq (B.24) are proved directly with the hypothesis of induction. On the other hand, the proof of (B.14) \leq (B.20) is analogous to the previous case¹. Finally, please note that $Z' = Z - 1$ and $K > 0$, then the inequality (B.13) \leq (B.19) is proved.

□

¹If the number of busy channels is greater than $C - b_2$, the admission control decision is known, then the number of combinations to evaluate is fewer than in case 1

B.2 Proof of Proposition 2

Proof. Inequality holds for $n = 0$ by definition. Assuming the inequality holds for $n - 1$, we show that it holds for n . We divide the problem in two cases: preempted and non-preempted situations.

- case 1: $b_1X + b_2(Y + 1) \leq C - b_1$;

$$\begin{aligned}
 V_n(X, Y + 1) - V_n(X, Y) &= \lambda'_1(V_{n-1}(X + 1, Y + 1) - V_{n-1}(X + 1, Y)) + \\
 &\quad \lambda'_2 \max\{V_{n-1}(X, Y + 1), V_{n-1}(X, Y + 2) + b_2R\} - \\
 &\quad \lambda'_2 \max\{V_{n-1}(X, Y), V_{n-1}(X, Y + 1) + b_2R\} + \\
 &\quad \mu'_1 X (V_{n-1}(X - 1, Y + 1) - V_{n-1}(X - 1, Y)) + \\
 &\quad \mu'_2 Y (V_{n-1}(X, Y) - V_{n-1}(X, Y - 1)) + \\
 &\quad \mu'_2 V_{n-1}(X, Y) - \mu'_2 V_{n-1}(X, Y) + \\
 &\quad \left(C \left(\frac{\mu'_1}{b_1} + \frac{\mu'_2}{b_2} \right) - \mu'_1 X - \mu'_2 (Y + 1) \right) \\
 &\quad (V_{n-1}(X, Y + 1) - V_{n-1}(X, Y)) \\
 &\geq -b_2K
 \end{aligned}$$

Using induction hypothesis we have $V_n(X, Y + 1) - V_n(X, Y) \geq (1 - \lambda'_2 - \alpha')(-b_2K) - \mu'_2(V_{n-1}(X, Y + 1) - V_{n-1}(X, Y)) + \lambda'_2(\max\{V_{n-1}(X, Y + 1), V_{n-1}(X, Y + 2) + b_2R\} - \max\{V_{n-1}(X, Y), V_{n-1}(X, Y + 1) + b_2R\})$. We can observe that the second term $(-\mu'_2(V_{n-1}(X, Y + 1) - V_{n-1}(X, Y)))$ is always positive or zero (being zero the worst case). Then, if $K \geq R$ we can prove that $\lambda'_2(\max\{V_{n-1}(X, Y + 1), V_{n-1}(X, Y + 2) + b_2R\} - \max\{V_{n-1}(X, Y), V_{n-1}(X, Y + 1) + b_2R\}) \geq -\lambda'_2 b_2 K$. This proves the result $\forall \alpha'$.

- case 2: $C - b_1 < b_1X + b_2(Y + 1) \leq C$;

In the same way as in the previous proposition proof, we define Z and Z' as

$$Z = \left\lceil \frac{b_1X + b_2(Y + 1) - C + b_1}{b_2} + \mathbb{1}_{\{ \text{mod } \{b_1X + b_2(Y + 1) - C + b_1, b_2\} \neq 0 \}} \right\rceil \text{ and}$$

$$Z' = \max \left\{ \left\lceil \frac{b_1X + b_2Y - C + b_1}{b_2} + \mathbb{1}_{\{ \text{mod } \{b_1X + b_2Y - C + b_1, b_2\} \neq 0 \}} \right\rceil, 0 \right\}; \text{ we have:}$$

$$\begin{aligned}
 V_n(X, Y + 1) - V_n(X, Y) &= \lambda'_1(V_{n-1}(X + 1, Y + 1 - Z) - Zb_2K - V_{n-1}(X + 1, Y - Z') + Z'b_2K) + \\
 &\quad \lambda'_2 \max\{V_{n-1}(X, Y + 1), V_{n-1}(X, Y + 2) + b_2R\} - \\
 &\quad \lambda'_2 \max\{V_{n-1}(X, Y), V_{n-1}(X, Y + 1) + b_2R\} + \\
 &\quad \mu'_1 X (V_{n-1}(X - 1, Y + 1) - V_{n-1}(X - 1, Y)) + \\
 &\quad \mu'_2 Y (V_{n-1}(X, Y) - V_{n-1}(X, Y - 1)) + \\
 &\quad \mu'_2 V_{n-1}(X, Y) - \mu'_2 V_{n-1}(X, Y) + \\
 &\quad \left(C \left(\frac{\mu'_1}{b_1} + \frac{\mu'_2}{b_2} \right) - \mu'_1 X - \mu'_2 (Y + 1) \right) (V_{n-1}(X, Y + 1) - V_{n-1}(X, Y)) \\
 &\geq -b_2K
 \end{aligned}$$

We can observe that $Z' = Z - 1$ and using the same arguments as in case 1, the proof is completed. When we have to evaluate the terms that implies the decision (the maximization), we have used that $K \geq R$.

□

B.3 Proof of Proposition 3

Proof. Inequality holds for $n = 0$ by definition. Assuming the inequality holds for $n - 1$, we show that it holds for n . We divide the problem in two cases: preempted and non-preempted situations.

- case 1: $b_1(X + 1) + b_2(Y + 1) \leq C - b_1$;

$$V_n(X + 1, Y + 1) - V_n(X + 1, Y) = \lambda'_1(V_{n-1}(X + 2, Y + 1) - V_{n-1}(X + 2, Y)) + \quad (\text{B.25})$$

$$\lambda'_2(\max\{V_{n-1}(X + 1, Y + 1), V_{n-1}(X + 1, Y + 2) + b_2R\} - \max\{V_{n-1}(X + 1, Y), V_{n-1}(X + 1, Y + 1) + b_2R\}) + \quad (\text{B.26})$$

$$\mu'_1X(V_{n-1}(X, Y + 1) - V_{n-1}(X, Y)) + \quad (\text{B.27})$$

$$\mu'_2Y(V_{n-1}(X + 1, Y) - V_{n-1}(X + 1, Y - 1)) + \quad (\text{B.28})$$

$$\mu'_1(V_{n-1}(X, Y + 1) - V_{n-1}(X, Y)) + \quad (\text{B.29})$$

$$\left(C \left(\frac{\mu'_1}{b_1} + \frac{\mu'_2}{b_2} \right) - \mu'_1(X + 1) - \mu'_2(Y + 1) \right) (V_{n-1}(X + 1, Y + 1) - V_{n-1}(X + 1, Y)) \quad (\text{B.30})$$

$$V_n(X, Y + 1) - V_n(X, Y) = \lambda'_1(V_{n-1}(X + 1, Y + 1) - V_{n-1}(X + 1, Y)) + \quad (\text{B.31})$$

$$\lambda'_2(\max\{V_{n-1}(X, Y + 1), V_{n-1}(X, Y + 2) + b_2R\} - \max\{V_{n-1}(X, Y), V_{n-1}(X, Y + 1) + b_2R\}) + \quad (\text{B.32})$$

$$\mu'_1X(V_{n-1}(X - 1, Y + 1) - V_{n-1}(X - 1, Y)) + \quad (\text{B.33})$$

$$\mu'_2Y(V_{n-1}(X, Y) - V_{n-1}(X, Y - 1)) + \quad (\text{B.34})$$

$$\mu'_1(V_{n-1}(X, Y + 1) - V_{n-1}(X, Y)) + \quad (\text{B.35})$$

$$\left(C \left(\frac{\mu'_1}{b_1} + \frac{\mu'_2}{b_2} \right) - \mu'_1(X + 1) - \mu'_2(Y + 1) \right) (V_{n-1}(X, Y + 1) - V_{n-1}(X, Y)) \quad (\text{B.36})$$

(B.25) \leq (B.31), (B.27) \leq (B.33), (B.28) \leq (B.34), (B.30) \leq (B.36) are proved directly by induction hypothesis. In addition, we have (B.29) = (B.35).

The last inequality requires a degree of algebraic manipulation:

$$\begin{aligned} & \lambda'_2(\max\{V_{n-1}(X, Y + 1), V_{n-1}(X, Y + 2) + b_2R\} - \max\{V_{n-1}(X, Y), V_{n-1}(X, Y + 1) + b_2R\}) = \\ & \lambda'_2(\max\{V_{n-1}(X, Y + 2) - V_{n-1}(X, Y + 1) + b_2R, 0\} - \max\{V_{n-1}(X, Y) - V_{n-1}(X, Y + 1), b_2R\}) = \\ & \lambda'_2(\max\{V_{n-1}(X, Y + 2) - V_{n-1}(X, Y + 1) + b_2R, 0\} + \min\{-V_{n-1}(X, Y) + V_{n-1}(X, Y + 1), -b_2R\}) \\ & \geq \\ & \lambda'_2(\max\{V_{n-1}(X + 1, Y + 2) - V_{n-1}(X + 1, Y + 1) + b_2R, 0\} + \min\{-V_{n-1}(X + 1, Y) + V_{n-1}(X + 1, Y + 1), -b_2R\}) = \\ & \lambda'_2(\max\{V_{n-1}(X + 1, Y + 1), V_{n-1}(X + 1, Y + 2) + b_2R\} - \max\{V_{n-1}(X + 1, Y), V_{n-1}(X + 1, Y + 1) + b_2R\}) \end{aligned}$$

B.3. Proof of Proposition 3

- case 2: $C - b_1 < b_1(X + 1) + b_2(Y + 1) \leq C$;

Defining Z, Z', Z^+ and Z^* :

$$\begin{aligned} Z &= \left\lfloor \frac{b_1(X+1)+b_2(Y+1)-C+b_1}{b_2} + \mathbb{1}_{\{\text{mod } \{b_1(X+1)+b_2(Y+1)-C+b_1, b_2\} \neq 0\}} \right\rfloor, \\ Z' &= \max \left\{ \left\lfloor \frac{b_1(X+1)+b_2Y-C+b_1}{b_2} + \mathbb{1}_{\{\text{mod } \{b_1(X+1)+b_2Y-C+b_1, b_2\} \neq 0\}} \right\rfloor, 0 \right\}, \\ Z^+ &= \max \left\{ \left\lfloor \frac{b_1X+b_2(Y+1)-C+b_1}{b_2} + \mathbb{1}_{\{\text{mod } \{b_1X+b_2(Y+1)-C+b_1, b_2\} \neq 0\}} \right\rfloor, 0 \right\} \text{ and} \\ Z^* &= \max \left\{ \left\lfloor \frac{b_1X+b_2Y-C+b_1}{b_2} + \mathbb{1}_{\{\text{mod } \{b_1X+b_2Y-C+b_1, b_2\} \neq 0\}} \right\rfloor, 0 \right\}, \end{aligned}$$

$$\begin{aligned} V_n(X+1, Y+1) - V_n(X+1, Y) &= \lambda'_1(V_{n-1}(X+2, Y+1-Z) - Zb_2K) - \\ &\quad \lambda'_1(V_{n-1}(X+2, Y-Z') - Z'b_2K) + \tag{B.37} \\ &\quad \lambda'_2(\max\{V_{n-1}(X+1, Y+1), V_{n-1}(X+1, Y+2) + b_2R\} - \\ &\quad \max\{V_{n-1}(X+1, Y), V_{n-1}(X+1, Y+1) + b_2R\}) + \tag{B.38} \\ &\quad \mu'_1X(V_{n-1}(X, Y+1) - V_{n-1}(X, Y)) + \\ &\quad \mu'_2Y(V_{n-1}(X+1, Y) - V_{n-1}(X+1, Y-1)) + \\ &\quad \mu'_1(V_{n-1}(X, Y+1) - V_{n-1}(X, Y)) + \\ &\quad \left(C \left(\frac{\mu'_1}{b_1} + \frac{\mu'_2}{b_2} \right) - \mu'_1(X+1) - \mu'_2(Y+1) \right) \\ &\quad (V_{n-1}(X+1, Y+1) - V_{n-1}(X+1, Y)) \end{aligned}$$

$$\begin{aligned} V_n(X, Y+1) - V_n(X, Y) &= \lambda'_1(V_{n-1}(X+1, Y+1-Z^+) - Z^+b_2K) - \\ &\quad \lambda_1(V_{n-1}(X+1, Y-Z^*) - Z^*b_2K) + \tag{B.39} \end{aligned}$$

$$\begin{aligned} &\quad \lambda'_2(\max\{V_{n-1}(X, Y+1), V_{n-1}(X, Y+2) + b_2R\} \\ &\quad - \max\{V_{n-1}(X, Y), V_{n-1}(X, Y+1) + b_2R\}) + \tag{B.40} \\ &\quad \mu'_1X(V_{n-1}(X-1, Y+1) - V_{n-1}(X-1, Y)) + \\ &\quad \mu'_2Y(V_{n-1}(X, Y) - V_{n-1}(X, Y-1)) + \\ &\quad \mu'_1(V_{n-1}(X, Y+1) - V_{n-1}(X, Y)) + \\ &\quad \left(C \left(\frac{\mu'_1}{b_1} + \frac{\mu'_2}{b_2} \right) - \mu'_1(X+1) - \mu'_2(Y+1) \right) \\ &\quad (V_{n-1}(X, Y+1) - V_{n-1}(X, Y)) \end{aligned}$$

(B.37) \leq (B.39) is valid according to Prop. 2 and observing that $Z' = Z - 1$ and $Z^* = Z^+ - 1$. The other inequalities can be demonstrated in the same way as in the previous case. In particular, we have to be careful in the proof of (B.38) \leq (B.40) in the scenarios where the number of allocated channels is greater $C - b_2$.

□

B.4 Proof of Proposition 4

Proof. Inequality holds for $n = 0$ by definition. Assuming the inequality holds for $n - 1$, we show that it holds for n . We divide the problem in two cases: preempted and non-preempted situations.

- case 1: $b_1X + b_2(Y + 2) \leq C - b_1$;

$$V_n(X, Y) - V_n(X, Y + 1) = \lambda'_1(V_{n-1}(X + 1, Y) - V_{n-1}(X + 1, Y + 1)) + \quad (\text{B.41})$$

$$\lambda'_2(\max\{V_{n-1}(X, Y), V_{n-1}(X, Y + 1) + b_2R\} \quad (\text{B.42})$$

$$- \max\{V_{n-1}(X, Y + 1), V_{n-1}(X, Y + 2) + b_2R\}) + \mu'_1X(V_{n-1}(X - 1, Y) - V_{n-1}(X - 1, Y + 1)) + \quad (\text{B.43})$$

$$\mu'_2Y(V_{n-1}(X, Y - 1) - V_{n-1}(X, Y)) + \quad (\text{B.44})$$

$$\mu'_2V_{n-1}(X, Y) - \mu'_2V_{n-1}(X, Y + 1) + \quad (\text{B.45})$$

$$\left(C \left(\frac{\mu'_1}{b_1} + \frac{\mu'_2}{b_2} \right) - \mu'_1X - \mu'_2(Y + 2) \right) \quad (\text{B.46})$$

$$(V_{n-1}(X, Y) - V_{n-1}(X, Y + 1))$$

$$V_n(X, Y + 1) - V_n(X, Y + 2) = \lambda'_1(V_{n-1}(X + 1, Y + 1) - V_{n-1}(X + 1, Y + 2)) + \quad (\text{B.47})$$

$$\lambda'_2(\max\{V_{n-1}(X, Y + 1), V_{n-1}(X, Y + 2) + b_2R\} \quad (\text{B.48})$$

$$- \max\{V_{n-1}(X, Y + 2), V_{n-1}(X, Y + 3) + b_2R\}) + \mu'_1X(V_{n-1}(X - 1, Y + 1) - V_{n-1}(X - 1, Y + 2)) + \quad (\text{B.49})$$

$$\mu'_2Y(V_{n-1}(X, Y) - V_{n-1}(X, Y + 1)) + \quad (\text{B.50})$$

$$\mu'_2V_{n-1}(X, Y) - \mu'_2V_{n-1}(X, Y + 1) + \quad (\text{B.51})$$

$$\left(C \left(\frac{\mu'_1}{b_1} + \frac{\mu'_2}{b_2} \right) - \mu'_1X - \mu'_2(Y + 2) \right) \quad (\text{B.52})$$

$$(V_{n-1}(X, Y + 1) - V_{n-1}(X, Y + 2))$$

The relations (B.41) \leq (B.47), (B.43) \leq (B.49), (B.44) \leq (B.50) and (B.46) \leq (B.52) are direct consequences of the induction hypothesis. The (B.45) and (B.51) terms cancel out each other.

Next we show that (B.48) \geq (B.42):

$$\begin{aligned} & \lambda'_2(\max\{V_{n-1}(X, Y + 1), V_{n-1}(X, Y + 2) + b_2R\} - \max\{V_{n-1}(X, Y + 2), V_{n-1}(X, Y + 3) + b_2R\}) = \\ & \lambda'_2(\max\{V_{n-1}(X, Y + 1) - V_{n-1}(X, Y + 2), b_2R\} - \max\{0, V_{n-1}(X, Y + 3) - V_{n-1}(X, Y + 2) + b_2R\}) = \\ & \lambda'_2(\max\{V_{n-1}(X, Y + 1) - V_{n-1}(X, Y + 2), b_2R\} + \min\{0, -V_{n-1}(X, Y + 3) + V_{n-1}(X, Y + 2) - \\ & b_2R\}) \geq \lambda'_2(\max\{V_{n-1}(X, Y) - V_{n-1}(X, Y + 1), b_2R\} + \min\{0, -V_{n-1}(X, Y + 2) + V_{n-1}(X, Y + \\ & 1) - b_2R\}) = \lambda'_2(\max\{V_{n-1}(X, Y) - V_{n-1}(X, Y + 1), b_2R\} - \max\{0, V_{n-1}(X, Y + 2) - V_{n-1}(X, Y + \\ & 1) + b_2R\}) = \\ & \lambda'_2(\max\{V_{n-1}(X, Y), V_{n-1}(X, Y + 1) + b_2R\} - \max\{V_{n-1}(X, Y + 1), V_{n-1}(X, Y + 2) + b_2R\}) \end{aligned}$$

- case 2: $C - b_1 < b_1X + b_2(Y + 2) \leq C$;

Defining Z , Z' and Z^* :

B.4. Proof of Proposition 4

$$\begin{aligned}
Z &= \left\lfloor \frac{b_1X + b_2(Y+2) - C + b_1}{b_2} + \mathbb{1}_{\{\text{mod } \{b_1X + b_2(Y+2) - C + b_1, b_2\} \neq 0\}} \right\rfloor, \\
Z' &= \max \left\{ \left\lfloor \frac{b_1X + b_2(Y+1) - C + b_1}{b_2} + \mathbb{1}_{\{\text{mod } \{b_1X + b_2(Y+1) - C + b_1, b_2\} \neq 0\}} \right\rfloor, 0 \right\} \text{ and} \\
Z^* &= \max \left\{ \left\lfloor \frac{b_1X + b_2Y - C + b_1}{b_2} + \mathbb{1}_{\{\text{mod } \{b_1X + b_2Y - C + b_1, b_2\} \neq 0\}} \right\rfloor, 0 \right\}, \\
V_n(X, Y) - V_n(X, Y + 1) &= \lambda'_1(V_{n-1}(X + 1, Y - Z^*) - Z^*b_2K) - \tag{B.53}
\end{aligned}$$

$$\lambda'_1(V_{n-1}(X + 1, Y + 1 - Z') - Z'b_2K) \tag{B.54}$$

$$\lambda'_2(\max\{V_{n-1}(X, Y), V_{n-1}(X, Y + 1) + b_2R\} \tag{B.54}$$

$$- \max\{V_{n-1}(X, Y + 1), V_{n-1}(X, Y + 2) + b_2R\}) + \tag{B.55}$$

$$\mu'_1X(V_{n-1}(X - 1, Y) - V_{n-1}(X - 1, Y + 1)) + \tag{B.55}$$

$$\mu'_2Y(V_{n-1}(X, Y - 1) - V_{n-1}(X, Y)) + \tag{B.56}$$

$$\mu'_2V_{n-1}(X, Y) - \mu'_2V_{n-1}(X, Y + 1) + \tag{B.57}$$

$$\left(C \left(\frac{\mu'_1}{b_1} + \frac{\mu'_2}{b_2} \right) - \mu'_1X - \mu'_2(Y + 2) \right) \tag{B.58}$$

$$(V_{n-1}(X, Y) - V_{n-1}(X, Y + 1))$$

$$V_n(X, Y + 1) - V_n(X, Y + 2) = \lambda'_1(V_{n-1}(X + 1, Y + 1 - Z') - Z'b_2K) - \tag{B.59}$$

$$\lambda'_1(V_{n-1}(X + 1, Y + 2 - Z) - Zb_2K) +$$

$$\lambda'_2(\max\{V_{n-1}(X, Y + 1), V_{n-1}(X, Y + 2) + b_2R\} - \tag{B.60}$$

$$\max\{V_{n-1}(X, Y + 2), V_{n-1}(X, Y + 3) + b_2R\}) +$$

$$\mu'_1X(V_{n-1}(X - 1, Y + 1) - V_{n-1}(X - 1, Y + 2)) + \tag{B.61}$$

$$\mu'_2Y(V_{n-1}(X, Y) - V_{n-1}(X, Y + 1)) + \tag{B.62}$$

$$\mu'_2V_{n-1}(X, Y) - \mu'_2V_{n-1}(X, Y + 1) + \tag{B.63}$$

$$\left(C \left(\frac{\mu'_1}{b_1} + \frac{\mu'_2}{b_2} \right) - \mu'_1X - \mu'_2(Y + 2) \right) \tag{B.64}$$

$$(V_{n-1}(X, Y + 1) - V_{n-1}(X, Y + 2))$$

(B.53) \leq (B.59) is true according to Prop. 2 (in particular, the result of Prop. 2 is used in the limit case: $Z' = Z^* = 0$). The relations (B.55) \leq (B.61), (B.56) \leq (B.62) and (B.58) \leq (B.64) are direct consequences of the induction hypothesis, and (B.57) = (B.63) is trivial. In order to analyze the inequality (B.54) \leq (B.60) the same arguments as case 1 can be applied. It is important to highlight that if the number of busy resources in the system is greater than $C - b_2$, the admission control decision has no sense (no SU will be accepted). So, if for example $b_1X + b_2(Y + 2) > C - b_2$ (and $b_1X + b_2(Y + 1) \leq C - b_2$), we can demonstrate the inequality in the following way: $\lambda'_2(\max\{V_{n-1}(X, Y + 1), V_{n-1}(X, Y + 2) + b_2R\} - V_{n-1}(X, Y + 2)) = \lambda'_2(\max\{V_{n-1}(X, Y + 1) - V_{n-1}(X, Y + 2), b_2R\}) \geq \lambda'_2(\max\{V_{n-1}(X, Y) - V_{n-1}(X, Y + 1), b_2R\}) = \lambda'_2(\max\{V_{n-1}(X, Y), V_{n-1}(X, Y + 1) + b_2R\} - V_{n-1}(X, Y + 1))$, then

- if $\max\{V_{n-1}(X, Y + 1), V_{n-1}(X, Y + 2) + b_2R\} = V_{n-1}(X, Y + 1)$ the proof is completed.
- if $\max\{V_{n-1}(X, Y + 1), V_{n-1}(X, Y + 2) + b_2R\} = V_{n-1}(X, Y + 2) + b_2R$, then $\lambda_2(\max\{V_{n-1}(X, Y), V_{n-1}(X, Y + 1) + b_2R\} - V_{n-1}(X, Y + 1)) \geq \lambda_2(\max\{V_{n-1}(X, Y), V_{n-1}(X, Y + 1) + b_2R\} - V_{n-1}(X, Y + 2) - b_2R)$ and the proof is over.

Appendix B. Proposition proofs of Chapter 2

□

Appendix C

Stochastic Geometry proofs

C.1 Proof of Proposition 10

Proof. Let \mathcal{F}_{p,f_k} and \mathcal{F}_s be the σ -algebras generated by the realizations of Φ_{p,f_k}^* , $k \in \{1 \dots n\}$ and Φ_s respectively. Using the fact that f_r (fading) is an exponential random variable with parameter μ which is independent of all other random elements involved, let k' be a specific k value, and considering that $|r(0)| = r_p$, we have:

$$\begin{aligned}
 P_{\Phi_{p,f_{k'}}^*}^0 (SINR^p(0, r(0), f_{k'}) > \gamma) | \mathcal{F}_{p,f_k}, \mathcal{F}_s, f, r(0) &= P_{\Phi_{p,f_{k'}}^*}^0 \left(\frac{f_r(0,0)l(r_p)}{N + I_{pp}^{f_{k'}}(0) + I_{sp}^{f_{k'}}(0)} > \gamma | \mathcal{F}_{p,f_k}, \mathcal{F}_s, f, r(0) \right) \\
 &= E_{\Phi_{p,f_{k'}}^*}^0 \left[e^{\frac{-\mu\gamma(N + I_{pp}^{f_{k'}}(0) + I_{sp}^{f_{k'}}(0))}{l(r_p)}} | \mathcal{F}_{p,f_{k'}}, \mathcal{F}_s, r(0), f \right] \\
 &= e^{\frac{-\mu\gamma N}{l(r_p)}} E_{\Phi_{p,f_{k'}}^*}^0 \left[e^{\frac{-\mu\gamma I_{sp}^{f_{k'}}(0)}{l(r_p)}} | \mathcal{F}_{p,f_k}, \mathcal{F}_s, r(0), f \right] \\
 &= E_{\Phi_{p,f_{k'}}^*}^0 \left[e^{\frac{-\mu\gamma I_{sp}^{f_{k'}}(0)}{l(r_p)}} | \mathcal{F}_{p,f_k}, \mathcal{F}_s, r(0), f \right].
 \end{aligned}$$

Obs: Intuitively, the conditional with $\mathcal{F}_{p,f_k}, \mathcal{F}_s, f$ can be seen as we already know which are the active transmitters.

Continuing with the calculus, on the one hand we have:

$$\begin{aligned}
 E_{\Phi_{p,f_{k'}}^*}^0 \left[e^{\frac{-\mu\gamma I_{sp}^{f_{k'}}(0)}{l(r_p)}} | \mathcal{F}_{p,f_k}, \mathcal{F}_s, r(0), f \right] &= E_{\Phi_{p,f_{k'}}^*}^0 \left[e^{\frac{-\mu\gamma \sum_{\{y \in \Phi_{p,f_{k'}}^* \setminus \{0\}\}} fr(y,0)l(|y-r(0)|)}{l(r_p)}} | \mathcal{F}_{p,f_{k'}}, r(0) \right] \\
 &= \prod_{y \in \Phi_{p,f_{k'}}^* \setminus \{0\}} E \left[e^{\frac{-\mu\gamma fr(y,0)l(|y-r(0)|)}{l(r_p)}} \right] \\
 &= \prod_{y \in \Phi_{p,f_{k'}}^* \setminus \{0\}} \frac{l(r_p)}{l(r_p) + \gamma l(|y-r(0)|)}.
 \end{aligned}$$

(C.1)

Appendix C. Stochastic Geometry proofs

Please note that the other conditionals ($\mathcal{F}_{p,f_k}, k \neq k', \mathcal{F}_s, f$) do not matter for previous calculation.

On the other hand,

$$\begin{aligned}
E_{\Phi_{p,f_{k'}}}^0 \left[e^{-\frac{\mu \gamma_{s_p}^{f_{k'}}(0)}{l(r_p)}} \mid \mathcal{F}_{p,f_k}, \mathcal{F}_s, r(0), f \right] &= E_{\Phi_{p,f_{k'}}}^0 \left[e^{-\frac{-\mu \gamma \sum_{\{x \in \Phi_s^*\}} \{f_r(x,0)l(|x-r(0)|)\}}{l(r_p)}} \mid \mathcal{F}_{p,f_k}, \mathcal{F}_s, r(0), f \right] \\
&= E_{\Phi_{p,f_{k'}}}^0 \left[e^{-\sum_{\{x \in \Phi_s\}} \frac{-\mu \gamma f_r(x,0)l(|x-r(0)|)U(x)}{l(r_p)}} \mid \mathcal{F}_{p,f_k}, \mathcal{F}_s, r(0), f \right] \\
&= E_{\Phi_{p,f_{k'}}}^0 \left[\prod_{x \in \Phi_s} E \left[e^{-\frac{\mu \gamma f_r(x,0)l(|x-r(0)|)U(x)}{l(r_p)}} \right] \mid \mathcal{F}_{p,f_k}, \mathcal{F}_s, r(0), f \right],
\end{aligned} \tag{C.2}$$

where $U(x) = \{0, 1\}$ being 1 if $x \in \Phi_s$ can transmit and has choose $f_{k'}$. In other words, $U(x) = \mathbb{1}_{\{f(x)=f_{k'}\}}$. In this sense:

$$E_{\Phi_{p,f_{k'}}}^0 \left[e^{-\frac{\mu \gamma_{s_p}^{f_{k'}}(0)}{l(r_p)}} \mid \mathcal{F}_{p,f_k}, r(0), f \right] = \exp \left\{ -\lambda_s \int_{\mathbb{R}^2} \frac{\gamma l(|x-r(0)|)}{\gamma l(|x-r(0)|) + l(r_p)} U(x) dx \right\}. \tag{C.3}$$

Using the same arguments of [49] that $\exp\{-x\} \leq 1 - (1 - \exp\{-y\})^{\frac{x}{y}} \forall 0 \leq x \leq y$ and defining $c(r_p) = \int_{\mathbb{R}^2} \frac{\gamma l(|x-r(0)|)}{\gamma l(|x-r(0)|) + l(r_p)} dx$, we have

$$E_{\Phi_{p,f_{k'}}}^0 \left[e^{-\frac{\mu \gamma_{s_p}^{f_{k'}}(0)}{l(r_p)}} \mid \mathcal{F}_{p,f_k}, r(0), f \right] \leq 1 - (1 - e^{-\lambda_s c(r_p)})^{\frac{\int_{\mathbb{R}^2} \frac{\gamma l(|x-r(0)|)}{\gamma l(|x-r(0)|) + l(r_p)} U(x) dx}{c(r_p)}}. \tag{C.4}$$

To sum up, we have obtained

$$\begin{aligned}
P_{\Phi_{p,f_{k'}}}^0 (SINR^p(0, f_{k'}, r(0)) > \gamma \mid \mathcal{F}_{p,f_k}, \mathcal{F}_s, r(0), f) &\leq e^{-\frac{\mu \gamma N}{l(r_p)}} \prod_{y \in \Phi_{p,f_{k'}}^* \setminus \{0\}} \frac{l(r_p)}{l(r_p) + \gamma l(|y-r(0)|)} \\
&\left(1 - (1 - e^{-\lambda_s c(r_p)})^{\frac{\int_{\mathbb{R}^2} \frac{\gamma l(|x-r(0)|)}{\gamma l(|x-r(0)|) + l(r_p)} U(x) dx}{c(r_p)}} \right).
\end{aligned} \tag{C.5}$$

In order to simplify the demonstration, in the following steps we will consider $\{f_1, f_2\}$ as the set of possible frequency bands and we assume that an active primary transmitter chooses f_1 with p_f probability (i.e. f_2 is chosen with $(1 - p_f)$). We will concentrate on $P_{\Phi_{p,f_1}}^0 (SINR(0, r(0), f_1) >$

C.1. Proof of Proposition 10

$\gamma|\mathcal{F}_{p,f_k}, r(0), f$ ($k' = 1$). In this case we have:

$$\begin{aligned}
U(x) &= \mathbb{1}_{\{|N_x^{p,f_1}|=0\}} \mathbb{1}_{\{|N_x^{p,f_2}|>0\}} + \mathbb{1}_{\{P(f_1)\}} \mathbb{1}_{\{|N_x^{p,f_1}|=0\}} \mathbb{1}_{\{|N_x^{p,f_2}|=0\}} \\
&= \mathbb{1}_{\{f(0,x)l(|x|)<\rho\}} \prod_{y \in \Phi_{p,f_1}^* \setminus 0} \mathbb{1}_{\{f(y,x)l(|y-x|)<\rho\}} \mathbb{1}_{\{\prod_{z \in \Phi_{p,f_2}^*} \mathbb{1}_{\{f(z,x)l(|z-x|)<\rho\}}=0\}} + \\
&\quad \mathbb{1}_{\{P(f_1)\}} \mathbb{1}_{\{f(0,x)l(|x|)<\rho\}} \prod_{y \in \Phi_{p,f_1}^* \setminus 0} \mathbb{1}_{\{f(y,x)l(|y-x|)<\rho\}} \prod_{z \in \Phi_{p,f_2}^*} \mathbb{1}_{\{f(z,x)l(|z-x|)<\rho\}}.
\end{aligned} \tag{C.6}$$

If each band has the same probability to be chosen, we have $P(f_1) = \frac{1}{2}$.

Working with Eq. (C.5) we can identify one term that only depends on Φ_{p,f_1}^* :

$$E_{\Phi_{p,f_1}^*}^0 \left[\prod_{y \in \Phi_{p,f_1}^* \setminus 0} \frac{l(r_p)}{l(r_p) + \gamma l(|y - r(0)|)} \right] = e^{-\lambda_p p_e p_f c(r_p)}. \tag{C.7}$$

The other one depends on Φ_{p,f_1}^* and Φ_{p,f_2}^* , since they are independent we can separate in A , B and C such as:

$$\begin{aligned}
&E_{\Phi_{p,f_1}^*}^0 \left[\prod_{y \in \Phi_{p,f_1}^* \setminus 0} \frac{l(r_p)}{l(r_p) + \gamma l(|y - r(0)|)} \mathbb{1}_{\{f(y,x)l(|y-x|)<\rho\}} (1 - e^{\frac{-\mu\rho}{l(|x|)}}) \right] = \\
&(1 - e^{\frac{-\mu\rho}{l(|x|)}}) E_{\Phi_{p,f_1}^*}^0 \left[\prod_{y \in \Phi_{p,f_1}^* \setminus 0} \frac{l(r_p)}{l(r_p) + \gamma l(|y - r(0)|)} \mathbb{1}_{\{f(y,x)l(|y-x|)<\rho\}} \right] = \\
&\quad (1 - e^{\frac{-\mu\rho}{l(|x|)}}) E_{\Phi_{p,f_1}^*}^0 \left[\prod_{y \in \Phi_{p,f_1}^* \setminus 0} \frac{l(r_p)(1 - e^{\frac{-\mu\rho}{l(|y-x|)}})}{l(r_p) + \gamma l(|y - r(0)|)} \right] = \\
&(1 - e^{\frac{-\mu\rho}{l(|x|)}}) \exp \left\{ -\lambda_p p_e p_f \int_{\mathbb{R}^2} \frac{\gamma l(|y - r(0)|) + l(r_p) e^{\frac{-\mu\rho}{l(|y-x|)}}}{l(r_p) + \gamma l(|y - x|)} dy \right\} = A.
\end{aligned} \tag{C.8}$$

$$\begin{aligned}
E_{\Phi_{p,f_2}^*}^0 \left[\mathbb{1}_{\{\prod_{z \in \Phi_{p,f_2}^*} \mathbb{1}_{\{f(z,x)l(|z-x|)<\rho\}}=0\}} \right] &= 1 - \exp \left\{ -\lambda_p p_e (1 - p_f) \int_{\mathbb{R}^2} e^{\frac{-\mu\rho}{l(|z-x|)}} dz \right\} \\
&= B.
\end{aligned} \tag{C.9}$$

$$\begin{aligned}
E_{\Phi_{p,f_2}^*}^0 \left[\prod_{z \in \Phi_{p,f_2}^*} \mathbb{1}_{\{f(z,x)l(|z-x|)<\rho\}} \right] &= \exp \left\{ -\lambda_p p_e (1 - p_f) \int_{\mathbb{R}^2} e^{\frac{-\mu\rho}{l(|z-x|)}} dz \right\} \\
&= C.
\end{aligned} \tag{C.10}$$

Appendix C. Stochastic Geometry proofs

Finally,

$$P_{\Phi_{p,f_1}}^0 (SINR^p(0, f_1, r(0)) > \gamma) \leq e^{\frac{-\mu\gamma N}{l(r_p)}} \left(e^{-\lambda_p p_e p_f c(r_p)} - \frac{(1 - e^{-\lambda_s c(r_p)})}{c(r_p)} \int_{\mathbb{R}^2} \frac{\gamma l(|x - r(0)|)}{\gamma l(|x - r(0)|) + l(r_p)} (AB + \frac{1}{2}AC) dx \right). \quad (\text{C.11})$$

□

C.2 Proof of Proposition 11

Proof. Working with $\{f_1, f_2\}$ as the set of possible frequency bands, let $U(x)$ and $Y(x)$ be:

$$U(x) = \mathbb{1}_{\{|N_x^{p,f_1}|=0\}} \mathbb{1}_{\{|N_x^{p,f_2}|>0\}} + \mathbb{1}_{\{P(f_1)\}} \mathbb{1}_{\{|N_x^{p,f_1}|=0\}} \mathbb{1}_{\{|N_x^{p,f_2}|=0\}} \quad (\text{C.12})$$

and

$$Y(x) = \mathbb{1}_{\{|N_x^{p,f_2}|=0\}} \mathbb{1}_{\{|N_x^{p,f_1}|>0\}} + \mathbb{1}_{\{P(f_2)\}} \mathbb{1}_{\{|N_x^{p,f_1}|=0\}} \mathbb{1}_{\{|N_x^{p,f_2}|=0\}}. \quad (\text{C.13})$$

Considering 0 as a typical secondary user, and assuming that each band has the same probability to be chosen if both are free of primaries, we have:

$$\begin{aligned} P(U(0) = 1) &= P(|N_0^{p,f_1}| = 0)P(|N_0^{p,f_2}| > 0) + \frac{1}{2}P(|N_0^{p,f_1}| = 0)P(|N_0^{p,f_2}| = 0) \\ &= e^{-\lambda_p p_e p_f \bar{N}_0} (1 - e^{-\lambda_p p_e (1-p_f) \bar{N}_0}) + \frac{1}{2} e^{-\lambda_p p_e p_f \bar{N}_0} e^{-\lambda_p p_e (1-p_f) \bar{N}_0}, \end{aligned} \quad (\text{C.14})$$

and

$$\begin{aligned} P(Y(0) = 1) &= P(|N_0^{p,f_1}| > 0)P(|N_0^{p,f_2}| = 0) + \frac{1}{2}P(|N_0^{p,f_1}| = 0)P(|N_0^{p,f_2}| = 0) \\ &= (1 - e^{-\lambda_p p_e p_f \bar{N}_0}) e^{-\lambda_p p_e (1-p_f) \bar{N}_0} + \frac{1}{2} e^{-\lambda_p p_e p_f \bar{N}_0} e^{-\lambda_p p_e (1-p_f) \bar{N}_0}. \end{aligned} \quad (\text{C.15})$$

Please note that we can deduce Eq. (7.13) using the previous expressions by

$$MAP_s = P(U(0) = 1) + P(Y(0) = 1). \quad (\text{C.16})$$

In order to obtain COP_s , in the same way as in the previous demonstration, we will work on determining $P_{\Phi_s}^0 (SINR^s(0, r(0), f_1) > \gamma, U(0))$. Then,

$$P_{\Phi_s}^0 (SINR^s(0, r(0), f_1) > \gamma, U(0) | \mathcal{F}_{p,f_1}, \mathcal{F}_{p,f_2}, \mathcal{F}_s, r(0), f) = e^{\frac{-\mu\gamma N}{l(rs)}} E_{\Phi_s}^0 \left[e^{\frac{-\mu\gamma_{ps}^{f_1}(0)}{l(rs)}} U(0) | \mathcal{F}_{p,f_1}, \mathcal{F}_{p,f_2}, \mathcal{F}_s, r(0), f \right] E_{\Phi_s}^0 \left[e^{\frac{-\mu\gamma_{ss}^{f_1}(0)}{l(rs)}} | \mathcal{F}_{p,f_1}, \mathcal{F}_{p,f_2}, \mathcal{F}_s, r(0), f \right].$$

C.2. Proof of Proposition 11

We have considered that $r(0) = r_s$. Working with the second term of Eq. (C.17),

$$\begin{aligned}
 & E_{\Phi_s}^0 \left[e^{\frac{-\mu\gamma f_{ps}^1(0)}{l(r_s)}} U(0) \mid \mathcal{F}_{p,f_1}, \mathcal{F}_{p,f_2}, \mathcal{F}_s, r(0), f \right] = \\
 & E_{\Phi_s}^0 \left[\exp \left\{ \frac{-\mu\gamma \sum_{\{y \in \Phi_{p,f_1}^*\}} f_r(y,0) l(|y-r(0)|)}{l(r_s)} \right\} U(0) \mid \mathcal{F}_{p,f_1}, r(0) \right] = \\
 & \prod_{y \in \Phi_{p,f_1}^*} E \left[\exp \left\{ \frac{-\mu\gamma f_r(y,0) l(|y-r(0)|)}{l(r_s)} \right\} \right] U(0).
 \end{aligned} \tag{C.17}$$

Please note that $U(0)$ depends on Φ_{p,f_1}^* and Φ_{p,f_2}^* .

In the other term, we have:

$$\begin{aligned}
 E_{\Phi_s}^0 \left[e^{\frac{-\mu\gamma f_{ss}^1(0)}{l(r_s)}} \mid \mathcal{F}_{p,f_1}, \mathcal{F}_{p,f_2}, \mathcal{F}_s, r(0), f \right] &= E_{\Phi_s}^0 \left[e^{\frac{-\mu\gamma \sum_{\{x \in \Phi_{s,f_1}^* \setminus \emptyset\}} f_r(x,0) l(|x-r(0)|)}{l(r_s)}} \mid \mathcal{F}_{p,f_1}, \mathcal{F}_{p,f_2}, \mathcal{F}_s, r(0), f \right] \\
 &= E_{\Phi_s}^0 \left[e^{\sum_{\{x \in \Phi_s \setminus \emptyset\}} \frac{-\mu\gamma f_r(x,0) l(|x-r(0)|) U(x)}{l(r_s)}} \mid \mathcal{F}_{p,f_1}, \mathcal{F}_{p,f_2}, \mathcal{F}_s, r(0), f \right] \\
 &= \prod_{x \in \Phi_s \setminus \emptyset} E \left[e^{\frac{-\mu\gamma f_r(x,0) l(|x-r(0)|) U(x)}{l(r_s)}} \right] \\
 &= \prod_{x \in \Phi_s \setminus \emptyset} \left(1 - \left(1 - E \left[e^{\frac{-\mu\gamma f_r(x,0) l(|x-r(0)|)}{l(r_s)}} \right] \right) U(x) \right) \\
 &= \prod_{x \in \Phi_s \setminus \emptyset} \left(1 - \frac{l(r_s)}{l(r_s) + \gamma l(|x-r(0)|)} U(x) \right).
 \end{aligned} \tag{C.18}$$

We have also:

$$E_{\Phi_s}^0 \left[e^{\frac{-\mu\gamma f_{ss}^1(0)}{l(r_s)}} \mid \mathcal{F}_{p,f_1}, \mathcal{F}_{p,f_2}, r(0), f \right] = \exp \left\{ -\lambda_s \int_{\mathbb{R}^2} \frac{\gamma l(|x-r(0)|)}{\gamma l(|x-r(0)|) + l(r_s)} U(x) dx \right\}. \tag{C.19}$$

Applying the same strategy from previous demonstration, we have

$$\begin{aligned}
 P_{\Phi_s}^0(SINR^s(0, r(0), f_1) > \gamma, U(0) \mid \mathcal{F}_{p,f_1}, \mathcal{F}_{p,f_2}, r(0), f) &\leq e^{\frac{-\mu\gamma N}{l(r_s)}} \prod_{y \in \Phi_{p,f_1}^*} \frac{l(r_s)}{l(r_s) + \gamma l(|y-r(0)|)} U(0) \\
 &\quad \left(1 - (1 - e^{-\lambda_s c(r_s)}) \frac{\int_{\mathbb{R}^2} \frac{\gamma l(|x-r(0)|)}{\gamma l(|x-r(0)|) + l(r_s)} U(x) dx}{c(r_s)} \right).
 \end{aligned}$$

where $U(0) = \mathbb{1}_{\{|N_0^{p,f_1}|=0\}} \mathbb{1}_{\{|N_0^{p,f_2}|>0\}} + \mathbb{1}_{\{P(f_1)\}} \mathbb{1}_{\{|N_0^{p,f_1}|=0\}} \mathbb{1}_{\{|N_0^{p,f_2}|=0\}}$. In other words,

$$U(0) = \prod_{y \in \Phi_{p,f_1}^*} \mathbb{1}_{\{f(y,0)l(|y-0|)<\rho\}} \mathbb{1}_{\{\prod_{z \in \Phi_{p,f_2}^*} \mathbb{1}_{\{f(z,0)l(|z-0|)<\rho\}}=0\}} + \mathbb{1}_{\{P(f_1)\}} \prod_{y \in \Phi_{p,f_1}^*} \mathbb{1}_{\{f(y,0)l(|y-0|)<\rho\}} \prod_{z \in \Phi_{p,f_2}^*} \mathbb{1}_{\{f(z,0)l(|z-0|)<\rho\}}$$

Appendix C. Stochastic Geometry proofs

□

Appendix D

Proposition proofs of Chapter 8

D.1 A Proof of Theorem 2

According to Theorem 1, we have defined, during the primary sensing phase, the normalized processes:

- $\tilde{A}_t^P = A_t^P / N_P$,
- $\tilde{E}_t^P(i, j) = E_t^P(i, j) / N_P$ and $\tilde{E}_t^S(i, j) = E_t^S(i, j) / N_S$,
- $\tilde{U}_t^{PP} = U_t^{PP} / N_P$ and $\tilde{U}_t^{SP} = U_t^{SP} / N_P$,

which converge in probability to $(a_t^P, e_t^P(i, j), e_t^S(i, j), u_t^{PP}, u_t^{PS})$ solution of the following differential equation system:

$$\frac{da_t^P}{dt} = \sum_{k,l \in \mathbb{N}} e_t^P(k, l); \quad (\text{D.1})$$

$$\frac{de_t^P(i, j)}{dt} = -e_t^P(i, j) - \frac{ie_t^P(i, j)}{u_t^{PP}} \sum_{k,l \in \mathbb{N}} ke_t^P(k, l); \quad \forall i, j \in \mathbb{N}; \quad (\text{D.2})$$

$$\frac{de_t^S(i, j)}{dt} = -\frac{2ie_t^S(i, j)}{u_t^{PS}} \sum_{k,l \in \mathbb{N}} le_t^P(k, l); \quad \forall i, j \in \mathbb{N}; \quad (\text{D.3})$$

$$\frac{du_t^{PP}}{dt} = -2 \sum_{k,l \in \mathbb{N}} ke_t^P(k, l); \quad (\text{D.4})$$

$$\frac{du_t^{PS}}{dt} = -2 \sum_{k,l \in \mathbb{N}} le_t^P(k, l); \quad (\text{D.5})$$

Appendix D. Proposition proofs of Chapter 8

where

$$\begin{aligned} a_0^P &= 0; \\ e_0^P(i, j) &= \frac{\mu(i, j)}{N_P}; \forall i, j \in \mathbb{N} \text{ and } e_0^S(i, j) = \frac{\nu(i, j)}{N_S}; \forall i, j \in \mathbb{N}; \\ u_0^{PP} &= \frac{1}{N_P} \sum_{i=0}^{\infty} \sum_{j=0}^{\infty} i\mu(i, j) \text{ and } u_0^{PS} = \frac{1}{N_P} \sum_{i=0}^{\infty} \sum_{j=0}^{\infty} 2j\mu(i, j). \end{aligned}$$

Defining $h_t(i, j) = e^t e_t^P(i, j) \forall i, j \in \mathbb{N}$ and introducing a new time variable τ_t such that $\frac{d\tau_t}{dt} = \frac{\sum_i \sum_j i e_t^P(i, j)}{u_t^{PP}}$; it is possible to decouple the system of equations (D.2) and (D.4). Please note that the mapping $t \rightarrow \tau_t$ is a bijection of $[0, \infty)$ onto $[0, \tau_\infty)$ (the detail explanation and justification of this time transformation can be found in [96]). In order to simplify the notation, in the following calculus we will drop the time dependence in τ_t : $\tau_t = \tau$.

Working with the rescaled time variables: $u_\tau^{PP} = u_{t(\tau)}^{PP}$ and $h_\tau(i, j) = h_{t(\tau)}(i, j); \forall i, j \in \mathbb{N}$, we can obtain the following system of differential equations:

$$\frac{du_\tau^{PP}}{d\tau} = -2u_\tau^{PP}; \quad (\text{D.6})$$

$$\frac{dh_\tau(i, j)}{d\tau} = -ih_\tau(i, j); \forall i, j \in \mathbb{N}; \quad (\text{D.7})$$

where

$$u_0^{PP} = \frac{1}{N_P} \sum_{i=0}^{\infty} \sum_{j=0}^{\infty} i\mu(i, j) \text{ and } h_0(i, j) = e_0^P(i, j); \forall i, j \in \mathbb{N}.$$

The system has the following unique solution:

$$u_\tau^{PP} = u_0^{PP} e^{-2\tau}; \quad (\text{D.8})$$

$$h_\tau(i, j) = h_0(i, j) e^{-i\tau}. \quad (\text{D.9})$$

By $h_\tau(i, j)$ definition, we have that

$$e_\tau^P(i, j) = e^{-t} e_0^P(i, j) e^{-i\tau}; \forall i, j \in \mathbb{N}. \quad (\text{D.10})$$

Substituting Eqs. (D.8), (D.9) and (D.10) in τ definition, we obtain

$$\frac{d\tau_t}{dt} = e^{-t} \frac{\sum_i \sum_j i e_0^P(i, j) e^{-i\tau}}{u_\tau^{PP}}, \quad (\text{D.11})$$

that represents the transformation between τ and t and vice versa. τ_∞ is obtained from Eq. (D.11) by solving:

$$\int_0^{\tau_\infty} \frac{u_0^{PP} e^{-2\sigma}}{\sum_i \sum_j i e_0^P(i, j) e^{-i\sigma}} d\sigma = 1. \quad (\text{D.12})$$

Working with the rescaled time $e_\tau^S(i, j)$ and once u_τ^{PS} is totally determined with Eq. (D.5) and Eq. (D.10), we have that

$$e_\tau^S(i, j) = e_0^S(i, j) \left(\frac{u_\tau^{PS}}{u_0^{PS}} \right)^i; \forall i, j \in \mathbb{N}, \quad (\text{D.13})$$

where

$$u_\tau^{PS} = u_0^{PS} + \int_0^\tau -2 \sum_i \sum_j j e_0^P(i, j) e^{-i\sigma} \frac{u_0^{PP} e^{-2\sigma}}{\sum_i \sum_j i e_0^P(i, j) e^{-i\sigma}} d\sigma \quad (\text{D.14})$$

□

D.2 A Proof of Theorem 4

Defining the normalized processes $\tilde{A}_t^S = A_t^S/N_S$, $\tilde{E}_t^S(j) = E_t^S(j)/N_S$, and $\tilde{U}_t^{SS} = U_t^{SS}/N_S$. Then, as $N_S \rightarrow \infty$, they converge in probability to the solution of the following set of differential equations:

$$\frac{da_t^S}{dt} = \sum_{l \in \mathbb{N}} e_t^S(l); \quad (\text{D.15})$$

$$\frac{de_t^S(j)}{dt} = -e_t^S(j) - \frac{je_t^S(j)}{u_t^{SS}} \sum_{l \in \mathbb{N}} l e_t^S(l); \forall j \in \mathbb{N}; \quad (\text{D.16})$$

$$\frac{du_t^{SS}}{dt} = -2 \sum_{l \in \mathbb{N}} l e_t^S(l); \quad (\text{D.17})$$

where

$$\begin{aligned} a_0^S &= 0; \\ e_0^S(j) &= \sum_{k \in \mathbb{N}} e_\infty^S(k, j) \forall j \in \mathbb{N} \\ u_0^{SS} &= \frac{1}{N_S} \sum_{l \in \mathbb{N}} l v(k, l); \end{aligned}$$

By similar manipulations of the differential equations, defining $h_t(j) = e^t e_t^S(j) \forall j \in \mathbb{N}$ and using the analogous definition of τ_t as in Theorem 2, we have:

$$u_\tau^{SS} = u_0^{SS} e^{-2\tau}; \quad (\text{D.18})$$

$$e_\tau^S(j) = e^{-t} e_0^S(j) e^{-j\tau}; \forall i, j \in \mathbb{N}; \quad (\text{D.19})$$

where

$$\frac{d\tau_t}{dt} = \frac{\sum_j j e_t^S(j)}{u_t^{SS}}. \quad (\text{D.20})$$

We are interested on the limit of a_t^S as t goes to infinity (when the secondary sensing phase is over). Please note that it is the same as τ goes to τ_∞ , being τ_∞ the solution of:

$$\int_0^{\tau_\infty} \frac{u_0^{SS} e^{-2\sigma}}{\sum_{l \in \mathbb{N}} l e_0^S(l) e^{-l\sigma}} d\sigma = 1. \quad (\text{D.21})$$

Appendix D. Proposition proofs of Chapter 8

Then, working with Eq. (D.15), the proportion of active secondary transmitters converges in probability to:

$$a_{\infty}^S = \int_0^{\tau_{\infty}} \sum_{j \in \mathbb{N}} e_0^S(j) e^{-j\tau} \frac{u_0^{SS} e^{-2\tau}}{\sum_{j \in \mathbb{N}} j e_0^S(j) e^{-j\tau}} d\tau \quad (\text{D.22})$$

□

Bibliography

- [1] J. Xue, Z. Feng, and K. Chen, "Beijing spectrum survey for cognitive radio applications," in *2013 IEEE 78th Vehicular Technology Conference (VTC Fall)*, pp. 1–5, Sept 2013.
- [2] J. Jacob and B. R. Jose, "Spectrum occupancy measurement and analysis in Kochi-India from a cognitive radio perspective," in *2016 Sixth International Symposium on Embedded Computing and System Design (ISED)*, pp. 328–333, Dec 2016.
- [3] V. Blaschke, H. Jaekel, T. Renk, C. Kloeck, and F. Jondral, "Occupation measurements supporting dynamic spectrum allocation for cognitive radio design," in *Cognitive Radio Oriented Wireless Networks and Communications, 2007. CrownCom 2007. 2nd International Conference on*, pp. 50–57, Aug 2007.
- [4] F. S. P. T. Force, "Report of the spectrum efficiency working group," tech. rep., Federal Communications Commission, 2002.
- [5] I. F. Akyildiz, W.-Y. Lee, M. C. Vuran, and S. Mohanty, "Next generation/dynamic spectrum access/cognitive radio wireless networks: A survey," *Computer Networks*, vol. 50, no. 13, pp. 2127 – 2159, 2006.
- [6] M. Shafi, A. F. Molisch, P. J. Smith, T. Haustein, P. Zhu, P. D. Silva, F. Tufvesson, A. Benjebbour, and G. Wunder, "5G: A tutorial overview of standards, trials, challenges, deployment, and practice," *IEEE Journal on Selected Areas in Communications*, vol. 35, pp. 1201–1221, June 2017.
- [7] H. Mu and T. Hu, *Cognitive Radio and the New Spectrum Paradigm for 5G*, pp. 265–286. Singapore: Springer Singapore, 2017.
- [8] F.-L. Luo and C. Zhang, *5G Standard Development: Technology and Roadmap*, pp. 616–. Wiley-IEEE Press, 2016.
- [9] Cisco, "Cisco visual networking index: Global mobile data traffic forecast update, 2016–2021 white paper," tech. rep., Cisco, Feb 2017.
- [10] F. Akhtar, M. H. Rehmani, and M. Reisslein, "White space: Definitional perspectives and their role in exploiting spectrum opportunities," *Telecommunications Policy*, vol. 40, no. 4, pp. 319 – 331, 2016.

Bibliography

- [11] S. Sasipriya and R. Vigneshram, "An overview of cognitive radio in 5g wireless communications," in *2016 IEEE International Conference on Computational Intelligence and Computing Research (ICIC)*, pp. 1–5, Dec 2016.
- [12] Z. Wang and W. Zhang, "Opportunistic spectrum sharing with limited feedback in poisson cognitive radio networks," *IEEE Transactions on Wireless Communications*, vol. 13, pp. 7098–7109, Dec 2014.
- [13] M. R. Hassan, G. Karmakar, J. Kamruzzaman, and B. Srinivasan, "Exclusive use spectrum access trading models in cognitive radio networks: A survey," *IEEE Communications Surveys Tutorials*, vol. PP, no. 99, pp. 1–1, 2017.
- [14] "Cognitive radio for m2m and internet of things," *Comput. Commun.*, vol. 94, pp. 1–29, Nov. 2016.
- [15] J. Mitola and G. Q. Maguire, "Cognitive radio: making software radios more personal," *IEEE Personal Communications*, vol. 6, pp. 13–18, Aug 1999.
- [16] G. I. Tsiropoulos, O. A. Dobre, M. H. Ahmed, and K. E. Baddour, "Radio resource allocation techniques for efficient spectrum access in cognitive radio networks," *IEEE Communications Surveys Tutorials*, vol. 18, pp. 824–847, Firstquarter 2016.
- [17] S. K. Sharma, E. Lagunas, S. Chatzinotas, and B. Ottersten, "Application of compressive sensing in cognitive radio communications: A survey," *IEEE Communications Surveys Tutorials*, vol. 18, pp. 1838–1860, thirdquarter 2016.
- [18] J. Ren, Y. Zhang, N. Zhang, D. Zhang, and X. Shen, "Dynamic channel access to improve energy efficiency in cognitive radio sensor networks," *IEEE Transactions on Wireless Communications*, vol. 15, pp. 3143–3156, May 2016.
- [19] G. Capdehourat, F. Larroca, and P. Belzarena, "Decentralized robust spectrum allocation for cognitive radio wireless mesh networks," *Ad Hoc Networks*, vol. 36, Part 1, pp. 1 – 20, 2016.
- [20] A. Goldsmith, S. A. Jafar, I. Maric, and S. Srinivasa, "Breaking spectrum gridlock with cognitive radios: An information theoretic perspective," *Proceedings of the IEEE*, vol. 97, pp. 894–914, May 2009.
- [21] "Ieee standard for information technology– local and metropolitan area networks– specific requirements– part 22: Cognitive wireless ran medium access control (mac) and physical layer (phy) specifications: Policies and procedures for operation in the tv bands," *IEEE Std 802.22-2011*, pp. 1–680, July 2011.
- [22] "Ieee standard for information technology - telecommunications and information exchange between systems - local and metropolitan area networks - specific requirements - part 11: Wireless lan medium access control (mac) and physical layer (phy) specifications amendment 5: Television white spaces (tvws) operation," *IEEE Std 802.11af-2013 (Amendment to IEEE Std 802.11-2012, as amended by IEEE Std 802.11ae-2012, IEEE Std 802.11aa-2012, IEEE Std 802.11ad-2012, and IEEE Std 802.11ac-2013)*, pp. 1–198, Feb 2014.

- [23] "Ieee standard for local and metropolitan area networks part 16: Air interface for broadband wireless access systems amendment 2: Improved coexistence mechanisms for license-exempt operation," *IEEE Std 802.16h-2010 (Amendment to IEEE Std 802.16-2009)*, pp. 1–223, July 2010.
- [24] "Ieee standard for information technology–telecommunications and information exchange between systems – local and metropolitan area networks – specific requirements – part 19: Tv white space coexistence methods," *IEEE Std 802.19.1-2014*, pp. 1–326, June 2014.
- [25] "Ieee draft standard for local and metropolitan area networks - part 15.4: Low rate wireless personal area networks (lr-wpans) - amendment 6: Tv white space between 54 mhz and 862mhz physical layer," *P802.15.4m/D3*, May 2013, pp. 1–138, Oct 2013.
- [26] K. Nolan, "Research and development efforts in software-defined radio (sdr), cognitive radio (cr), and dynamic spectrum access (dsa) technologies.," in *2008 IET Seminar on Cognitive Radio and Software Defined Radios: Technologies and Techniques*, pp. 1–24, Sept 2008.
- [27] J. C. Merlano-Duncan, T. E. Bogale, and L. B. Le, "Sdr implementation of spectrum sensing for wideband cognitive radio," in *2015 IEEE 82nd Vehicular Technology Conference (VTC2015-Fall)*, pp. 1–5, Sept 2015.
- [28] M. M. Butt, C. Galiotto, and N. Marchetti, "Fair and regulated spectrum allocation in licensed shared access networks," in *2016 IEEE 27th Annual International Symposium on Personal, Indoor, and Mobile Radio Communications (PIMRC)*, pp. 1–6, Sept 2016.
- [29] W. Dong, S. Rallapalli, L. Qiu, K. K. Ramakrishnan, and Y. Zhang, "Double auctions for dynamic spectrum allocation," *IEEE/ACM Transactions on Networking*, vol. 24, pp. 2485–2497, Aug 2016.
- [30] A. Turhan, M. Alanyali, E. Kavurmacioglu, and D. Starobinski, "Dynamic pricing of preemptive service for secondary demand," *IEEE Transactions on Cognitive Communications and Networking*, vol. 2, pp. 208–222, June 2016.
- [31] Y. Zhang, C. Lee, D. Niyato, and P. Wang, "Auction approaches for resource allocation in wireless systems: A survey," *IEEE Communications Surveys Tutorials*, vol. 15, pp. 1020–1041, Third 2013.
- [32] G. Wu, P. Ren, and Q. Du, "Dynamic spectrum auction with time optimization in cognitive radio networks," in *IEEE Vehicular Technology Conference (VTC Fall)*, pp. 1–5, Sept 2012.
- [33] X. Wang, Z. Li, P. Xu, Y. Xu, X. Gao, and H.-H. Chen, "Spectrum sharing in cognitive radio networks – an auction-based approach," *Systems, Man, and Cybernetics, Part B: Cybernetics, IEEE Transactions on*, vol. 40, pp. 587–596, June 2010.

Bibliography

- [34] A. Turhan, M. Alanyali, and D. Starobinski, "Optimal admission control of secondary users in preemptive cognitive radio networks," in *Modeling and Optimization in Mobile, Ad Hoc and Wireless Networks (WiOpt), 10th International Symposium on*, pp. 138–144, May 2012.
- [35] L. Xie, J. Xiang, and Y. Zhang, "Revenue-based admission control for cognitive radio cellular systems," in *Communications and Networking in China, 2008. ChinaCom 2008. Third International Conference on*, pp. 1200–1204, Aug 2008.
- [36] B. Kim and S.-S. Ko, "Optimal admission control and state space reduction in two-class preemptive loss systems," *ETRI Journal*, vol. 37, pp. 917–921, Oct 2015.
- [37] D. Niyato and E. Hossain, "Competitive pricing for spectrum sharing in cognitive radio networks: Dynamic game, inefficiency of nash equilibrium, and collusion," *IEEE Journal on Selected Areas in Communications*, vol. 26, pp. 192–202, Jan 2008.
- [38] Y. Zhu, W. Sun, J. Yu, T. Liu, and B. Li, "Distributed spectrum sharing in cognitive radio networks: A pricing-based decomposition approach," *International Journal of Distributed Sensor Networks*, vol. 2014, 2014.
- [39] H. Yu, L. Gao, Z. Li, X. Wang, and E. Hossain, "Pricing for uplink power control in cognitive radio networks," *Vehicular Technology, IEEE Transactions on*, vol. 59, pp. 1769–1778, May 2010.
- [40] Z.-q. Wang, L.-g. Jiang, and C. He, "Price-based power control algorithm in cognitive radio networks based on monotone optimization," *Journal of Shanghai Jiao-tong University (Science)*, vol. 20, no. 6, pp. 654–659, 2015.
- [41] E. Altman, T. Jimenez, and G. Koole, "On optimal call admission control in resource-sharing system," *IEEE Transactions on Communications*, vol. 49, pp. 1659–1668, Sep 2001.
- [42] S. V. Savin, M. A. Cohen, N. Gans, and Z. Katalan, "Capacity management in rental businesses with two customer bases," *Operations Research*, vol. 53, no. 4, pp. 617–631, 2005.
- [43] F. Baccelli and B. Blaszczyszyn, *Stochastic Geometry and Wireless Networks, Volume I - Theory*, vol. 1 of *Foundations and Trends in Networking Vol. 3: No 3-4*, pp 249-449. NoW Publishers, 2009.
- [44] F. Baccelli and B. Blaszczyszyn, *Stochastic Geometry and Wireless Networks, Volume II - Applications*, vol. 2 of *Foundations and Trends in Networking: Vol. 4: No 1-2*, pp 1-312. NoW Publishers, 2009.
- [45] P. Bermolen, M. Jonckheere, F. Larroca, and P. Moyal, "Estimating the transmission probability in wireless networks with configuration models," *ACM Trans. Model. Perform. Eval. Comput. Syst.*, vol. 1, pp. 9:1–9:23, Apr. 2016.

- [46] M. Haenggi, J. G. Andrews, F. Baccelli, O. Dousse, and M. Franceschetti, “Stochastic geometry and random graphs for the analysis and design of wireless networks,” *IEEE Journal on Selected Areas in Communications*, vol. 27, pp. 1029–1046, September 2009.
- [47] F. H. Panahi and T. Ohtsuki, “Stochastic geometry based analytical modeling of cognitive heterogeneous cellular networks,” in *2014 IEEE International Conference on Communications (ICC)*, pp. 5281–5286, June 2014.
- [48] H.-M. Wang and T.-X. Zheng, *Random Cellular Networks and Stochastic Geometry*, pp. 21–40. Singapore: Springer Singapore, 2016.
- [49] T. V. Nguyen and F. Baccelli, “A probabilistic model of carrier sensing based cognitive radio,” in *New Frontiers in Dynamic Spectrum, 2010 IEEE Symposium on*, pp. 1–12, April 2010.
- [50] M. L. Puterman, *Markov Decision Processes: Discrete Stochastic Dynamic Programming*. New York, NY, USA: John Wiley & Sons, Inc., 1st ed., 1994.
- [51] D. P. Bertsekas, *Dynamic Programming and Optimal Control*. Athena Scientific, 2nd ed., 2000.
- [52] O. Alagoz and M. U. Ayvaci, *Uniformization in Markov Decision Processes*. John Wiley & Sons, Inc., 2010.
- [53] E. Ormeci and J. van der Wal, “Admission policies for a two class loss system with general interarrival times,” *Stochastic Models*, vol. 22, no. 1, pp. 37–53, 2006.
- [54] E. L. Örmeci, A. Burnetas, and J. van der Wal, “Admission policies for a two class loss system,” *Stochastic Models*, vol. 17, no. 4, pp. 513–539, 2001.
- [55] G. A. J. F. Brouns and J. van der Wal, “Optimal threshold policies in a two-class preemptive priority queue with admission and termination control,” *Queueing Systems*, vol. 54, pp. 21–33, Sep 2006.
- [56] M. Y. Ulukus, R. Gullu, and L. Ormeci, “Admission and termination control of a two class loss system,” *Stochastic Models*, vol. 27, no. 1, pp. 2–25, 2011.
- [57] L. De Nardis and O. Holland, *Deployment Scenarios for Cognitive Radio*, pp. 49–116. Cham: Springer International Publishing, 2014.
- [58] C. Jiang, L. Duan, and J. Huang, “Joint spectrum pricing and admission control for heterogeneous secondary users,” in *Modeling and Optimization in Mobile, Ad Hoc, and Wireless Networks (WiOpt), 2014 12th International Symposium on*, pp. 497–504, May 2014.
- [59] E. Pashenkova, I. Rish, and R. Dechter, “Value iteration and policy iteration algorithms for markov decision problem,” tech. rep., Department of Information and Computer Science, University of California at Irvine, 1996.

Bibliography

- [60] B. Hajek, “Optimal control of two interacting service stations,” *IEEE Transactions on Automatic Control*, vol. 29, pp. 491–499, Jun 1984.
- [61] S. M. Ross, *Stochastic Processes*. John Wiley & Sons, 2nd ed., 1996.
- [62] M. El-Taha and S. S. Jr., *Sample-Path Analysis of Queueing Systems*. Springer US, 1999.
- [63] Z. Liu, P. Nain, and D. Towsley, “Sample path methods in the control of queues,” *Queueing Systems*, vol. 21, no. 3, pp. 293–335, 1995.
- [64] M. L. Puterman and M. C. Shin, “Modified policy iteration algorithms for discounted markov decision problems,” *Management Science*, vol. 24, no. 11, pp. 1127–1137, 1978.
- [65] R. Darling and J. Norris, “Differential equation approximations for markov chains,” *Probab. Surveys*, vol. 5, pp. 37–79, 2008.
- [66] M. Benaïm and J.-Y. L. Boudec, “A class of mean field interaction models for computer and communication systems,” *Performance Evaluation*, vol. 65, no. 11, pp. 823 – 838, 2008. Performance Evaluation Methodologies and Tools: Selected Papers from ValueTools 2007.
- [67] S. N. Ethier and T. G. Kurtz, *Markov processes : characterization and convergence*. Wiley series in probability and mathematical statistics, New York, Chichester: J. Wiley & Sons, 1986.
- [68] V. Acary and B. Brogliato, *Numerical Methods for Nonsmooth Dynamical Systems: Applications in Mechanics and Electronics*, vol. 35 of *Lecture Notes in Applied and Computational Mechanics*. Springer Verlag, 2008.
- [69] N. Gast and B. Gaujal, “Mean field limit of non-smooth systems and differential inclusions,” *SIGMETRICS Perform. Eval. Rev.*, vol. 38, pp. 30–32, Oct. 2010.
- [70] N. Gast and B. Gaujal, “Markov chains with discontinuous drifts have differential inclusion limits,” *Performance Evaluation*, vol. 69, no. 12, pp. 623 – 642, 2012.
- [71] M. Jonckheere and S. Shneer, “Stability of multi-dimensional birth-and-death processes with state-dependent 0-homogeneous jumps,” *Advances in Applied Probability*, vol. 46, no. 1, p. 59–75, 2014.
- [72] L. Bortolussi, “Hybrid limits of continuous time markov chains,” in *2011 Eighth International Conference on Quantitative Evaluation of SysTems*, pp. 3–12, Sept 2011.
- [73] L. Bortolussi, “Hybrid behaviour of markov population models,” *Information and Computation*, pp. –, In Press.
- [74] L. Aspirot, E. Mordecki, and G. Rubino, “Fluid limits applied to peer to peer network analysis,” *Quantitative Evaluation of Systems, International Conference on*, vol. 0, pp. 13–20, 2011.

- [75] F. Baccelli, F. Mathieu, I. Norros, and R. Varloot, “Can P2P networks be super-scalable?,” *CoRR*, vol. abs/1304.6489, 2013.
- [76] A. Ferragut and F. Paganini, “Fluid models of population and download progress in p2p networks,” *IEEE Transactions on Control of Network Systems*, vol. 3, pp. 34–45, March 2016.
- [77] D. Qiu and R. Srikant, “Modeling and performance analysis of bittorrent-like peer-to-peer networks,” in *SIGCOMM '04: Proceedings of the 2004 conference on Applications, technologies, architectures, and protocols for computer communications*, (New York, NY, USA), pp. 367–378, ACM, 2004.
- [78] M. Tschaikowski and M. Tribastone, “Spatial fluid limits for stochastic mobile networks,” *Performance Evaluation*, vol. 109, pp. 52 – 76, 2017.
- [79] G. Sharma, A. Ganesh, and P. Key, “Performance analysis of contention based medium access control protocols,” *IEEE Transactions on Information Theory*, vol. 55, pp. 1665–1682, April 2009.
- [80] M. Jonckheere and J. Mairesse, “Towards an erlang formula for multiclass networks,” *Queueing Systems*, vol. 66, pp. 53–78, Sep 2010.
- [81] S. Wang, J. Zhang, and L. Tong, “Delay analysis for cognitive radio networks with random access: A fluid queue view,” in *Proceedings of the 29th Conference on Information Communications, INFOCOM'10*, (Piscataway, NJ, USA), pp. 1055–1063, IEEE Press, 2010.
- [82] C. Yin, L. Gao, and S. Cui, “Scaling laws for overlaid wireless networks: A cognitive radio network versus a primary network,” *IEEE/ACM Transactions on Networking*, vol. 18, pp. 1317–1329, Aug 2010.
- [83] C. Zhang, X. Wang, X. Guan, and H. H. Chen, “Quality-of-service in cognitive radio networks with collaborative sensing,” in *GLOBECOM 2009 - 2009 IEEE Global Telecommunications Conference*, pp. 1–5, Nov 2009.
- [84] M. Benaïm and J.-Y. Le Boudec, “A class of mean field interaction models for computer and communication systems,” *Perform. Eval.*, vol. 65, no. 11-12, pp. 823–838, 2008.
- [85] J.-Y. Le Boudec, “The Stationary Behaviour of Fluid Limits of Reversible Processes is Concentrated on Stationary Points,” tech. rep., 2010.
- [86] Z. Zhao, “A preemptive connection pool manager for web-based application collaboration,” in *8th International Conference on Collaborative Computing: Networking, Applications and Worksharing, CollaborateCom 2012, Pittsburgh, PA, USA, October 14-17, 2012*, pp. 326–334, 2012.
- [87] P. J. Smith, A. Firag, P. Dmochowski, and M. Shafi, “Analysis of the m/m/n/n queue with two types of arrival process: Applications to future mobile radio systems,” vol. 2012, 01 2012.

Bibliography

- [88] P. Robert, *Stochastic Networks and Queues*. Stochastic Modelling and Applied Probability Series, New York: Springer-Verlag, 2003.
- [89] L. Aspirot, *Fluid Approximations for Stochastic Telecommunication Models*. PhD thesis, Universidad de la República, 2017. unpublished thesis.
- [90] D. Stoyan, W. S. Kendall, and J. Mecke, *Stochastic geometry and its applications*. Wiley series in probability and mathematical statistics, Chichester, W. Sussex, New York: Wiley, 1987. Rev. translation of: Stochastische Geometrie.
- [91] R. van der Hofstad, “Random graphs and complex networks.” Lecture Notes, 2013.
- [92] B. Bollobas, *Random Graphs*. Cambridge, UK: Cambridge University Press, 2001.
- [93] T. V. Nguyen and F. Baccelli, “A stochastic geometry model for cognitive radio networks,” *The Computer Journal*, 2011.
- [94] S. Lee and G. Hwang, *Throughput Analysis of Multichannel Cognitive Radio Networks Based on Stochastic Geometry*, pp. 63–71. Cham: Springer International Publishing, 2016.
- [95] P. Bermolen, M. Jonckheere, and P. Moyal, “The jamming constant of uniform random graphs,” *Stochastic Processes and their Applications*, 2016. To appear.
- [96] G. Brightwell, S. Janson, and M. Luczak, “The greedy independent set in a random graph with given degrees,” *Random Structures Algorithms*, Oct. 2016. To appear.
- [97] L. Langwagen, “Geometría aleatoria con aplicaciones al modelado de redes inalámbricas,” bachelor’s thesis, Universidad de la República(Uruguay). Facultad de Ciencias., 2014.
- [98] D. Zhang, Z. Chen, J. Ren, N. Zhang, M. Awad, H. Zhou, and X. Shen, “Energy harvesting-aided spectrum sensing and data transmission in heterogeneous cognitive radio sensor network,” *IEEE Transactions on Vehicular Technology*, vol. PP, no. 99, pp. 1–1, 2016.
- [99] N. Tadayon and S. Aissa, “Multi-channel cognitive radio networks: Modeling, analysis and synthesis,” *IEEE Journal on Selected Areas in Communications*, vol. 32, pp. 2065–2074, November 2014.
- [100] N. Tadayon and S. Aïssa, “Modeling and analysis framework for multi-interface multi-channel cognitive radio networks,” *IEEE Transactions on Wireless Communications*, vol. 14, pp. 935–947, Feb 2015.
- [101] A. Busson, B. Jabbari, A. Babaei, and V. Vèque, “Interference and throughput in spectrum sensing cognitive radio networks using point processes,” *Journal of Communications and Networks*, vol. 16, pp. 67–80, Feb 2014.
- [102] C. h. Lee and M. Haenggi, “Interference and outage in poisson cognitive networks,” *IEEE Transactions on Wireless Communications*, vol. 11, pp. 1392–1401, April 2012.

- [103] A. Rabbachin, T. Q. S. Quek, H. Shin, and M. Z. Win, “Cognitive network interference,” *IEEE Journal on Selected Areas in Communications*, vol. 29, pp. 480–493, February 2011.
- [104] H. ElSawy and E. Hossain, “Channel assignment and opportunistic spectrum access in two-tier cellular networks with cognitive small cells,” in *2013 IEEE Global Communications Conference (GLOBECOM)*, pp. 4477–4482, Dec 2013.
- [105] G. Yuchen, N. Kai, and L. Jiaru, “Stochastic geometric analysis of the uplink throughput in cognitive radio cellular networks,” *China Communications*, vol. 10, pp. 44–53, Aug 2013.
- [106] H. ElSawy and E. Hossain, “Two-tier hetnets with cognitive femtocells: Downlink performance modeling and analysis in a multichannel environment,” *IEEE Transactions on Mobile Computing*, vol. 13, pp. 649–663, March 2014.
- [107] D. J. Daley and D. Vere-Jones, *An introduction to the theory of point processes. Vol. II. Probability and its Applications* (New York), New York: Springer, second ed., 2008. General theory and structure.
- [108] S. Helif, R. Abdulla, and S. Kumar, “A review of energy detection and cyclostationary sensing techniques of cognitive radio spectrum,” in *2015 IEEE Student Conference on Research and Development (SCOReD)*, pp. 177–181, Dec 2015.
- [109] P. Erdős and A. Rényi, “On random graphs. I,” *Publ. Math. Debrecen*, vol. 6, pp. 290–297, 1959.
- [110] M. Molloy and B. Reed, “A critical point for random graphs with a given degree sequence,” *Random Structures & Algorithms*, vol. 6, no. 2-3, pp. 161–180, 1995.
- [111] D. Dawson, “Measure-valued processes, stochastic partial differential equations, and interacting systems,” in *CRM Proceedings & Lecture Notes*, vol. 5, American Mathematical Society, 1991.
- [112] “Opencellid, [online], <https://opencellid.org/>.”
- [113] M. Ulm, P. Widhalm, and N. Brändle, “Characterization of mobile phone localization errors with opencellid data,” in *2015 4th International Conference on Advanced Logistics and Transport (ICALT)*, pp. 100–104, May 2015.
- [114] Y. J. Chun, M. O. Hasna, and A. Ghayeb, “Modeling heterogeneous cellular networks interference using poisson cluster processes,” *IEEE Journal on Selected Areas in Communications*, vol. 33, pp. 2182–2195, Oct 2015.
- [115] M. Afshang and H. S. Dhillon, “Poisson cluster process based analysis of hetnets with correlated user and base station locations,” *CoRR*, vol. abs/1612.07285, 2016.
- [116] M. Haenggi, *Stochastic Geometry for Wireless Networks*. New York, NY, USA: Cambridge University Press, 1st ed., 2012.

Bibliography

- [117] D. J. Daley and D. Vere-Jones, *An introduction to the theory of point processes. Vol. I. Probability and its Applications* (New York), New York: Springer-Verlag, second ed., 2003. Elementary theory and methods.

Esta es la última página.
Compilado el Friday 23rd February, 2018.
<http://iie.fing.edu.uy/>